Graduate Theses and Dissertations

Iowa State University Capstones, Theses and Dissertations

2019

Geoenvironmental aspects of recycled materials in pavement applications: Leaching characterizations

Masrur Mahedi

Iowa State University

Follow this and additional works at: https://lib.dr.iastate.edu/etd

Part of the Civil Engineering Commons, Geochemistry Commons, and the Geotechnical Engineering Commons

Recommended Citation

Geoenvironmental aspects of recycled materials in pavement applications: Leaching characterizations

by

Masrur Mahedi

A dissertation submitted to the graduate faculty

in partial fulfillment of the requirements for the degree of

DOCTOR OF PHILOSOPHY

Major: Civil Engineering (Geotechnical Engineering)

Program of Study Committee:
Bora Cetin, Major Professor
Jeramy C. Ashlock
Chris R. Rehmann
Robert Horton
Halil Ceylan

The student author, whose presentation of the scholarship herein was approved by the program of study committee, is solely responsible for the content of this dissertation. The Graduate College will ensure this dissertation is globally accessible and will not permit alterations after a degree is conferred.

Iowa State University
Ames, Iowa
2019

DEDICATION

For the two most important women in my life,

My mom & my wife

TABLE OF CONTENTS

LIST OF FIGURES

LIST OF TABLES

ACKNOWLEDGMENTS

I would like to express my deepest gratitude to my committee chair, Dr. Bora Cetin for his guidance, motivation and extensive patience throughout my Ph.D. studies. I am thankful to him for advising and helping me with my research, technical writing, presentations, and for all the opportunities offered while working with him. Without his constant supports, this work would not have been completed. I am grateful to my mentor and minor representative professor, Dr. Robert Horton for his teaching, tremendous encouragements, research suggestions and help in my personal life. He has always been a savior in crucial and challenging times. I would like to thank my committee members Dr. Halil Ceylan, Dr. Chris R. Rehmann and Dr. Jeramy C. Ashlock for their time, suggestions and support throughout the course of this research study. It was a great opportunity for me to learn under their supervision. My special thanks to Dr. Kristen Cetin and Dr. Kaoru Ikuma for reviewing my papers and providing me with valuable feedback. My utmost appreciation to Kendra Lee, former CCEE Environmental Lab Manager, for her support in laboratory investigations. The assistance and effort of Ben Popken and Anish Bhatt, Undergraduate Research Assistant, are greatly appreciated. Thanks to my advisor at UT Arlington, Dr. Sahadat Hossain for his unconditional support during my graduate studies. In addition, I would also like to thank my friends, colleagues, the department faculty and staff for making my time at Iowa State University a wonderful experience. Last but not the least, I want to express my deepest love to my parents, wife, sisters and in-laws for their supports and encouragements throughout my study.

ABSTRACT

Industrial byproducts, fly ash and steel slag are widely used in pavement subgrade soil stabilization. Similarly, recycled concrete aggregates (RCA) are one of the most commonly used waste materials in pavement base construction. These materials are known to leach heavy metals and other elements of environmental concerns. On the other hand, cement is frequently used as an activator during fly ash and slag stabilization, which considerably increases the material pH, and hence, the leaching potentials of toxic constituents. The pH of RCA greatly varies with age, source and storage conditions due to carbonation. Additionally, the influence of matric potential on the leaching behaviors of RCA remains unknown. This study investigated the leaching characteristics of RCA and cement activated fly ash and steel slag stabilized soils through laboratory batch water leach test, toxicity characteristic leaching procedure, synthetic precipitation leaching procedure and pH-dependent leach tests. The effluent concentrations of calcium (Ca), magnesium (Mg), aluminum (Al), barium (Ba), chromium (Cr), copper (Cu), iron (Fe), zinc (Zn), manganese (Mn), sulfur (S), dissolved inorganic/organic carbon (DIC/DOC), sulfate (SO_4), pH, electrical conductivity (EC) and alkalinity were quantified. Moreover, geochemical modeling was performed to evaluate the leaching mechanisms of these elements. The effluent concentrations of Ca, Ba, Al, SO_4 increased; Mg, Cu and DIC concentrations decreased; Fe, Zn and DOC fluctuated; and Cr and Mn concentrations remained unaffected by cement addition. Cement activation altered the pH dependent release of Ca, Cr, Ba, Zn, S, SO_4, DIC and DOC, noticeably. Multiple batch tests were required for the comprehensive leaching assessment. Geochemical modeling indicated that, except for Cr, the releases of elements from cement activated fly ash and slag stabilized soils were solubility controlled. In case of RCA, leaching characteristics were considerably influenced by carbonation, particle sizes and liquid to solid ratios (L/S). Distinct pH dependent releases of

elements were observed relying on degree of carbonation. The selection of appropriate leach tests depended on RCA carbonation and constituent of potential concern. Matric potentials at different saturation conditions were found to have an impact on the release of elements from RCA. The highest solution pH and leached concentrations of Ca and Ba were originated in the matric potential range of 2 kPa to 5 kPa.

CHAPTER 1.   GENERAL INTRODUCTION

In the United States, a number of state highway agencies are adopting the use of industrial byproducts and waste materials in their roadway construction practices. The use of industrial by-products such as fly ash and slag in soil stabilization are very common, owing to their suitable physical properties, mechanical properties and economic advantages. Fly ash is a coal combustion pozzolanic byproduct of coal power plants. It is collected from exhaust gas either by mechanical or electrostatic procedures (Wen et al., 2011). According to American Coal Ash Association (ACAA, 2018), in 2016 around 37.8 million tons of fly ash were generated only in the U.S., and 60% of these were reused. Some of the fly ashes have self-cementitious properties (e.g., Class C fly ash) derived from higher amount of calcium oxides (CaO), while others (e.g., Class F fly ash, high carbon fly ash) are rich in silica (SiO_2), alumina (Al_2O_3) and iron oxides (Fe_2O_3) which can react with an activator such as cement and lime to produce additional cementitious compounds (Cetin et al., 2010; Thomas, 2007). However, during the combustion process at high temperatures, coal minerals undergo phase transformations which may render subsequent leaching of toxic elements from the fly ashes (Jones, 1995).

Similarly, steel slag is produced as a by-product of iron manufacturing industry, consisting of silicates and alumino-silicates of lime and other bases (primarily, magnesium) which can offer cementitious properties (Engström et al., 2013). According to United States Geological Survey (USGS) Mineral Commodity Summaries (U.S. Geological Survey, 2018), in the year of 2016, the estimated ferrous slag production was 15 to 20 million tons in the United States. These slags predominantly consist of $CaO-MgO-SiO_2-Fe_2O_3$ quaternary system and can be considered as weak cement clinkers (Shi, 2004). Slags are more efficient to improve the soil strength, especially in the presence of high sulfate salts (Mahedi et al. 2018). Nevertheless, Dayioglu et al. (2018)

reported the leaching of toxic, heavy and trace metals from steel slag at different environmental conditions.

Several studies have evaluated the leaching behavior and leaching mechanisms of metals from fly ash and slag stabilized soils (Bin-Shafique et al., 2006; Cappuyns et al., 2014; Cetin et al., 2013; Cetin and Aydilek, 2013; Gomes and Pinto, 2006; Kogbara et al., 2013; Kogbara and Al-Tabbaa, 2011; Komonweeraket et al., 2015b, 2015c, 2015a; Windt et al., 2011; Zhang et al., 2016). Fly ashes and slags are often used with cement in soil stabilization for strength and stiffness requirements due to their low self-cementing potentials. Cement addition substantially enhances the pH of soil which may induce further leaching of certain amphoteric metals such as aluminum (Al), Barium (Ba), chromium (Cr), copper (Cu) and zinc (Zn). Therefore, the leaching behavior and leaching controlling mechanisms of fly ash or slag treated soil are specifically important, when a calcium-based activator such as cement is used. There is a lack of information on the leaching behavior and leaching mechanisms of contaminants from these widely implemented cement activated fly ash or slag stabilized soils. In addition, previous studies evaluated the leaching of metals for a limited pH range, disregarding the influence of commonly occurred benign elements such as Ca, Mg, sulfate (SO_4), nitrate (NO_3), dissolved organic carbon (DOC), dissolved inorganic carbon (DIC) etc. These elements are largely released from fly ash and slag and their mode of occurrence, precipitation and substitution essentially control the leaching of other environmentally sensitive elements.

Correspondingly, aggregates derived from natural sources have been used traditionally as pavement base materials. In recent times, the extraction of natural aggregates has become more labor intensive and costly due to high quality resource depletion and environmental concerns (Faysal et al., 2016). Therefore, crushed waste concrete commonly termed as recycled concrete

aggregates (RCA) are being considered as a possible alternative to virgin aggregates (Chen et al., 2012). Demolition of existing structures such as buildings, concrete pavements, bridges, curbs and gutters are the main sources of recycled crushed concrete aggregates which may also be generated from concrete over-runs associated with new constructions. After the process of recycling, cement paste left attached to the surface of the aggregates which can be a potential source of leached constituents (Bestgen et al., 2016a, 2016b).

Previous studies evaluated the leaching potential of RCA based on pH and standard test procedures (Bestgen et al., 2016a; Chen et al., 2012, 2009, Engelsen et al., 2012, 2010, 2009). However, inconsistency within the results of previous studies are often apparent owing to the variety of test procedures, age, location and derived material sources (i.e., building demolition, concrete pavement, stockpile). Additionally, Engelsen et al. (2010) pointed out that the leaching potentials of RCA materials greatly varies depending on RCA degree of carbonation. Therefore, a comprehensive assessment of the leaching behavior of the elements from these materials is required, encompassing the widely used test procedures and diverse sources. Moreover, in all conventional leach test procedures influent solutions are added in excess to the materials of interest. Test procedure varies based on extraction fluid type, liquid to solid ratio, shaking period, shaking rate and extraction/filtration procedure. However, these methods may not represent the actual field conditions because RCA may become saturated only during/just after a rainfall event or in an inundation scenario. In most cases, the RCA used as pavement base materials remains unsaturated. Nonetheless, there is continuous infiltration or seepage of water from the unsaturated RCA towards the ground water table. The leaching behavior of metals in this unsaturated flow yet remained unexplored.

1.1 Research Goal and Objectives

The objectives of this proposed study are to (1) investigate the leaching behavior of elements from cement activated fly ash and slag stabilized soils and RCAs; (2) evaluate the effects of leaching regulatory factors such as stabilizer types and their addition rates, liquid to solid ratios, total metal contents, environmental conditions, pH and particle sizes; (3) identify and access the leaching controlling mechanisms; (4) provide quantitative comparisons between standard leach test procedures; (5) investigate the effect of carbonation on the leaching from RCA; and (6) evaluate the leaching behavior of elements under different saturated conditions and matric potentials. The experimental program to achieve these goals consists of the following tasks:

1. Determining physical and chemical properties of the materials used in this study by exploiting particle size distribution, compaction, X-ray diffraction (XRD) and X-ray fluorescence (XRF) analyses.

2. Performing acid digestions of cement, fly ash, slag, soil and RCAs to measure total metal contents.

3. Preparing different combinations of cement activated fly ash and slag treated samples. Collecting RCAs from a variety of geographic location and source of origin.

4. Performing batch water leach tests (WLT) for a quick estimation of the leaching behavior of metals.

5. Performing toxicity characteristic leaching procedure (TCLP) to evaluate the leaching behavior in landfill containment condition.

6. Performing synthetic precipitation leaching procedure (SPLP) to evaluate the leaching behavior in acid rain condition.

7. Performing USGS leach test to evaluate the field leachability.

8. Performing pH dependent leach test to identify the leaching patter of metals and minerals.

9. Implementing pressure cell method to evaluate the leaching behavior of metals at different matric potentials.

10. Quantifying effluent cations and anions concentrations and other chemical properties of interests from cement activated fly ash and slag treated soils, fly ash, slag, cement and soil alone; and RCAs.

11. Identifying the leaching controlling mechanisms via geochemical modeling program Visual MINTEQ.

This study investigates the leaching behavior of 10 metals (Aluminum (Al), Barium (Ba), Calcium (Ca), Chromium (Cr), Copper (Cu), Iron (Fe), Magnesium (Mg), Manganese (Mn), Sulfur (S) and Zinc (Zn)) and 5 different elements of significance (Sulfate-SO_4, Nitrite-NO_2, Nitrate-NO_3, Dissolved Inorganic Carbon-DIC, and Dissolved Organic Carbon-DOC). In addition, effluent pH, electric conductivity and alkalinity were quantified.

1.2 Organization of the Dissertation

This dissertation consists of six chapters: general introduction, four research papers, and conclusions and recommendations. Chapter 1 provides the general introduction, describing the requirements and objective of this research endeavor. Chapter 2 explores the leaching characteristics of the elements from cement activated fly ash and slag treated soils in TCLP, SPLP, WLT effluents. Geochemical modeling was performed based on the solution concentrations of the elements from these standard batch tests. Chapter 3 describes the pH dependent leaching behavior of Al, Cu, Fe and Zn from cement activated fly ash and slag treated soils. Geochemical modeling was performed to investigate the leaching controlling mechanisms of the selected elements based on pH dependent leach tests concentrations. Chapter 4 focus the leaching behavior and leaching

controlling mechanisms of Ca, Mg, Ba, Mn, Cr and S based on pH dependent leach tests. Chapter 5 discusses the influence of carbonation on the leaching characteristics of recycled concrete aggregates (RCA). Geochemical modeling was performed to investigate on the leaching controlling mechanisms of the elements from the RCAs with a varying degree of carbonation. Chapter 7 summarizes the key findings of this study. Several research directions are provided for future studies.

CHAPTER 2. LEACHING OF ELEMENTS FROM CEMENT ACTIVATED FLY ASH AND SLAG AMENDED SOILS

A paper submitted to *Chemosphere*

Masrur Mahedi and Bora Cetin

2.1 Abstract

The leaching behavior and leaching controlling mechanisms of four elements: chromium (Cr), copper (Cu), iron (Fe) and sulfur (S) from cement activated fly ash and slag stabilized pavement subgrade soils were evaluated. Synthetic precipitation leaching procedure (SPLP), batch water leach test (WLT), toxicity characteristic leaching procedure (TCLP) and pH-adjusted leach tests were conducted. Several factors such as stabilizer type and addition rate, cement content, elemental concentration and pH were considered for parametric study. Geochemical equilibrium model MINTEQA2 was implemented to identify the leaching controlling mechanisms of the metals. Effluent pH played the most vital role on the leaching behavior of the elements. Quantitative assessments between the test methods indicated significant variations in the leached metal concentrations. Cr and Cu showed amphoteric leaching behaviors, whereas Fe and S followed cationic leaching patterns. Cr^{3+}, Cu^{2+}, Fe^{3+} and S^{6+} were identified to be the dominant oxidation states of the metals of interest. According to the geochemical analyses, leaching of these elements were solubility controlled. Dissolution-precipitation of oxide and hydroxide minerals controlled the leaching of Cr, Cu, Fe and S from cement activated fly ash and slag stabilized subgrade soils.

Keywords: Metal leaching, Soil stabilization, Cement, Fly ash, Slag, Geochemical modeling

2.2   Introduction

In the United States, a number of state highway agencies are adopting the use of waste materials and industrial byproducts in their construction applications. The recycling of the materials considerably reduces the natural resource depletion, construction cost, labor and declination of landfill spacing. Fly ash and steel slag are the two widely used recycled materials in pavement constructions with great applicability in subgrade soil stabilization. Fly ashes are byproducts from coal burning electric power plants, whereas steel slags are the non-metallic offshoots generated in different stages of steel production (Engström et al. 2013; Cetin et al. 2014). Some of the fly ashes (e.g. Class C) have self-cementing properties resulting from higher amount of calcium oxides (CaO), while others (e.g. Class F, high-carbon fly ash) are effective pozzolans owing to the presence of silica (SiO^2), alumina (Al^2O^3) and iron oxides (Fe^2O^3), capable of producing cementitious compounds with the presence of an activator such as lime and cement (Mahedi et al. 2018). The combustion of lignite or subbituminous coal generates Class C fly ash, whereas Class F fly ash is generated when bituminous coal is used (Thomas 2007; Senapati 2011). Besides, steel slags are frequently represented by CaO–MgO–SiO^2–Fe^2O^3 quaternary system and can be considered as weak cement clinkers (Shi 2004). Therefore, soil stabilization becomes more practical and economical with fly ashes or slags, where other traditional and nontraditional techniques (e.g. cement, lime, excavation and replacement, polymer, enzyme, biocementation) are proven to be costly and labor intensive (Yilmaz et al. 2019).

Strength, stiffness and durability properties of fly ash and slag treated soils are deemed to be satisfactory by previous studies (Cetin et al. 2010; Tastan et al. 2011; Dayioglu et al. 2014, 2018; Mahedi et al. 2018; Yilmaz et al. 2019). Nevertheless, limited information exists on their environmental impacts because of the leaching of toxic substances into the surface and groundwater (Cetin et al. 2012b, 2014). As the coal minerals undergo phase changes during the

combustion processes, use of fly ashes may induce substantial leaching of ecologically harmful metals into the environment (Jones 1995; Qureshi et al. 2018). Gomes and Pinto (2006) reported leaching of heavy metals from steelmaking slags. Dayioglu et al. (2018) concluded that leaching of heavy and toxic metals from steel slags is largely dependent on the environmental conditions. Therefore, conflicts within the previous studies are often apparent (Bestgen et al. 2016a), owing to the variety of leach test procedures. A comprehensive assessment of the leaching behavior of the metals is required, encompassing the widely used test procedures. Moreover, the effect of pH is often isolated, though the pH plays an important role on the leaching behavior of metals from fly ash and slag treated soils (Komonweeraket et al. 2015b). Furthermore, leaching behavior of steel slag relating mineralogy and element availability is still inadequate (Spanka et al. 2018).

Besides, fly ashes and slags are often used with cement in soil stabilization to initiate pozzolanic reactions due to their lower cementing potential. Cement addition substantially enhances the pH of soil which may induce further leaching of metals such as chromium (Cr), selenium (Se), and arsenic (As) (Cetin et al. 2012a). Therefore, the leaching behavior and leaching controlling mechanisms of fly ash and steel slag treated soil are specifically important, when a calcium-based activator such as cement is used. Furthermore, leaching controlling mechanisms from slag treated soil have not yet been investigated. It is necessary to understand the leaching mechanisms, since the toxicity of the metals largely depends on their speciation and/or oxidation states.

The main objective of this study was to evaluate the leaching behavior and leaching controlling mechanisms of metals from cement activated fly ash and steel slag treated subgrade soil based on SPLP, WLT, TCLP and pH-adjusted leach tests. Cr, Cu, Fe and S were selected as the elements of potential concern based on their environmental impacts determined by previous

studies (Bestgen et al. 2016a, b). The U.S. EPA listed Cr and Cu on the priority contaminant list, whereas Fe and S (as SO_4^{2-}) are listed on secondary priority list. Finally, experimental data were utilized to identify the predominant metal species and leaching controlling mechanisms by implementing the geochemical modeling program MINTEQA2.

2.3   Materials

Collapsible and frost susceptible Iowa loess soil treated with two different fly ashes and ground granulated blast-furnace steel slag was used for the experimental setup of the study. According to Unified Soil Classification System (USCS), loess soil was classified as low plasticity silt (ML) with 82% fines (< 0.05 mm) and 11% clay (< 0.02 mm) size particles. The liquid limit (LL) and plasticity index (PI) of the soil were found to be 24 and 4, respectively; following the standard method designated by ASTM D4318. The American Association of State Highway and Transportation Officials (AASHTO) classification of the soil was A-4.

Type I/II Portland cement was utilized as an activator to enhance the pozzolanic reactions of fly ashes and slag. The basic oxide components of the materials used in this study are provided in Table 2.1. Based on the chemical components, fly ashes were classified and Class C and F following the guidelines provided in ASTM C618. As indicated earlier, Class C and F are the most widely implemented fly ashes in soil stabilization due to their self-cementing capacities and pozzolanic activities. The CaO content of steel slag was found to be 39.8%, indicating its cementation potentials. The SiO2, Al2O3 and Fe2O3 contents of steel slag were 35.7%, 9.9% and 0.6% respectively, which could contribute significantly in the stabilization process. Additionally, the total metals content of the materials was determined based on EPA Method 3050B and are reported in Table 2.1. As presented in Table 2.1, the Cr, Cu and Fe contents were the highest in Class C fly ash, whereas the maximum amount of S was found in cement. Except for Fe, all the metal contents were the lowest in loess soil. The minimum amount of Fe was found in steel slag.

2.4 Method

2.4.1 Leach Test Sample Preparation

An array of soil-fly ash-cement and soil-slag-cement mixtures was prepared on weight basis by varying the fly ash or steel slag content in the range of 10% to 40%. Previous studies recommend the maximum use of 20% fly ash and slag in soil stabilization for strength and stiffness requirements (Tastan et al. 2011; Oormila and Preethi 2014; Aldeeky and Al Hattamleh 2017; Yilmaz et al. 2019). In this study, 40% soil-fly ash and soil-slag mixtures were prepared for comparative purposes. Cement was implemented as an additive at the addition rates of 3% and 6%. Due to relatively lower self-cementing properties of Class C fly ash, cement and Class C fly ash were used together as a composite grout (Mahedi et al. 2019). All mixtures were prepared at optimum moisture content (w_0) to ensure adequate compaction and maximum dry density (γ_d). Then, the mixtures were cured for 7 days at 21°C temperature and 100% relative humidity room. After curing, mixtures were sieved through U.S. No. 10 sieve before being subjected to the leach tests. Furthermore, leach tests were also performed on fly ashes, steel slag, cement and soil alone. A summary of the mixtures is provided in Table 2.2 along with their corresponding w_0, γ_d and total metal contents of the blends.

2.4.2 SPLP Leach Test

Synthetic precipitation leaching procedure (SPLP) designated by U.S. EPA method 1312 was performed on soil, fly ashes, slag, cement, soil-fly ash-cement and soil-slag-cement blends to simulate the acid rain condition (Kosson et al. 2002). The extraction fluid was prepared with a mixture of reagent grade sulfuric and nitric acid (60%/40% by weight) and diluting the solution with nanopure water to a pH of 5±0.05. A constant liquid to solid (L/S) ratio of 20 was maintained for all the SPLP sample preparation. Samples were rotated end-to-end for 18±2 hours at a rotation rate of 28 rpm. The pH of the solutions was then measured, considering the equilibrium condition

was met. Finally, the samples were subjected to vacuum filtration using 0.7-μm borosilicate glass fiber filters. Filtered samples were acidified with 10% trace metal grade nitric acid (HNO_3) to a pH less than 2, and stored for further analysis in acid-washed 50 mL centrifuged tubes at temperature less than 4°C.

2.4.3   Batch Water Leach Test

Standard method designated by ASTM D3987 was followed for batch water leach test (WLT). Two basic modifications were done to the standard method. Firstly, samples were prepared with a liquid to solid (L/S) ratio of 10 to simulate the representative field condition. According to Kosson et al. (2002), L/S ratios higher than 10 could occurred in fields with relatively very high infiltration rates. Secondly, to provide stable reaction conditions, 0.02 M sodium chloride (NaCl) was used as the influent solution (Cetin et al. 2014). Samples were rotated end-over-end fashion at a rate of 29 rpm for 18±0.25 hours. Samples were then pressure filtered through 0.45-μm pore size and 25 mm diameter membrane disk filter papers using filter holders and 60 mL plastic syringes. Filtered samples were stored for further metal analysis following the same storage procedure described in SPLP method section.

2.4.4   TCLP Leach Test

To simulate the leaching behavior in landfill containment condition, toxicity characteristic leaching procedure (TCLP) designated by U.S. EPA method 1311 was implemented (Bestgen et al. 2016a). The extraction solution for the test was prepared by adding 5.7 mL glacial acetic acid (CH_3COOH) and 64.3 mL 1 N sodium hydroxide (NaOH) into nanopure water and diluting the solution to 1 liter. Properly prepared leachant always had the pH of 4.93±0.05. The leachate samples were prepared with a liquid to solid (L/S) ratio of 20. The agitation, filtration and storage procedure were the same for both TCLP and SPLP methods.

2.4.5   pH-Adjusted Leach Test

The effect of pH on the leaching behavior of metals was investigated by regulating the sample pH at acidic (pH $\cong$ 2), neutral (pH $\cong$ 7), and basic (pH $\cong$ 13) conditions, with tolerance of ± 0.5 unit. The U.S. EPA method 1313 defined in Leaching Environmental Assessment Framework (LEAF) was implemented. Samples were prepared at a constant liquid to solid ratio of 10, and the pH adjustments were performed by adding specific amount of 2 N trace metal grade nitric acid (HNO_3) or 1 N ACS grade potassium hydroxide (KOH) into nanopure water. The required amount of acid/base for a target pH condition was predetermined from the acid neutralizing capacity of the mixtures and is presented in Table 2.3. The samples were agitated for 48±2 hours at a rotation rate of 28 rpm to achieve stable pH conditions. Subsequently, pressure filtration through 0.2-μm pore size and 25 mm diameter membrane disk filter papers was applied following the common preservation method implemented in this study.

2.4.6   Total Metal Content

To determine the total metal content of the materials, acid digestions were performed following the U.S. EPA method 3050B. The digestion technique dissolves almost all the elements that could become environmentally available. A representative 1 g sample was digested with the repeated additions of concentrated trace metal grade nitric acid (HNO_3) and 30% hydrogen peroxide (H_2O_2). For complete digestion, heating at 95±5 °C temperature and refluxing were applied according to the standard. Concentrated hydrochloric acid (HCl) was also added to the nitric acid-peroxide digestate, heated and refluxed. Finally, the digestate was filtered through Whatman No. 41 filter paper. The residue and filter paper were washed with hot HCl and hot water subsequently, to increase the solubility of the metals. The filtrate was then stored in 100 mL volumetric flasks at temperature less than 4°C for further analysis.

2.4.7 Metal Analysis

Metal concentrations in the preserved samples were determined by utilizing inductively coupled plasma optical emission spectroscopy (ICP-OES). Commercially produced multi-element standard solutions were used to standardize the instrument with linear calibration curves. The calibration curves were verified by analyzing blanks and check standards of know concentrations at every 9 samples. The minimum detection limits (MDLs) of ICP-OES for Cr, Cu, Fe and S were 0.5 µg/L, 0.07 µg/L, 3.2 µg/L and 22 µg/L, respectively.

2.4.8 Geochemical Modeling

Based on the thermodynamic data, geochemical equilibrium models are capable of predicting the aqueous concentrations of elements, assuming an equilibrium between the effluent and solubility controlling minerals of the elements of potential concern (Allison et al. 1991). Therefore, the numerical model MINTEQA2 was used to identify the predominant oxidation states and speciation analysis of the metals. The geochemical equilibrium model MINTEQA2 was run in two steps. Initially, the speciation analyses were performed to identify the dominant oxidation states of the elements using their aqueous concentrations and effluent pH values. An equilibrium between the leachate and atmospheric carbon dioxide was assumed at 25 °C, since the sample preparation, collection and filtration processes were exposed to the atmosphere. The redox sensitive elements were specified, and the dominant oxidation states of the elements were estimated from the MINTEQA2 predicted aqueous concentrations of the species. In the second step, the log activities of all the element species in the solution and the saturation indices of the effluents with respect to the minerals were calculated by entering the elemental concentrations as per their oxidation states determined previously. An activity diagram for each of the elements was generated by plotting the MINTEQA2 calculated log activities of the elements against the laboratory measured effluent pH values. If the leaching of an element was controlled by the mineral

solubility, the activities of the element fell in close proximity to the solubility/stability line of the minerals (Garavaglia and Caramuscio 1994).

2.5   Results and Discussion

2.5.1   Effect of Cement Content on the Leaching Behavior

Figure 2.1 presents the influence of cement content on the leaching behavior of the elements, along with the effluent concentrations from cement only. As observed in Fig. 2.1, Cr and Cu concentrations increased with the increase in cement content. It is well known that Cr and Cu follow amphoteric leaching patterns where concentrations are minimum at neutral conditions but increase in both acidic and alkaline pH (Komonweeraket et al. 2015b). With the increase in cement content, the effluent pH increased in alkaline condition which eventually raised the leached concentrations of Cr and Cu. Moreover, aqueous concentrations of these elements were also higher for cement. In contrast, Fe concentrations decreased with the increase in cement content from 3% to 6%. Fe followed a cationic leaching pattern where concentrations decreased as the effluent pH increased with an increase in the cement dosage. Moreover, 100% cement leached a lower amount of Fe compared to soil-fly ash-cement and soil-slag-cement mixtures. S concentrations slightly increased with 3% cement incorporation but remained almost unchanged at 6% addition rates. 100% cement leached a higher amount of S, which may have occurred due to higher elemental concentrations of S in cement (Table 2.1).

2.5.2   Effect of Fly Ash and Slag Content on the Leaching Behavior

Leached concentrations of Cr, Cu, Fe and S from SPLP tests as a function of fly ash and slag content are presented in Fig. 2.2. As seen in Figs. 2.2a and 2.2b, leached Cr and Cu concentrations were higher for specimens mixed with fly ashes compared to slag mixtures. For the initial addition rates (10%), Cr and Cu concentrations increased noticeably, but remained within a narrow range at higher application dosages. It is anticipated that the pH of the solution played a

vital role on the leaching behavior of these metals. As seen in Table 2.4, except the initial addition rates, pH of the mixtures does not change significantly with the increase in fly ash and slag content, which is the most probable reason for the observed leaching behavior. However, the highest amounts of Cu leached from Class C fly ash, whereas leached Cr concentrations were lower compared to Class F fly ash blends. Based on the total metal analysis, Class C fly ash mixtures have the highest Cu content (Table 2.4) which may have induced higher leaching of Cu. Cr contents in Class C and F fly ash are comparable (Table 2.1, 70 mg/kg and 69.3 mg/kg, respectively), yet Class F fly ash blends may have leached higher amounts of Cr due to its lower CaO content (12%) compared to Class C fly ash (26%). Higher CaO content of Class C fly ash released higher Ca^{2+} into the solution which could have complexed with Cr and precipitated as insoluble $Ca\text{-}Cr^{3+}$ complexes at alkaline conditions (Cornelis et al. 2008). Thus, Cr leaching was reduced from Class C fly ash mixtures.

Leached Fe concentrations fluctuated with fly ash and slag content (Fig. 2.2c). Varying degree of hydration of the mixture may have caused the erratic nature of Fe leaching. According to Goswami and Mahanta (2007), degree of pozzolanic activity largely influences the leaching behavior of Fe. Furthermore, 100% Class C fly ash leached lower amount of Fe compared to the cement activated Class C fly ash treated mixtures, whereas the observed behavior is opposite for Class F fly ash and slag blends.

Sulfur concentrations initially increased with the addition of fly ash and slag content (Fig. 2.2d). After the initial increase, no significant change in concentrations was observed for Class C fly ash mixtures, whereas concentrations kept increasing with the increase in Class F fly ash content. Fruchter et al. (1990) claimed that sulfur mostly exists as sulfate (SO_4^{2-}) in fly ashes, especially in oxidizing conditions. At higher pH, at the presence of free lime, sulfate precipitates

as insoluble ettringite and reduces the solution concentrations (Hassett et al. 2005). Small variations in pH of Class C mixtures, and lower Ca content of Class F fly ash possibly influenced the leaching behavior of sulfur. For slag mixtures, S concentrations fluctuated within a narrow range (18.2-23.6 mg/L), indicating lesser influence of pH and application dosage on the leaching of sulfur from soils mixed with slag and cement.

2.5.3   Comparisons between SPLP, WLT and TCLP

An attempt was made to compare the leachability of the elements in different test methods, representing varying environmental conditions. As depicted in Fig. 2.3, leached Cr and Cu concentrations from cement activated fly ash and slag treated soils were the highest in TCLP effluent, whereas the lowest concentrations were observed in SPLP extracts. WLT concentrations were intermediate, falling between TCLP and SPLP concentrations. Among three different test methods, TCLP extraction fluid was the most acidic (pH = 4.93±0.05), which had increased the degradation of the blends and hence, the solubility of the elements (Bestgen et al. 2016a). WLT effluent solutions contained a significant amount of dissolved Cl- ions since the extraction fluid was prepared with 0.02 M NaCl. Mobile metal-Cl- complexes in the WLT effluents are thought to be the main reason for higher Cr and Cu concentrations in WLT compared to SPLP (Engelsen et al. 2012). Sulfur also showed a similar leaching behavior, with higher concentrations in TCLP extract and comparable leachability in SPLP and WLT solutions (Figs. 2.4a-c). As seen in Figs. 2.4d-e, with few exceptions, the highest concentrations of Fe were associated with WLT which was followed by the SPLP and TCLP concentrations ($Fe_{WLT} > Fe_{SPLP} > Fe_{TCLP}$). Bestgen et al. (2016b) reported an increase in Fe concentrations at pH higher than 12, which may have induced by the hydrolysis of Fe^{3+} in the form of $Fe(OH)^{4-}$ (Allanore et al. 2007). The effluent pH of the mixtures in SPLP and WLT were in the range of 11.82-12.14, whereas the pH for TCLP solutions

was between 7.92 and 11.41 (Table 2.4). Therefore, formation of Fe(OH)$^{4-}$ was less likely in TCLP effluent which probably yielded lower Fe concentrations.

2.5.4 Influence of Total Metal Content

Fly ashes and slag contained higher amounts of metals, but as indicated in Fig. 2.5, regardless of the test methodology, higher elemental concentrations do not necessarily induce higher leaching of metals. Figure 2.5 illustrates the leaching of Cr, Cu, Fe and S in SPLP, WLT and TCLP solutions along with the total metal contents of the mixtures. As seen in Figs. 2.5a-c, total metal contents did not influence the effluent concentrations of Cr, Cu and Fe. Sulfur concentrations tend to increase with the increase in total metal content (Fig. 2.5d), indicating a direct effect of source additions on the leaching behavior of sulfur. Iwashita et al. (2005) also claimed that, the leaching of S is correlated to its total concentration in fly ash.

2.5.5 pH Conditions and the Leaching of Elements

Figures 2.6 and 2.7 show the leaching of Cr, Cu, Fe and S from soil, cement, fly ashes, slag, and cement activated soil-fly ash and soil-slag mixtures at three different pH conditions (acidic, neutral and basic). Leached concentrations of Cr, Cu, Fe and S were highest in acidic conditions. Cr and Cu concentrations decreased monotonically in both neutral and alkaline conditions (Fig. 2.6). Fe concentrations decreased rapidly at neutral pH and remained low throughout the basic conditions (Fig. 2.7). Sulfur concentrations did not differ much in acidic and neutral conditions, though a subsequent decrease in concentrations was observed in an alkaline environment. Under an acidic environment, dissolution of metal bearing minerals such as Eskolaite (Cr$_2$O$_3$), Tenorite (CuO), Hematite (Fe$_2$O$_3$), gypsum (CaSO$_4\cdot$2H$_2$O), anhydrite (CaSO$_4$) and ettringite (Ca$_6$Al$_2$(SO$_4$)$_3$(OH)$_{12}\cdot$26H$_2$O) increased the release of the elements into the aqueous solutions (Komonweeraket et al. 2015b). As the pH increased, concentrations of elements decreased due to the precipitation and/or adsorption of the ions (Mizutani et al. 1996).

However, at acidic conditions, Class F fly ash mixtures leached the highest Cr concentrations (Figs. 2.6a-c) whereas, Cu and Fe leaching were the highest for the Class C fly ash blends (Figs. 2.6d-f and 2.6a-c). Similar leaching behaviors were also observed in neutral conditions with a few exceptions in Cu and Fe concentrations (20% and 40% slag blends). Mass of elements in the mixtures played an important role on the leaching concentrations at these pH conditions. From the elemental analyses, the highest concentrations of Cu and Fe were detected in the Class C fly ash, while Cr concentrations were the highest in the Class F fly ash (Table 2.1). 20% and 40% slag treated blends had the lowest pH (Table 2.4) among all of the samples prepared in neutral conditions. This is the most probable reason for higher Cu and Fe leaching from these blends at neutral conditions. In contrast, the highest concentrations of Cr, Cu and Fe in alkaline conditions occurred in the leachate of Class F fly ash blends. Under alkaline conditions, Ca^{2+} precipitates as calcite ($CaCO_3$) and/or aragonite ($CaCO_3$) which work as an effective absorbent of the metals of interest (Ahmad et al. 2012; Komonweeraket et al. 2015c, a). Lower CaO content of Class F fly ash reduced the formation and precipitation of $CaCO_3$. Therefore, higher amounts of Cr, Cu and Fe cations remained in the effluent of Class F fly ash mixtures. However, slag mixtures showed the highest leaching of sulfur in all of the environmental conditions (Figs. 2.7d-f), indicating that ettringite formation was less likely to occur in slag blends (Zhang et al. 2016).

Depending on the pH conditions, 100% cement showed less variation in Cr, Cu and S concentrations. Additionally, at neutral and basic pH, cement leached the highest amount of Cr, Cu, and S. Cement had the highest pH buffering capacity among all of the materials used in this study. This required larger amounts of acid or base additions to the solution for the pH adjustment. Higher amount of acid or base may have degraded the cement paste vigorously and increased the effluent metal concentrations. However, leached Fe concentrations from cement decreased

gradually toward neutral and alkaline environments. 100% slag leached higher Fe concentrations at these pH conditions, yet Fe concentrations from cement were higher compared to those leached from fly ashes. Relatively lower pH of slag yielded higher Fe concentrations in these pH conditions.

From the aforementioned observations, it is evident that pH played the most vital role on the leaching behavior of the elements from cement activated fly ash and slag stabilized soils. Therefore, aqueous concentrations of the elements from all of the leach tests (SPLP, WLT, TCLP and pH controlled) are plotted against their corresponding pH values in Fig. 2.8. Table 2.4 tabulates the pH values of the blends in different test methods, and pH conditions. However, as indicated in Figs. 2.8a and 2.8b, the amphoteric leaching patterns of Cr and Cu were observed, where concentrations increase in both acidic and alkaline conditions. Minimum concentrations of Cr and Cu were associated with the pH ranges of 10.5-11. Similar amphoteric leaching patterns of Cr and Cu were also reported by the previous studies (Komonweeraket et al. 2015b; Bestgen et al. 2016a, b; Li et al. 2018). Dissolution and precipitation of oxide and hydroxide minerals greatly influenced the solubility of these amphoteric leaching elements (Komonweeraket et al. 2011). However, in the most cases, Cr concentrations exceeded the maximum contaminant level (MCL) of 0.1 mg/L specified by the U.S. EPA for drinking water. Excluding extreme acidic conditions (pH $\leq$ 2), Cu concentrations were lower than the U.S. EPA specified MCL of 1.3 mg/L.

As depicted in Figs. 2.8c and 2.8d, Fe and S showed cationic leaching patterns, where concentrations decreased with the increase in pH. A sharp drop in Fe concentrations was observed in the pH range of 6-7, whereas S concentrations decreased dramatically at pH higher than 10. With the increase in pH towards the neutral conditions, Fe precipitates as the amorphous oxy-hydroxide and subsequently reduces the aqueous concentrations (Warren and Dudas 1989). Sulfur

concentrations may have also been reduced due to the precipitation of ettringite at pH higher than 10.7 (Gabrisová et al. 1991). Except for the acidic pH, Fe and S (as SO_4) concentrations were lower than the U.S. EPA specified MCLs of 0.3 and 250 mg/L, respectively.

2.6   Geochemical Modeling

Numerical model MINTEQA2 was implemented to determine the predominant oxidation states and leaching controlling mechanisms of the elements from cement activated fly ash and slag amended soils. Two main equilibrium mechanisms, solubility and sorption control the leaching of elements from industrial by-products such as fly ash and steel slag (Fruchter et al. 1990; Mudd et al. 2004). In the cases where solubility controls the leaching of elements, based on thermodynamic data, geochemical equilibria models are found to be successful in predicting aqueous concentration of the elements (Komonweeraket et al. 2015b; Bestgen et al. 2016a). Therefore, leached metals concentrations from all the leach tests and the corresponding solution pH were used as input for the MINTEQA2 program. Saturation indices and activity of the elements were calculated along with the identification of leaching controlling minerals of the elements of interest. The analyses indicated that the dominant oxidation states of Cr, Cu, Fe and S were Cr^{3+}, Cu^{2+}, Fe^{3+} and S^{6+}, respectively. The leached Cr concentrations in this study largely exceeded the EPA specified MCL of 0.1 mg/L. Nonetheless, speciation revealed that the majority of the Cr was in the form of trivalent Cr (III), which was a much less concern to human health than the Cr (VI) (Izquierdo et al. 2011; Izquierdo and Querol 2012). According to Huggins et al. (1999), Cr^{6+} could easily reduce by SO_2 in furnace flue gas, and therefore Cr^{3+} may become the dominant one in the fly ash leachates.

Despite of different stabilizer types and addition rates, similarities in leaching behavior and leaching controlling mechanisms were observed. As indicated in Fig. 2.9a, the leaching of Cr^{3+} is solubility controlled in the pH range of 7 to 13. Amorphous $Cr(OH)_3$ and eskolaite (Cr_2O_3) have

comparable solubility and are identified as the controlling hydroxide and oxide minerals for the leaching of Cr^{3+}. Previous studies also reported that leaching of Cr^{3+} is controlled by amorphous and crystalline $Cr(OH)_3$ (Reardon et al. 1995; Komonweeraket et al. 2015b). Presence of Cr_2O_3 also promotes the formation of aqueous chromium hydroxides (Komonweeraket et al. 2015b).

Tenorite (CuO) and $Cu(OH)_2$ were recognized as the potential solids, controlling the leaching of Cu at pH higher than 10 (Fig. 2.9b) while $CuCO_3$ and $Cu(OH)_2$ likely controlled the solubility of Cu at pH between 7 and 10. Fruchter et al. (1990) concluded that tenorite is the most probable solubility controlling phase for Cu^{2+} leaching among other Cu minerals commonly present in near surface geological conditions. However, undersaturation of Cu was observed at higher pH indicating the effect of adsorption mechanisms (Theis and Wirth 1977). Additionally, at acidic pH conditions, Cu^{2+} leaching was found to be adsorption controlled.

Geochemical modeling indicates that, leached Fe^{3+} concentrations were mostly controlled by the Fe-hydroxides such as ferrihydrite ($Fe(OH)_3$) and goethite (α-FeO(OH)) (Fig. 2.9c). Garavaglia and Caramuscio (1994) reported that leaching of Fe3+ from fly ashes is controlled by ferrihydrite. Hematite (Fe_2O_3), a primary mineral of iron in fly ash was also predicted by MINTEQA2. According to Rai (1987) the leaching of Fe^{3+} in long term and short-term leaching experiments is controlled by the dissolution and precipitation of both Fe oxide and hydroxide minerals. Patel and Devatha (2019) who studied biomedical ash for iron also identified ferrihydrite, goethite and hematite as the solubility controlling minerals for Fe. Oversaturation of Fe3+ was observed which could be due to smaller crystal sizes of iron minerals, resulting in an increase in the solubility product constant (K_{sp}). The K_{sp} of the iron minerals could increase by several orders of magnitude due to decreasing crystal size (Schwertmann 1991). Komonweeraket et al. (2015b) also reported the oversaturation of Fe3+ in the pH range of 5 to 12 from soil-fly ash mixtures.

Additionally, as seen from the Fig. 2.9d, SO_4^{2-} ion activities were controlled by both gypsum ($CaSO_4 \cdot 2H_2O$) and anhydrite ($CaSO_4$). It is well known that fly ashes and slag are rich in gypsum and anhydrite, and hence leach sulfate in considerable amounts (Zhang et al. 2016). After investigating the leaching of sulfate from recycled concrete aggregate, Abbaspour et al. (2016) also concluded that leaching of SO_4^{2-} is controlled by gypsum rather than the ettringite. However, oversaturation with respect to gypsum and anhydrite was observed in a few cases (typically for slag blends), where epsomite ($MgSO_4 \cdot 7H_2O$) might have controlled the solubility of sulfate.

2.7   Conclusions

A series of SPLP, WLT and TCLP tests were conducted to explore the leaching behavior of Cr, Cu, Fe and S from Type I/II cement activated Class C fly ash, Class F fly ash and slag stabilized Iowa loess soil. The leaching potential of the elements at acidic, neutral and basic conditions were also evaluated. Leaching controlling mechanisms were studied by implementing the geochemical modeling program MINTEQA2. Some of the salient findings of this study are summarized below:

- An increase in cement content increased the leached concentrations of Cr, Cu and S, while the Fe concentrations decreased with the increase in cement content.

- Aqueous concentrations of the elements increased when the fly ash or slag content was increased from 0 to 10%. Further increases in addition rates did not influence the leaching of elements significantly.

- Cr, Cu and S concentrations were the highest in TCLP, intermediate in WLT and the lowest in SPLP effluents. Comparable leachability of S was observed in WLT and SPLP solutions. The highest concentrations of Fe were observed in WLT and were the lowest in TCLP leachates.

- Regardless the test type, additions of metal sources did not impact the leachate concentrations of metals from cement activated soil-fly ash and soil-slag mixtures. However, sulfur concentrations tended to increase with the increase in total metal content in materials.

- Leached concentrations of Cr, Cu, Fe and S were the highest in acidic conditions. Cr and Cu concentrations gradually decreased in both neutral and basic pH. Fe concentrations dropped sharply in neutral pH and remained low throughout the basic conditions. Small variations in S concentrations were observed in both acidic and neutral pH but decreased rapidly in basic environments.

- pH played an important role on the leaching behavior of the elements. Cr and Cu showed amphoteric leaching behaviors, whereas Fe and S followed cationic leaching patterns.

- The dominant oxidation states of Cr, Cu, Fe and S were determined as Cr^{3+}, Cu^{2+}, Fe^{3+} and S^{6+} (as SO_4^{2-}), respectively. Under natural pH conditions, Cr concentrations exceeded the EPA specified MCL for drinking water. However, previous studies identified trivalent Cr (III) to be less detrimental compared to Cr (VI) for human health.

- Despite of the differences in fly ashes, slag, cement and soil compositions, similarities in leaching behavior of elements were observed during geochemical modelling analyses. Resemblances were mostly due to the similar leaching regulatory factors and controlling mechanisms.

- Dissolution and precipitation of oxide and hydroxide minerals were identified as the major leaching controlling mechanism of the elements. Amorphous $Cr(OH)_3$ and eskolaite; tenorite and $Cu(OH)_2$; ferrihydrite, goethite and hematite; gypsum and

anhydrite; were determined to be the primary minerals controlling the leaching of Cr, Cu, Fe and S, respectively.

- The leaching of the elements from cement activated fly ash and slag treated soils were effected by both cement and fly ash/slag addition rates. Presence of cement as an activator influenced the material pH, and hence, the leaching characteristics of the elements. Though the effluent concentrations of Cr exceeded the EPA specified MCL, the use of fly ash and slag with cement in soil stabilization could be environmentally safe, since the Cr was found to be in Cr(III) oxidation state which is nontoxic.

2.8   References

Abbaspour A, Tanyu BF, Cetin B (2016) Impact of aging on leaching characteristics of recycled concrete aggregate. Environ Sci Pollut Res 23:20835–20852. doi: 10.1007/s11356-016-7217-9

Ahmad K, Bhatti IA, Muneer M, et al (2012) Removal of heavy metals (Zn, Cr, Pb, Cd, Cu and Fe) in aqueous media by calcium carbonate as an adsorbent. Int J Chem Biochem Sci 2:48–53

Aldeeky H, Al Hattamleh O (2017) Experimental study on the utilization of fine steel slag on stabilizing high plastic subgrade soil. Adv Civ Eng 2017:1–11. doi: 10.1155/2017/9230279

Allanore A, Lavelaine H, Valentin G, et al (2007) Electrodeposition of metal iron from dissolved species in alkaline media. J Electrochem Soc 154:E187. doi: 10.1149/1.2790285

Allison JD, Brown DS, Novo-Gradac KJ (1991) MINTEQA2/PRODEFA2, A geochemical assessment model for environmental systems: Version 3.0 User's Manual. Environmental Research Laboratory, Office of Research and Development, US Environmental Protection Agency, Athens, Georgia

Bestgen JO, Cetin B, Tanyu BF (2016a) Effects of extraction methods and factors on leaching of metals from recycled concrete aggregates. Environ Sci Pollut Res 23:12983–13002. doi: 10.1007/s11356-016-6456-0

Bestgen JO, Hatipoglu M, Cetin B, Aydilek AH (2016b) Mechanical and environmental suitability of recycled concrete aggregate as a highway base material. J Mater Civ Eng 28:04016067. doi: 10.1061/(ASCE)MT.1943-5533.0001564

Cetin B, Aydilek AH, Guney Y (2010) Stabilization of recycled base materials with high carbon fly ash. Resour Conserv Recycl 54:878–892. doi: 10.1016/J.RESCONREC.2010.01.007

Cetin B, Aydilek AH, Guney Y (2012a) Leaching of trace metals from high carbon fly ash stabilized highway base layers. Resour Conserv Recycl 58:8–17. doi:

10.1016/J.RESCONREC.2011.10.004

Cetin B, Aydilek AH, Li L (2014) Trace metal leaching from embankment soils amended with high-carbon fly ash. J Geotech Geoenvironmental Eng 140:1–13. doi: 10.1061/(ASCE)GT.1943-5606.0000996

Cetin B, Aydilek AH, Li L (2012b) Experimental and numerical analysis of metal leaching from fly ash-amended highway bases. Waste Manag 32:965–978. doi: 10.1016/J.WASMAN.2011.12.012

Cornelis G, Johnson CA, Gerven T Van, Vandecasteele C (2008) Leaching mechanisms of oxyanionic metalloid and metal species in alkaline solid wastes: A review. Appl Geochemistry 23:955–976. doi: 10.1016/J.APGEOCHEM.2008.02.001

Dayioglu AY, Aydilek AH, Cetin B (2014) Preventing swelling and decreasing alkalinity of steel slags used in highway infrastructures. Transp Res Rec J Transp Res Board 2401:52–57. doi: 10.3141/2401-06

Dayioglu AY, Aydilek AH, Cimen O, Cimen M (2018) Trace metal leaching from steel slag used in structural fills. J Geotech Geoenvironmental Eng 144:04018089. doi: 10.1061/(ASCE)GT.1943-5606.0001980

Engelsen CJ, Wibetoe G, van der Sloot HA, et al (2012) Field site leaching from recycled concrete aggregates applied as sub-base material in road construction. Sci Total Environ 427–428:86–97. doi: 10.1016/J.SCITOTENV.2012.04.021

Engström F, Adolfsson D, Samuelsson C, et al (2013) A study of the solubility of pure slag minerals. Miner Eng 41:46–52. doi: 10.1016/j.mineng.2012.10.004

Fruchter JS, Rai D, Zachara JM (1990) Identification of solubility-controlling solid phases in a large fly ash field lysimeter. Environ Sci Technol 24:1173–1179. doi: 10.1021/es00078a004

Gabrisová A, Havlica J, Sahu S (1991) Stability of calcium sulphoaluminate hydrates in water solutions with various pH values. Cem Concr Res 21:1023–1027. doi: 10.1016/0008-8846(91)90062-M

Garavaglia R, Caramuscio P (1994) Coal fly-ash leaching behaviour and solubility controlling solids. Stud Environ Sci 60:87–102. doi: 10.1016/S0166-1116(08)71450-X

Gomes JFP, Pinto CG (2006) Leaching of heavy metals from steelmaking slags. Rev Metal 42:409–416. doi: 10.3989/revmetalm.2006.v42.i6.39

Goswami RK, Mahanta C (2007) Leaching characteristics of residual lateritic soils stabilised with fly ash and lime for geotechnical applications. Waste Manag 27:466–481. doi: 10.1016/J.WASMAN.2006.07.006

Hassett DJ, Pflughoeft-Hassett DF, Heebink L V. (2005) Leaching of CCBs: Observations from over 25 years of research. In: Hower JC (ed) Fuel. Elsevier, pp 1378–1383

Huggins FE, Najih M, Huffman GP (1999) Direct speciation of chromium in coal combustion by-products by X-ray absorption fine-structure spectroscopy. Fuel 78:233–242. doi: 10.1016/S0016-2361(98)00142-2

Iwashita A, Sakaguchi Y, Nakajima T, et al (2005) Leaching characteristics of boron and selenium for various coal fly ashes. Fuel 84:479–485. doi: 10.1016/J.FUEL.2004.11.002

Izquierdo M, Koukouzas N, Touliou S, et al (2011) Geochemical controls on leaching of lignite-fired combustion by-products from Greece. Appl Geochemistry 26:1599–1606. doi: 10.1016/j.apgeochem.2011.04.013

Izquierdo M, Querol X (2012) Leaching behaviour of elements from coal combustion fly ash: An overview. Int J Coal Geol 94:54–66. doi: 10.1016/J.COAL.2011.10.006

Jones DR (1995) The Leaching of major and trace elements from coal ash. In: Environmental Aspects of Trace Elements in Coal. Springer, Dordrecht, Netherlands, pp 221–262

Komonweeraket K, Benson CH, Edil TB, Bleam WF (2011) Leaching behavior and mechanisms controlling the release of elements from soil stabilized with fly ash. In: Geo-Frontiers 2011. American Society of Civil Engineers, Reston, VA, pp 1101–1110

Komonweeraket K, Cetin B, Aydilek A, et al (2015a) Geochemical analysis of leached elements from fly ash stabilized soils. J Geotech Geoenvironmental Eng 141:04015012. doi: 10.1061/(ASCE)GT.1943-5606.0001288

Komonweeraket K, Cetin B, Aydilek AH, et al (2015b) Effects of pH on the leaching mechanisms of elements from fly ash mixed soils. Fuel 140:788–802. doi: 10.1016/J.FUEL.2014.09.068

Komonweeraket K, Cetin B, Benson CH, et al (2015c) Leaching characteristics of toxic constituents from coal fly ash mixed soils under the influence of pH. Waste Manag 38:174–184. doi: 10.1016/J.WASMAN.2014.11.018

Kosson DS, van der Sloot HA, Sanchez F, Garrabrants AC (2002) An integrated framework for evaluating leaching in waste management and utilization of secondary materials. Environ Eng Sci 19:159–204. doi: 10.1089/109287502760079188

Li J, Zeng M, Ji W (2018) Characteristics of the cement-solidified municipal solid waste incineration fly ash. Environ Sci Pollut Res 25:36736–36744. doi: 10.1007/s11356-018-3600-z

Mahedi M, Cetin B, Cetin KS (2019) Freeze-thaw performance of phase change material (PCM) incorporated pavement subgrade soil. Constr Build Mater 202:449–464. doi: 10.1016/J.CONBUILDMAT.2018.12.210

Mahedi M, Cetin B, White DJ (2018) Performance evaluation of cement and slag stabilized expansive soils. Transp Res Rec J Transp Res Board 036119811875743. doi: 10.1177/0361198118757439

Mizutani S, Yoshida T, Sakai S, Takatsuki H (1996) Release of metals from MSW I fly ash and availability in alkali condition. Waste Manag 16:537–544. doi: 10.1016/S0956-053X(96)00095-5

Mudd GM, Weaver TR, Kodikara J (2004) Environmental geochemistry of leachate from leached brown coal ash. J Environ Eng 130:1514–1526. doi: 10.1061/(ASCE)0733-9372(2004)130:12(1514)

Oormila T., Preethi TV (2014) Effect of stabilization using flyash and GGBS in soil characteristics. Int J Eng Trends Technol 11:284–289. doi: 10.14445/22315381/IJETT-V11P254

Patel KM, Devatha CP (2019) Investigation on leaching behaviour of toxic metals from biomedical ash and its controlling mechanism. Environ Sci Pollut Res 1–8. doi: 10.1007/s11356-018-3953-3

Qureshi A, Maurice C, Öhlander B (2018) Effects of the co-disposal of lignite fly ash and coal mine waste rocks on AMD and leachate quality. Environ Sci Pollut Res 1–12. doi: 10.1007/s11356-018-3896-8

Rai D (1987) Inorganic and organic constituents in fossil fuel combustion residues: Volume 2, An annotated bibliography. Pacific Northwest Lab., Richland, WA (USA); Electric Power Research Inst., Palo Alto, CA (USA)

Reardon EJ, Czank CA, Warren CJ, et al (1995) Determining controls on element concentrations in fly ash leachate. Waste Manag Res 13:435–450. doi: 10.1016/S0734-242X(05)80023-0

Schwertmann U (1991) Solubility and dissolution of iron oxides. Plant Soil 130:1–25. doi: 10.1007/BF00011851

Senapati MR (2011) Fly ash from thermal power plants – waste management and overview. Curr Sci 100:1791–1794. doi: 10.2307/24077549

Shi C (2004) Steel Slag—its production, processing, characteristics, and cementitious properties. J Mater Civ Eng 16:230–236. doi: 10.1061/(ASCE)0899-1561(2004)16:3(230)

Spanka M, Mansfeldt T, Bialucha R (2018) Sequential extraction of chromium, molybdenum, and vanadium in basic oxygen furnace slags. Environ Sci Pollut Res 25:23082–23090. doi: 10.1007/s11356-018-2361-z

Tastan EO, Edil TB, Benson CH, Aydilek AH (2011) Stabilization of organic soils with fly ash. J Geotech Geoenvironmental Eng 137:819–833. doi: 10.1061/(ASCE)GT.1943-5606.0000502

Theis TL, Wirth JL (1977) Sorptive behavior of trace metals on fly ash in aqueous systems. Environ Sci Technol 11:1096–1100. doi: 10.1021/es60135a006

Thomas M (2007) Optimizing the use of fly ash in concrete. Skokie, Ill Portl Cem Assoc 24. doi: 10.15680/IJIRSET.2015.0409047

Warren CJ, Dudas MJ (1989) Leachability and partitioning of elements in ferromagnetic fly ash particles. Sci Total Environ 84:223–236. doi: 10.1016/0048-9697(89)90385-9

Yilmaz Y, Coban HS, Cetin B, Edil TB (2019) Use of standard and off-spec fly ashes for soil stabilization. J Mater Civ Eng 31:04018390. doi: 10.1061/(ASCE)MT.1943-5533.0002599

Zhang Y, Cetin B, Likos WJ, Edil TB (2016) Impacts of pH on leaching potential of elements from MSW incineration fly ash. Fuel 184:815–825. doi: 10.1016/J.FUEL.2016.07.089

2.9 Tables and Figures

Table 2.1 Chemical composition and total metal content of the materials

Chemical Composition[*]	C FA	F FA	Cement	Slag	Soil
CaO (%)	25.9	11.8	64	39.8	5.2
SiO_2 (%)	37.6	56.3	20	35.7	67.7
Al_2O_3 (%)	18	18.6	4.4	9.9	9.6
Fe_2O_3 (%)	5.9	5.5	3	0.6	3.3
$SiO_2 + Al_2O_3 + Fe_2O_3$ (%)	61.5	80.4	27.4	46.2	80.6
Loss on Ignition, LOI (%)	0.24	0.14	2.45	N/A	6.91
Moisture Content (%)	0.05	0.03	N/A	0.07	1.34
SO_3, max %	1.2	0.4	2.9	1.1	0.03
Classification	Class C[a]	Class F[a]	Type I/II[b]	-	ML[c], A-4[d]
Total Metal Analysis (mg/kg) [**]					
Chromium (Cr)	70.3	69.3	35	35.3	29.6
Copper (Cu)	148.1	63.7	27	19.8	17.7
Iron (Fe)	34348	21686	10476	2289	13370
Sulfur (S)	9103	3176	18200	12600	916

Note: [*]X-ray fluorescence spectrometry (XRF); FA: Fly ash; N/A: Not available; [a]ASTM C618; [b]ASTM C150/C150M; Hyphen: not applicable; [c]ASTM D2487; [d]AASHTO classification; [**]U.S. EPA Method 3050B

Table 2.2 Composition of the mixtures along with optimum moisture content, maximum dry density and elemental concentrations

Sample Name	FA or Slag Content (%)	Cement Content (%)	Optimum moisture, w_o (%)	Max. Dry density, γ_d (kN/m³)	Cr (mg/kg)	Cu (mg/kg)	Fe (mg/kg)	S (mg/kg)
Loess Soil	0	0	16.2	16.7	29.63	17.66	13370	916
10CFA3PC	10	3	18.8	16.6	33.35	29.49	15150	2100
10CFA6PC	10	6	17	16.6	33.38	29.42	15029	2516
20CFA6PC	20	6	14.5	17	36.32	38.84	16562	3039
40CFA6PC	40	6	14	16.7	40.97	53.81	18999	3870
10FFA3PC	10	3	17.5	16.5	33.26	22.02	14029	1575
10FFA6PC	10	6	18	16.6	33.3	22.15	13937	2005
20FFA6PC	20	6	17	16.8	36.16	25.44	14552	2098
40FFA6PC	40	6	15.2	17	40.7	30.68	15529	2246
10BFS3PC	10	3	18.5	16.3	30.25	18.13	12313	2409
10BFS6PC	10	6	18	16.6	30.37	18.36	12265	2818
20BFS6PC	20	6	17	16.7	30.76	18.48	11473	3594
40BFS6PC	40	6	18.7	16.8	31.38	18.66	10215	4828

Note: FA: Fly ash; CFA: Class C fly ash; FFA: Class F fly ash; BFS: Blast-furnace steel slag; PC: Type I/II Portland cement; 10CFA3PC: 10% Class C fly ash + 3% Type I/II Portland cement blend

Table 2.3 Required amount of acid/base added for a target pH in pH-dependent leach tests for cement activated fly ash and slag treated mixtures

Mixture ID	Target pH 2		Target pH 7		Target pH 13	
	Acid Added[*] (meq/g)	Final pH	Acid Added[*] (meq/g)	Final pH	Base Added[*] (meq/g)	Final pH
Loess Soil	3.07	1.91	0.19	7.37	-1.32	13.08
C FA	18.96	2.01	6	6.87	-1.06	12.93
F FA	7.49	1.83	0.92	6.83	-1.26	12.99
Slag	20	3.2	13.65	6.74	-1.32	13.11
Cement	20	4.51	19.11	7.49	-1.11	13.11
10CFA3PC	4.9	1.79	1.4	6.96	-1.06	12.99
10CFA6PC	5.57	1.69	1.44	8.02	-1.28	12.99
20CFA6PC	6.62	1.8	1.97	7.23	-1.26	13
40CFA6PC	8.5	1.71	2.29	7.22	-1.13	12.98
10FFA3PC	3.83	1.77	0.64	6.82	-1.39	13.04
10FFA6PC	4.42	1.87	1.5	7.06	-1.13	12.98
20FFA6PC	4.73	1.81	1.51	6.9	-1.49	13.06
40FFA6PC	5	2.17	1.33	7.1	-1.25	13
10BFS3PC	5.59	1.53	2.08	6.94	-1.41	13.12
10BFS6PC	5.73	2.69	2.46	6.98	-1.38	13.1
20BFS6PC	9.36	1.67	3.34	6.73	-1.17	13.03
40BFS6PC	10.15	2.19	4.01	6.83	-1.14	13.03

Note: [*]Dry weight basis; FA: Fly ash; CFA: Class C fly ash; FFA: Class F fly ash; BFS: Blast-furnace steel slag; PC: Type I/II Portland cement; 10CFA3PC: 10% Class C fly ash + 3% Type I/II Portland cement blend

Table 2.4 pH of the cement activated soil-fly ash and soil-slag mixtures in different test methods and pH conditions

Mixture ID	pH					
	WLT	TCLP	SPLP	Acidic Condition	Neutral Condition	Basic Condition
Loess Soil	8.57	6.46	9.3	1.91	7.37	13.08
C FA	12	11.41	11.92	2.01	6.87	12.93
F FA	11.64	6.69	11.71	1.83	6.83	12.99
Slag	11.6	9.93	11.68	3.2	6.74	13.11
Cement	12.39	12.6	12.51	4.51	7.49	13.11
10CFA3PC	11.79	8.88	11.82	1.79	6.96	12.99
10CFA6PC	11.92	10.62	12.02	1.69	8.02	12.99
20CFA6PC	11.95	11.16	12.01	1.8	7.23	13
40CFA6PC	11.97	11.21	12.03	1.71	7.22	12.98
10FFA3PC	11.75	7.92	11.78	1.77	6.83	13.04
10FFA6PC	11.98	9.08	12.08	1.87	7.06	12.98
20FFA6PC	11.98	10.65	12.08	1.81	6.9	13.06
40FFA6PC	12.01	10.34	12.02	2.17	7.1	13
10BFS3PC	11.83	9.88	11.94	1.53	6.94	13.12
10BFS6PC	12.01	11.18	12.11	2.69	6.98	13.1
20BFS6PC	12.02	11.31	12.11	1.67	6.73	13.03
40BFS6PC	12.03	11.41	12.14	2.19	6.83	13.03

Note: FA: Fly ash; CFA: Class C fly ash; FFA: Class F fly ash; BFS: Blast-furnace steel slag; PC: Type I/II Portland cement; 10CFA3PC: 10% Class C fly ash + 3% Type I/II Portland cement blend
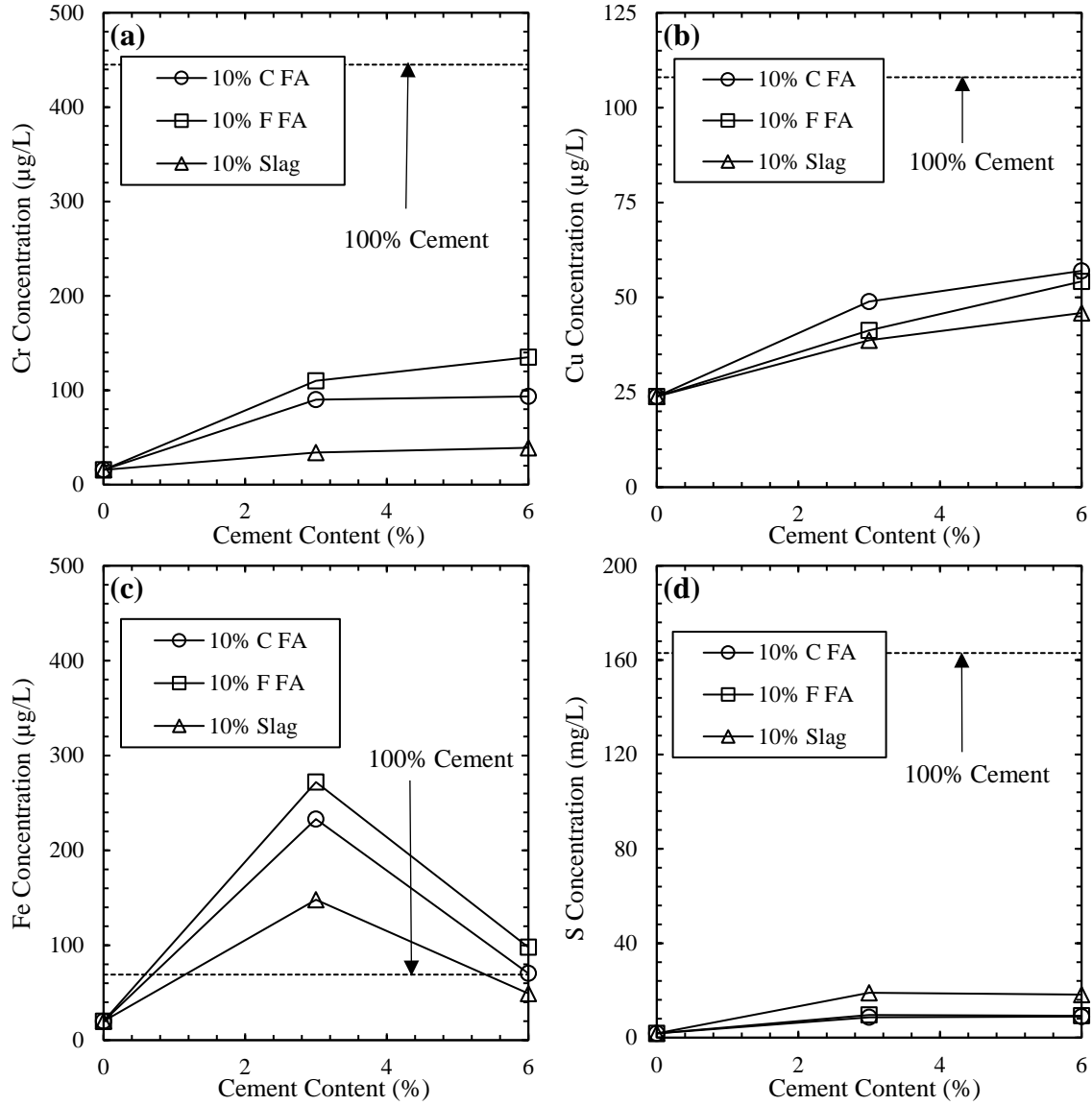
Figure 2.1 Effect of cement content on the leached concentrations of (a) Cr, (b) Cu, (c) Fe, and (d) S in SPLP effluent. *Note:* 0% corresponds to soil only; FA: Fly ash
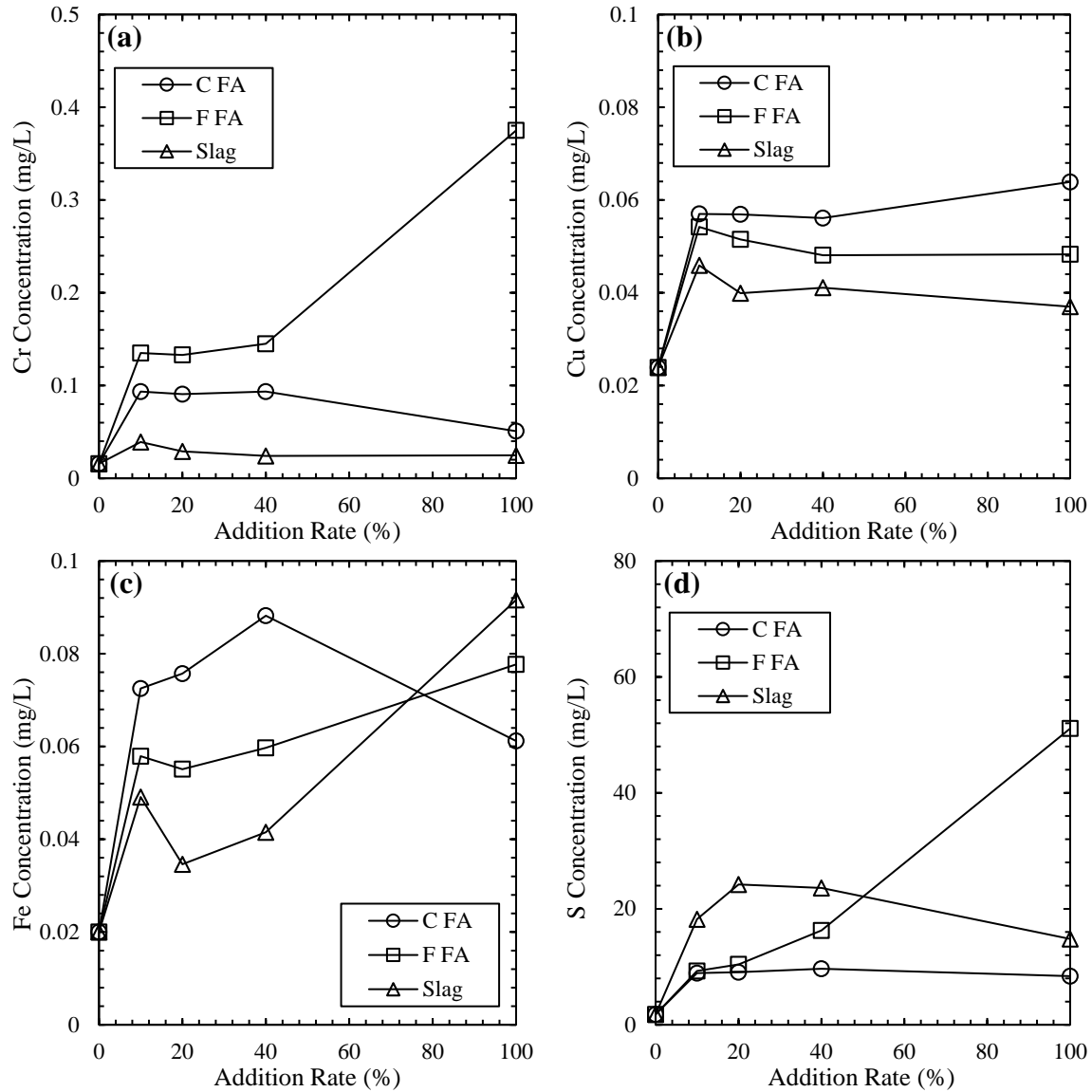
Figure 2.2 Effluent concentrations of (a) Cr, (b) Cu, (c) Fe, and (d) S as a function of fly ash or slag addition rate in SPLP effluent. *Note:* In addition to fly ash or slag content, mixtures were prepared with 6% type I/II cement. 0% and 100% correspond to soil, and FA (or slag) only samples; FA: Fly ash
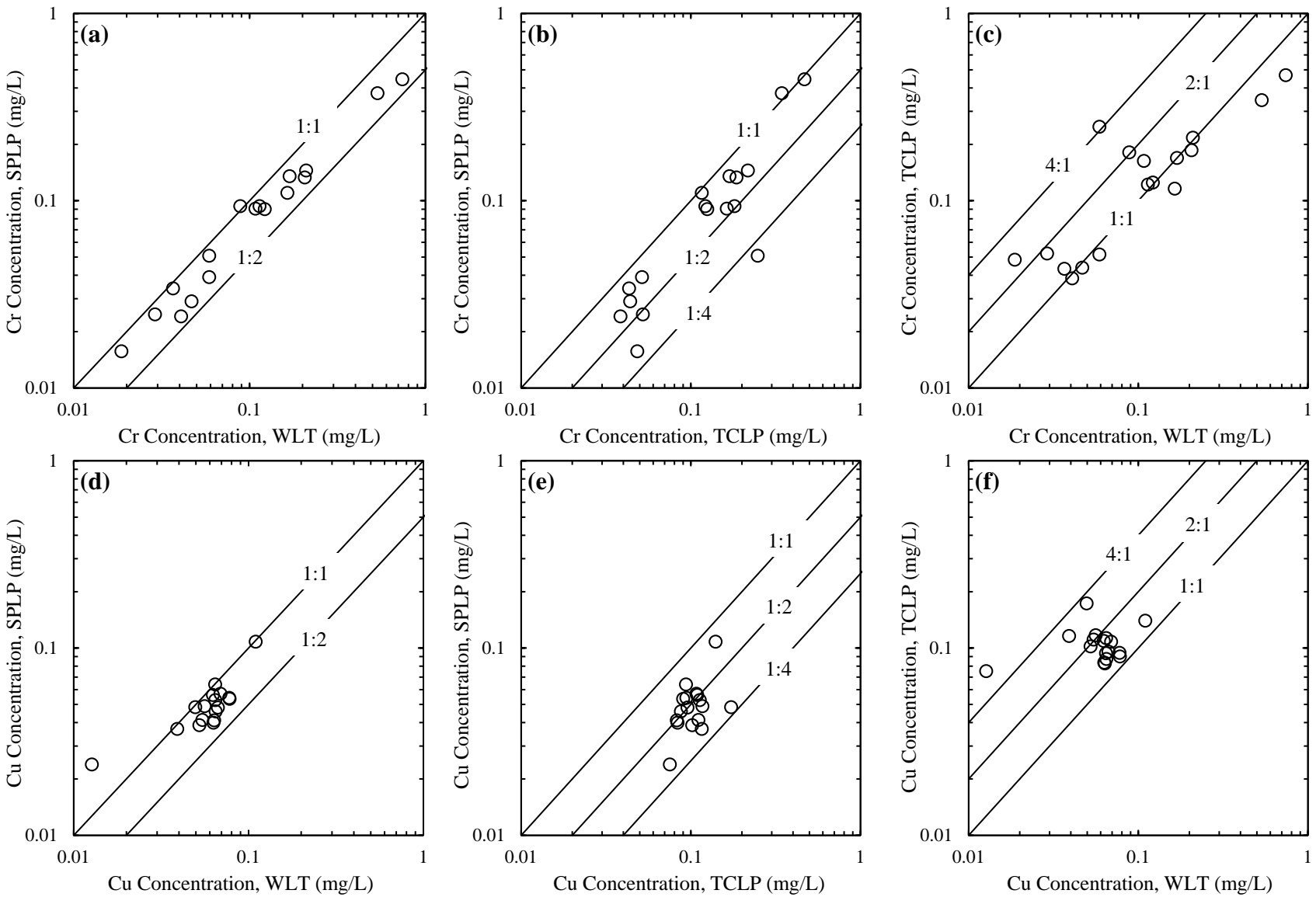
Figure 2.3   Method comparisons of Cr and Cu concentrations from cement activated soil-fly ash and soil–slag mixtures
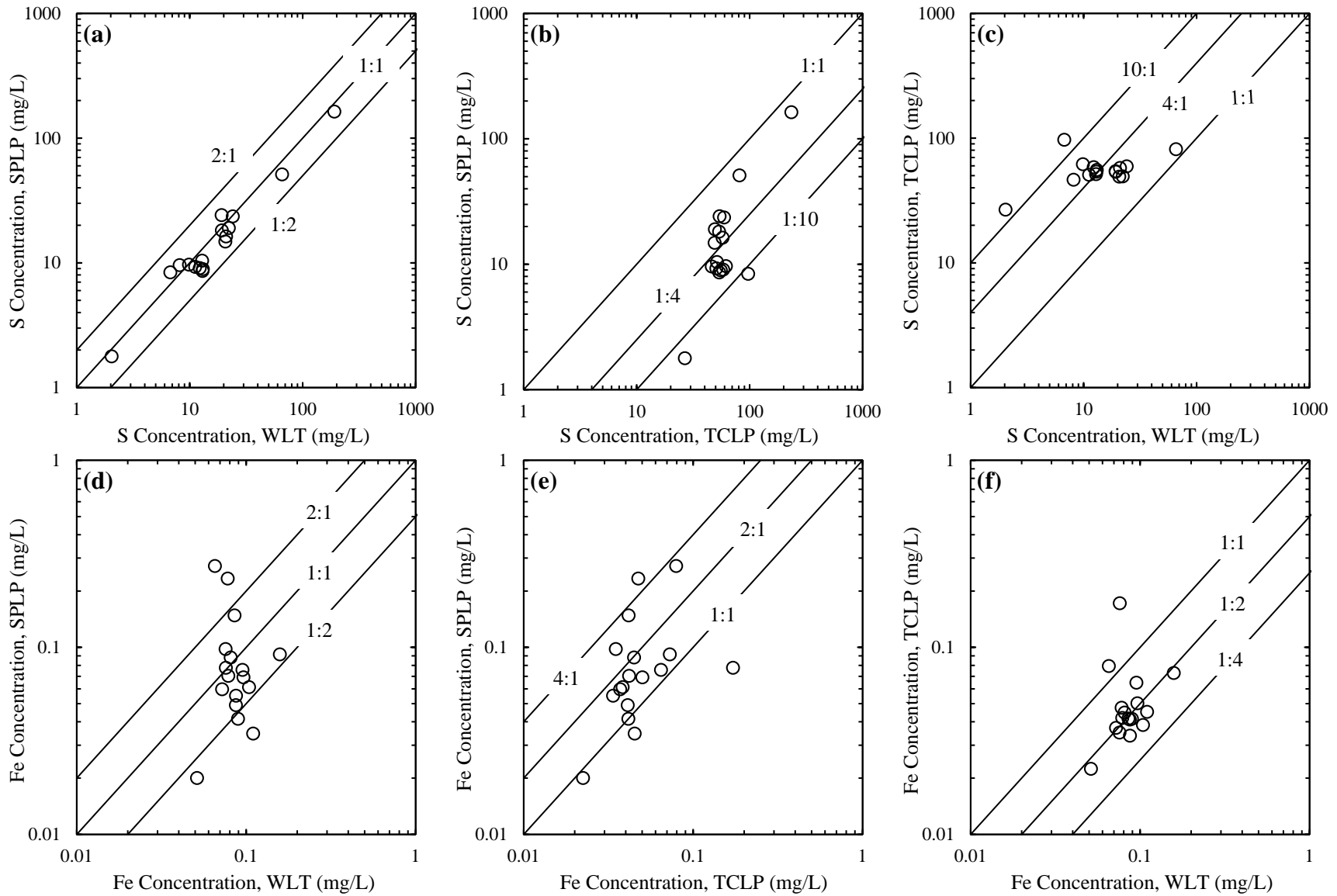
Figure 2.4 Method comparisons of S and Fe concentrations from cement activated soil-fly ash and soil–slag mixtures

38
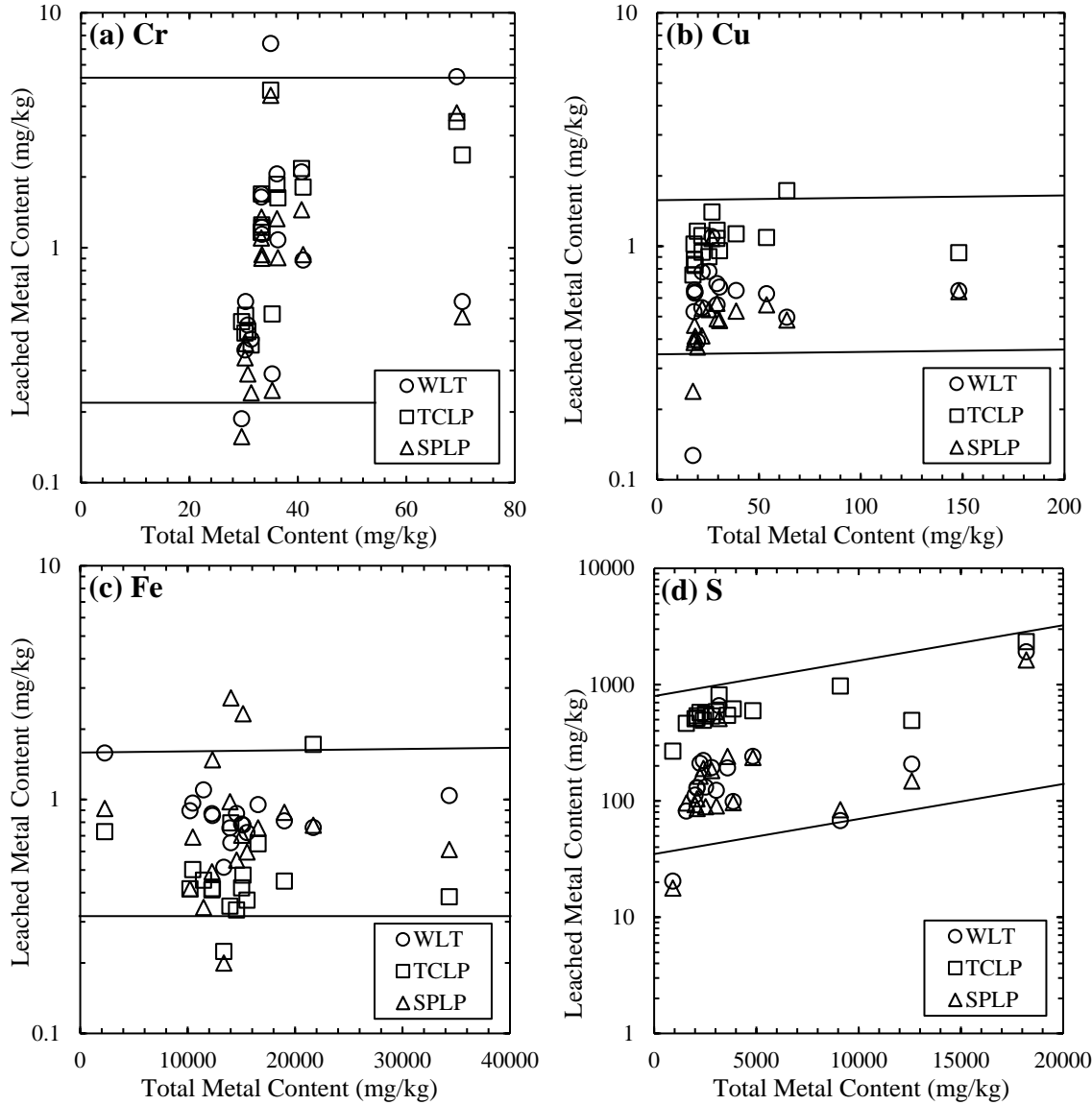
Figure 2.5 Effluent concentrations of (a) Cr, (b) Cu, (c) Fe, and (d) S from WLT, TCLP and SPLP leach tests as the function of total metal content of the soil-fly ash-cement and soil-slag-cement mixtures
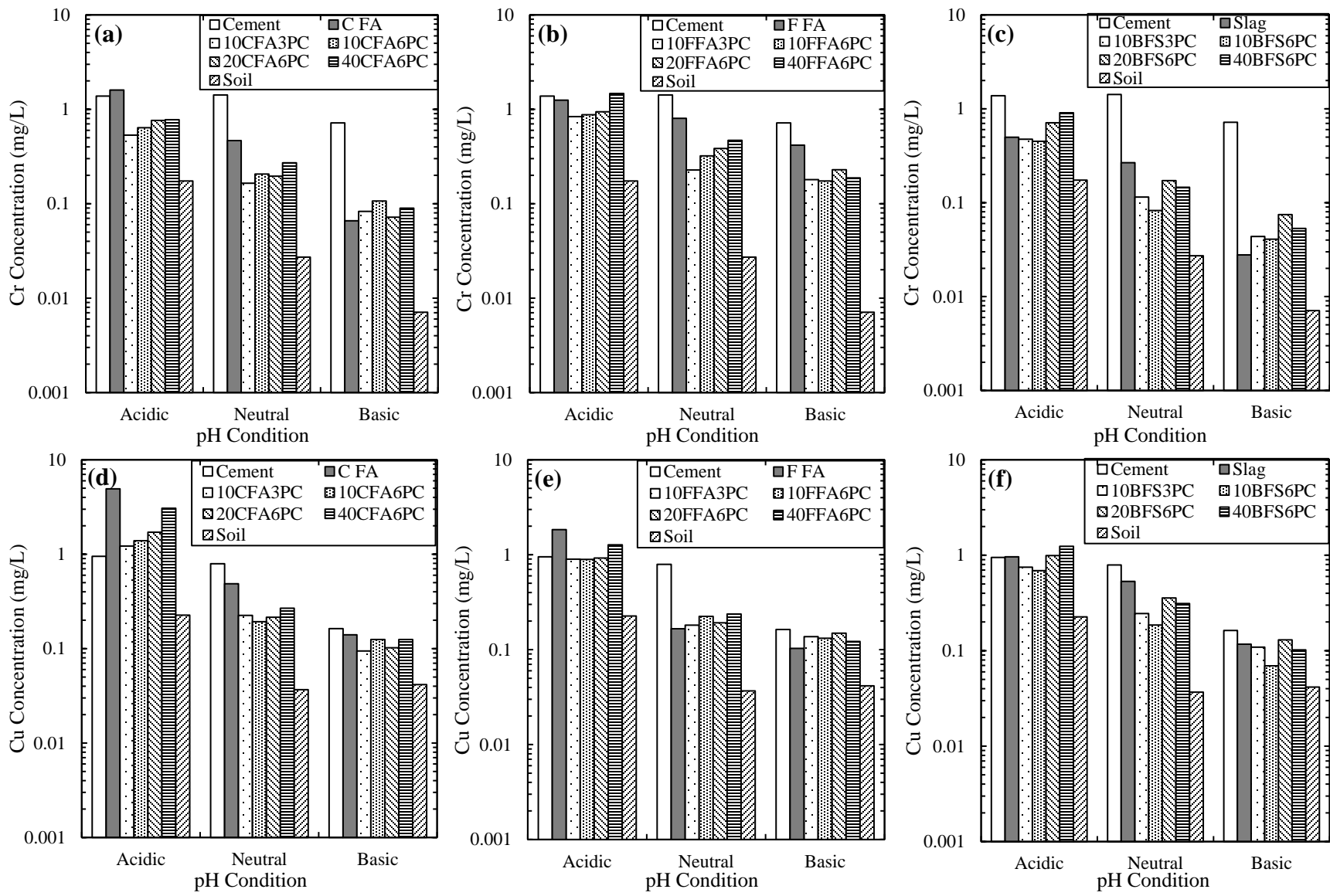
Figure 2.6 Leaching of Cr and Cu at acidic, neutral and basic conditions. *Note:* 10CFA3PC: 10% Class C fly ash+3% cement mixture
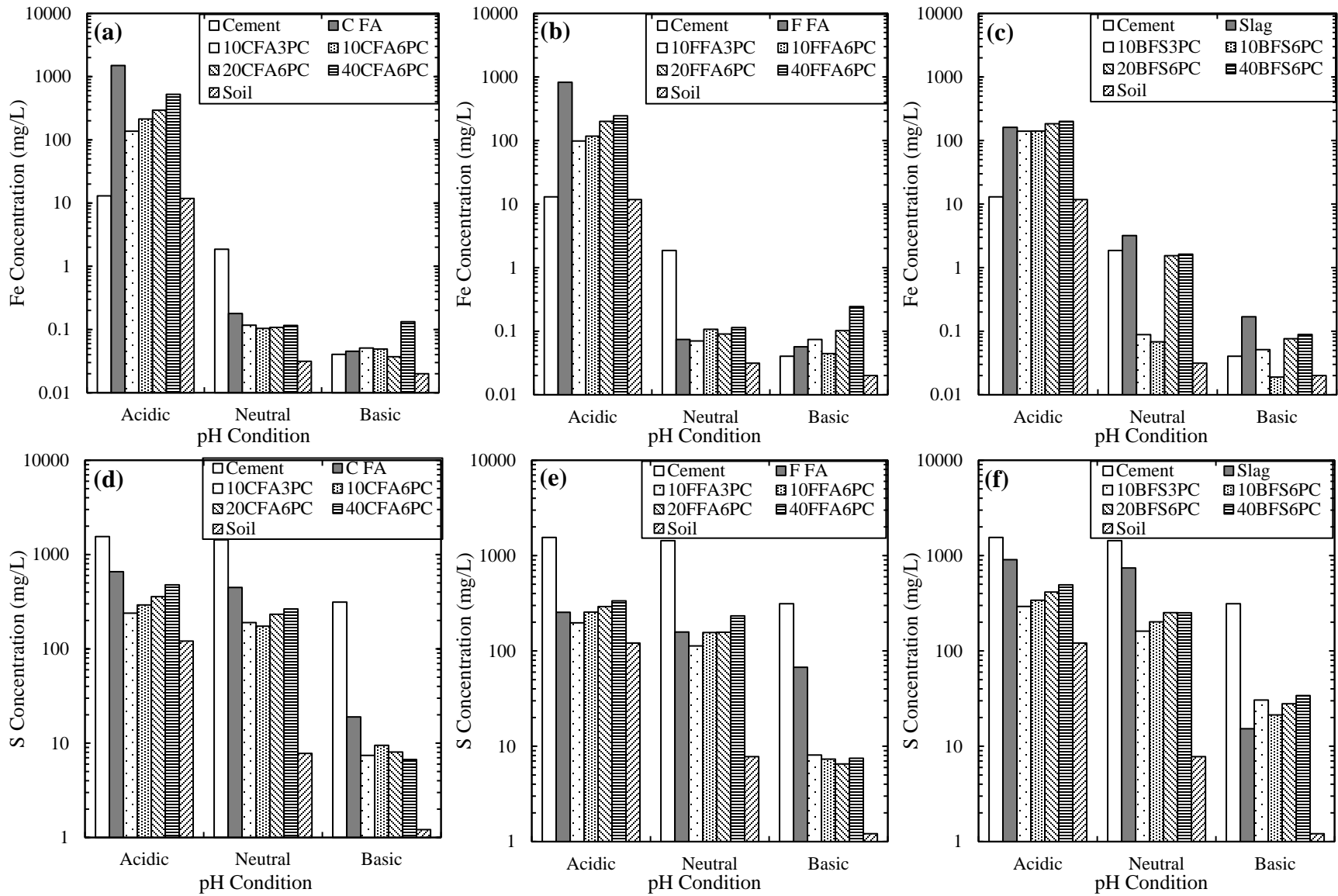
Figure 2.7 Leaching of Fe and S at acidic, neutral and basic conditions. *Note:* 10CFA3PC: 10% Class C fly ash+3% cement mixture
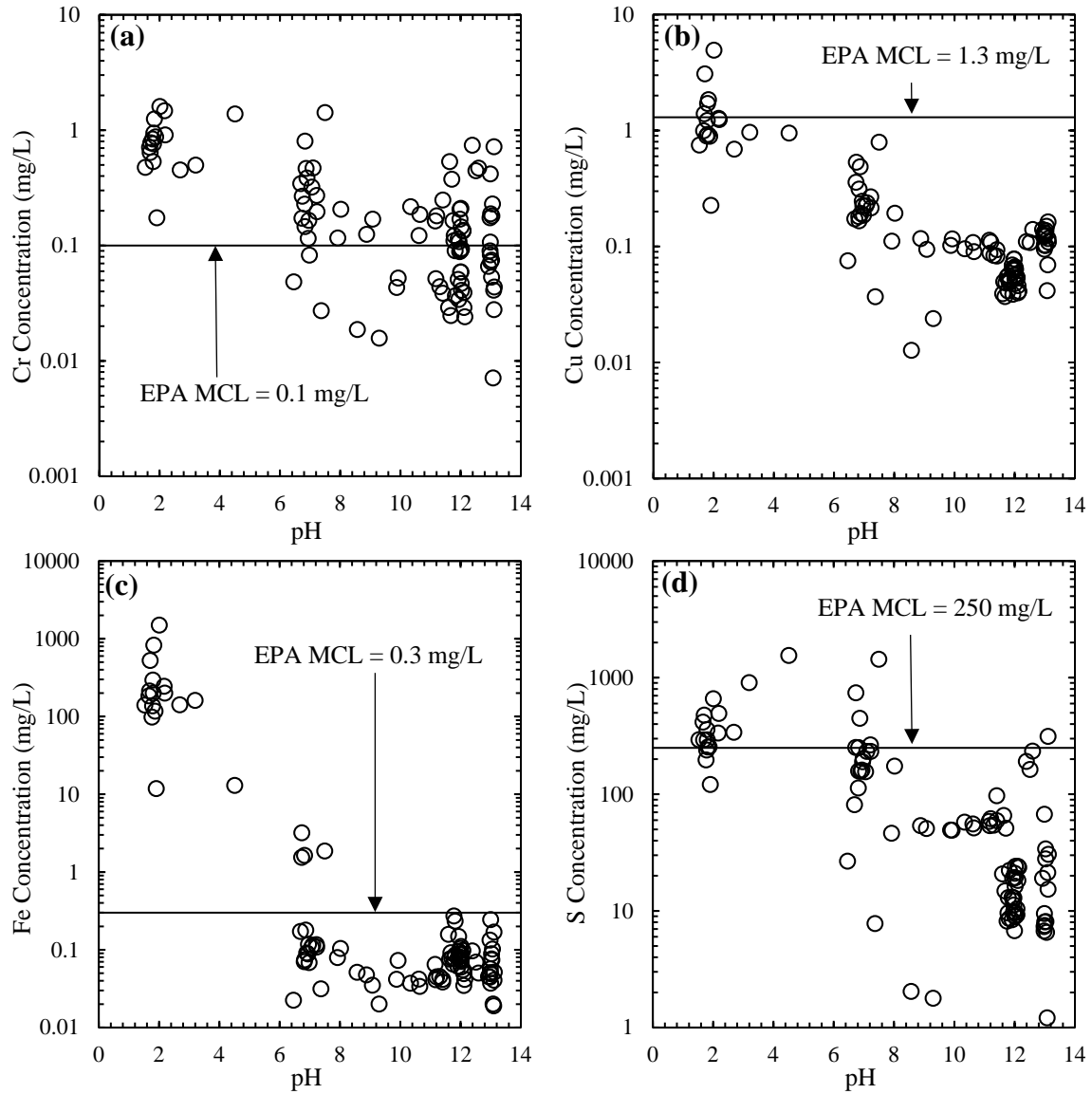
Figure 2.8 Effect of pH on the leached concentrations of (a) Cr, (b) Cu, (c) Fe, and (d) S from cement activated fly ash and slag treated mixtures
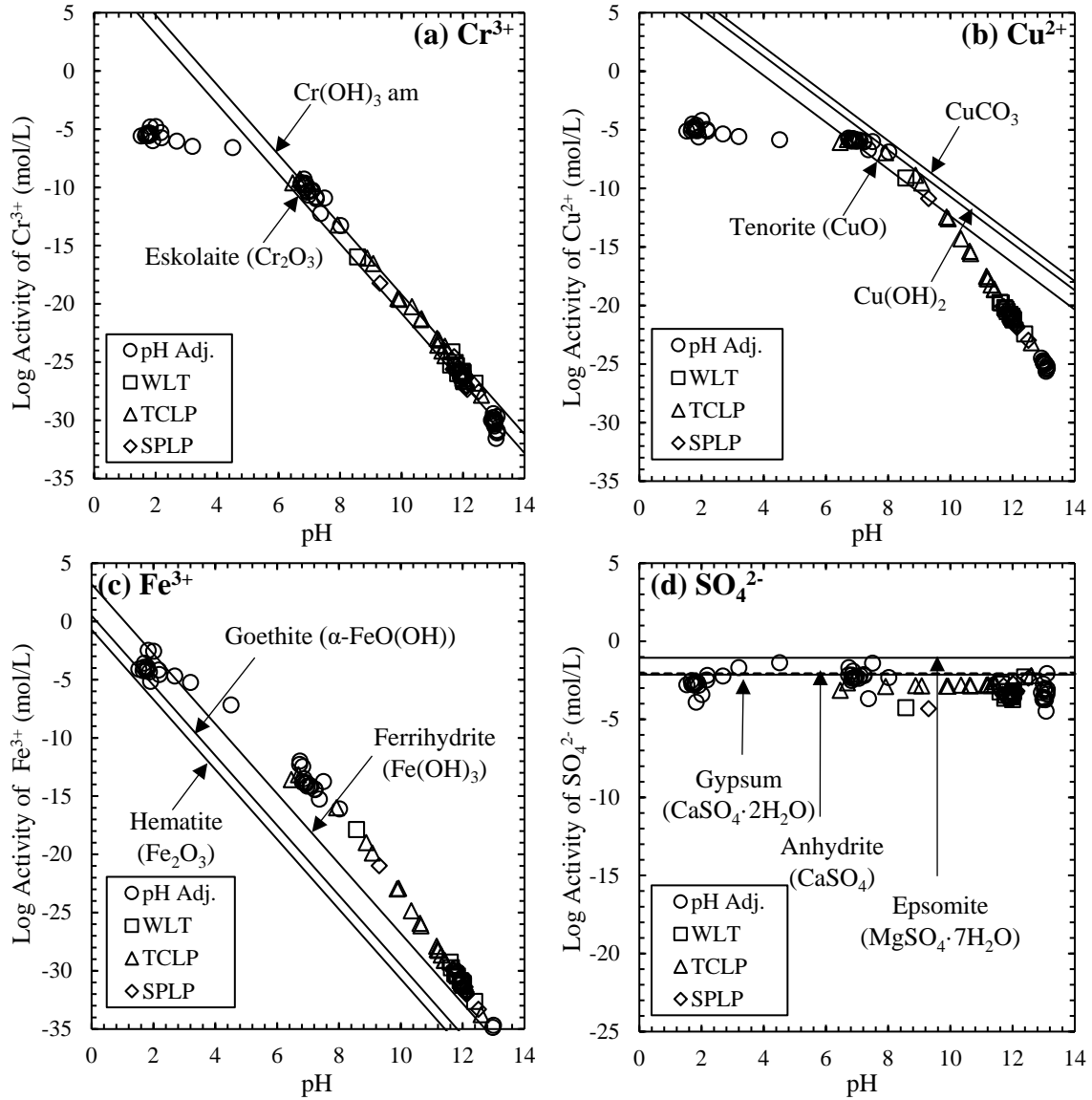
Figure 2.9 Log activity of (a) Cr^{3+}, (b) Cu^{2+}, (c) Fe^{3+}, and (d) SO_4^{2-} in the effluent of cement activated fly ash and slag treated mixtures

CHAPTER 3.   LEACHING BEHAVIOR OF ALUMINUM, COPPER, IRON AND ZINC FROM FLY ASH AND SLAG STABILIZED SOILS

Masrur Mahedi, Bora Cetin and Asli Y. Dayioglu

3.1   Abstract

The use of industrial by-products such as fly ash and slag have become very prevalent in soil stabilization owing to its suitable physical and mechanical properties, and economical advantages. However, fly ash and slag have been identified as the potential source of toxic substances, and may pose environmental risk by leaching heavy and trace metals into soil, surface and groundwater. Toxicity characteristic leaching procedure (TCLP) tests were conducted to investigate the environmental hazards associated with the leaching of Aluminum (Al), Copper (Cu), Iron (Fe) and Zinc (Zn) from fly ashes, slag, type I/II cement and cement activated fly ash and slag stabilized soils. Sulfate (SO_4), dissolved inorganic carbon (DIC) and dissolved organic carbon (DOC) concentrations were also quantified to evaluate their influence on metal leaching. To understand the effect of pH on the leaching behavior, pH-dependent leach tests were conducted at the pH ranges of 2 to 14. An increase in fly ash or slag content might not necessarily increase the effluent metal concentrations. Al, Cu, Zn and DOC followed an amphoteric leaching pattern where concentrations increased in both acidic and basic conditions. In contrast, maximum DIC concentrations occurred at neutral or near neutral pH values. Fe and SO_4 showed cationic leaching behavior where concentrations decreased with an increase in effluent pH. Additionally, dominant oxidation states of the metals and their leaching controlling mechanisms were identified by implementing the geochemical modeling program Visual MINTEQ. The geochemical analyses indicated that the solubility of Al^{3+} and Fe^{3+} were controlled by precipitation/dissolution reactions

of oxide/hydroxide minerals at all pH values. Leaching of Cu^{2+} was only solubility controlled at pH higher than 7, whereas Zn^{2+} leaching was solubility controlled in the pH range of 8 to 12.

Keywords: Leaching, metals, pH-dependent, fly ash, slag, geochemical modeling

3.2   Introduction

Fly ash is a coal combustion byproduct from coal power plants, collected from exhaust gas either by mechanical or electrostatic procedures (Wen et al., 2011). According to the U.S. Energy Information Administration, about 40% of the electricity generated in the United States in 2016 was reliant on coal combustion (EIA, 2018). As of 2016, more than 37 million tons of fly ashes were produced and approximately 60% of them were recycled (ACAA, 2017). Some of these fly ashes have cementitious properties (e.g., Class C fly ash) derived from higher amount of calcium oxides (CaO), while others (e.g., Class F fly ash, high carbon fly ash) are rich in silica (SiO_2), alumina (Al_2O_3) and iron oxides (Fe_2O_3) which can react with an activator such as cement and lime to produce additional cementitious compounds (Cetin et al., 2010; Thomas, 2007). Similarly, steel slag is the non-metallic byproduct generated in different stages of steel production (Engström et al., 2013; Yin et al., 2018), mostly consisting silicates and aluminosilicates of calcium and other bases, having the potential to be a functioning substitute of cement clinkers (Shi, 2004). Therefore, soil stabilization with fly ash and slag have emerged as an economical and practical alternative to the conventional chemical stabilization methods. However, the use of fly ash and slag in construction purposes may pose potential environmental hazards as they contain heavy and trace metals (Bin-Shafique et al., 2006; Cetin et al., 2014; Dayioglu et al., 2014; Langová and Matýsek, 2010). On the other hand, Mahedi et al. (2018) showed that fly ashes and slags are more efficient to improve the soil strength when they are mixed with cement. In addition to the strength increase, it is expected that cement inclusion would alter the leaching behavior of metals from these soil-fly ash and soil-slag mixtures. However, this has not been quantified.

In recent years, the leaching of metals from fly ashes and slags has received significant attentions. Several studies demonstrated the influence of fly ash content, fly ash type and soil type on the leaching potential of metals (Cetin et al., 2013; Cetin and Aydilek, 2013; Gwenzi and Mupatsi, 2016; Kogbara et al., 2014, 2013; Tsiridis et al., 2015; Zhang et al., 2016). The leaching of metals with slag aging (Gomes and Pinto, 2006), carbonation sequestration (Huijgen and Comans, 2006), leaching kinetics (De Windt et al., 2011), environmental and geotechnical assessment (Sas et al., 2015), pH dependent leaching (Cappuyns et al., 2014) are some significant and recent works on the leaching behavior of slag. However, limited works have been reported on the leaching characterization of metals from cement activated fly ash and slag stabilized soils. None of the previous studies has investigated the leaching properties of cement activated fly ash and slag stabilized soils as a function of fly ash/slag/cement content and pH dependence, though mineralogy of these additives affects the particle surface charge, buffering capacity, and hence the leaching behaviors of metals (Dayioglu et al., 2018; Komonweeraket et al., 2015b). An assessment regarding the influence of pH on the leaching behavior of metals is vitally important, since pH plays an important role in controlling the leaching of both organic and inorganic substances (Fruchter et al., 1990; Komonweeraket et al., 2015b, 2015a; Mudd et al., 2004). Leaching behavior of metals is reflected by effluent pH, and an investigation involving pH would offers a better understanding on the environmental impacts of soils mixed with fly ash and slag. Moreover, inclusion of an activator (e.g. cement, lime) in soil-fly ash and soil-slag mixtures contributes to the basic effluent pH significantly. Higher effluent pH may induce leaching of amphoteric metals such as Aluminum (Al), Copper (Cu) and Zinc (Zn) from fly ash and slag stabilized soils. Furthermore, leaching controlling mechanisms related to the effluent pH from soil-fly ash-cement and soil-slag-cement mixtures have not yet been investigated. Leaching mechanisms are vitally important in

predicting the metal concentrations in leachate from cement activated fly ash and slag stabilized soils. Therefore, the knowledge on leaching mechanisms is at prime position in quantifying the risks associated with the use of fly ash-cement and slag-cement in soil stabilization.

The objectives of this study are to (1) investigate the metal leaching behavior from commonly used fly ashes and slag in geotechnical purposes, (2) access the effects of fly ash, slag and cement contents on the leaching characteristics, (3) examine the influence of pH on the leaching behavior, (4) identify the mechanisms controlling the release of metals and minerals, and (5) determine the effect of stabilizers' type on metal leaching potentials and mechanisms. Two different fly ashes (Class C and F) and blast-furnace steel slag were selected for laboratory evaluation purposes. Type I/II cement was considered as an activator. A series of pH dependent leach test was performed to investigate the leaching behavior of Aluminum (Al), Copper (Cu), Iron (Fe) and Zinc (Zn). These metals were selected as the leaching characteristics of the designated metals are highly pH sensitive (Fruchter et al., 1990; Mudd et al., 2004). Toxicity characteristic leaching procedure (TCLP) leach test was implemented to relate the leached concentrations of the selected metals with regulatory limits defined by the U.S. EPA. In addition, leached concentrations of sulfate (SO_4), dissolved inorganic carbon (DIC) and dissolve organic carbon (DOC) were quantified due to their influence on metal leaching behavior (van der Sloot et al., 2017). Furthermore, geochemical modeling program MINTEQ was implemented to identify the leaching controlling mechanisms and determine the dominant oxidation states of metals in the effluents from fly ash-cement and slag-cement treated soils.

3.3 Materials

Iowa loess soil was stabilized with fly ash-cement and ground granulated blast furnace slag-cement grout. Loess soil was collected from the loess hill areas of Monona County, Iowa. ASTM C136/C136M was followed for sieve analysis of the soil. Approximately 82% of the soil

consists of fine particles (< 0.075 mm), while rest of it is predominantly sand size particles. The Liquid Limit (LL) and Plasticity Index (PI) determined in accordance to ASTM D4318 were found to be 24 and 4, respectively. The soil was classified as low plasticity silt (ML) according to Unified Soil Classification System (USCS). The specific gravity (G_s) of the soil was determined to be 2.74 following the standard method designated by ASTM D854.

Two different fly ashes (Class C and Class F) and a ground granulated blast furnace slag were used in the current study. As described in previous studies (Cetin et al., 2010; Mahedi et al., 2018) fly ashes and slag worked more efficiently when it was used with a calcium based activator. Therefore, Type I/II Portland cement was considered to initiate the pozzolanic reactions. The chemical compositions and the total elemental analysis of the materials used in this study are summarized in Table 3.1 and Table 3.2, respectively. For convenience, Class C fly ash and Class F fly ash are designated herein as C FA and F FA, correspondingly. The CaO content of the slag was 39.8% by weight indicating that it had high soil stabilization potential. Loess soil was found to be calcareous with the presence of Al_2O_3 (9.6%) and CaO (5.2%). X-ray diffraction analysis (not included for brevity) revealed the presence of albite ($NaAlSi_3O_8$), calcite ($CaCO_3$) and dolomite ($CaMg(CO_3)_2$) in loess soil. The pH of the stabilizers ranged from 11.6 to 12.7, while the pH of Loess soil was slightly alkaline (pH = 8.57). Both the fly ashes and slag primarily consisted of silt-sized particles with fines ranging from 73-91% (passing U.S. No. 200 sieve size) (Table 3.3). The G_s of the C FA was the highest (2.7), whereas it was the lowest for the slag (2.55) (Table 3.3).

3.4   Methods

3.4.1   Sample Preparation

The fly ash/slag and cement percentages for the mixtures were selected based on the strength and stiffness requirements determined by previous studies (Cetin et al., 2010; Mahedi et

al., 2018). A summary of the batches is provided in Table 3.4. Soil was mixed with 10%, 20%, and 40% fly ashes and slag by weight. The lower percentages (10% and 20%) of fly ash and slag are within the typical application range for soil stabilization. Cement was added as an activator at rates of 3% and 6%. All mixture proportions were measured gravimetrically and mixed thoroughly at their corresponding optimum moisture content (OMC) using nano-pure water. OMC and maximum dry density (γ_{dmax}) of soil and the mixtures were pre-determined by implementing standard compaction effort as per ASTM D698. As reported in Table 3.4, the γ_{dmax} of the mixtures were within the range of 16.3 to 17 kN/m^3, while the optimum moisture content varied between 14 to 18.8%. Mixtures were then cured in plastic bags for 7 days at 19 °C $\pm$ 2 and 95 % $\pm$ 5 relative humidity. After curing, samples were crushed and sieved through U.S. No. 10 sieve for leaching tests.

3.4.2 Toxicity Characteristic Leaching Procedure (TCLP)

Toxicity characteristic leaching procedure (TCLP) designated by U.S. EPA method 1311 was performed on soil, fly ashes, slag and soil-fly ash/slag-cement mixtures. The extraction solution for TCLP was prepared by adding 5.7 mL glacial acetic acid (CH_3COOH) and 64.3 mL 1 N sodium hydroxide (NaOH) into 500 mL nano-pure water. The solution was then diluted to 1 L, yielding a pH of 4.93±0.05. Specimens were prepared at a constant liquid-to-solid ratio (L:S) of 20:1. 200 mL of extraction fluid was added to 10 g of soil mixture in a 1-liter high-density polyethylene (HDPE) bottle. The samples were rotated for 18±2 hours at a rotation rate of 28 rpm as described in Cetin and Aydilek (2013). After rotation, solution pH and conductivity were measured. Finally, samples were vacuum filtered using 0.7-μm borosilicate glass fiber filters. The filtered samples were divided into two aliquots: one non-acidified, and the other acidified to a pH < 2 with 10% trace metal grade nitric acid (HNO_3). Both aliquots were stored in refrigerator at temperature lower than 4 ºC for further analyses.

3.4.3 pH Dependent Leach Test

Standard test method designated by U.S. EPA Method 1313 was followed to evaluate the effect of pH on the leaching behavior of metals and minerals. A liquid-to-solid ratio (L:S) of 10:1 was utilized with 40 g sample, and the samples were prepared at nine target pH values of 2, 4, 5.5, 7, 8, 9, 10.5, 12 and 13 ($\pm$0.5). The pH of the solutions was adjusted with either 1 N potassium hydroxide (KOH) or 2 N trace metal grade HNO_3. The appropriate amount of acid/base and water required for a target pH were pre-determined by evaluating the acid neutralizing capacity (ANC) of the mixtures. The acid neutralizing capacity was assessed by adding various amount of 1 N KOH or 2 N HNO_3 into water. A liquid-to-solid ratio (L:S) of 10:1 was implemented and the solution was rotated for 48$\pm$2 hours at a rotation rate of 28 rpm. After rotation, pH and electric conductivity of the solutions were measured. The pH dependent leach test samples were also rotated at 28 rpm for 48$\pm$2 hours. After measuring the pH and conductivity, samples were pressure filtered using 60-mL plastic syringes through 25-mm diameter, 0.2-μm pore size membrane filters fitted in 25-mm Easy Pressure syringe filter holders. All the syringes, filter holders and centrifuged tubes were acid-washed and rinsed with nano-pure water prior to use. The filtered extract was acidified with 10% trace metal grade nitric acid (HNO_3) to the pH lower than 2 and stored in refrigerator at temperature lower than 4 ℃. Another non-acidified aliquot of sample was stored for DIC, DOC and SO_4 measurements.

3.4.4 Measurement Methods

The elemental analysis of the samples was performed by inductively coupled plasma optical emission spectroscopy (ICP-OES). Known concentrations of commercially produced multi-element standard solutions were used to calibrate the ICP. The calibration curves were verified at every 9 samples and at the end of analysis sessions by running blank solutions and checking standards. The minimum detection limits (MDLs) of Al, Cu, Fe and Zn were 2.5 µg/L,

1.5 µg/L, 3.2 µg/L and 1 µg/L, respectively. Dissolved inorganic and organic carbon analyses were measured by the Shimadzu TOC-V analyzer. The instrument was calibrated by standard sodium bicarbonate ($NaHCO_3$) and sodium carbonate (Na_2CO_3) solutions for inorganic carbon, and potassium hydrogen phthalate ($C_8H_5KO_4$) solutions for organic carbon measurements. Inorganic carbon was converted to carbon dioxide (CO_2) in IC reactor by acidifying the samples with 17% phosphoric acid (H_3PO_4) solution. Organic carbon was also converted to CO_2 separately by the persulfate oxidizer solution and heating at 680 ℃. Finally, DIC and DOC concentrations were measured by quantifying CO_2 in a non-dispersive infrared (NDIR) gas analyzer. Sulfate measurements were carried out by the SEAL AQ2 analyzer, implementing the U.S. EPA method no: EPA-123-A Rev. 5. The detection limits for the sulfate was 1 mg SO_4/L. Under controlled conditions, dissolved sulfates were converted to barium sulfate ($BaSO_4$) suspension and the resulting turbidity was determined by a filter photometer at 405 nm. A new calibration curve was prepared for every analysis session by the standard anhydrous sodium sulfate (Na_2SO_4) solution which provided 1000 mg/L aqueous concentration of sulfates.

3.5   Results

3.5.1   Toxicity Characteristic Leaching Procedure (TCLP)

3.5.1.1 pH and electric conductivity (EC)

Fig. 3.1a shows the change of effluent pH (in TCLP) of the mixtures with fly ash and slag content when mixed with 6% cement by weight. Effluent pH greatly influences the leaching behavior of metals and is considered as an important safety criterion for soil stabilization (Daniels and Das, 2006). Fig. 3.1b indicates that the mixtures prepared with slag have the highest pH values whereas the pH of the specimens prepared with Class F fly ash were the lowest. It is well known that, effluent pH increases with the increase in CaO and MgO content of materials (Bin-Shafique et al., 2006; Quina et al., 2009). Table 3.1 indicates that CaO content is higher for slag and Class

C fly ash (39.8, 25.9; respectively) compared to the Class F fly ash (11.8%) used in the current study. Effluent pH of mixtures increased with an increase in fly ash/slag content (except the one prepared with 40% Class F fly ash), though the increase rates were insignificant beyond 10%. In case of 40% F fly ash mixture, the effluent pH (10.34) was slightly lower than that of 20% F fly ash blend (10.65). Izquierdo et al. (2011) concluded that effluent pH increased when $CaO/Ca(OH)_2$ ratio within the soil matrix was higher. Hydrated calcium silicate (C-S-H) produced by pozzolanic reactions may have reduced the free lime content of 40% F fly ash mixture and decreased the solution pH eventually. Moreover, Class F fly ash and slag mixtures have higher pH values compared to Class F fly ash alone and slag alone, proving the greater influence of cement (6% by weight) on the pH controlling mechanism. CaO content of Class F fly ash alone seemed to be inadequate to neutralize the free protons in TCLP extraction solution. For pure slag, effluent pH was lower due to slow dissolution rate of primary slag minerals (merwinite, akermanite and gehlenite) at alkaline conditions (Engström et al., 2013). Additionally, Fig. 3.1b shows that the effluent pH of the mixtures increases significantly with an increase in cement content, reflecting higher discharge of free lime and portlandite from type I/II cement. The pH of 100% cement in TCLP effluent solution was found to be the highest (12.6).

Impacts of fly ash/slag content and cement content on electrical conductivity (EC) of mixtures are presented in Figs. 3.1c and 1d, respectively. EC is associated with cation and anion concentrations in the solution which provides an estimation of effluent ionic strength (Gräfe et al., 2009). Higher ionic strength may induce additional metal leaching by decreasing surface negativity of soil mixtures through electrostatic effects (Sparks, 2003). Cetin et al. (2012) observed enhanced leaching of metals at increased ionic strengths. Fig. 3.1c shows that EC of Class C and slag mixtures increases with an increase in Class C fly ash and slag content. On the other hand, such

trend was not observed for the mixtures prepared with Class F fly ash. EC of soil-Class F fly ash-cement mixtures increased initially (10%), but remained almost unaffected at addition rates beyond 10% by weight. Class F fly ash alone had the lowest EC in all materials including the soil alone. Fig. 3.1d shows that EC of mixtures are not affected noticeably with an increase in cement content from 3% to 6% by weight.

3.5.1.2 Effect of fly ash and slag content on the leaching of elements

Fig. 3.2 shows the variation of TCLP effluent concentrations of the elements (Al, Cu, Fe, Zn, SO_4 and DIC) with fly ash and slag content. Metals were analyzed by compiling leached concentrations from soil, fly ashes, slag and 6% cement activated fly ash and slag treated soil mixtures. As seen from Fig. 3.2a, Al concentrations increase with the increase in fly ash and slag content. Murarka et al. (1991) claimed that Al concentration in aqueous solution is controlled by the dissolution and precipitation of aluminum (hydro) oxide. Free Al^{3+} starts to precipitate as gibbsite and $Al(OH)_3$ in the pH range of 6 to 9 (Astrup et al., 2006). With the increase in fly ash or slag content, pH raised beyond this range (Figs. 3.1a and 3.1b) and increased the leached concentrations of Al. Class F fly ash blends leached the lowest amount of Al. Leached Al concentrations from the mixtures were significantly lower than those observed in fly ashes only. Al became immobilized by incorporating in cement hydrates. As seen in Fig. 3.2a, 100% Class F fly ash leached higher amount of Al, though the solution pH (6.69) was low. At this pH, $Al(OH)_2^+$ dominates as the pH is lower than the point of zero charge (PZC) of alumina (8.1) (Tombácz, 2009). $Al(OH)_2^+$ may have complexed with acetate ligands and remained in the solution, which eventually increased the effluent concentrations of Al. For other mixtures, ligands were initially complexed with Ca^{2+} because of their higher CaO content, and greater reactivity of Ca^{2+} compared to Al^{3+} cations. It should be pointed out that in all cases, Al concentrations exceeded 0.2 mg/L

specified by U.S. EPA maximum contaminant level (MCL) for drinking water. However, cement treatment may considerably reduce Al leaching from fly ashes.

The leached concentrations of Cu and Fe in TCLP extracts followed very similar leaching trends (Figs. 3.2b and 3.2c). Untreated loess soil leached higher amount of Cu and Fe than the soil-fly ash-cement and soil-slag-cement mixtures. Aqueous concentrations of these metals fluctuated with fly ash or slag content. Yet, with few exceptions, Cu and Fe concentrations decreased with the increase in fly ash or slag content. Effluent pH mostly controls the leaching of these two metals. Komonweeraket et al. (2015b) claimed that Cu follows a cationic leaching pattern, where concentrations decrease with an increase in pH due to the precipitation of copper oxide (CuO) and hydroxide ($Cu(OH)_2$) minerals. Fe also precipitates in neutral and alkaline conditions (pH > 6) forming insoluble cationic species (Goswami and Mahanta, 2007). Therefore, the soil-fly ash/slag-cement mixtures leached less due to high alkaline pH conditions (pH > 12) than the loess soil which has a pH = 6.46. Furthermore, Class C fly ash alone leached lower amount of Cu and Fe compared to the soil-Class C fly ash mixtures, whereas the observed behavior was opposite for Class F fly ash and slag blends. Lower pH of 100% Class F fly ash and slag (6.69 and 9.93, respectively) compared to Class C fly ash (pH = 11.41) was the reason for the observed behavior. In addition, acidic nature of soil effluent (pH = 6.46) was identified as the potential reason of higher Cu and Fe leaching from untreated soil. However, in all cases, Cu and Fe concentrations were lower than the U.S. EPA specified MCLs for drinking waters (1.3 and 0.3 mg/L, respectively).

Fig. 3.2d shows that Zn concentrations increase consistently with Class C fly ash content. Zn follows an amphoteric leaching pattern and the dissolution and/or precipitation of zincite and $Zn(OH)_2$ control the aqueous concentrations of Zn (Murarka et al., 1991). Bestgen et al. (2016)

reported that the lowest concentrations of Zn occur at pH around 10.5. With the increase in fly ash content, solution pH of Class C fly ash mixtures raised to the range of 10.6 to 11.2 which caused an increase in Zn concentrations. For Class F fly ash mixtures, concentrations fluctuated depending on the effluent pH. In contrast, after an initial increase, Zn concentrations decreased with an increase in slag content, though the pH increased above 10.5. From elemental analysis, Zn content (Table 3.2) was the lowest for slag which may have resulted in lower leaching of Zn. Cetin et al. (2014) reported minor leaching of Zn at elevated pHs due to lower elemental concentrations.

Sulfate concentrations also increased with fly ash content, whereas a decreasing trend was observed for slag mixtures with an initial increase at 10% addition rate (Fig. 3.2e). At higher pH levels (pH > 10.7), with the presence of free lime SO_4 precipitates as ettringite (Gabrisová et al., 1991). Higher CaO content (Table 3.1) of slag may have facilitated the formation and precipitation of ettringite which eventually reduced the effluent concentrations of SO_4. Lower amount of CaO in fly ashes inhibited the formation of ettringite and therefore, higher amount of SO_4 remained in the solutions. Moreover, oxyanions such as AsO_4^{3-}, SeO_3^{-2} may replace SO_4 in ettringite and increased the aqueous concentrations (Zhang and Reardon, 2003). Yet, this claim cannot be verified as As and Se concentrations were not measured in the current study.

DIC concentrations decreased significantly with an increase in fly ash or slag content (Fig. 3.2f). DIC occurs mainly in three inorganic forms: dissolved carbon dioxide ($CO_{2(aq)}$), bicaronate (HCO_3^-) and carbonate (CO_3^{2-}) (Schulz et al., 2006). At alkaline conditions and with the presence of atmospheric $CO_{2(g)}$, carbonate (CO_3^{2-}) predominates and precipitates as insoluble carbonates of divalent cations such as Ca^{2+}, Cd^{2+}, Mg^{2+}, and Sr^{2+} (Langmuir, 1997; Stumm and Morgan, 1996). Komonweeraket et al. (2015a) reported the oversaturation and precipitation of calcite and/or aragonite ($CaCO_3$) in soil-fly ash leachates at pH higher than 9. In this study, pH values of soil-fly

ash-cement and soil-slag-cement mixtures were very basic which resulted in reduction of DIC concentrations by inducing insoluble carbonate precipitations.

3.5.1.3 Effect of cement content on the leaching of elements

TCLP effluent concentrations of the elements with cement content are presented in Fig. 3.3. Mixtures prepared with 10% fly ash or slag content, and varying dosages (3% and 6%) of cement were considered to evaluate the influence of cement on the leaching behaviors. As seen from Fig. 3.3, Al and SO_4 concentrations increased with cement content. The rate of increases in concentrations of Al and SO_4 were not linear, though the mass of metals in the mixtures increased linearly with cement content. The increase rates were greater when cement content was increased from 0% to 3% rather than the increase from 3% to 6%. Effluent concentrations of these ions were higher for 100% cement which was the most probable reason for higher concentrations at elevated cement content. For Fe and Zn, concentrations increased at the initial cement content (3%), but subsequently decreased at 6% addition rate. Cu concentrations monotonically decreased with an increase in cement content. Cu and Fe may have followed a cationic leaching pattern and concentrations decreased as the pH increased along with the increase in cement content (Komonweeraket et al., 2015b; Liu et al., 2008). Conversely, Zn shows amphoteric leaching pattern with minimum concentrations at pH around 10.5 (Bestgen et al., 2016). With an increase in cement content, pH increased to 10.5 which caused a reduction in leached Zn concentrations. Furthermore, Zn concentration was lower in 100% cement compared to the mixtures. In case of DIC, concentrations decreased with cement content due to the precipitation of divalent metal carbonates at alkaline conditions. 100% cement also had lower DIC as the cement pH was very alkaline (pH=12.6).

3.5.2 pH-dependent Leaching Behavior

3.5.2.1 Acid neutralizing capacity (ANC)

ANC of the mixtures along with loess soil, cement, fly ashes and slag are illustrated in Fig. 3.4. Negative values in ANC curves indicate base addition in terms of meq/g weight of dry sample. As seen in Fig. 3.4a, loess soil showed very low neutralizing capacities (-0.315 to 0.19 meq/g soil) in the pH range of 12.4 to 7.4. Acid neutralizing capacities of Class F fly ash were almost identical to loess soil, with a large buffer zone at pH lower than 4. According to Zhang et al. (2016), the plateau indicates that, environmental conditions can affect the effluent pH of Class F fly ash. Class C fly ash also showed higher neutralizing capacities at pH < 4. Compared to Class F fly ash and soil, greater buffering capacities of Class C fly ash were observed throughout the whole pH range due to its higher CaO content (Table 3.1). Two different plateaus at pH values of 8.6 and 6.4 were identified in the ANC curve of Class C fly ash. Silicates and aluminosilicates have a buffering capacity at pH value of 8 which is the reason for the observed plateau at pH of 8.6 (Roy and Cartledge, 1997). Calcium carbonate, gypsum and gibbsite are most likely responsible for the plateau at pH around 6.4. These minerals have the buffering capacities in the pH range of 5 to 6 (Chen et al., 2009). The variations in equilibrium pH were observed depending on the Ca-contents of the minerals (Giampaolo et al., 2002).

Compared to the fly ashes, slag showed higher neutralizing capacities. A large buffer region from pH 9 to 6.7 was identified, which may have happened due to higher CaO and MgO contents of slag (Table 3.1). As expected, the strongest acid neutralizing capacities were observed for cement with three distinct plateaus ranging the pH of 13.1 to 12.3, 12.3 to 10.3 and 10.3 to 9.0 (Fig. 3.4a). The first plateau was ascribed due to the presence of soluble portlandite along with Ca-rich (Ca/Si = 1.8) calcium-silicate-hydrates (C-S-H) (Isenburg and Moore, 1992; Stronach and Glasser, 1997). The second plateau was associated with C-S-H of low Ca/Si ratio (<1.5) which

showed acid neutralizing capacities at pH around 10 (Stegemann and Buenfeld, 2002). The third plateau was due to MgO in dolomitic lime causing a pH detention within the pH range of 9 to 11 (Fernández et al., 2003).

Fig. 3.4 shows that acid neutralizing capacities of the mixtures are influenced by their soil, cement and fly ash or slag contents. For Class C fly ash and slag mixtures, acid neutralizing capacities fall between the neutralizing capacities of soil and 100% Class C fly ash or slag materials (Fig. 3.4b and 3.4d). Buffering capacity of these mixtures increased with fly ash and slag content. The influences of cement on ANC curves were less pronounced. Higher CaO and MgO content (Table 3.1) of Class C fly ash and slag, and lower cement addition rates (3%-6%) validate the observed behavior. In contrast, soil-Class F fly ash mixtures have higher neutralizing capacities than those of soil and 100% Class F fly ash (Fig. 3.4c). This indicates larger influence of cement on the buffering capacities of Class F fly ash mixtures. Lower amount of CaO and MgO content (Table 3.1) in Class F fly ash and higher acid buffering capacity of cement is the reason for the observed inclination. Trivial improvement in buffering capacities with fly ash contents also justifies the aforementioned claim.

3.5.2.2 pH dependent leaching patterns

Fig. 3.5 shows the leached concentrations of Al from the mixtures and materials alone as a function of pH. Al showed amphoteric leaching pattern with minimum concentration at neutral pH, and maximum concentrations at acidic and basic conditions (Freire et al., 2015). In this study, minimum concentrations of Al were observed at somewhat alkaline environment. At neutral and slightly basic pHs (6-9), Al precipitates as amorphous $Al(OH)_3$ which decreases Al concentrations in the effluent (Gitari et al., 2009). Fig. 3.5 also indicates that leached Al concentrations are higher in acidic conditions compared to the ones in alkaline conditions. Gibbsite and amorphous $Al(OH)_3$ controls the leaching of Al in acidic fly ash solutions, whereas boehmite [γ-AlO(OH)] controls Al

at alkaline conditions (Roy et al., 1984). However, for 100% cement (Fig. 3.5a), a decrease in Al concentration was observed at higher pH (pH > 12) which is consistent with the leachability of Si and other oxyanions, linked to the precipitation of ettringite (Cornelis et al., 2008). Moreover, as seen from Fig. 3.5d, leached Al concentrations were stable in a pH range of 5.5 to 11 for slag mixtures. Slower dissolution rates of Al bearing slag minerals such as gehlenite ($Ca_2Al_2SiO_7$) and tricalcium aluminate ($Ca_3Al_2O_6$) are the most probable reason of the observed leaching behavior for slag mixtures (Engström et al., 2013). Dudas (1981) also reported limited leachability of Al due to extremely slow dissolution rates of glassy matrix and crystalline aluminosilicate phases.

The concentrations of Cu were the highest in acidic conditions which kept decreasing until the pH was around 12 (Fig. 3.6). A subsequent increase in Cu concentrations beyond the pH of 12 indicated amphoteric leaching behavior of Cu. Chandler et al. (1997) reported mild amphoteric leaching of Cu from fly ashes and municipal solid waste incinerator residues. Fruchter et al. (1990) indicated that the release of Cu was solubility controlled and dependent on the dissolution/precipitation of CuO and $Cu(OH)_2$. It is well known that CuO is an amphoteric oxide with higher solubility in both acidic and basic solutions. In addition, loess soil showed robust amphoteric leaching of Cu with minimum concentration at pH around 9.5. Cu solubility is also strongly influenced by the complexation with DOC (Dijkstra et al., 2008). Higher DOC concentrations in soil is the most probable reason for the strong amphoteric leaching pattern of Cu from soil only. In contrast, cationic leaching of Cu was observed for 100% cement (Fig. 3.6a). It is assumed that under alkaline conditions Cu is included in the precipitates such as calcite ($CaCO_3$) and/or aragonite ($CaCO_3$) and reduced in concentrations (Cetin et al., 2012; Komonweeraket et al., 2015b).

The leachability of Fe sharply decreased towards slight acidic to neutral environments (pH $\cong$ 5-7) and remained low throughout the remaining pH range (Fig. 3.7). It is well known that Fe is solubility controlled and dependent on the dissolution and precipitation of oxide and hydroxide minerals such as hematite (Fe_2O_3) and $Fe(OH)_3$. With an increase in pH, Fe precipitated as amorphous oxyhydroxide (Warren and Dudas, 1989) which decreased solution Fe concentrations. For soil-Class F fly ash/slag-cement mixtures, an increase in Fe concentration was observed at extreme caustic conditions (pH $\geq$ 13). At extreme pH conditions (pH > 12), Fe concentrations may have increased due to the hydrolysis of Fe^{3+} in the form of $Fe(OH)_4^-$ (Allanore et al., 2007).

The leaching of Zn also presented amphoteric characteristics with higher concentrations in acidic conditions (pH < 4), followed by a rapid decrease in the pH range of 4 to 11 (Fig. 3.8). An elevated release of Zn at pH higher than 11 specified the expected U/V-shaped curve for Zn leaching (Bestgen et al., 2016; Du et al., 2018; Engelsen et al., 2010). Theis et al. (1982) has identified Zincite (ZnO) as the primary Zn containing mineral in fly ashes which controls the effluent Zn concentrations (Garavaglia and Caramuscio, 1994). The formation of anionic hydroxo-complexes enhanced Zn concentrations in strong alkaline conditions (Izquierdo and Querol, 2012).

As indicated in Fig. 3.9, SO_4 concentrations remained almost unaffected across the pH range of 2 to 10.5, decreased sharply at pH values of 10.5 to 12, and remained constant beyond pH > 12. Similar leaching behavior of SO_4 from fly ashes and soil-fly ash mixtures has also been recognized by Zhang et al. (2016) and De Gianfilippo et al. (2018). With the presence of sufficient lime (CaO), SO_4 forms insoluble ettringite and precipitates when the pH rises above 10.7 (Gabrisová et al., 1991). At pH lower than 10, SO_4 solubility appears to be controlled by anhydrite ($CaSO_4$) and gypsum ($CaSO_4 \cdot 2H_2O$). Onori et al. (2011) identified anhydrite and gypsum as the potential solubility controlling minerals for SO_4 leaching from bottom ashes at pH lower than 10.

In contrast, amphoteric leaching of SO_4 was observed for loess soil (Fig. 3.9a), with minimum concentrations at near neutral condition. It is speculated that SO_4 anions were absorbed and precipitated with $Al(OH)_3$ at neutral environment. A positive correlation between the solution SO_4 and Al concentrations was also observed for loess soil (not included for brevity). Pommerenk and Schafran (2005) reported adsorption of SO_4 onto precipitated hydrous aluminum oxide and concluded that, electrostatic forces at the surface-water interface plays a vital role on SO_4 adsorption mechanism.

Fig. 3.10 depicts the DIC concentrations of mixtures as a function of pH. The highest DIC concentrations were observed at neutral condition, with a sharp decrease in both acidic and alkaline environments. An increase in DIC concentrations were also observed at a pH higher than 12. Dissolved carbon dioxide ($CO_{2(aq)}$ and H_2CO_3), bicaronate (HCO_3^-) and carbonate (CO_3^{2-}) are the major forms of dissolved inorganic carbon (Schulz et al., 2006). In neutral pH, the major contribution to DIC arises from the concentrations of HCO_3^- (Clark, 2015). At pH higher than 10.3, CO_3^{2-} becomes the main species (Cole and Prairie, 2009) and precipitates with divalent cations, resulting a decrease in DIC concentrations (Langmuir, 1997). Under the acidic condition, $CO_{2(aq)}$ and H_2CO_3 are the dominant species which increased CO_2 partial pressure in the solution (Clark, 2015). For an equilibrium with the overlying atmosphere, CO_2 is released from the solution and decreased the DIC concentrations. Nonetheless, effluent DIC concentrations were supersaturated by more than an order of magnitude relative to atmospheric pCO_2 (380 µatm), especially for loess soil and the mixtures. Loess soil was found to be calcareous which increased pCO_2 in extraction vessel at lower pH values and increased the solubility of CO_2. However, this assumption could not be verified as the change in partial pressure (pCO_2) was not measured during the sample extraction process.

On the contrary to the DIC leaching behavior, DOC concentrations were higher in both acidic and basic conditions while they were minimum at neutral and/or near neutral pH conditions (Fig. 3.11). This observation is consistent with Komonweeraket et al. (2015c). Dissolution of high molecular weight humic acids in acidic and alkaline pH is the most probable reason of increased DOC concentrations (Langmuir, 1997). Also, with the increase in pH, sorption of organic substances to the mineral surfaces decreased (Dijkstra et al., 2002). The leached DOC from soil-slag mixtures were the least pH sensitive in both acidic and basic environments. 100% slag and cement also showed no sensitivity to the effluent pH in terms of DOC leaching. According to Guimaraes et al. (2006), DOC also depends on calcium leaching and possibly forms DOC-Ca complexes. Higher CaO content (Table 3.1) in slag and cement may have leached additional Ca^{2+} which complexed with DOC and remained in the solution.

3.5.3 Geochemical Modeling

In order to determine whether the release of a metal is solubility controlled or sorption controlled, geochemical analyses were carried out on all samples subjected to pH dependent test by utilizing Visual MINTEQ, an equilibrium speciation model (Gustafsson, 2014). The model was used to calculate the equilibrium composition of the samples as well as their saturation indices at a fixed pH measured in laboratory conditions and by allowing only aqueous complexation reactions, following the suggestions of Komonweeraket et al. (2015b) and Apul et al. (2005). Input data were the pH, EC, SO_4, DIC, DOC and metal concentrations of the pH dependent test samples. In addition, the dominant oxidation states of the redox sensitive metals were specified. The predominant oxidation states assumed for the elements of interest were Al^{3+}, Cu^{2+}, Fe^{3+} and Zn^{2+}. The analyses were performed on assumption that reactions took place in an open system at a temperature of 25 °C under atmospheric partial pressure of $CO_2(g)$ and that the leachate was in equilibrium with the minerals controlling the solubility (Gustafsson, 2014). The calculated log

activities of the metals were plotted with respect to the leachate pH. The plots were then used to determine if that particular metal was solubility or sorption controlled. In case the metal is solubility controlled, the data points should lie in close proximity to the solubility line of the mineral controlling the solubility (Garavaglia and Caramuscio, 1994; Komonweeraket et al., 2015b; Zhang et al., 2016).

Fig. 3.12 indicates that leaching of Al^{3+} for all samples is controlled by dissolution/precipitation reactions of aluminium-(hydr)oxides. The geochemical analyses show that both gibbsite $(Al(OH)_3)$ and boehmite $(AlO(OH))$ may be the solubility controlling mineral phases for all pH values. These findings are in agreement with the previous studies conducted on the leaching mechanisms of fly ash (Astrup et al., 2006; Komonweeraket et al., 2015b; Zhang et al., 2016). Bhattacharyya et al. (2011) performed an experimental study on solubility behavior of fly ash and found out that the saturation index values of gibbsite, which are an important indicator if the sample is oversaturated, under-saturated or in equilibrium with respect to a particular mineral, vary between -1 and +1, showing that gibbsite might be a solubility controlling mineral. Similarly, Masindi et al. (2018) performed geochemical analysis on blast furnace (BF) slag leachate and found out that gibbsite controls the solubility of slag leachates at different pH values.

Mechanisms that control Cu^{2+} leaching from waste materials has been extensively studied in the past by various researchers (Bestgen et al., 2016; Engelsen et al., 2010; Fruchter et al., 1990; Garavaglia and Caramuscio, 1994; Komonweeraket et al., 2015b; Murarka et al., 1991; Zhang et al., 2016). The findings of previous studies are in good agreement with the results obtained in this study. Visual MINTEQ analysis results indicated that Tenorite (CuO) was the solubility controlling mineral at neutral to alkaline pH values (Fig. 3.13). At pH values lower than 6, Cu^{2+} leaching was reported to be adsorption controlled. Apul et al. (2005) also indicated that the under-

saturation at acidic conditions were quiet prominent for [$Cu(OH)_2(s)$], suggesting that at acidic pH values, Cu interacts with sorptive surfaces and aqueous complexes other than malachite and tenorite and sorption becomes the controlling mechanism.

As in Al^{3+}, Fe-(hydr)oxides controlled the Fe leaching from materials alone and their mixtures. Fig. 3.14 shows that hematite (Fe_2O_3) and goethite ($FeO(OH)$) are the two major solubility controlling phases for Fe at all pHs. In the literature, ferrihydrite ($Fe(OH)_3$) was also reported to govern the solubility mechanism of fly ash (Gitari et al., 2009; Komonweeraket et al., 2015b). However, the saturation indices for hematite and goethite were lower in this study, similar to the results of Bestgen et al. (2016). Thus, they were controlling the leaching mechanism of Fe.

Fig. 3.15 shows that leaching of Zn^{2+} is partially controlled by solubility in case different types of waste materials are utilized. For each treatment method (Class C fly ash-cement, Class F fly ash-cement and slag-cement) as well as control materials, for pH values greater than 8 and smaller than 12, leaching mechanism is governed by solubility. However, for neutral to acidic pH values as well as extremely alkaline values, the calculated Zn^{2+} activities were under-saturated with respect to zincite (ZnO) and $Zn(OH)_2$, pointing out an adsorption controlled mechanism for that pH range. This observation is similar to the results provided in the literature (Bestgen et al., 2016; Garavaglia and Caramuscio, 1994; Komonweeraket et al., 2015b; Murarka et al., 1991; Zhang et al., 2016). Engelsen et al. (2010) proposed that at very high pH values, $CaZn_2(OH)_6.2H_2O(s)$ may have controlled the solubility of Zn^{2+}. However, Visual MINTEQ database does not include this mineral, thus no information could be obtained.

3.6   Conclusions

A study was conducted to investigate the leaching behavior of Al, Cu, Fe and Zn from loess soil, Class C and F fly ashes, blast-furnace steel slag, type I/II cement and soil-fly ash/slag-cement mixtures. In addition, leachability of SO_4, DOC and DIC along with pH and EC were evaluated.

To understand the leaching mechanisms, geochemical modelling was performed using Visual MINTEQ and pH dependent leach test data. The major findings of this study are summarized as follows:

Addition of fly ash and slag caused an increase in leached Al and SO_4 concentrations in TCLP solution. After the initial increase, leached Al concentrations did not vary depending on fly ash or slag content. Soil-slag-cement mixtures leached the lowest amount of SO_4. In all cases, concentrations of Al exceeded the regulatory limits determined by U.S. EPA Maximum Contaminant Limits (MCLs).

TCLP concentrations of Cu, Fe and Zn fluctuated with the increase in fly ash or slag addition rates. It was anticipated that the leaching behavior of these metals was dependent on both effluent pH and total metal content of materials. Concentrations of these metals were below the U.S. EPA specified MCLs. DIC concentrations significantly decreased with an increase in fly ash or slag content due to the precipitation of divalent metal carbonates.

The influences of cement content on leaching behavior of elements can be divided into three broad sections: (1) Al and SO_4 concentrations increased with an increase in cement content, (2) Fe and Zn concentrations initially increased and then decreased at higher addition rates, (3) Cu and DIC concentrations decreased with an increase in cement content. The change in concentrations with cement content was not linear, though the constituents' mass in the mixtures increased/decreased monotonically with cement content.

The pH dependent leaching of Al, Cu and Zn followed an amphoteric pattern with minimum concentrations at neutral/near neutral pH values and higher concentrations at acidic and alkaline conditions. Leached concentrations of these elements were significantly higher in acidic

conditions compared to those observed in alkaline conditions. Minimum concentrations of Cu and Zn were mostly observed at basic pH conditions.

Fe showed cationic leaching behavior with sharp decrease in concentrations in slight acidic to neutral conditions (pH $\cong$ 5-7). In rest of the pH range, Fe concentrations remained considerably low. For Class C fly ash and slag mixtures, small increase in Fe concentrations was observed at extreme basic conditions (pH$\geq$ 13) due to the hydrolysis of Fe^{3+} in the form of $Fe(OH)_4^-$.

The leaching of SO_4 was unaffected in the pH range of 2 to 10.5 but decreased abruptly with consequent increase in pH. DIC concentrations were maximum at neutral pH values, whereas DOC concentrations were higher in acidic and alkaline conditions.

Similarity in leaching behavior for a given element was observed, regardless the compositional differences of the stabilizing materials (fly ashes, slag and cement). This similarity indicates homogeneity in leaching controlling mechanisms such as solubility, sorption and solid-solution interaction and factors such as pH, redox conditions and ionic strength.

The geochemical analyses conducted via Visual MINTEQ indicated that precipitation/dissolution reactions of oxide/hydroxide minerals controlled the solubility of Al^{3+} and Fe^{3+} at all pH values. On the other hand, leaching of Cu^{2+} is only solubility controlled at pH values larger than 7, whereas Zn^{2+} leaching is controlled by solubility for pH values between 8 and 12.

In general, from the leaching assessment of the materials, it was concluded that cement activated fly ash and slag could be used in pavement subgrade soil stabilization. However, cautions should be taken regarding the leaching of Al, since the leached concentrations of Al exceeded the EPA specified MCL in all cases.

3.7   Acknowledgements

The authors thank Kendra Lee, ISU Environmental Lab Manager, for her support in laboratory investigations. The assistance and effort of Ben Popken and Anish Bhatt, Undergraduate Research Assistant, are appreciated. The findings and claims reported in this study are solely those of the authors. Endorsement by the fly ash and suppliers is not implied and should not be assumed.

3.8   References

ACAA, 2017. 2016 Production and Use Survey Results News Release. Washington, D.C., USA.

Allanore, A., Lavelaine, H., Valentin, G., Birat, J.P., Lapicque, F., 2007. Electrodeposition of metal iron from dissolved species in alkaline media. J. Electrochem. Soc. 154, E187. https://doi.org/10.1149/1.2790285

Apul, D.S., Gardner, K.H., Eighmy, T.T., Fällman, A.M., Comans, R.N.J., 2005. Simultaneous application of dissolution/precipitation and surface complexation/surface precipitation modeling to contaminant leaching. Environ. Sci. Technol. 39, 5736–5741. https://doi.org/10.1021/ES0486521

Astrup, T., Dijkstra, J.J., Comans, R.N.J., Sloot, H.A. van der, Christensen, T.H., 2006. Geochemical modeling of leaching from MSWI air-pollution-control residues. Environ. Sci. Technol. 40, 3551–3557. https://doi.org/10.1021/ES052250R

Bestgen, J.O., Cetin, B., Tanyu, B.F., 2016. Effects of extraction methods and factors on leaching of metals from recycled concrete aggregates. Environ. Sci. Pollut. Res. 23, 12983–13002. https://doi.org/10.1007/s11356-016-6456-0

Bhattacharyya, P., Reddy, K.J., Attili, V., 2011. Solubility and fractionation of different metals in fly ash of powder river basin coal. Water, Air, Soil Pollut. 220, 327–337. https://doi.org/10.1007/s11270-011-0757-1

Bin-Shafique, S., Benson, C.H., Edil, T.B., Hwang, K., 2006. Leachate concentrations from water leach and column leach tests on fly ash-stabilized soils. Environ. Eng. Sci. 23, 53–67. https://doi.org/10.1089/ees.2006.23.53

Cappuyns, V., Alian, V., Vassilieva, E., Swennen, R., 2014. pH dependent leaching behavior of Zn, Cd, Pb, Cu and As from mining wastes and slags: Kinetics and mineralogical control. Waste and Biomass Valorization 5, 355–368. https://doi.org/10.1007/s12649-013-9274-3

Cetin, B., Aydilek, A.H., 2013. pH and fly ash type effect on trace metal leaching from embankment soils. Resour. Conserv. Recycl. 80, 107–117. https://doi.org/10.1016/J.RESCONREC.2013.09.006

Cetin, B., Aydilek, A.H., Guney, Y., 2010. Stabilization of recycled base materials with high carbon fly ash. Resour. Conserv. Recycl. 54, 878–892. https://doi.org/10.1016/J.RESCONREC.2010.01.007

Cetin, B., Aydilek, A.H., Li, L., 2014. Trace metal leaching from embankment soils amended with high-carbon fly ash. J. Geotech. Geoenvironmental Eng. 140, 1–13. https://doi.org/10.1061/(ASCE)GT.1943-5606.0000996

Cetin, B., Aydilek, A.H., Li, L., 2013. Leaching behavior of aluminum, arsenic, and chromium from highway structural fills amended with high-carbon fly ash. Transp. Res. Rec. J. Transp. Res. Board 2349, 72–80. https://doi.org/10.3141/2349-09

Cetin, B., Aydilek, A.H., Li, L., 2012. Experimental and numerical analysis of metal leaching from fly ash-amended highway bases. Waste Manag. 32, 965–978. https://doi.org/10.1016/J.WASMAN.2011.12.012

Chandler, A.J., Eighmy, T.T., Hjelmar, O., Kosson, D.S., Sawell, S.E., Vehlow, J., Sloot, H.A. van der, Hartlen, J., 1997. Municipal Solid Waste Incinerator Residues, Volume 67, 1st ed. Elsevier, Amsterdam, Netherlands.

Chen, Q., Zhang, L., Ke, Y., Hills, C., Kang, Y., 2009. Influence of carbonation on the acid neutralization capacity of cements and cement-solidified/stabilized electroplating sludge. Chemosphere 74, 758–764. https://doi.org/10.1016/J.CHEMOSPHERE.2008.10.044

Clark, I.D., 2015. Groundwater Geochemistry and Isotopes, 1st ed. CRC press, Boca Raton, Florida, USA.

Cole, J.J., Prairie, Y.T., 2009. Dissolved CO2, in: Likens, G.E. (Ed.), Encyclopedia of Inland Waters. Elsevier, Amsterdam, Netherlands, pp. 30–34.

Cornelis, G., Johnson, C.A., Gerven, T. Van, Vandecasteele, C., 2008. Leaching mechanisms of oxyanionic metalloid and metal species in alkaline solid wastes: A review. Appl. Geochemistry 23, 955–976. https://doi.org/10.1016/J.APGEOCHEM.2008.02.001

Daniels, J.L., Das, G.P., 2006. Leaching behavior of lime–fly ash mixtures. Environ. Eng. Sci. 23, 42–52. https://doi.org/10.1089/ees.2006.23.42

Dayioglu, A.Y., Aydilek, A.H., Cetin, B., 2014. Preventing swelling and decreasing alkalinity of steel slags used in highway infrastructures. Transp. Res. Rec. J. Transp. Res. Board 2401, 52–57. https://doi.org/10.3141/2401-06

Dayioglu, A.Y., Aydilek, A.H., Cimen, O., Cimen, M., 2018. Trace metal leaching from steel slag used in structural fills. J. Geotech. Geoenvironmental Eng. 144, 04018089. https://doi.org/10.1061/(ASCE)GT.1943-5606.0001980

De Windt, L., Chaurand, P., Rose, J., 2011. Kinetics of steel slag leaching: Batch tests and modeling. Waste Manag. 31, 225–235. https://doi.org/10.1016/J.WASMAN.2010.05.018

Di Gianfilippo, M., Hyks, J., Verginelli, I., Costa, G., Hjelmar, O., Lombardi, F., 2018. Leaching behaviour of incineration bottom ash in a reuse scenario: 12 years-field data vs. lab test results. Waste Manag. 73, 367–380. https://doi.org/10.1016/j.wasman.2017.08.013

Dijkstra, J.J., Meeussen, J.C.L., Van der Sloot, H.A., Comans, R.N.J., 2008. A consistent geochemical modelling approach for the leaching and reactive transport of major and trace elements in MSWI bottom ash. Appl. Geochemistry 23, 1544–1562. https://doi.org/10.1016/J.APGEOCHEM.2007.12.032

Dijkstra, J.J., van der Sloot, H.A., Comans, R.N.J., 2002. Process identification and model development of contaminant transport in MSWI bottom ash. Waste Manag. 22, 531–541. https://doi.org/10.1016/S0956-053X(01)00034-4

Du, B., Li, J., Fang, W., Liu, Y., Yu, S., Li, Y., Liu, J., 2018. Characterization of naturally aged cement-solidified MSWI fly ash. Waste Manag. 80, 101–111. https://doi.org/10.1016/J.WASMAN.2018.08.053

Dudas, M.J., 1981. Long-term leachability of selected elements from fly ash. Environ. Sci. Technol. 15, 840–843. https://doi.org/10.1021/es00089a013

EIA, 2018. Electric Power Annual 2017. Washington, D.C., USA.

Engelsen, C.J., van der Sloot, H.A., Wibetoe, G., Justnes, H., Lund, W., Stoltenberg-Hansson, E., 2010. Leaching characterisation and geochemical modelling of minor and trace elements released from recycled concrete aggregates. Cem. Concr. Res. 40, 1639–1649. https://doi.org/10.1016/J.CEMCONRES.2010.08.001

Engström, F., Adolfsson, D., Samuelsson, C., Sandström, Å., Björkman, B., 2013. A study of the solubility of pure slag minerals. Miner. Eng. 41, 46–52. https://doi.org/10.1016/j.mineng.2012.10.004

Fernández, A.I., Chimenos, J.M., Raventós, N., Miralles, L., Espiell, F., 2003. Stabilization of electrical arc furnace dust with low-grade MgO prior to landfill. J. Environ. Eng. 129, 275–279. https://doi.org/10.1061/(ASCE)0733-9372(2003)129:3(275)

Freire, M., Lopes, H., Tarelho, L.A.C., 2015. Critical aspects of biomass ashes utilization in soils: Composition, leachability, PAH and PCDD/F. Waste Manag. 46, 304–315. https://doi.org/10.1016/J.WASMAN.2015.08.036

Fruchter, J.S., Rai, D., Zachara, J.M., 1990. Identification of solubility-controlling solid phases in a large fly ash field lysimeter. Environ. Sci. Technol. 24, 1173–1179. https://doi.org/10.1021/es00078a004

Gabrisová, A., Havlica, J., Sahu, S., 1991. Stability of calcium sulphoaluminate hydrates in water solutions with various pH values. Cem. Concr. Res. 21, 1023–1027. https://doi.org/10.1016/0008-8846(91)90062-M

Garavaglia, R., Caramuscio, P., 1994. Coal fly-ash leaching behaviour and solubility controlling solids. Stud. Environ. Sci. 60, 87–102. https://doi.org/10.1016/S0166-1116(08)71450-X

Giampaolo, C., Mastro, S.L., Polettini, A., Pomi, R., Sirini, P., 2002. Acid neutralisation capacity and hydration behaviour of incineration bottom ash–Portland cement mixtures. Cem. Concr. Res. 32, 769–775. https://doi.org/10.1016/S0008-8846(01)00760-8

Gitari, W.M., Fatoba, O.O., Petrik, L.F., Vadapalli, V.R.K., 2009. Leaching characteristics of selected South African fly ashes: Effect of pH on the release of major and trace species. J. Environ. Sci. Heal. Part A 44, 206–220. https://doi.org/10.1080/10934520802539897

Gomes, J.F.P., Pinto, C.G., 2006. Leaching of heavy metals from steelmaking slags. Rev. Metal. 42, 409–416. https://doi.org/10.3989/revmetalm.2006.v42.i6.39

Goswami, R.K., Mahanta, C., 2007. Leaching characteristics of residual lateritic soils stabilised with fly ash and lime for geotechnical applications. Waste Manag. 27, 466–481. https://doi.org/10.1016/J.WASMAN.2006.07.006

Gräfe, M., Power, G., Klauber, C., 2009. Review of bauxite residue alkalinity and associated chemistry. CSIRO Doc. DMR-3610. Proj. ATF-06-3 Manag. Bauxite Residues 51.

Guimaraes, A.L., Okuda, T., Nishijima, W., Okada, M., 2006. Organic carbon leaching behavior from incinerator bottom ash. J. Hazard. Mater. 137, 1096–1101. https://doi.org/10.1016/J.JHAZMAT.2006.03.047

Gustafsson, J.P., 2014. Visual MINTEQ 3.0 User Guide. KTH, Department of Land and Water Recources, Stockholm, Sweden.

Gwenzi, W., Mupatsi, N.M., 2016. Evaluation of heavy metal leaching from coal ash-versus conventional concrete monoliths and debris. Waste Manag. 49, 114–123. https://doi.org/10.1016/J.WASMAN.2015.12.029

Huijgen, W.J.J., Comans, R.N.J., 2006. Carbonation of steel slag for CO2 sequestration: Leaching of products and reaction mechanisms. Environ. Sci. Technol. 40, 2790–2096. https://doi.org/10.1021/ES052534B

Isenburg, J., Moore, M., 1992. Generalized acid neutralization capacity test, in: Stabilization and Solidification of Hazardous, Radioactive, and Mixed Wastes: 2nd Volume. ASTM International, 100 Barr Harbor Drive, PO Box C700, West Conshohocken, PA 19428-2959, pp. 361-361–17. https://doi.org/10.1520/STP19564S

Izquierdo, M., Koukouzas, N., Touliou, S., Panopoulos, K.D., Querol, X., Itskos, G., 2011. Geochemical controls on leaching of lignite-fired combustion by-products from Greece. Appl. Geochemistry 26, 1599–1606. https://doi.org/10.1016/j.apgeochem.2011.04.013

Izquierdo, M., Querol, X., 2012. Leaching behaviour of elements from coal combustion fly ash: An overview. Int. J. Coal Geol. 94, 54–66. https://doi.org/10.1016/J.COAL.2011.10.006

Kogbara, R.B., Al-Tabbaa, A., Stegemann, J.A., 2014. Comparisons of operating envelopes for contaminated soil stabilised/solidified with different cementitious binders. Environ. Sci. Pollut. Res. 21, 3395–3414. https://doi.org/10.1007/s11356-013-2276-7

Kogbara, R.B., Al-Tabbaa, A., Yi, Y., Stegemann, J.A., 2013. Cement–fly ash stabilisation/solidification of contaminated soil: Performance properties and initiation of operating envelopes. Appl. Geochemistry 33, 64–75. https://doi.org/10.1016/J.APGEOCHEM.2013.02.001

Komonweeraket, K., Cetin, B., Aydilek, A., Benson, C.H., Edil, T.B., 2015a. Geochemical analysis of leached elements from fly ash stabilized soils. J. Geotech. Geoenvironmental Eng. 141, 04015012. https://doi.org/10.1061/(ASCE)GT.1943-5606.0001288

Komonweeraket, K., Cetin, B., Aydilek, A.H., Benson, C.H., Edil, T.B., 2015b. Effects of pH on the leaching mechanisms of elements from fly ash mixed soils. Fuel 140, 788–802. https://doi.org/10.1016/J.FUEL.2014.09.068

Komonweeraket, K., Cetin, B., Benson, C.H., Aydilek, A.H., Edil, T.B., 2015c. Leaching characteristics of toxic constituents from coal fly ash mixed soils under the influence of pH. Waste Manag. 38, 174–184. https://doi.org/10.1016/J.WASMAN.2014.11.018

Langmuir, D., 1997. Aqueous Environmental Geochemistry. Prentice Hall, Upper Saddle River, New Jersey, USA.

Langová, Š., Matýsek, D., 2010. Zinc recovery from steel-making wastes by acid pressure leaching and hematite precipitation. Hydrometallurgy 101, 171–173. https://doi.org/10.1016/J.HYDROMET.2010.01.003

Liu, Y., Li, Y., Li, X., Jiang, Y., 2008. Leaching behavior of heavy metals and PAHs from MSWI bottom ash in a long-term static immersing experiment. Waste Manag. 28, 1126–1136. https://doi.org/10.1016/J.WASMAN.2007.05.014

Mahedi, M., Cetin, B., White, D.J., 2018. Performance evaluation of cement and slag stabilized expansive soils. Transp. Res. Rec. 036119811875743. https://doi.org/10.1177/0361198118757439

Masindi, V., Osman, M.S., Mbhele, R.N., Rikhotso, R., 2018. Fate of pollutants post treatment of acid mine drainage with basic oxygen furnace slag: Validation of experimental results with a geochemical model. J. Clean. Prod. 172, 2899–2909. https://doi.org/10.1016/J.JCLEPRO.2017.11.124

Mudd, G.M., Weaver, T.R., Kodikara, J., 2004. Environmental geochemistry of leachate from leached brown coal ash. J. Environ. Eng. 130, 1514–1526. https://doi.org/10.1061/(ASCE)0733-9372(2004)130:12(1514)

Murarka, I., Rai, D., Ainsworth, C., 1991. Geochemical basis for predicting leaching of inorganic constituents from coal-combustion residues, in: Waste Testing and Quality Assurance: Third Volume. ASTM International, 100 Barr Harbor Drive, PO Box C700, West Conshohocken, PA 19428-2959, pp. 279-279–10. https://doi.org/10.1520/STP25484S

Onori, R., Polettini, A., Pomi, R., 2011. Mechanical properties and leaching modeling of activated incinerator bottom ash in Portland cement blends. Waste Manag. 31, 298–310. https://doi.org/10.1016/J.WASMAN.2010.05.021

Pommerenk, P., Schafran, G.C., 2005. Adsorption of inorganic and organic ligands onto hydrous aluminum oxide: Evaluation of surface charge and the impacts on particle and NOM removal during water treatment. Environ. Sci. Technol. 39, 6429–6434. https://doi.org/10.1021/ES050087U

Quina, M.J., Bordado, J.C.M., Quinta-Ferreira, R.M., 2009. The influence of pH on the leaching behaviour of inorganic components from municipal solid waste APC residues. Waste Manag. 29, 2483–2493. https://doi.org/10.1016/j.wasman.2009.05.012

Roy, A., Cartledge, F.K., 1997. Long-term behavior of a Portland cement-electroplating sludge waste form in presence of copper nitrate. J. Hazard. Mater. 52, 265–286. https://doi.org/10.1016/S0304-3894(96)01812-2

Roy, W.R., Griffin, R.A., Dickerson, D.R., Schuller, R.M., 1984. Illinois basin coal fly ashes. 1. Chemical characterization and solubility. Environ. Sci. Technol. 18, 734–739. https://doi.org/10.1021/es00128a003

Sas, W., Głuchowski, A., Radziemska, M., Dzięcioł, J., Szymański, A., 2015. Environmental and geotechnical assessment of the steel slags as a material for road structure. Materials (Basel). 8, 4857–4875. https://doi.org/10.3390/ma8084857

Schulz, K.G., Riebesell, U., Rost, B., Thoms, S., Zeebe, R.E., 2006. Determination of the rate constants for the carbon dioxide to bicarbonate inter-conversion in pH-buffered seawater systems. Mar. Chem. 100, 53–65. https://doi.org/10.1016/J.MARCHEM.2005.11.001

Shi, C., 2004. Steel Slag—its production, processing, characteristics, and cementitious properties. J. Mater. Civ. Eng. 16, 230–236. https://doi.org/10.1061/(ASCE)0899-1561(2004)16:3(230)

Sparks, D.L., 2003. Environmental Soil Chemistry. Academic Press, San Diego, California, USA. https://doi.org/https://doi.org/10.1016/B978-0-12-656446-4.X5000-2

Stegemann, J.A., Buenfeld, N.R., 2002. Prediction of leachate pH for cement paste containing pure metal compounds. J. Hazard. Mater. 90, 169–188. https://doi.org/10.1016/S0304-3894(01)00338-7

Stronach, S.A., Glasser, F.P., 1997. Modelling the impact of abundant geochemical components on phase stability and solubility of the CaO—SiO2 —H2O system at 25°C: Na+, K+, SO42-, Cl- and CO32-. Adv. Cem. Res. 9, 167–181. https://doi.org/10.1680/adcr.1997.9.36.167

Stumm, W., Morgan, J.J., 1996. Aquatic Chemistry : Chemical Equilibria and Rates in Natural Waters. Wiley & Sons, Hoboken, New Jersey, USA.

Theis, T.L., Halvorson, M., Levine, A., Stankunas, A., Unites, D., 1982. Fly ash attenuation mechanisms, Report and Technical Studies on the Disposal and Utilization of Fossil-Fuel Combustion By-products. USEPA, Washington, D.C., USA.

Thomas, M., 2007. Optimizing the use of fly ash in concrete. Skokie, Ill. Portl. Cem. Assoc. 24. https://doi.org/10.15680/IJIRSET.2015.0409047

Tombácz, E., 2009. pH-dependent surface charging of metal oxides. Period. Polytech. Chem. Eng. 53, 77. https://doi.org/10.3311/pp.ch.2009-2.08

Tsiridis, V., Petala, M., Samaras, P., Sakellaropoulos, G.P., 2015. Evaluation of interactions between soil and coal fly ash leachates using column percolation tests. Waste Manag. 43, 255–263. https://doi.org/10.1016/J.WASMAN.2015.05.031

van der Sloot, H.A., Kosson, D.S., van Zomeren, A., 2017. Leaching, geochemical modelling and field verification of a municipal solid waste and a predominantly non-degradable waste landfill. Waste Manag. 63, 74–95. https://doi.org/10.1016/J.WASMAN.2016.07.032

Warren, C.J., Dudas, M.J., 1989. Leachability and partitioning of elements in ferromagnetic fly ash particles. Sci. Total Environ. 84, 223–236. https://doi.org/10.1016/0048-9697(89)90385-9

Wen, H., Baugh, J., Edil, T., Wang, J., 2011. Cementitious high-carbon fly ash used to stabilize recycled pavement materials as base course. Transp. Res. Rec. J. Transp. Res. Board 2204, 110–113. https://doi.org/10.3141/2204-14

Yin, K., Ahamed, A., Lisak, G., 2018. Environmental perspectives of recycling various combustion ashes in cement production – A review. Waste Manag. 78, 401–416. https://doi.org/10.1016/J.WASMAN.2018.06.012

Zhang, M., Reardon, E.J., 2003. Removal of B, Cr, Mo, and Se from wastewater by incorporation into hydrocalumite and ettringite. Environ. Sci. Technol. 37, 2947–2952. https://doi.org/10.1021/ES020969I

Zhang, Y., Cetin, B., Likos, W.J., Edil, T.B., 2016. Impacts of pH on leaching potential of elements from MSW incineration fly ash. Fuel 184, 815–825. https://doi.org/10.1016/J.FUEL.2016.07.089

3.9   Tables and Figures

Table 3.1 Chemical composition of fly ashes, slag, cement and soil by X-ray fluorescence spectrometry (XRF)

Soil/Fly Ash/Slag	pH[*]	LOI (%)	SiO_2 (%)	Al_2O_3 (%)	Fe_2O_3 (%)	CaO (%)	SO_3 (%)	MgO (%)	Classification
FA-1	12.01	0.24	37.6	18.0	5.9	25.9	1.2	5.2	C FA[**]
FA-2	11.64	0.14	56.3	18.6	5.5	11.8	0.4	2.9	F FA[**]
Slag	11.60	-	35.7	9.9	0.6	39.8	1.1	10.4	N/A
Cement	12.65	2.45	20.0	4.4	3.0	64.0	2.9	2.2	Type I/II[***]
Loess	8.57	6.91	67.7	9.6	3.3	5.2	0.03	2.1	ML[****]

Note: FA: Fly ash; [*]ASTM D 4793; LOI: Loss on ignition; Hyphen: not available; C FA: Class C fly ash; F FA: Class F fly ash; [**]ASTM C618-17a; [***]ASTM C150/C150M -18; N/A: Not applicable; [****]USGS classification.

Table 3.2 Total metal content of the fly ashes, slag, cement and loess soil determined following the U.S. EPA Method 3050B

Soil/Fly Ash/Slag	Al (mg/kg)	Cu (mg/kg)	Fe (mg/kg)	Zn (mg/kg)	S (mg/kg)
C FA	59700	148	34348	98	9103
F FA	35143	64	21686	49	3176
Cement	10514	27	10476	43	18200
Slag	29529	20	2289	26	12600
Loess	5725	18	13370	44	916

Note: FA: Fly ash.

Table 3.3 Basic properties of fly ashes, slag and soil used in study

Soil/Fly Ash/Slag	Percent Fine (%)	Percent Clay (%)	Initial Moisture, w/w (%)	C_u	C_c	G_s	LL (%)	PI (%)
C FA	91	8	0.05	3.33	1.31	2.70	NP	NP
F FA	88	3	0.03	22.78	12.19	2.67	NP	NP
Slag	73	7	0.07	3.18	1.5	2.55	NP	NP
Loess	92	11	1.34	10.67	3.38	2.74	24	4

Notes: Fine < 75 µm; Clay < 0.02 mm; C_u: Coefficient of uniformity; C_c: Coefficient of curvature; G_s: Specific gravity; LL: Liquid limit; PI: Plasticity index; NP: Nonplastic.

Table 3.4 Experimental setup of the study

Fly Ash/ Slag Type	Soil Content (%)	Fly Ash Content (%)	Type I/II Cement Content (%)	Optimum Moisture, OMC (%)	Max. Dry Density, γ_{dmax} (kN/m^3)
Class C FA	87	10	3	18.8	16.6
	84	10	6	17.0	16.6
	74	20	6	14.5	17.0
	54	40	6	14.0	16.7
Class F FA	87	10	3	17.5	16.5
	84	10	6	18.0	16.6
	74	20	6	17.0	16.8
	54	40	6	15.2	17.0
Slag	87	10	3	18.5	16.3
	84	10	6	18.0	16.6
	74	20	6	17.0	16.7
	54	40	6	18.7	16.8
Loess	100	0	0	16.2	16.7

Note: FA: Fly ash; OMC: Weight basis.
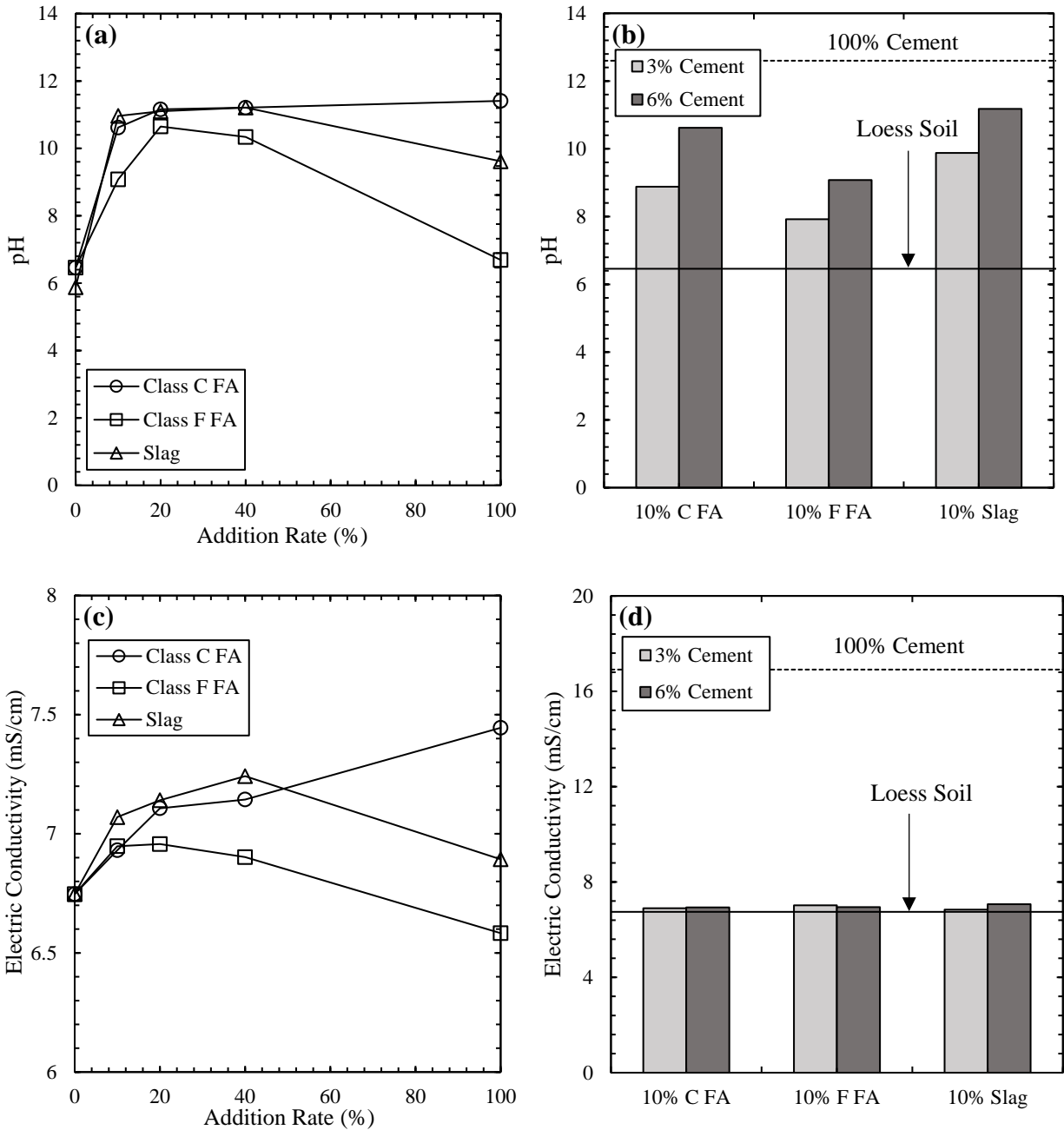
Figure 3.1 Change in (a) pH with FA and slag content, (b) pH with cement content, (c) EC with FA and slag content and (d) EC with cement content in TCLP effluent. *Note:* Zero and hundred percent corresponds to soil and FA/slag only. FA- Fly ash. EC- electric conductivity
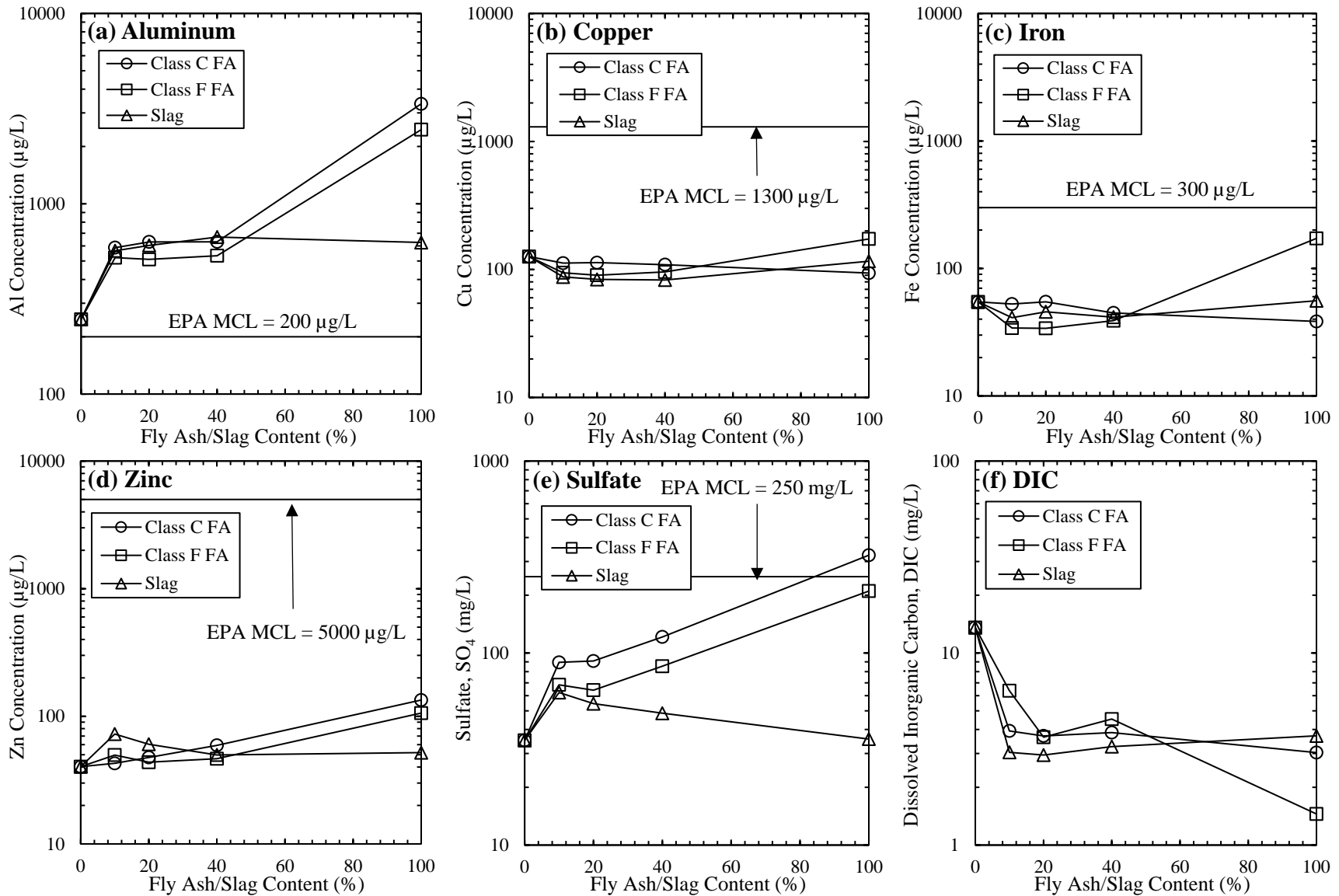
Figure 3.2 Effect of FA/slag content on effluent concentration of (a) Al, (b) Cu, (c) Fe, (d) Zn, (e) SO₄ and (f) DIC in TCLP effluent
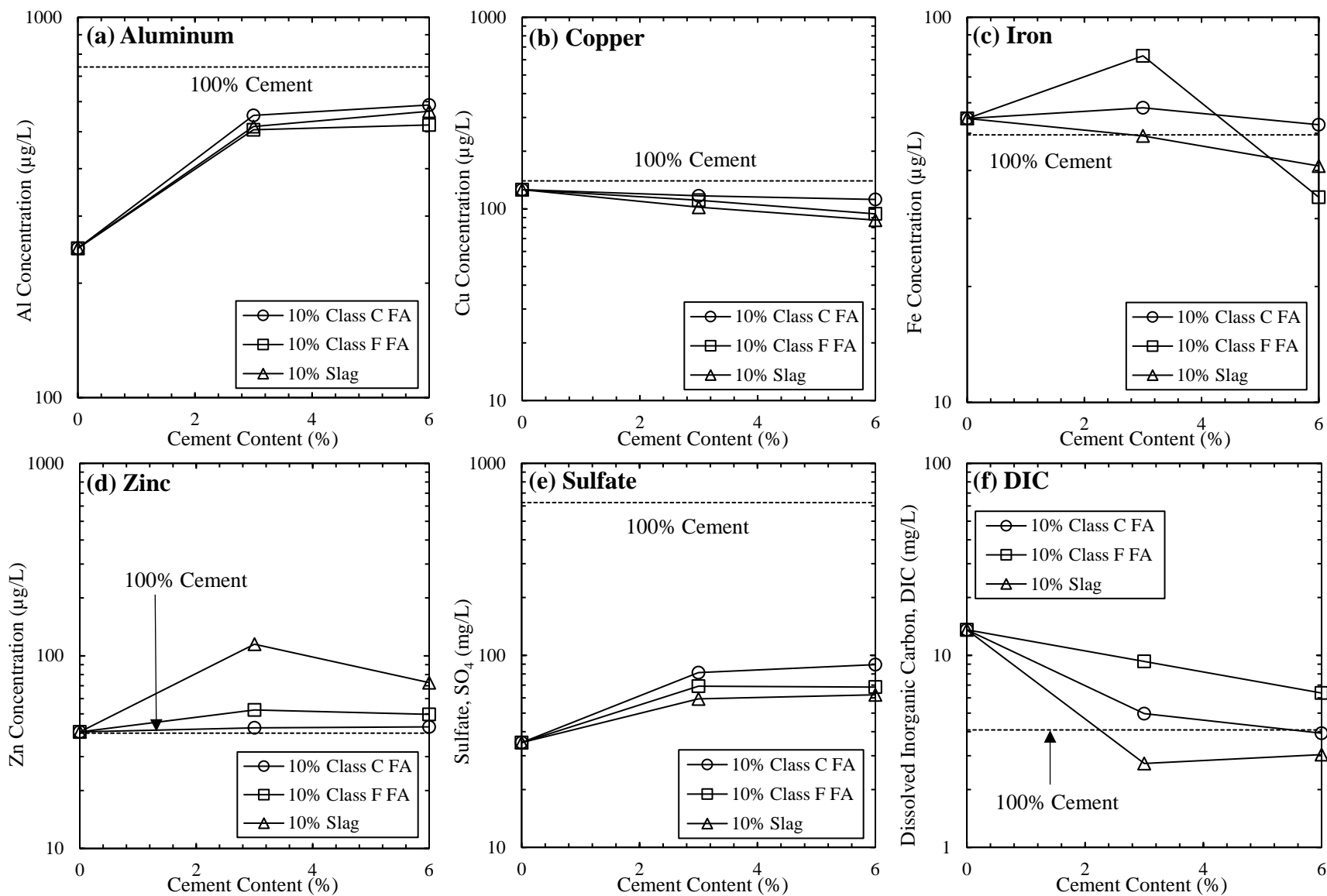
Figure 3.3 Effect of cement content on effuent concentration of (a) Al, (b) Cu, (c) Fe, (d) Zn, (e) SO₄ and (f) DIC in TCLP
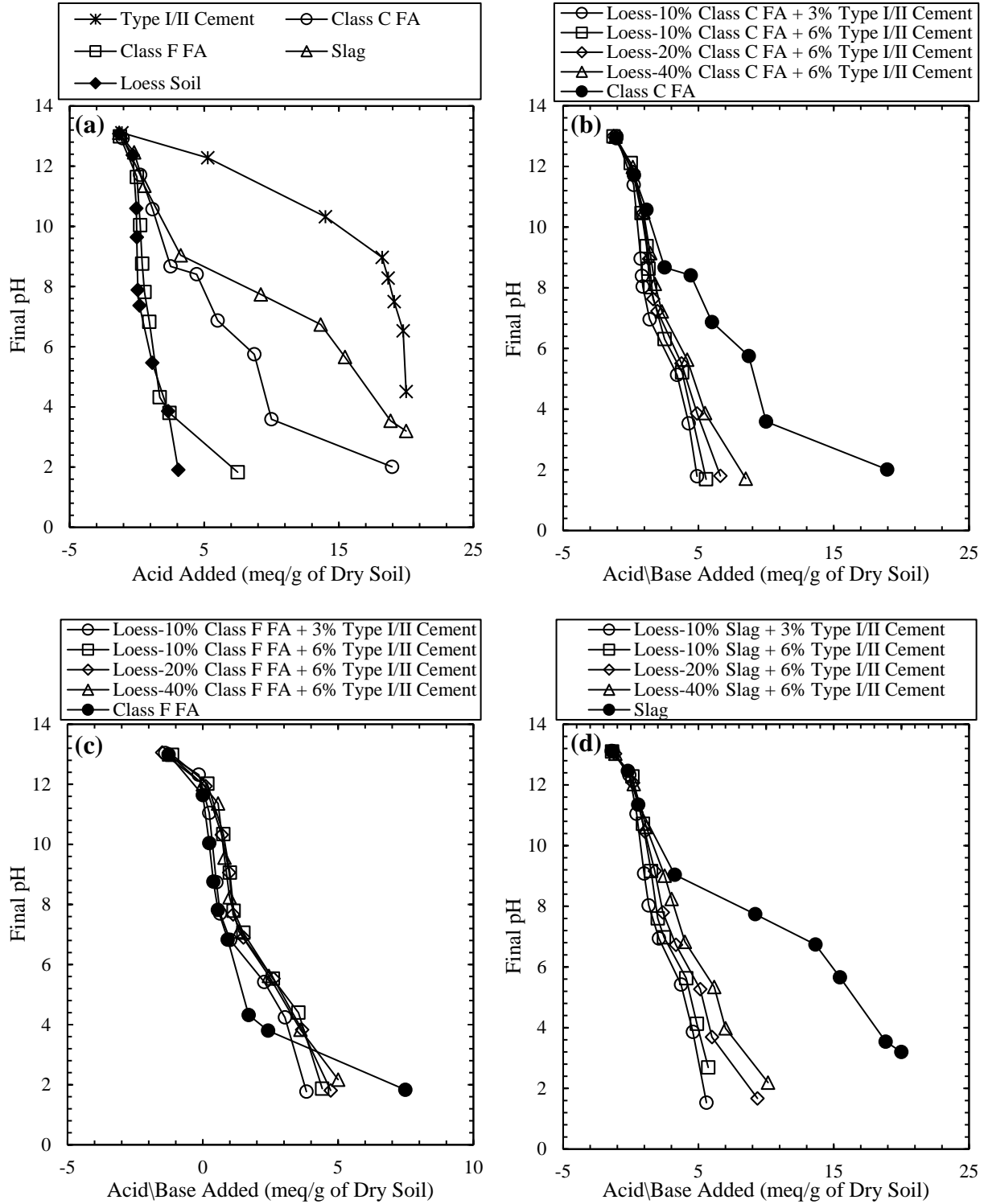
Figure 3.4 Acid neutralizing capacity (ANC) of (a) soil, cement, fly ashes and slag, (b) Class C FA mixtures, (c) Class F FA mixtures and (d) slag mixtures. *Note:* FA- Fly ash
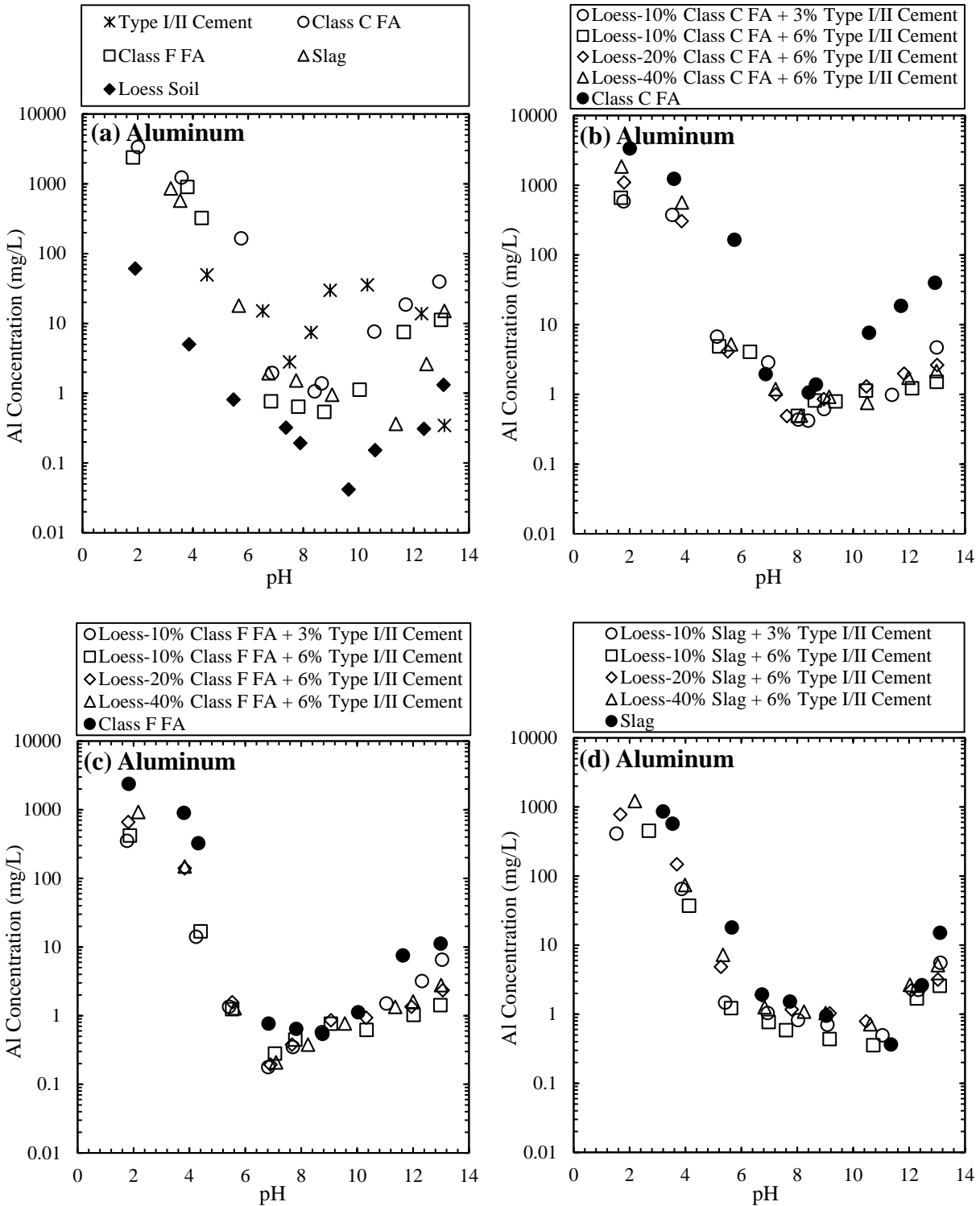
Figure 3.5 pH dependent leaching of Al in the leachates from (a) soil, cement, fly ashes and slag, (b) Class C FA mixtures, (c) Class F FA mixtures and (d) slag mixtures. *Note:* FA- Fly ash
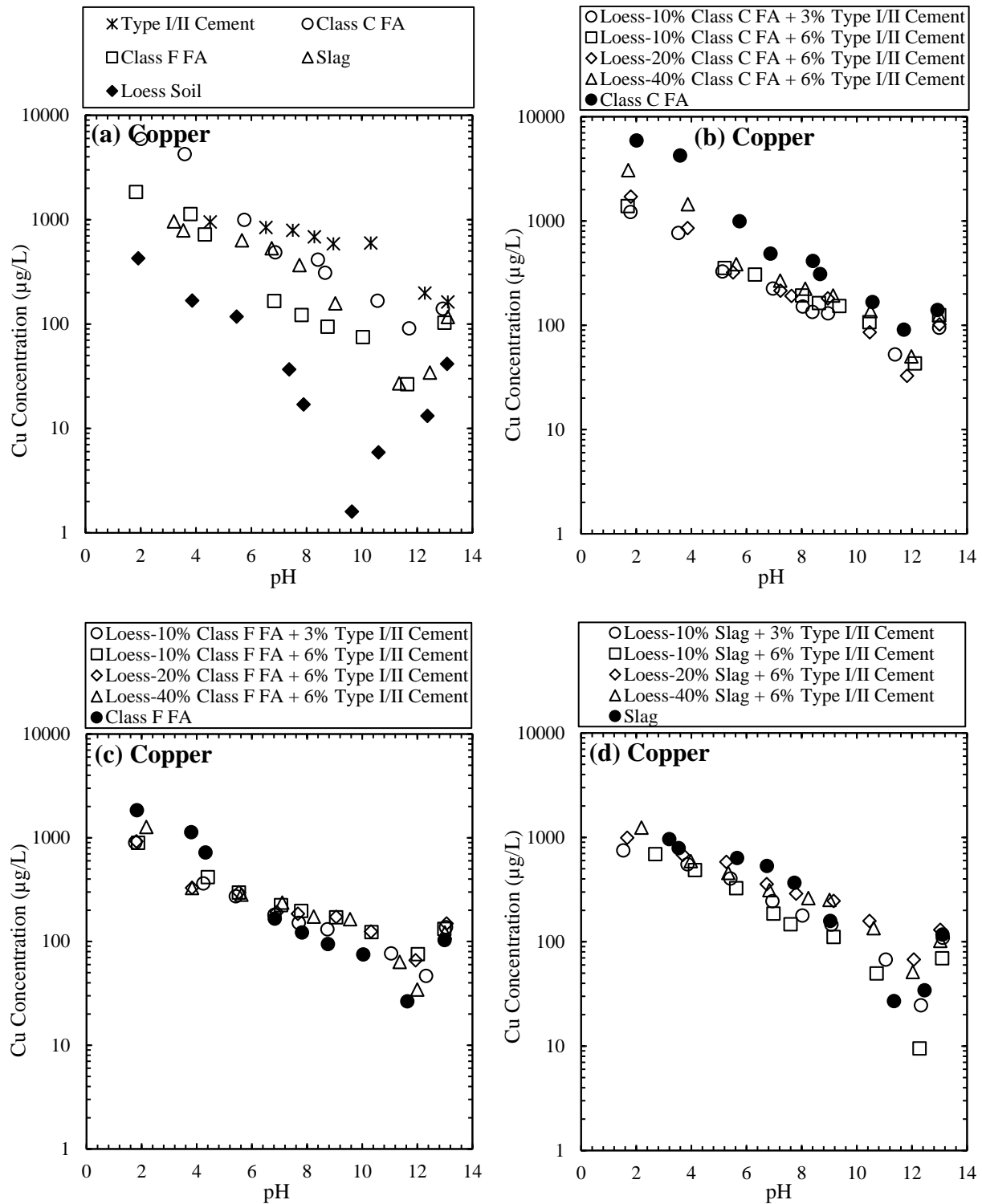
Figure 3.6 pH dependent leaching of Cu in the leachates from (a) soil, cement, fly ashes and slag, (b) Class C FA mixtures, (c) Class F FA mixtures and (d) slag mixtures. *Note:* FA- Fly ash

83
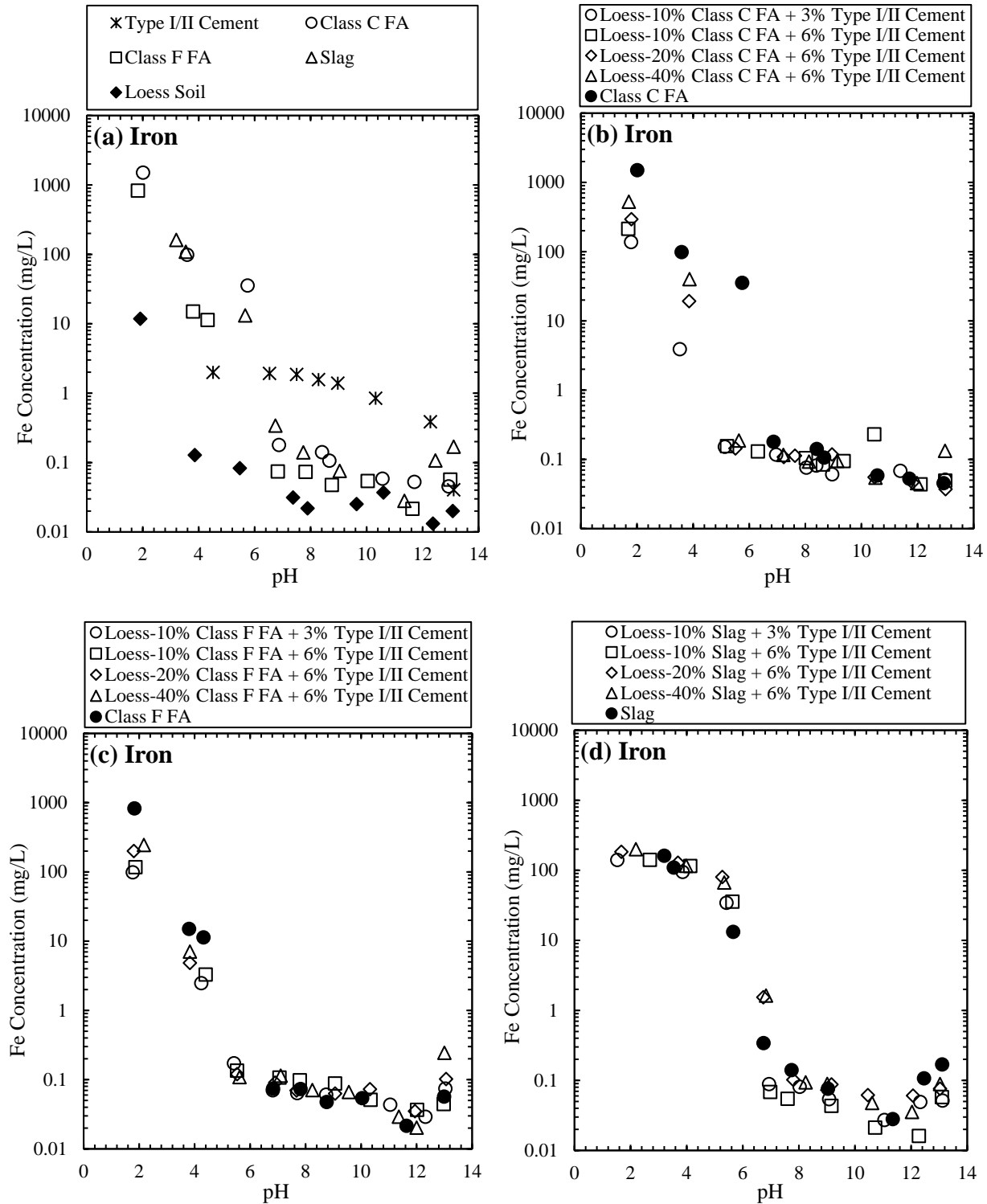
Figure 3.7 pH dependent leaching of Fe in the leachates from (a) soil, cement, fly ashes and slag, (b) Class C FA mixtures, (c) Class F FA mixtures and (d) slag mixtures. *Note:* FA- Fly ash
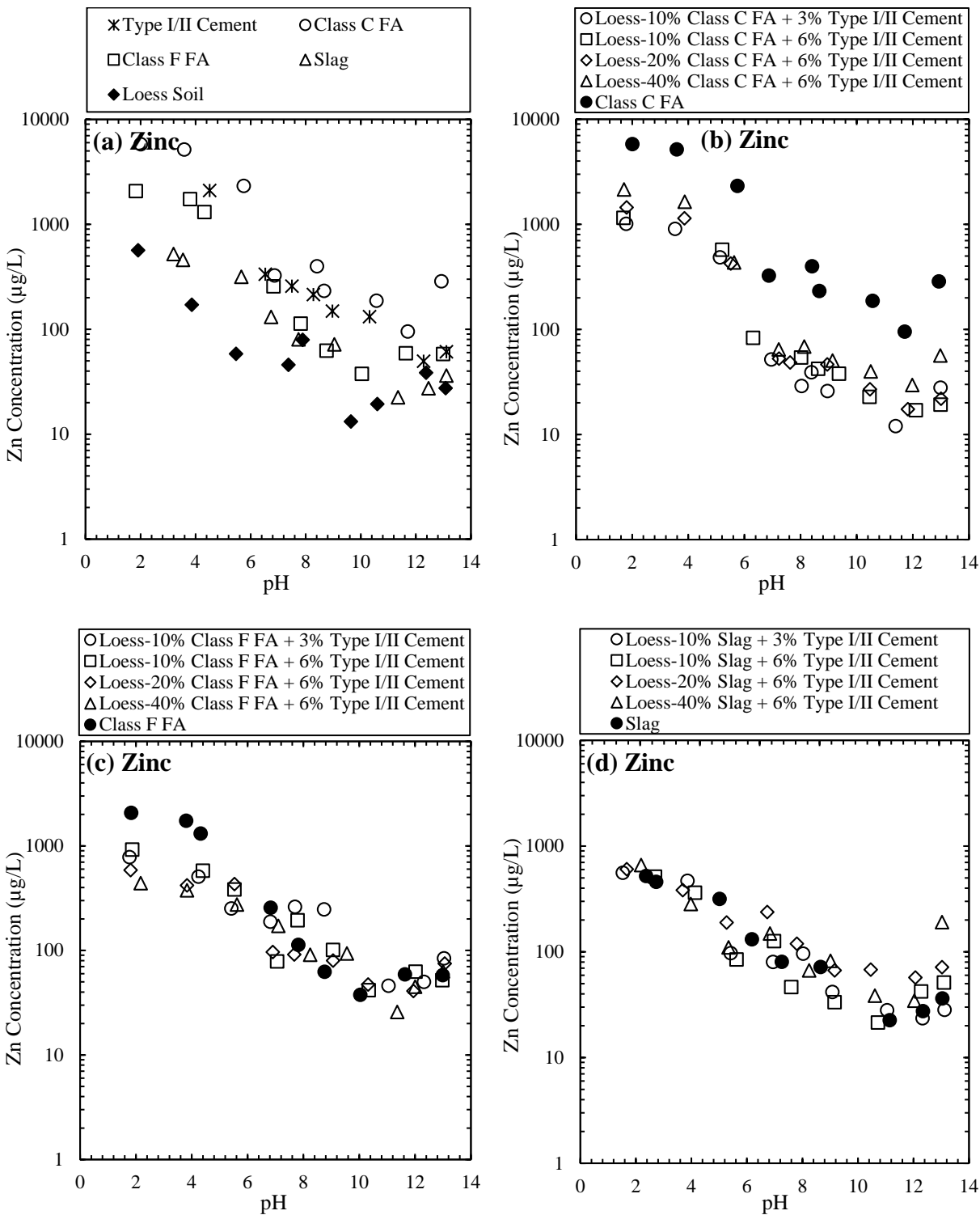
Figure 3.8 pH dependent leaching of Zn in the leachates from (a) soil, cement, fly ashes and slag, (b) Class C FA mixtures, (c) Class F FA mixtures and (d) slag mixtures. *Note:* FA- Fly ash
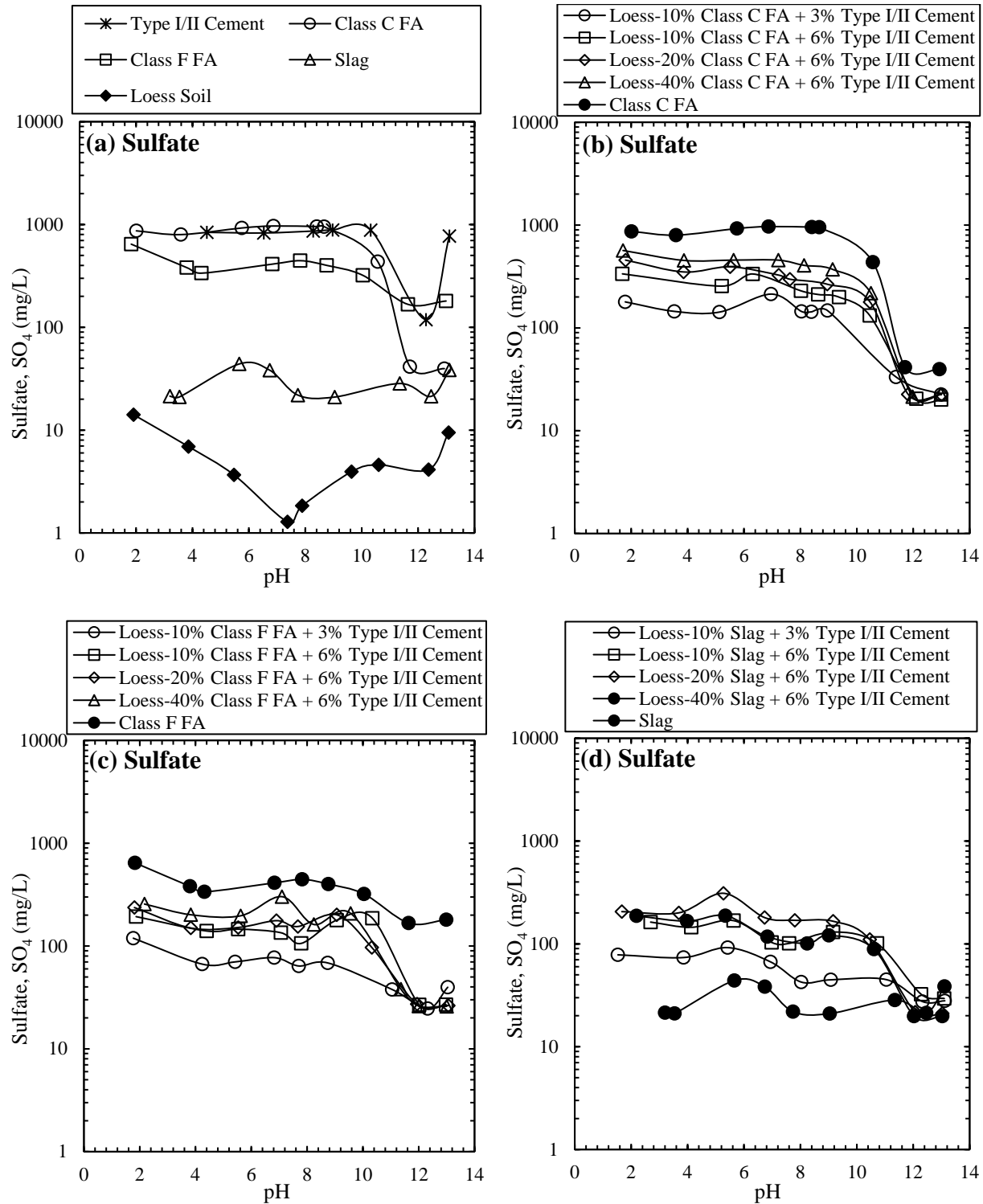
Figure 3.9 pH dependent leaching of SO4 in the leachates from (a) soil, cement, fly ashes and slag, (b) Class C FA mixtures, (c) Class F FA mixtures and (d) slag mixtures. *Note:* FA- Fly ash
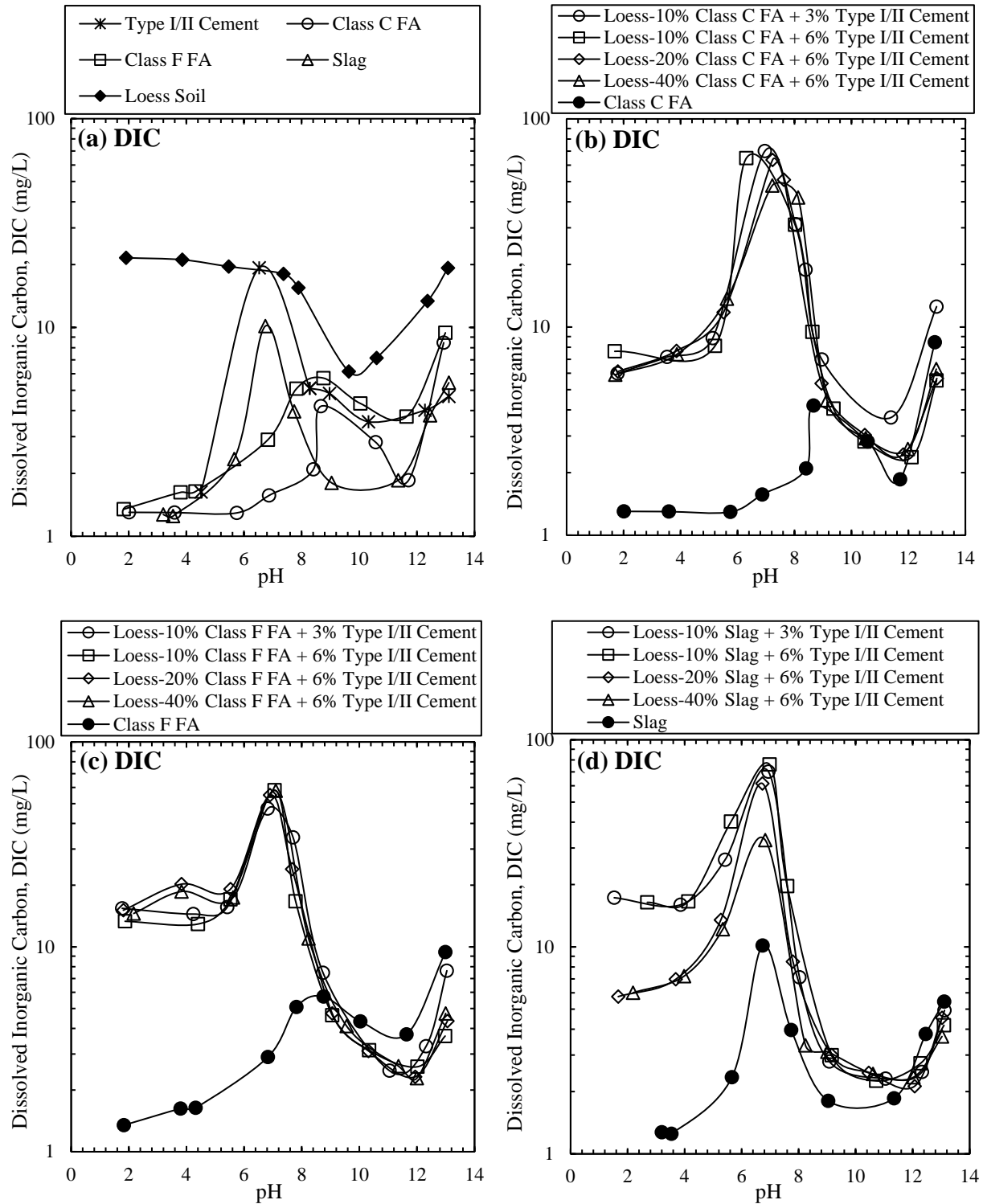
Figure 3.10 pH dependent leaching of DIC in the leachates from (a) soil, cement, fly ashes and slag, (b) Class C FA mixtures, (c) Class F FA mixtures and (d) slag mixtures. *Note:* FA- Fly ash
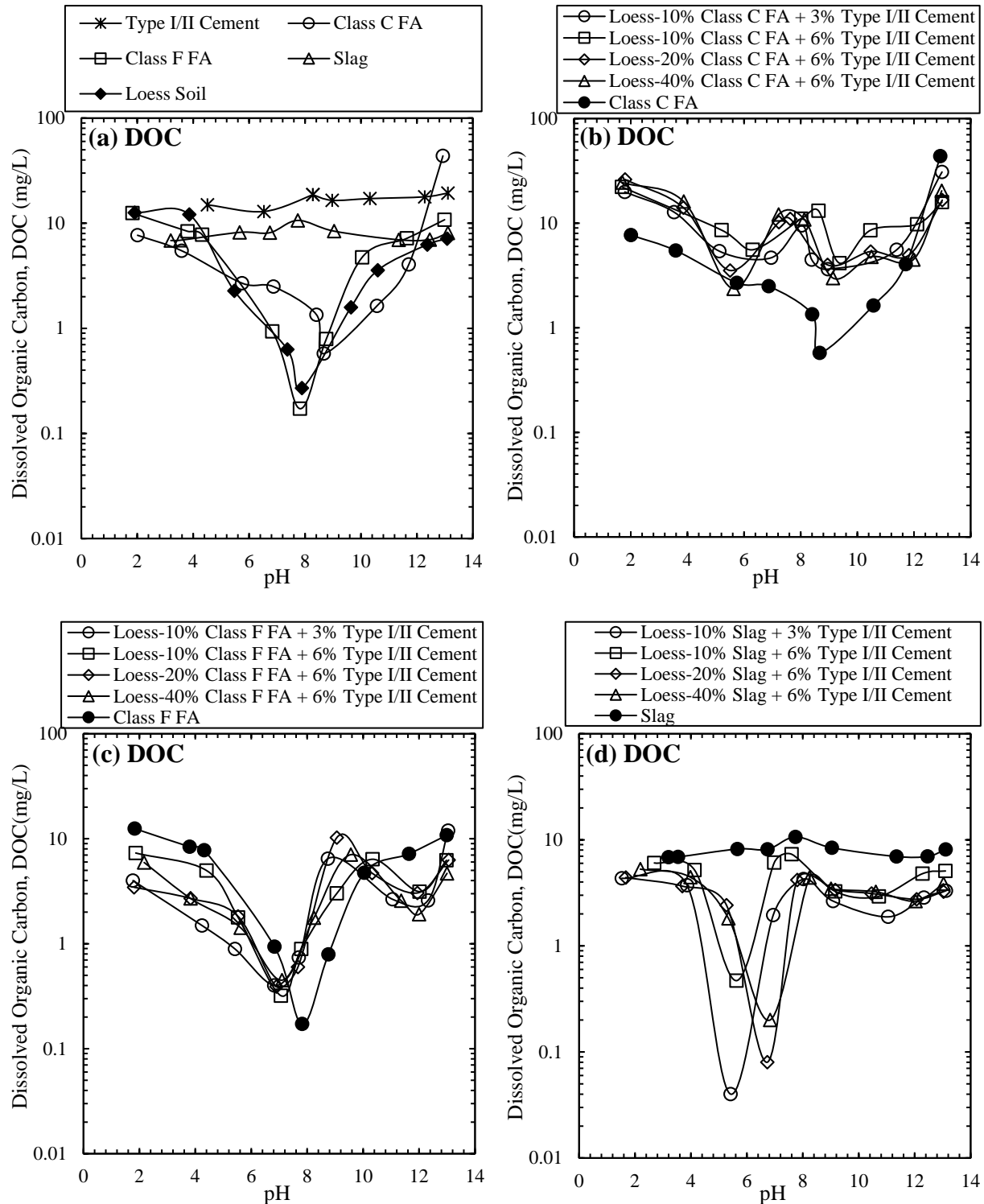
Figure 3.11   pH dependent leaching of DOC in the leachates from (a) soil, cement, fly ashes and slag, (b) Class C FA mixtures, (c) Class F FA mixtures and (d) slag mixtures. *Note:* FA- Fly ash
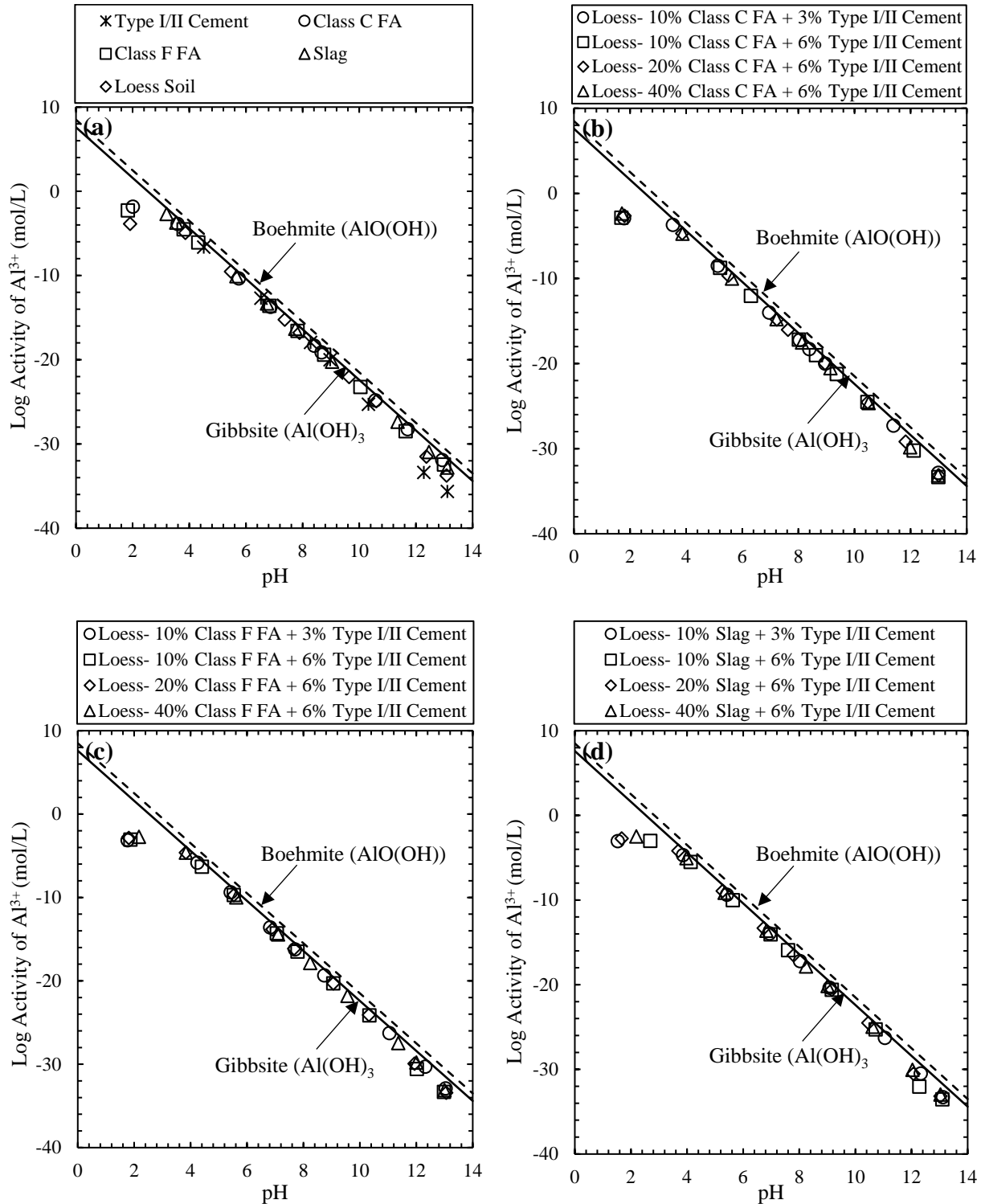
Figure 3.12 Log activity of Al^{3+} with pH in the effluent from (a) soil, cement, fly ashes and slag, (b) Class C FA mixtures, (c) Class F FA mixtures and (d) slag mixtures. *Note:* FA- Fly ash
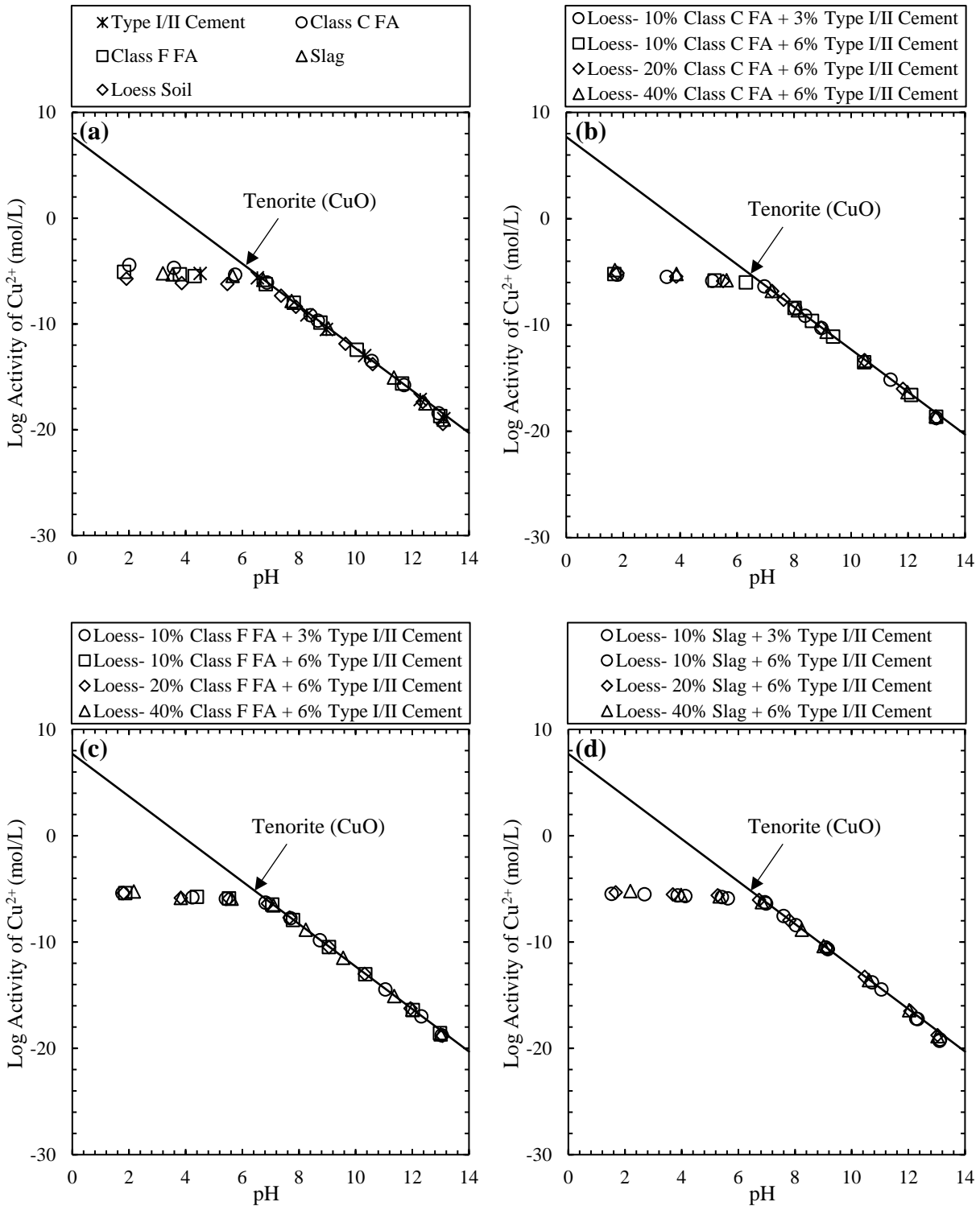
Figure 3.13   Log activity of Cu^{2+} with pH in the effluent from (a) soil, cement, fly ashes and slag, (b) Class C FA mixtures, (c) Class F FA mixtures and (d) slag mixtures. *Note:* FA- Fly ash
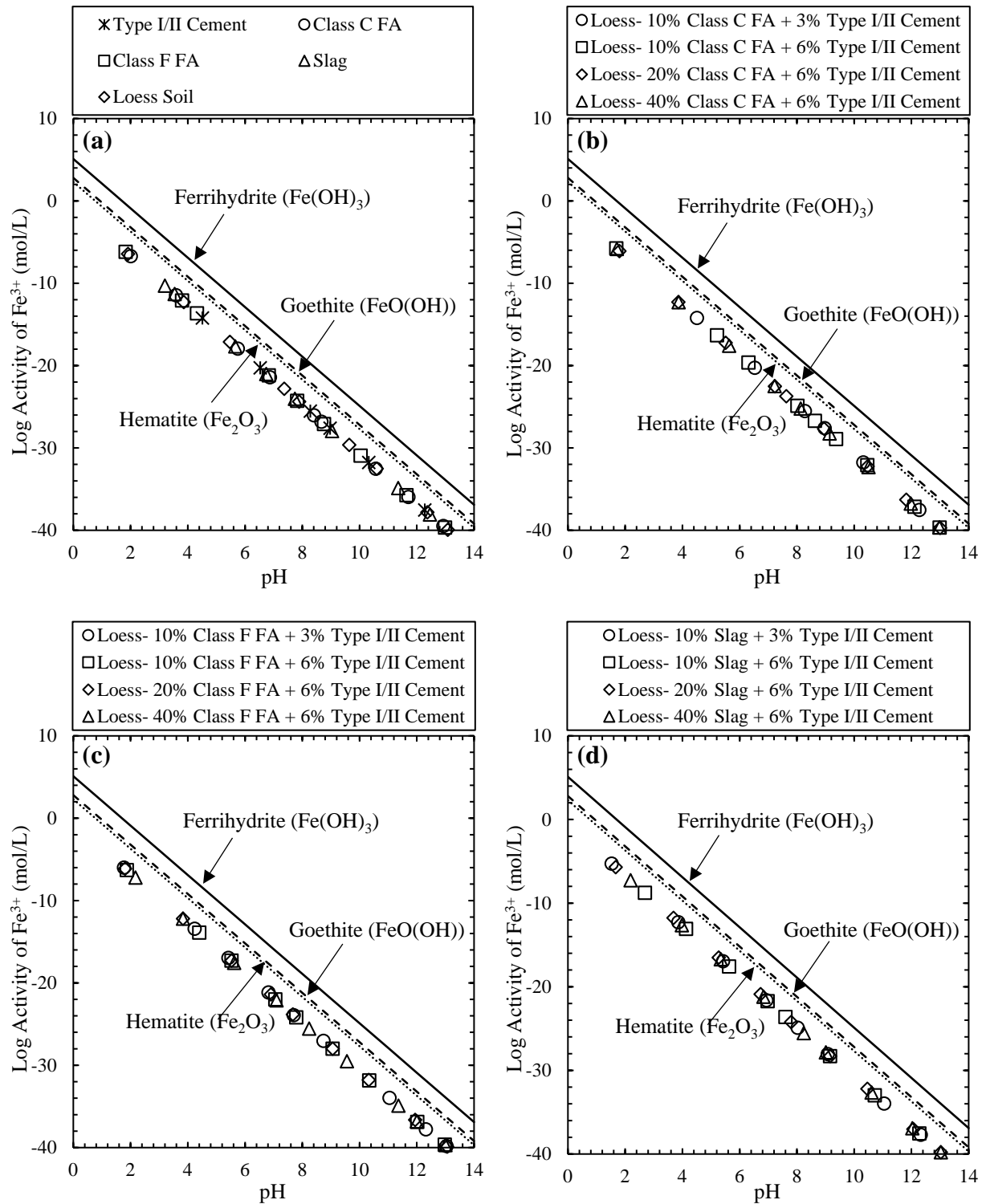
Figure 3.14 Log activity of Fe^{3+} with pH in the effluent from (a) soil, cement, fly ashes and slag, (b) Class C FA mixtures, (c) Class F FA mixtures, and (d) slag mixtures. *Note:* FA- Fly ash
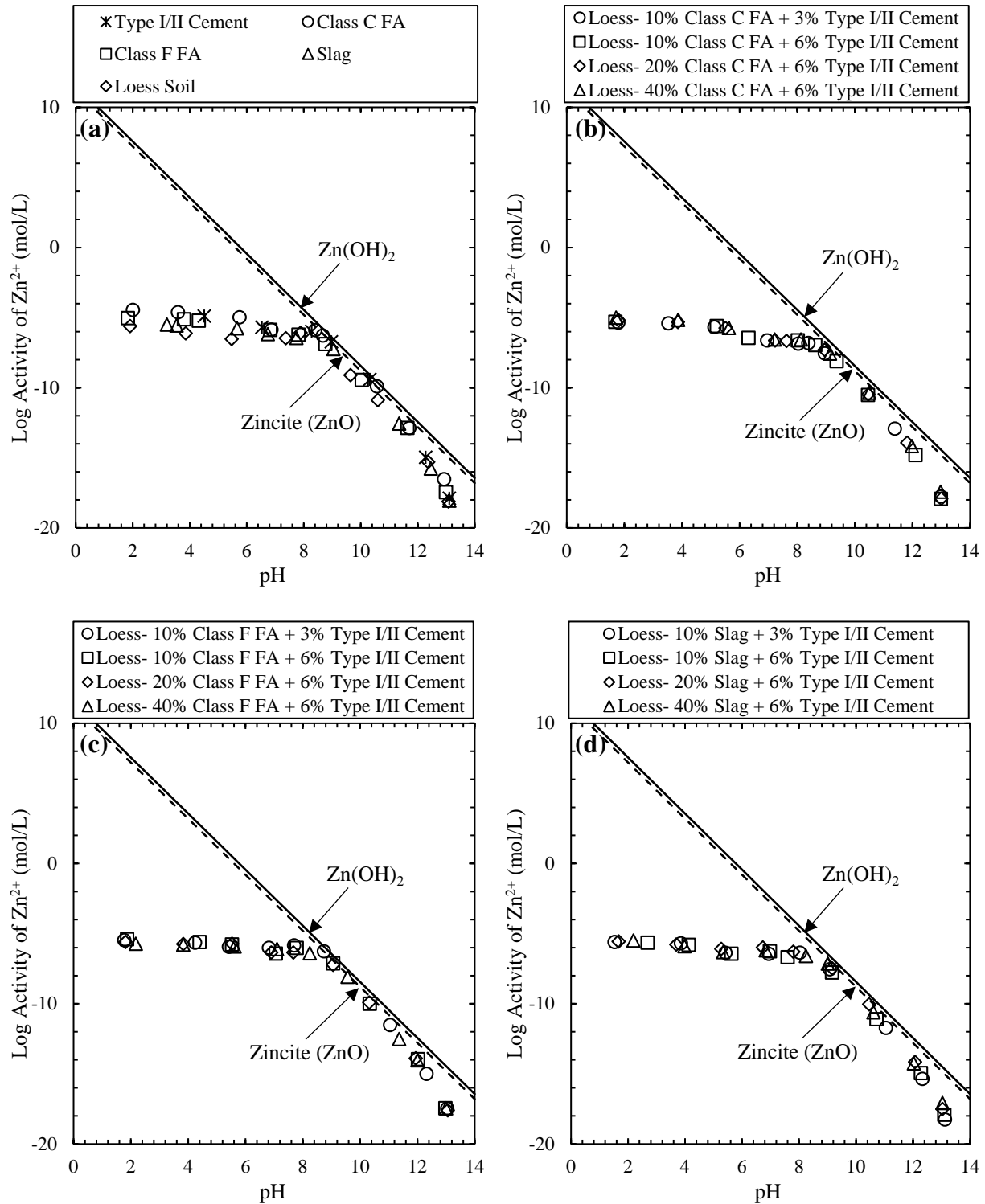
Figure 3.15 Log activity of Zn^{2+} with pH in the effluent from (a) soil, cement, fly ashes and slag, (b) Class C FA mixtures, (c) Class F FA mixtures and (d) slag mixtures. *Note:* FA- Fly ash

CHAPTER 4. GEO-ENVIRONMENTAL ASSESSMENT OF CEMENT ACTIVATED FLY ASH AND SLAG STABILIZED SOILS: LEACHING BEHAVIORS

A paper to be submitted to *Journal of Environmental Management*

Masrur Mahedi, Bora Cetin and Asli Y. Dayioglu

4.1   Abstract

Very few studies have investigated the leaching behavior of elements from cement activated fly ash and slag treated soils, although the inclusion of cement significantly enhances the material pH and may alter the leachability of the elements. This study sought the leaching behavior of Ca, Mg, S, Mn, Ba, Cr and total dissolved carbon (TDC) from cement activated soil-fly ash, soil-slag mixtures and soil, fly ash, slag and cement alone. Batch water leach tests, acid neutralization capacity (ANC) and pH-dependent leach tests were performed on type I/II Portland cement activated Class C fly ash, Class F fly ash and ground granulated blast-furnace slag stabilized soils. Effluent concentrations of Ca and Ba increased, Mg decreased, S and TDC varied, and Cr and Mn remained unaffected by cement content. Solution pH had the greatest influence on the leaching behaviors of the elements. Ca, Mg, S and Mn followed cationic leaching patters, whereas Ba showed both cationic and amphoteric leaching characteristics. The highest concentrations of Cr were found at extreme acidic conditions, followed by a concentration plateau in the pH range of 5.5 to 10, and subsequent decrease and increase in concentrations at pH of 11.5 and 13, respectively. Geochemical modeling results suggested that except for Cr, the leaching mechanisms of the elements were controlled by their sulfate and (hydr)oxide minerals. The leaching of Cr was possibly controlled by $BaCrO_4$ and $CaCrO_4$. Carbonate minerals may not play a significant role on the leaching mechanisms when cement is used as an activator.

Keywords: Leaching, metals, batch water leach test, pH-dependent leach test, fly ash, slag, cement, geochemical modeling

4.2   Introduction

Despite of the potential of renewable energy, electricity demand surged by urbanization and industrial sprawl is largely dependent on the coal combustion power plants. These coal-based power plants generate huge amount of fly ashes in both industrialized and developing countries. According to American Coal Ash Association (ACAA), in 2017 around 38.2 million tons of fly ashes were generated in the United States, and 24.1 million tons of these were reused (ACAA, 2018). Fly ashes are pozzolanic materials, containing varying amount of lime (CaO), silica (SiO_2), alumina (Al_2O_3) and iron oxide (Fe_2O_3); capable of producing calcium-silicate and calcium-aluminate hydrates while reacting with water (Thomas, 2007). Some fly ashes (e.g., Class C fly ash) exhibit self-cementing capabilities owing to the presence of higher amount of CaO, while others (e.g., Class F fly ash, high carbon fly ash) produce supplementary cementitious compounds by reacting with an activator (i.e., lime, cement, kiln dust) (Cetin et al., 2010). Similarly, steel slags are produced as the by-product from iron manufacturing industries, consisting silicates and alumino-silicates of calcium and magnesium (Shi, 2004). As of 2017, the estimated ferrous slag production in the U.S. was 15 to 20 million tons (U.S. Geological Survey, 2018). These materials: fly ash and slag, have been successfully utilized in a variety of civil engineering applications for many years. Previous studies showed the effectivity of fly ashes and slags in soil stabilization by ensuring adequate strength, stiffness and durability requirements (Dayioglu et al., 2014; Mahedi et al., 2019, 2018; Tastan et al., 2011; Yilmaz et al., 2019). In-situ soil stabilization becomes more practical and economical by fly ash and slag, especially in places with fine-grained soils where excavation and replacement are costly and labor intensive. However, during the coal combustion process at high temperatures, coal minerals undergo phase transformations which may cause subsequent leaching of toxic elements from fly ashes (Jones, 1995). In addition, Dayioglu et al.

(2018), Gomes and Pinto (2006) reported the leaching of heavy and toxic metals from steel slags at different environmental conditions.

Toxic elements from fly ashes and slag are likely to leach with water, regardless the application, storage and disposal conditions. Deportation of these harmful elements contaminate surface and groundwater posing significant threat to the living organisms, including substantial human health hazard (Cetin et al., 2012b; Chowdhury et al., 2016). Therefore, leaching potential and behavior of toxic elements from these recycled products have become a growing concern. Previous studies investigated the leaching behavior of elements from different fly ash, slag, and fly ash stabilized soils focusing the elements of environmental concern; while overlooking other non-hazardous elements such as Ca, Mg and total dissolved carbon (TDC) (Cappuyns et al., 2014; Cetin et al., 2012b, 2012c; Komonweeraket et al., 2015b; Kosson et al., 2014; Sas et al., 2015; Windt et al., 2011; Zhang et al., 2016). These nontoxic elements are largely released from fly ash and slag and their mode of occurrence, precipitation and substitution essentially control the effluent pH and subsequently the leachability of toxic elements (Izquierdo and Querol, 2012). Moreover, inadequate information exists on the leaching behavior of elements from cement activated fly ash and slag stabilized soils. It is anticipated that cement inclusion would alter the leachability of elements by enhancing the solution pH significantly.

Few studies have been undertaken on the leaching behavior of fly ash-cement and slag-cement stabilized soils (Akhter et al., 1990; Allan and Kukacka, 1995; Kogbara et al., 2014, 2013; Li et al., 2018; Wang et al., 2018). Most of these studies focused on the leachability of contaminated soils, which were prepared in controlled laboratory conditions by adding aqueous metal solutions to an unadulterated soil. Fly ash-cement, and/or slag-cement were used as a composite grout where fly ash and slag application rates were limited. These grouts were used as

a remediation technique of the stabilized/solidified (S/S) contaminated soils. However, as mentioned earlier, fly ash and slag are identified as a potential source of leaching for toxic elements. The influence of fly ash or slag content on the leaching of elements from stabilized soils needs to be addressed. Additionally, the leaching of metals was only evaluated for a limited pH range, though the solution pH is the most crucial parameter controlling the leaching of substances from solid to liquid phase (Fruchter et al., 1990; Komonweeraket et al., 2015c; Mudd et al., 2004). Pertinent information for the assessment of leaching mechanisms are obtained by pH dependent leaching of elements (Dijkstra et al., 2002). Furthermore, to the best of our knowledge, the leaching controlling mechanisms of elements from cement activated fly ash and slag stabilized soils yet remained unexplored. The effect of cement as an activator also stayed uncharted.

Based on experimental and numerical assessments, the main objectives of this study were to investigate the leaching behavior and leaching mechanisms of elements from cement activated fly ash and slag stabilized soils. Two different fly ashes, Class C and F and ground granulated blast-furnace steel slag, were utilized because of their widespread implications in soil stabilization. Type I/II Portland cement was applied as an activator for fly ash and slag stabilization. Batch water leach tests (WLT) were performed on cement activated soil-fly ash, soil-slag mixtures and soil, fly ashes, slag and cement alone to evaluate the leaching behavior of metals as a function of fly ash, slag and cement contents. An experimental array of 17 blends were prepared, and the leached concentrations of Ca, Mg, S, Mn, Ba, Cr and TDC were considered. pH-dependent leach tests were performed to investigate the influence of pH on the leaching characteristics of elements in the pH range of 2 to 13. pH dependent leaching of the elements from soil-fly ash-cement and soil-slag-cement mixtures were compared to soil, fly ash, slag and cement alone. Furthermore, geochemical modeling program Visual MINTEQ was implemented for speciation analyses and to identify the

leaching controlling mechanisms of elements from cement activated fly ash and slag stabilized soils.

4.3   Materials

Two different fly ashes (FA) and ground granulated blast furnace steel slag (Slag) were used in the current study. Type I/II Portland cement was implemented as an activator due to lower cementation properties of fly ashes and slag. The chemical compositions of the fly ashes, slag and cement were determined by X-ray fluorescence spectrometry (XRF) and are reported in Table 4.1. Following ASTM C618, fly ashes were classified as Class C and F, respectively. As tabulated in Table 4.1, CaO content of slag was higher (39.8%) compared to the fly ashes, nonetheless the effluent pH was lower (11.6). This indicated the insoluble forms of Ca in slag and the necessity of an activator such as cement. The total metal contents of the stabilizers were also determined following the U.S. EPA Method 3050B and are summarized in Table 4.1. Table 4.1 indicates that Ca and S contents were the highest in cement, whereas maximum Mg and Mn contents were detected in slag. Class C fly ash had the highest Ba and Cr contents.

Frost susceptible Iowa loess soil, often subjected to the chemical treatments was selected for the current study. Grain size distributions of the soil, fly ashes and slag were performed in accordance with ASTM C136 and are presented in Figure 4.1. The liquid limit (LL) and plasticity index (PI) of the soil were determined to be 24 and 4, respectively (ASTM D4318). According to Unified Soil Classification System (USCS), the soil was classified as low plasticity silt (ML). Additionally, loess soil was found to be calcareous with higher Ca and Mg contents from total elemental analysis. The pH of the soil was 8.57 which is moderately alkaline. Moreover, the specific gravity of soil along with fly ashes and slag was determined following ASTM D854 and are reported in Table 4.1.

4.4   Method

4.4.1   Sample Preparation

Cement activated soil-fly ash and soil-slag mixtures were prepared by both varying fly ash/slag and cement contents to investigate the compositional influence of the stabilizing agents on the leaching behavior of elements. An array of mixtures was prepared based on strength and stiffness requirements determined by previous studies (Aldeeky and Al Hattamleh, 2017; Oormila and Preethi, 2014; Tastan et al., 2011; Yilmaz et al., 2019), where the recommended maximum use of fly ash or slag for soil stabilization was 20%. In addition, 40% soil-fly ash and soil-slag mixtures were prepared to investigate the leaching behavior of elements as a function of fly ash or slag content. All the blends contained either 3% or 6% of type I/II Portland cement. A summary of the blends along with the optimum moisture content (OMC) and maximum dry density (MMD) determined by ASTM D698 is provided in Table 4.2. The OMC and MMD of the mixtures were in the range of 14% to 18.8% and 16.3 kN/m3 to 17 kN/m3, respectively. All the soil-fly ash-cement and soil-slag-cement mixtures were prepared at OMC on dry weight basis. The mixtures were cured in plastic bags for 7 days at room temperature (21°C) and 100% relative humidity chamber. Cured samples were crushed and passed through U.S. No. 10 sieve for leach test sample preparation. Leach tests were also performed on untreated soil and stabilizers alone for an overall understanding of the leaching behaviors, leaching mechanisms and comparisons.

4.4.2   Batch Water Leach Test (WLT)

Batch water leach tests (WLT) were performed in accordance with ASTM D4793. A liquid to solid (L/S) ratio of 10 was used to simulate the representative field conditions (Kosson et al., 2002). The influent solution for WLT was prepared with 0.02 M NaCl (sodium chloride) to provide stable reaction conditions (Cetin et al., 2014). The mixtures were rotated at 29 rpm for 18±0.25 hours. Once the equilibrium condition was established, pH and electric conductivity of the

supernatant fluid were measured. The solutions were then pressure filtered through 0.2-µm pore size and 25 mm diameter membrane disk filter papers, using acid washed pressure filter holders fitted to 60 mL plastic syringes. A portion of the filtered extract was acidified with 10% trace metal grade nitric acid (HNO3) to a pH less than 2 and stored in refrigerator at temperature less than 4 ºC for metal analysis. Another non-acidified aliquot was immediately subjected to total dissolved carbon (TDC) measurements.

4.4.3 pH-Dependent Leach Test

pH-dependent leach tests were performed on cement activated soil-fly ash, soil-slag mixtures and soil, fly ashes, slag, cement alone following the U.S. EPA Method 1313 to quantify the effect of pH on the liquid-solid partitioning (LSP) curves of the elements. A liquid to solid (L/S) ratio of 10 was maintained throughout the experimental program. Samples were prepared at 9 different target pH values (2, 4, 5.5, 7, 8, 9, 10.5, 12 and 13; ±0.5). The target pH values represent diverse exposure conditions, such as natural stabilized soil, neutral environment, landfill situation, acid rain and field environment. Nano-pure water with 1 N potassium hydroxide (KOH) or 2 N trace metal grade nitric acid (HNO3) was used to attain the target pH values. The required volumes of acid, base and water for a specific pH were pre-determined by exploiting the acid neutralization capacity (ANC) of the mixtures. ANCs were evaluated by adding varying quantities of acid, base and water with a 40 g of mixtures at a constant liquid-solid (L/S) ratio of 10. Moisture content of the mixtures (i.e., OMC) was also considered. Solutions were then agitated at a rotation rate of 28 rpm for 48 ± 2 hours. Lastly, the pH of the solutions was determined to quantify the acid/base buffering capacity of the mixtures. Final pH-dependent leach test samples were also agitated for 48 ± 2 hours at a rotation rate of 28 rpm. After rotation, effluent pH and electric conductivity (EC)

were measured. The extracts were then pressure filtered and stored for chemical analyses following the same procedures adopted for WLTs.

4.4.4   Chemical Analysis

Inductively coupled plasma optical emission spectroscopy (ICP-OES) was utilized for the elemental analyses of the extracted leachate. The ICP-OES was calibrated with known concentrations of multi-element standards. Due to a wide range in metal concentrations, multiple calibration curves were prepared for pH-dependent leach test samples. Check standards and blanks were analyzed at every 9 samples to verify the calibration curves and to ensure uniform aspiration condition. The minimum detection limits (MDLs) of ICP-OES for Ca, Mg, Mn, Ba, S and Cr were 2.2 µg/L, 1.2 µg/L, 0.4 µg/L, 0.4 µg/L, 22 µg/L and 0.5 µg/L, respectively.

The concentrations of TDC in the extracts were measured by Shimadzu TOC-V analyzer with ASI-V auto-sampler. The instrument was calibrated by potassium hydrogen phthalate ($C_8H_5KO_4$) standard solutions. Samples were introduced to total carbon (TC) combustion tube and heated to 680 ℃ with the presence of an oxidizing catalyst. The oxidizing catalyst was prepared by dissolving specific amount of sodium persulfate ($Na_2S_2O_8$) and 85% phosphoric acid (H_3PO_4) into nano-pure water. The samples were oxidized, and the TC components were decomposed to form carbo dioxide (CO_2). The nitrogen carrier gas delivered the combustion products to the cell of a non-dispersive infrared (NDIR) gas analyzer, where CO_2 concentrations were quantified.

4.4.5   Geochemical Modeling

There are two known mechanisms that control the leaching of elements: solubility controlled and sorption controlled leaching (Komonweeraket et al., 2015b). To assess the leaching controlling mechanisms of the elements from cement activated soil-fly ash, soil-slag mixtures and soil, fly ashes, slag, cement alone; geochemical modeling programs VisualMINTEQ and Geochemist's Workbench (GWB) (Bethke and Yeakel, 2015) were employed. VisualMINTEQ

was utilized to calculate the ion activities, speciation and saturation indices whereas GWB was used to plot the Ternary and Schoeller diagrams. Input data used in VisualMINTEQ were the pH, electrical conductivity (EC) values of the leachates, major and trace element concentrations obtained from pH-dependent leaching tests.

4.5   Results and Discussion

4.5.1   Batch Water Leach Tests (WLT)

4.5.1.1 pH and electric conductivity (EC)

Solution pH is an important factor largely influencing the leaching criteria of metals and minerals (Daniels and Das, 2006). Electric conductivity (EC) depends on cation and anion concentrations, providing an estimation of the effluent ionic strength (Gräfe et al., 2009). Higher ionic strength decreases surface negativity of soil particles through electrostatic effects which may induce additional leaching of elements (Sparks, 2003). Figure 4.2 shows the effect of fly ash and slag content on pH and EC of the effluents from batch water leach tests. As presented in Figure 4.2a, the pH of the mixtures increased with fly ash and slag content, though the increases were not significant beyond the addition rate of 10%. These indicated the influence of cement as an activator. Mixtures prepared with slag showed slightly higher pH values, nonetheless the pH of 100% slag was the lowest. According to Engström et al. (2013), the dissolution rates of primary slag minerals are slow. Despite of higher CaO content in slag (Table 4.1), lower dissolution rates of Ca bearing minerals (merwinite, akermanite and gehlenite) were the most probable reason for lower pH of pure slag. To verify this hypothesis, slag was subjected to X-ray diffraction (XRD) analysis for the mineralogical investigation (not included for brevity). From XRD analysis, merwinite was identified as the primary mineral of slag used in this study. Additionally, elevated pH of the soil-slag-cement mixtures indicates the necessity and effectivity of cement as an activator. Cement may have improved the hydration of slag minerals, increasing the leached Ca^{2+}

concentrations. Release of Ca^{2+} produces $Ca(OH)_2$ which increases the pH of the effluent (Johnson et al., 1999). The variations of pH for Class F fly ash were almost the similar to slag mixtures. Cement incorporation resulted higher pH values of soil-F FA mixtures compared to F FA alone.

Like pH, EC significantly increased with the initial (10%) addition of fly ash or slag content (Figure 4.2b). After the initial increase, EC did not change noticeably for Class C fly ash and slag blends, signifying larger influence of cement addition. In contrast, a decrease in EC was observed with Class F fly ash content. It is anticipated that, the EC of the solutions was largely dependent on the leaching of alkaline earth metals such as Ca, Mg and Ba, along with common anions such as CO_3^{2-} and SO_4^{2-}. These cations and anions precipitate at elevated pH, decreasing the solution ion concentrations. As seen from Table 4.1, CaO and MgO contents of Class F fly ash were very low to compensate the precipitation of the ions. Therefore, effluent EC decreased with the increase in Class F fly ash content. Additionally, the lowest value of EC was observed for slag alone due to lower dissolution rates of slag minerals (Engström et al., 2013).

4.5.1.2 Effect of cement content on the leaching behavior

The effect of cement content on the effluent concentrations of Ca, Mg, S, Mn, Ba and Cr is illustrated in Figure 4.3. Mixtures prepared at 10% fly ash or slag content with varying percentage of cement (3% and 6%) were considered for the analyses. As indicated in Figure 4.3a and 4.43e, Ca and Ba concentrations increased, whereas Mg concentrations decreased with the increase in cement content (Figure 4.3b). With the addition of cement, elemental concentrations of Ca increased which subsequently increased the leached Ca concentrations. The leaching of Mg and Ba is largely dependent on the solution pH. Mg follows a cationic leaching pattern whereas the leaching behavior of Ba is amphoteric (Engelsen et al., 2010; Komonweeraket et al., 2015c). Therefore, an increase in cement content increased the solution pH significantly, which subsequently increased the leached Ba concentrations. The effluent Mg concentrations decreased

due to the precipitation of Mg cations as dolomite and/or magnesite at higher pH values (Komonweeraket et al., 2015a).

Except for Class F fly ash, S concentrations (Figure 4.3c) decreased with an increase in cement content. The effluent pH increased with cement addition which facilitated the formation and precipitation of insoluble ettrintige ($Ca_6Al_2(SO_4)_3(OH)_{12} \cdot 26H_2O$). Formation of ettringite was unlikely for Class F fly ash blends since CaO and SO_3 contents were the lowest in F FA (Table 4.1). Therefore, an increase in S concentration was observed for Class F fly ash at elevated cement content (6%). In case of Mn, leached concentrations almost remained unaffected by cement additions with variations less than 0.5 µg/L (Figure 4.4d). Small variations in Cr concentrations were also observed, especially for fly ash treated samples. However, leached Cr concentration slightly increased with the increase in cement content at the presence of slag in the mixtures.

4.5.1.3 Effect of fly ash or slag content on the leaching behavior of elements

Figure 4.4 shows the variation of Ca, Mg, S, Mn, Ba and Cr concentrations from cement activated fly ash and slag treated soils as a function of fly ash or slag content. Leached concentrations from soil-fly ash and soil-slag mixtures with 6% cement content were considered for the analyses. As seen from Figure 4.4a, Ca concentrations initially increased with the addition of fly ash and slag content. Higher CaO content (Table 4.1) of fly ashes and slag compared to soil contributed significantly to the leached concentrations of Ca. After the initial increase, a slight decrease in concentrations was observed, though the CaO content of the mixtures increased proportionally with the increase in fly ash or slag addition rates. Ca follows a cationic leaching pattern where leached concentration decreases with the increase in solution pH (Bestgen et al., 2016a; Engelsen et al., 2010). An increase in fly ash or slag content increased the solution pH which consequently decreased the aqueous concentrations of Ca. Furthermore, smaller variation

in Ca concentrations were observed, regardless the fly ash or slag type indicating greater influence of cement on the leaching of Ca.

As indicated in Figure 4.4b, the highest amount of Mg leached from loess soil (15.7 mg/L), which significantly decreased in the stabilization process. It is anticipated that, dissolution of dolomite and magnesite due to lower soil pH (pH = 8.57) was associated with the higher leaching of Mg. Dolomite and magnesite were detected in loess soil from XRD analysis (not included for brevity). For the cement activate soil-fly ash and soil-slag mixtures, Mg concentrations were near the detection limit because of higher effluent pH (> 11.5). 100% Class F fly ash leached higher amount of Mg compared to Class C fly ash. For slag mixtures, after the initial decrease at 10% addition rate, leached concentrations of Mg increased with the increase in slag content. As indicated in Table 4.1, the highest amount of Mg content was found in Slag (Table 4.1) which could have contributed to the effluent Mg concentrations.

Regardless the stabilizer type, S concentrations significantly increased at 10% addition rates (Figure 4.4c). After the initial increase in concentrations, three different leaching patterns of S were observed. For Class C fly ash mixtures, S concentrations decreased with the addition rates. This implies the formation and precipitation of insoluble ettringite at highly alkaline conditions (van der Sloot, 2002). An increasing trend of S leaching was observed for Class F fly ash mixtures, suggesting minor/no formation of ettringite. Ettringite occurs only when lime (CaO) is abundant in the solution (Hassett et al., 2005), which is unlikely due to lower CaO content of Class F fly ash (Table 4.1). For slag mixtures, S concentrations fluctuated within a narrow range (19.2-24.1 mg/L) indicating lesser influence of pH and the addition rates. Zhang et al. (2016) reported similar leaching behavior of sulfate, identifying gypsum and anhydrite as the major leaching controlling minerals.

The variation of effluent Mn concentrations as a function of fly ash or slag content is presented in Figure 4.4d. Leaching of Mn were very low ($< 10\,\mu g/L$) and remained within a narrow range. Mn is generally associated with the glass fraction and/or ferromagnetic particles in fly ashes (Kim et al., 2003; Warren and Dudas, 1988). Extremely low leaching rates of Mn from both glass fraction and ferromagnetic particles were reported by Querol et al. (2001). For Class C fly ash and slag mixtures, leached Mn concentrations slightly increased with addition rates, which was consistent with the findings by Cetin et al. (2012a). In all cases, Mn concentrations were lower than the U.S. EPA specified maximum concentration limits (MCL) for drinking waters ($50\,\mu g/L$).

As depicted in Figure 4.4e, Ba concentrations generally increased with an increase in fly ash or slag content. For Class F fly ash and slag alone, solution Ba concentrations were lower than their mixtures. As mentioned earlier, Ba follows an amphoteric leaching with higher concentrations in both acidic and alkaline pH conditions (Komonweeraket et al., 2015c). For all the mixtures, pH increased with fly ash or slag content beyond the pH of 11.75, which increase leached concentrations of Ba. The pH values for 100% F fly ash and slag were relatively lower which was the reason for lower leaching of Ba. The U.S. EPA lists Ba as the primary drinking water regulation standard. Leached Ba concentrations exceeded the U.S. EPA specified MCL of 2 mg/L for cement activated soil-fly ash mixtures.

Figure 4.4(f) shows that addition of fly ash or slag initially increased the effluent Cr concentrations. The highest concentrations of Cr were observed for Class F fly ash, whereas Cr concentrations were the lowest for slag mixtures. From total metal analysis, the lowest Cr content was observed in slag (Table 4.2). Additionally, after the initial increase, Cr concentrations decreased with Class C fly ash and slag content. It is anticipated that Cr has precipitated with Ca by forming Cr-Ca solid solutions, and subsequently reduced the effluent Cr concentrations

(Cornelis et al., 2008). A linear correlation was found when the effluent Cr concentrations were plotted against the leached concentrations of Ca from all the mixtures ($R^2 = 0.48$, not included for brevity). However, for Class F fly ash mixtures, Cr concentration increased with fly ash content, which might have happened due to low CaO content of Class F fly ash. For all Class F fly ash blends, Cr concentrations exceeded U.S. EPA specified MCL (100 µg/L) for drinking waters.

4.5.1.4 Total dissolved carbon (TDC) concentrations

Figure 4.5 shows the aqueous concentrations of TDC from the mixtures. As seen in Figure 5a, TDC concentrations increased with the increase in cement content for the fly ash mixtures. Both the organic and inorganic carbon contributed to the TDC concentrations of the effluents. Dissolution and desorption of organic matters from the mineral surfaces at higher pH are the most probable reasons for the increased concentrations of TDC with cement content (Dijkstra et al., 2002; Langmuir, 1997).

With few exceptions, TDC concentrations decreased with fly ash or slag content (Figure 4.5b). Dissolved carbon dioxide ($CO_{2(aq)}$), bicarbonate (HCO_3^-) and carbonate (CO_3^{2-}) are the forms of inorganic carbons in the solution (Schulz et al., 2006). Inorganic carbons count for the higher fraction in TDC (Jarvie et al., 2017). In the pH range of WLT effluents (Figure 4.2), carbonates dominated and precipitated with divalent cation which consequently decreased the TDC concentrations (Bestgen et al., 2016b). In addition, 100% slag leached the highest amount of TDC because of the lowest pH (11.6) of the effluent solutions. For soil-slag-cement, a decrease in TDC concentration was observed at higher cement content (Figure 4.5a). The precipitation of carbonates may have surpassed the desorption of organic matters and therefore, decreased the TDC concentration with cement content.

4.5.2   Acid-Base Neutralization Capacity (ANC)

Acid neutralization capacity (ANC) of cement activated soil-fly ash, soil-slag mixtures and soil, fly ashes, slag, cement alone was evaluated by adding varying amount of acid or base with the solids. Figure 4.6 shows the ANC of the mixtures, where the addition of base is characterized by negative milliequivalents per gram weight of dry sample. As seen from Figure 4.6a, loess soil and Class F fly ash showed very low buffering capacities in the pH range of 12.4 to 4.8. For Class F fly ash, slight improvement in ANC was observed at pH lower than 4. In contrast, Class C fly ash and slag showed greater neutralization capacities, resulting from their higher CaO and MgO content (Table 4.1). Two distinct plateaus were identified in the ANC curve of Class C fly ash at pH range of 8.26 to 6.23 and 4 to 2.43. For slag, the plateau was observed in between the pH values of 9.43 and 6.92. According to Roy and Cartledge (1997), silicates and aluminosilicates start to dissolve at pH 8, which is the most probable reason for the observed first plateau. Dissolution of gypsum, calcium carbonate and gibbsite may have shaped the second plateau, owing to their neutralization capacity at pH about 5 (Chen et al., 2009). Depending on Ca containing minerals, variations in equilibrium pH were observed (Giampaolo et al., 2002). The highest ANC was observed for type I/II cement with 3 plateaus identified at pH range of 12.6 to 12.4, 11.8 to 11.6 and 10.8 to 9.5. Soluble portlandite along with higher Ca/Si ratio (>1.8) of calcium-silicate-hydrate resulted the first plateau, whereas the second plateau was associated with lower Ca/Si ratio (<1.5) of calcium silicate hydrate (C-S-H) (Isenburg and Moore, 1992; Stronach and Glasser, 1997). The third plateau was ascribed due to $Mg(OH)_2$ causing a pH detention at around pH values of 9 (Fernández et al., 2003).

Cement, soil and fly ash type influenced the ANC of the mixtures. As seen in Figure 4.6b and 4.6d, ANC of cement activated soil-C FA and soil-slag mixtures lay in between the neutralization capacities of soil and C FA or slag alone. Buffering capacity of these mixtures

increased noticeably with the increase in fly ash and slag content. Influence of cement was less pronounced due to higher buffering capacities of C FA and slag. For cement activated soil-F FA mixtures, neutralization capacities were higher compared to both the soil and F FA alone, indicating larger influence of cement. Higher neutralization capacity of cement and lower CaO content (Table 4.1) of Class F fly ash are the probable reasons for the observed inclination.

4.5.3   pH-dependent Leach Test

4.5.3.1 Leaching of Ca, Mg and S

Leaching behavior of Ca, Mg and S from cement activated fly ash and slag treated soils followed cationic leaching patterns where concentrations decreased with the increase in solution pH (Figure 4.7, 4.8 and 4.9). Dissolution of minerals and desorption of cations at acidic conditions significantly increased their concentrations. Tiruta-Barna et al. (2006) found that strength of acid increased as the pH decreased which intensified the attack on the metal bearing minerals and thus increased the leached concentrations of cationic elements. Also, sorption of Ca, S and Mg is less favored at acidic conditions, especially at pH less than 6 (Komonweeraket et al., 2015c). For Class F fly ash mixtures, leached concentrations of Ca and S were higher compared to F FA alone, indicating the influence of cement incorporation. Additionally, higher leachability of Ca and S were observed for cement while, slag showed maximum leaching of Mg. At a fixed pH value, small variations in concentrations were observed, irrespective to fly ash or slag contents. The differences were even lower at alkaline conditions, indicating maximum leaching of the elements, regardless the addition rates.

According to Warren and Dudas (1985), gypsum ($CaSO_4$) and anhydrite ($CaSO_4 . 2H_2O$) are the potential solubility controlling minerals for the leaching of Ca at acidic to slight alkaline conditions (pH of 1.5 to 10). Sulfur concentrations within this pH range are also controlled by the dissolution and precipitation of gypsum and anhydrite. Fruchter et al. (1990) reported that sulfur

(S) predominantly existed as sulfate (SO_4^{2-}), especially at oxidizing conditions. At pH values higher than 10.7, SO_4 precipitated by forming insoluble ettringite resulting a decrease in both Ca and S concentrations (Gabrisová et al., 1991; Hassett et al., 2005). Moreover, at higher pH values (pH > 9), carbonates become more important and calcite ($CaCO_3$) and/or aragonite ($CaCO_3$) plays an important role on the leaching behavior of Ca (Stumm and Morgan, 1996). At higher pH, sulfate and carbonate minerals of Ca and Mg may have precipitated and decreased their effluent concentrations. Roy et al. (1984) also concluded that Ca concentrations at alkaline conditions in equilibrium with atmospheric carbon dioxide are controlled by the solubility of calcite. In addition, leaching of Ca from fly ashes could be controlled by unstable CaO, loosely attached at the surface of fly ash particles (Warren and Dudas, 1984).

Similarly, leaching behavior of Mg was controlled by the solubility of carbonate minerals such as magnesite ($CaMg(CO_3)_2$) and dolomite ($MgCO_3$). Previous studies have identified magnesite and dolomite as the major leaching controlling minerals for Mg in fly ash and slag effluents (Apul et al., 2005; Garavaglia and Caramuscio, 1994; Komonweeraket et al., 2015a).

4.5.3.2 Leaching of Mn

As seen in Figure 4.10, higher concentrations of Mn were observed up to the pH values of 6 to 7, which decreased drastically at pH around 7. The decrease rates were lower in the pH range of 10 to 13. Thus, Mn showed a cationic leaching pattern because of the dissolution and precipitation of manganese (hydro)oxides (Cetin et al., 2012c). In acidic and neutral condition, Mn^{2+} cations were freely available (Gitari et al., 2009), therefore increased the effluent concentrations. Moreover, the point of zero charge (PZC) of the mixtures could have a profound influence on the leaching behavior of Mn. According to Wang et al. (2007), the pH associated with the PZC of Class C and F fly ashes is in between 6.2 and 7.6. At pH lower than PZC, fly ash particles were positively charged which significantly decreased the sorption of the cations. As the

pH rises above PZC, fly ash particles developed negative charges and induced sorption of Mn cations, resulting an overall decrease in dissolved concentrations. For cement activated soil-slag mixtures similar observations were made, though the speculated PZC was in the pH range of 7.6 to 8. At pH higher than 10, the lower leaching of Mn could be controlled by the solubility of pyrochroite ($Mn(OH)_2$) (Komonweeraket et al., 2015b), which is further investigated in the geochemical modeling section.

4.5.3.3 Leaching of Ba

Figure 4.11 illustrates the leaching behavior of Ba as a function of pH from cement activated soil-fly ash, soil-slag mixtures and soil, fly ashes, slag alone. Two different leaching patterns of Ba were observed based on the materials used in this study. Loess soil, fly ashes and their mixtures showed amphoteric leaching pattern where Ba concentrations increased both in acidic and alkaline conditions. In contrast, cement, slag and slag mixtures showed cationic pattern with an inversely proportional relationship between concentration and effluent pH. Leaching of Ba from cement activated soil-F FA mixtures was relatively pH independent, showing lesser variations in concentrations depending on pH. Similar leaching behaviors of Ba were observed in previous studies from fly ashes and soil-fly ash mixtures (Komonweeraket et al., 2015a), MSWI air-pollution-control residue (Astrup et al., 2006) and steel slags (Fällman, 2000; Loncnar et al., 2016).

The leaching of Ba is believed to be associated with barite ($BaSO_4$) and witherite ($BaCO_3$). Komonweeraket et al. (2015a) claimed that in the pH range of 1.5 to 10, the leaching of Ba from fly ash treated soils was controlled by barite, whereas witherite controlled the Ba concentrations at pH higher than 10. Ba can also co-precipitate with sulfate and strontium (Sr) as barite-celestite [$(Ba,Sr)SO_4$], especially with the presence of large amount of Ca (Fruchter et al., 1990). From total metal analysis (Table 4.1), higher amount of Ca and S were detected in slag and cement.

Precipitation of Ba-Sr-sulfate solid solution at higher pH could be a reason for the cationic leaching of Ba from cement, slag and soil-slag mixtures. The leaching mechanisms of Ba are discussed more in details in geochemical modeling section.

4.5.3.4 Leaching of Cr

The leaching behavior of Cr demonstrated oxyanionic leaching patterns, with higher concentrations in acidic pH values (pH < 3), which decreased considerably at neutral or slightly acidic conditions (Figure 4.12). From pH values of 5.5 to 10, a concentration plateau was identified, followed by a decrease (pH $\cong$ 11.5), and subsequent increase in Cr concentrations at extreme pH conditions (pH $\cong$ 13). The observed plateau was less pronounced for soil-slag mixtures resulting in the pH range of 5.5 to 7. However, Komonweeraket et al. (2015b) indicated an amphoteric leaching behavior of Cr from soil-fly ash mixtures. The difference could be attributed to the presence of Cr as Cr(VI) and Cr(III) in this current and previous study. The pH of the fly ashes used in the previous study were close to neutral pH conditions, while due to cement activation, the pH of the mixtures prepared in this study were very high (pH > 11.5). Therefore, Cr in this study could be in its oxidized form (Cr^{6+}), whereas reduced form of Cr (i.e., Cr^{3+}) was identified by the previous study.

Additionally, an amphoteric leaching pattern of Cr was observed for loess soil. The leached Cr concentrations were significantly higher for cement and Class F fly ash alone (Figure 4.12a). For soil-F fly ash mixtures, leaching of Cr was nearly pH independent, with small variation in concentrations depending on pH. Previous studies claimed that Cr may become immobilized by replacing Silicon (Si) in C-S-H gel, as the ionic radius of and $Si(OH)_4$ and $Cr(OH)_4^-$ are comparable (Glasser, 1997; Olmo et al., 2001). Minor formation of C-S-H in cement and soil-F fly ash mixtures might have increased the effluent Cr concentrations. However, this claim could not be verified since Si concentrations were not measured in this study.

4.5.3.5 Leaching of TDC

The leached concentrations of total dissolved carbon (TDC) as a function of pH from soil-fly ash-cement, soil-slag-cement and soil, fly ashes, slag and cement alone are presented in Figure 4.13. Highest concentrations of TDC were observed at neutral or near neutral pH values, with slight increase in concentrations both in extreme acidic (pH < 2) and alkaline (pH > 12) conditions. Dissolved organic and inorganic carbon mutually contributed to the total dissolved carbon concentrations in the leachates. Organic carbon yields from soil organic matters and are bonded with oxygen and hydrogen, whereas inorganic carbon occurs mainly at three forms: carbonate (CO_3^{2-}), bicarbonate (HCO_3^-) and carbonic acid/dissolved carbon dioxide [$H_2CO_3/CO_2(aq)$)] (Schulz et al., 2006).

Generally, total dissolved carbon concentrations are dominated by inorganic carbon (Jarvie et al., 2017), which is also observed in this current study (not included for brevity). At neutral pH conditions, the higher concentrations of TDC were due to the presence of bicarbonates (Clark, 2015). As the pH increases, carbonates appear to be ubiquitous and become the major species at pH higher than 10.3 (Cole and Prairie, 2009). Subsequently, DIC concentrations decreased as the carbonates precipitated with divalent cations such as Ca, Mg, Sr and Ba (Garrabrants et al., 2004; Langmuir, 1997).

In acidic conditions, $H_2CO_3/CO_2(aq)$ dominated which increased the CO_2 partial pressure in the effluent (Clark, 2015). Consequently, CO_2 evaded for equilibrium with atmospheric CO_2 and decreased DIC concentrations. Nonetheless, the effluents were supersaturated with TDC relative to the partial pressure of atmospheric CO_2 (380 µatm), indicating the contribution of organic carbon. Dissolved organic carbon (DOC) are reliant on Ca leaching because of the possible formation of DOC-Ca complexes (Guimaraes et al., 2006). At acidic conditions, organic carbon may have remained in the solution by DOC-Ca complexes and contributed to TDC concentrations.

Additionally, high molecular weight humic acids could dissolved at alkaline conditions and increase the TDC concentrations (Langmuir 1997). Furthermore, at higher pH, the sorption of DOC to mineral surfaced decreases which contributes to TDC at pH higher than 12 (Dijkstra et al., 2002).

4.5.4 Geochemical Modeling

Geochemical modeling was performed based on the pH-dependent leach test results from all the cement activated soil-fly ash, soil-slag mixtures and soil, fly ashes, slag alone. The equilibrium speciation models, Visual MINTEQ and Geochemist's Workbench (GWB) were implemented. An equilibrium between the solubility controlling minerals and the leachate was assumed at $25°$ C and under the atmospheric CO_2 partial pressure ($10^{-3.5}$ atm). Aqueous complexation reactions at a fixed pH was allowed for geochemical modeling by Visual MINTEQ as suggested by Apul et al. (2005).

Figures 4.14 to 4.21 illustrate the geochemical modeling results. Figure 4.14 shows the results of Ternary diagrams for pure materials, soil-class C fly ash mixtures, soil-class F fly ash mixtures and soil-slag mixtures, respectively. The results show that except soil-slag mixtures (Fig 14d), the leachates have somewhat comparable concentrations of Ba^{2+}, Mn^{2+} and CrO_4^{2-}. The Ba/Mn and Ba/CrO_4^{2-} molar ratios are significantly large due to elemental composition of the materials (Table 4.1).

A Schoeller diagram (Schoeller, 1962) yields the concentrations of major cations and anions on a semi-logarithmic plot where the ion names are presented on the x-axis and the analyte concentrations are given on the logarithmically scaled y-axis in meq/L. The concentration of each analyte is plotted as a point and the diagram is generated by connecting the points and forming a "fingerprint diagram". This enables description of any sample by dominant cations and anions. The Schoeller diagrams of pure cement, FFA, CFA and slag at neutral pH values (pH = 6.53-6.83)

are given in Figure 4.15. The results indicate that even though all samples have similar fingerprints, the leachate concentrations differ significantly due to nature of the materials. Cement and FFA have the highest and lowest Ca^{2+} concentrations, respectively. Steel slag has been reported to have a considerable amount of Ca^{2+} and Mg^{2+} (Dayioglu et al 2018), hence the Ca^{2+} concentration is larger compared with FFA. After slag, cement, CFA and FFA have the largest to smallest Mg^{2+} concentrations. The interrelationships among the concentrations of sulfur, barium and chromium in steel slag and fly ash leachates have been extensively studied and evaluated in previous studies (Fruchter et al 1990, Fallman and Aurell 1996). On the contrary to the compounds above, despite of their low S percentage in the elemental compositions, CFA and FFA have similar and highest sulfate concentrations on natural pH within the leachates, followed by cement and slag, respectively. This might be due to fact that even though their S concentrations are low, SO_4^{2-} is reported to be the dominant species in fly ashes (Fruchter 1990, Izquierdo and Querol 2012). On the other hand, ettringite ($Ca_6(Al)_2(OH)_{12}(SO_4)_3:26H_2O$) has been shown to exist in steel slag, which might have caused free sulfate concentration to decrease (Huijgen and Comans, 2006). Similarly, Barite ($BaSO_4$) is known to control the Ba^{2+} solubility in steel slag, the horizontal line on the fingerprint diagram of slag (Fig 15d) agrees with previous findings (Fallman, 2000). Mn^{2+} leaching from the materials depends on the initial material composition, where highest concentration is observed in slag leachate, with remaining materials yielding similar concentrations (Table 4.1 and Figure 4.15).

Depending of effluent pH, the leaching of Ca, Mg and Ba are known to be controlled by sulfate and carbonate minerals (Komonweeraket et al., 2015a; Zhang et al., 2016). As shown in Figures 4.16, similar leaching mechanisms of Ca was observed for cement activated fly ash and slag treated soils. From the solubility lines of the minerals of Ca, gypsum and anhydrite were

identified as the potential solubility controlling minerals for Ca at the pH range of 2 to 7, whereas it may be controlled by gypsum, anhydrite and calcite between the pH of 7 and 8 (Figure 4.16). Previous studies indicated that, carbonate minerals control the leaching of Ca^{2+} from fly ash in alkaline solutions in equilibrium with atmosphere (Komonweeraket et al., 2015a; Mudd et al., 2004; Roy et al., 1984; Stumm and Morgan, 1996). However, in the leachate from cement activated soil-fly ash and soil-slag mixtures Ca^{2+} activity was controlled by gypsum and anhydrite up to the pH of 11. Dissolution of gypsum and anhydrite from the cement paste possibly contributed Ca cations into the leachate and subsequently precipitated calcite (Langmuir, 1997). Additionally, at pH higher than 11, portlandite started to influence the leaching mechanisms of Ca. These results indicated that calcite may not play a significant role on the leaching of Ca from soil-fly ash and soil-slag systems when cement is used as an activator.

Gypsum and anhydrite also controlled the solubility of sulfate from soil-fly ash-cement and soil-slag-cement mixtures throughout the whole pH range (Figure 4.17). Slight undersaturation was observed with respect to gypsum and anhydrite, which could have happened due to incomplete dissolution of these minerals. Inadequate presence of minerals in solid phase is also a possible reason of undersaturation. This observation is in agreement with the leaching mechanisms of sulfate from pure fly ash and slag materials (Dayioglu et al., 2018; Komonweeraket et al., 2015a).

The geochemical modeling results showed that Mg solubility was controlled by carbonate minerals (dolomite and magnesite) only in the pH range of 7 to 8 (Figure 4.18), although previous studies reported that the dolomite and magnesite are the solubility controlling solids for Mg throughout the alkaline pH conditions (Apul et al., 2005; Garavaglia and Caramuscio, 1994; Komonweeraket et al., 2015a). Conversely, brucite controlled the solubility of Mg in the pH range of 8 to 14 from cement activated fly ash and slag treated soils. At acidic pH values, disassociated

activities of Mg^{2+} with respect to the solubility lines indicated that Mg leaching was not solubility controlled. Apul et al (2005) concluded that at pH values lower than 7, the model predictions and the lab concentrations start to deviate, revealing the potentially adsorption controlled leaching mechanism at acidic pH values.

Figure 4.19 presents the log activity diagrams of Ba^{2+} with respect to the pH for pure materials as well as the mixtures. Leaching controlling mechanisms of Ba are quite complex, since it may be present in sulfate or carbonate minerals, or might react with other metals such as Sr or Cr and co-precipitate (Fruchter et al., 1990; Komonweeraket et al., 2015a; Mudd et al., 2004). As seen in Figure 4.19, the Ba^{2+} activities did not exhibit a pH dependent behavior and remained constant at all pH values, in close proximity to the solubility line of barite ($BaSO_4$) with slight oversaturation. The oversaturation indicated the possible formation of $Ba(S, Cr)O_4$ and/or $(Ba, Sr)SO_4$ solid solutions (Komonweeraket et al., 2015a). Between pH values of 8.5 and 10, Ba leaching may be controlled by witherite ($BaCO_3$) as well, as reported by (Zhang et al., 2016), however it should be noted that both solubility lines intersect within this region. Diversely, Komonweeraket et al. (2015) and Mudd et al. (2004) reported that at pH higher than 10, witherite controlled the leaching of Ba from fly ash and fly ash stabilized soils. In this study cement was used as an activator for fly ash and slag treatment, which possibly worked as an additional source of sulfate in the solution. Gypsum and anhydrite are the major sources of sulfate and were identified in cement and Class C fly ash by XRD analysis.

Figure 4.20 illustrates that Mn^{2+} leaching is controlled by the dissolution/precipitation reactions of manganese (hydro)oxides at alkaline pH values (pH > 7). Zhang et al (2016) also showed that the cationic leaching pattern of Mn was demonstrated by $Mn(OH)_2$ precipitation, and leaching mechanism of Mn was controlled by the dissolution/precipitation of $Mn(OH)_2$. Under

neutral and acidic conditions, Mn^{2+} are freely available and the dissolution of the tephroite-forsterite might control the leaching of Mn (Gitari et al., 2009; Pareuil et al., 2010).

Unlike some of the previous studies, leaching of CrO_4^{2-} from cement activated fly ash and slag mixtures was not controlled by the dissolution/precipitation reactions of its (hydr)oxides (Figure 4.21). Previous studies found the reduced form Cr3+ in the fly ash leachate and claimed that amorphous $Cr(OH)_3$, crystalline $Cr(OH)_3$, and Cr_2O_3 could control the leaching of Cr from fly ash and soil-fly ash mixtures (Gitari et al., 2009; Komonweeraket et al., 2015b; Loncnar et al., 2016; Mulugeta et al., 2011; Reardon et al., 1995; Theis et al., 1982). Lower pH of the fly ash and/or soil-fly ash mixtures used in these studies was the most probable reason for the observed inclination. However, current study propose that $BaCrO_4$ and $CaCrO_4$ could controlled the leaching of Cr(VI) from soil-fly ash-cement and soil-slag-cement mixtures due to high pH values resulted from cement activation. Figure 4.22 shows the log activities of CrO_4^{2-} with respect to the log activities of Ba^{2+} along with the solubility line of $BaCrO_4$. The log activities of Cr were 3 to 7 order of magnitude lower than the solubility line of BaCrO4, indicating that BaCrO4 may control the solubility of Cr. Fallman (2000) pointed out that concentrations of Ba and Cr may be controlled by the solubility of solid phases $BaSO_4$ and $Ba(S, Cr)O_4$. Similar observation was made with respect to $CaCrO_4$, but the Cr activities were approximately 7 to 12 magnitude lower than the saturation line of CaCrO4. Other studies also claimed that $BaCrO_4$ and $CaCrO_4$ might control the leaching of Cr(VI) in highly alkaline conditions such as the leachate from cement solidified refinery sludge and ash (Karamalidis and Voudrias, 2008), high pH fly ash (Zhang et al., 2016), recycled concrete aggregate (Bestgen et al., 2016; Engelsen et al., 2010) and MSWI air pollution-control residues (Astrup et al., 2006).

3.6   Conclusions

Batch water leach tests (WLT) and pH-dependent leach tests were performed to investigate the leaching behavior of major and trace elements (Ca, Mg, S, Mn, Ba and Cr) from cement activated soil-fly ash, soil-slag mixtures and soil, fly ash, slag and cement alone. Additionally, pH, electric conductivity (EC) and total dissolved carbon (TDC) concentrations in the test effluents were evaluated. Geochemical modeling program Visual MINTEQ was implemented to investigate the leaching controlling mechanisms of the elements. Based on this experimental study the following conclusions were obtained:

1.   Cement activation had diverse influences on the leached concentrations of the elements in batch water leach tests. Ca and Ba concentrations increased, Mg concentrations decreased, and S and TDC concentration varied with the increase in cement content. Aqueous concentrations of Mn and Cr remained unaffected by the addition of cement in soil-fly ash-cement and soil-slag-cement mixtures.

2.   Solution pH and EC initially increased with the addition of fly ash or slag content but stayed unchanged at further addition rates. Along with the basic oxide contents, fly ash/slag mineralogy and dissolution rates of the minerals played an important role on the solution pH and EC. Cement had the greater effect on pH and EC of the effluent of the mixtures.

3.   Effluent pH had the most significant influence on the leaching of elements rather than the fly ash or slag addition rates. Except for soil-slag-cement mixtures, WLT effluent concentrations of Ba and Cr exceeded the regulatory limits determined by the U.S. EPA MCLs (Maximum Contaminant Limits) of 2000 µg/L and 100 µg/L, respectively.

4.   Acid/base neutralizing capacity provided an indication of the hydration products and minerals of soil, fly ashes, slag, cement and their mixtures, along with a basis for qualitative

comparisons. Besides, ANCs revealed that the fly ashes and slag used in this study can produce pozzolanic reactions.

5.　　　Ca, Mg, S and Mn followed cationic leaching patterns, where concentrations decreased with the increase in solution pH. An increase in fly ash or slag content did not cause a significant increase in the leaching of metals from the mixtures. This indicates that the mode of occurrence played the major role compared to the total elemental concentrations of metals in the mixtures.

6.　　　The leaching of Ba followed both cationic and amphoteric patterns depending on the materials used in this study. Loess soil, fly ashes and their mixtures showed amphoteric leaching, where minimum concentrations occurred at neutral and near neutral pHs. Conversely, cement, slag and slag mixtures showed cationic leaching of Ba.

7.　　　Cr showed neither a cationic, an amphoteric, nor an oxyanionic leaching behavior. A concentration plateau was identified in the pH range of 5.5-10, which was followed by subsequent decrease and increase in concentrations at pH of 11.5 and 13, respectively. The variations could be due to the abundance of other divalent ions such as Ca, SO_4^{2-} and Mg, difference in speciation (Cr^{3+} vs Cr^{6+}) and complexation with other minerals and organic/inorganic carbons.

8.　　　Total dissolved carbon (TDC) concentrations were the highest at neutral/near neutral pH values, but decreased drastically in both acidic and alkaline conditions. Moreover, in extreme acidic and alkaline pH conditions, an increase in TCD was observed. The highest concentrations of TDC at neutral pH values were associated with inorganic carbons (bicarbonates), whereas at extreme pH conditions TDC increased because of the dissolution and desorption of organic matters.

9.   The geochemical analyses conducted via Visual MINTEQ indicated that solubility of Ca^{2+}, Ba^{2+} and S^{6+} were controlled by precipitation/dissolution reactions of sulfate minerals (gypsum, anhydrite, barite) at all pH values. At pH higher than 11, portlandite influenced the leaching mechanisms of Ca^{2+}. Carbonate minerals (calcite, aragonite, witherite) may not play an important role on the leaching mechanisms of these elements from cement activated fly ash and slag stabilized soils.

10.   Leaching of Mg^{2+} and Mn^{2+} was only solubility controlled at pH values higher than 8. Alike Ca^{2+}, Mg^{2+} leaching at higher pH values was controlled by brucite rather than the carbonate minerals such as dolomite, magnesite. Pyrochroite controlled the leaching of Mn^{2+} at alkaline conditions.

11.   Instead of reduced Cr^{3+}, oxidized form Cr^{6+} was found to be dominant in soil-fly ash-cement and soil-slag-cement leachate. Leaching of CrO_4^{2-} was not controlled by the solubility of its (hydr)oxides. The log activity diagrams showed that $BaCrO_4$ and $CaCrO_4$ may have control the leaching of CrO_4^{2-}, which is analogous with the leaching of Cr from highly alkaline waste materials.

12.   Results indicated that, the use of cement activated slag mixtures is the safer option compared to cement activated fly ash mixtures in soil stabilization considering the leaching characteristics of the elements. Cement activated slag stabilized soils leached lower concentrations of Ca, Mg, S, Mn, Ba and Cr compared to cement-fly ash-soil mixtures.

3.7   References

ACAA, 2018. Coal combustion products production & use statistics. Farmington Hills, MI.

Akhter, H., Butler, L.G., Branz, S., Cartledge, F.K., Tittlebaum, M.E., 1990. Immobilization of As, Cd, Cr and PB-containing soils by using cement or pozzolanic fixing agents. J. Hazard. Mater. 24, 145–155. https://doi.org/10.1016/0304-3894(90)87006-4

Aldeeky, H., Al Hattamleh, O., 2017. Experimental study on the utilization of fine steel slag on stabilizing high plastic subgrade soil. Adv. Civ. Eng. 2017, 1–11. https://doi.org/10.1155/2017/9230279

Allan, M.L., Kukacka, L.E., 1995. Blast furnace slag-modified grouts for in situ stabilization of chromium-contaminated soil. Waste Manag. 15, 193–202. https://doi.org/10.1016/0956-053X(95)00017-T

Apul, D.S., Gardner, K.H., Eighmy, T.T., Fällman, A.M., Comans, R.N.J., 2005. Simultaneous application of dissolution/precipitation and surface complexation/surface precipitation modeling to contaminant leaching. Environ. Sci. Technol. 39, 5736–5741. https://doi.org/10.1021/ES0486521

Astrup, T., Dijkstra, J.J., Comans, R.N.J., Sloot, H.A. van der, Christensen, T.H., 2006. Geochemical modeling of leaching from MSWI air-pollution-control residues. Environ. Sci. Technol. 40, 3551–3557. https://doi.org/10.1021/ES052250R

Bestgen, J.O., Cetin, B., Tanyu, B.F., 2016a. Effects of extraction methods and factors on leaching of metals from recycled concrete aggregates. Environ. Sci. Pollut. Res. 23, 12983–13002. https://doi.org/10.1007/s11356-016-6456-0

Bestgen, J.O., Hatipoglu, M., Cetin, B., Aydilek, A.H., 2016b. Mechanical and environmental suitability of recycled concrete aggregate as a highway base material. J. Mater. Civ. Eng. 28, 04016067. https://doi.org/10.1061/(ASCE)MT.1943-5533.0001564

Bethke, C.M., Yeakel, S., 2015. GWB Essentials Guide. The Geochemist's Workbench, Aqueous Solutions, LLC, Champaign, Illinois.

Cappuyns, V., Alian, V., Vassilieva, E., Swennen, R., 2014. pH dependent leaching behavior of Zn, Cd, Pb, Cu and As from mining wastes and slags: Kinetics and mineralogical control. Waste and Biomass Valorization 5, 355–368. https://doi.org/10.1007/s12649-013-9274-3

Cetin, B., Aydilek, A.H., Guney, Y., 2012a. Leaching of trace metals from high carbon fly ash stabilized highway base layers. Resour. Conserv. Recycl. 58, 8–17. https://doi.org/10.1016/J.RESCONREC.2011.10.004

Cetin, B., Aydilek, A.H., Guney, Y., 2010. Stabilization of recycled base materials with high carbon fly ash. Resour. Conserv. Recycl. 54, 878–892. https://doi.org/10.1016/J.RESCONREC.2010.01.007

Cetin, B., Aydilek, A.H., Li, L., 2014. Trace metal leaching from embankment soils amended with high-carbon fly ash. J. Geotech. Geoenvironmental Eng. 140, 1–13. https://doi.org/10.1061/(ASCE)GT.1943-5606.0000996

Cetin, B., Aydilek, A.H., Li, L., 2012b. Experimental and numerical analysis of metal leaching from fly ash-amended highway bases. Waste Manag. 32, 965–978. https://doi.org/10.1016/J.WASMAN.2011.12.012

Cetin, B., Aydilek, A.H., Li, L., 2012c. Experimental and numerical analysis of metal leaching from fly ash-amended highway bases. Waste Manag. 32, 965–978. https://doi.org/10.1016/j.wasman.2011.12.012

Chen, Q., Zhang, L., Ke, Y., Hills, C., Kang, Y., 2009. Influence of carbonation on the acid neutralization capacity of cements and cement-solidified/stabilized electroplating sludge. Chemosphere 74, 758–764. https://doi.org/10.1016/J.CHEMOSPHERE.2008.10.044

Chowdhury, S., Mazumder, M.A.J., Al-Attas, O., Husain, T., 2016. Heavy metals in drinking water: Occurrences, implications, and future needs in developing countries. Sci. Total Environ. 569–570, 476–488. https://doi.org/10.1016/J.SCITOTENV.2016.06.166

Clark, I.D., 2015. Groundwater Geochemistry and Isotopes, 1st ed. CRC press, Boca Raton, Florida, USA.

Cole, J.J., Prairie, Y.T., 2009. Dissolved CO2, in: Likens, G.E. (Ed.), Encyclopedia of Inland Waters. Elsevier, Amsterdam, Netherlands, pp. 30–34.

Cornelis, G., Johnson, C.A., Gerven, T. Van, Vandecasteele, C., 2008. Leaching mechanisms of oxyanionic metalloid and metal species in alkaline solid wastes: A review. Appl. Geochemistry 23, 955–976. https://doi.org/10.1016/J.APGEOCHEM.2008.02.001

Daniels, J.L., Das, G.P., 2006. Leaching behavior of lime–fly ash mixtures. Environ. Eng. Sci. 23, 42–52. https://doi.org/10.1089/ees.2006.23.42

Dayioglu, A.Y., Aydilek, A.H., Cetin, B., 2014. Preventing swelling and decreasing alkalinity of steel slags used in highway infrastructures. Transp. Res. Rec. J. Transp. Res. Board 2401, 52–57. https://doi.org/10.3141/2401-06

Dayioglu, A.Y., Aydilek, A.H., Cimen, O., Cimen, M., 2018. Trace metal leaching from steel slag used in structural fills. J. Geotech. Geoenvironmental Eng. 144, 04018089. https://doi.org/10.1061/(ASCE)GT.1943-5606.0001980

Dijkstra, J.J., van der Sloot, H.A., Comans, R.N.J., 2002. Process identification and model development of contaminant transport in MSWI bottom ash. Waste Manag. 22, 531–541. https://doi.org/10.1016/S0956-053X(01)00034-4

Engelsen, C.J., van der Sloot, H.A., Wibetoe, G., Justnes, H., Lund, W., Stoltenberg-Hansson, E., 2010. Leaching characterisation and geochemical modelling of minor and trace elements released from recycled concrete aggregates. Cem. Concr. Res. 40, 1639–1649. https://doi.org/10.1016/J.CEMCONRES.2010.08.001

Engström, F., Adolfsson, D., Samuelsson, C., Sandström, Å., Björkman, B., 2013. A study of the solubility of pure slag minerals. Miner. Eng. 41, 46–52. https://doi.org/10.1016/j.mineng.2012.10.004

Fällman, A.-M., 2000. Leaching of chromium and barium from steel slag in laboratory and field tests — a solubility controlled process? Waste Manag. 20, 149–154. https://doi.org/10.1016/S0956-053X(99)00313-X

Fernández, A.I., Chimenos, J.M., Raventós, N., Miralles, L., Espiell, F., 2003. Stabilization of electrical arc furnace dust with low-grade MgO prior to landfill. J. Environ. Eng. 129, 275–279. https://doi.org/10.1061/(ASCE)0733-9372(2003)129:3(275)

Fruchter, J.S., Rai, D., Zachara, J.M., 1990. Identification of solubility-controlling solid phases in a large fly ash field lysimeter. Environ. Sci. Technol. 24, 1173–1179. https://doi.org/10.1021/es00078a004

Gabrisová, A., Havlica, J., Sahu, S., 1991. Stability of calcium sulphoaluminate hydrates in water solutions with various pH values. Cem. Concr. Res. 21, 1023–1027. https://doi.org/10.1016/0008-8846(91)90062-M

Garavaglia, R., Caramuscio, P., 1994. Coal fly-ash leaching behaviour and solubility controlling solids. Stud. Environ. Sci. 60, 87–102. https://doi.org/10.1016/S0166-1116(08)71450-X

Garrabrants, A.C., Sanchez, F., Kosson, D.S., 2004. Changes in constituent equilibrium leaching and pore water characteristics of a Portland cement mortar as a result of carbonation. Waste Manag. 24, 19–36. https://doi.org/10.1016/S0956-053X(03)00135-1

Giampaolo, C., Mastro, S.L., Polettini, A., Pomi, R., Sirini, P., 2002. Acid neutralisation capacity and hydration behaviour of incineration bottom ash–Portland cement mixtures. Cem. Concr. Res. 32, 769–775. https://doi.org/10.1016/S0008-8846(01)00760-8

Gitari, W.M., Fatoba, O.O., Petrik, L.F., Vadapalli, V.R.K., 2009. Leaching characteristics of selected South African fly ashes: Effect of pH on the release of major and trace species. J. Environ. Sci. Heal. Part A 44, 206–220. https://doi.org/10.1080/10934520802539897

Glasser, F.P., 1997. Fundamental aspects of cement solidification and stabilisation. J. Hazard. Mater. 52, 151–170. https://doi.org/10.1016/S0304-3894(96)01805-5

Gomes, J.F.P., Pinto, C.G., 2006. Leaching of heavy metals from steelmaking slags. Rev. Metal. 42, 409–416. https://doi.org/10.3989/revmetalm.2006.v42.i6.39

Gräfe, M., Power, G., Klauber, C., 2009. Review of bauxite residue alkalinity and associated chemistry, CSIRO Document DMR-3610. Project ATF-06-3: Management of Bauxite Residues.

Guimaraes, A.L., Okuda, T., Nishijima, W., Okada, M., 2006. Organic carbon leaching behavior from incinerator bottom ash. J. Hazard. Mater. 137, 1096–1101. https://doi.org/10.1016/J.JHAZMAT.2006.03.047

Hassett, D.J., Pflughoeft-Hassett, D.F., Heebink, L. V., 2005. Leaching of CCBs: Observations from over 25 years of research, in: Hower, J.C. (Ed.), Fuel. Elsevier, pp. 1378–1383. https://doi.org/10.1016/J.FUEL.2004.10.016

Isenburg, J., Moore, M., 1992. Generalized acid neutralization capacity test, in: Stabilization and Solidification of Hazardous, Radioactive, and Mixed Wastes: 2nd Volume. ASTM International, 100 Barr Harbor Drive, PO Box C700, West Conshohocken, PA 19428-2959, pp. 361-361–17. https://doi.org/10.1520/STP19564S

Izquierdo, M., Querol, X., 2012. Leaching behaviour of elements from coal combustion fly ash: An overview. Int. J. Coal Geol. 94, 54–66. https://doi.org/10.1016/J.COAL.2011.10.006

Jarvie, H.P., King, S.M., Neal, C., 2017. Inorganic carbon dominates total dissolved carbon concentrations and fluxes in British rivers: Application of the THINCARB model – Thermodynamic modelling of inorganic carbon in freshwaters. Sci. Total Environ. 575, 496–512. https://doi.org/10.1016/J.SCITOTENV.2016.08.201

Johnson, C.A., Kaeppeli, M., Brandenberger, S., Ulrich, A., Baumann, W., 1999. Hydrological and geochemical factors affecting leachate composition in municipal solid waste incinerator bottom ash: Part II. The geochemistry of leachate from Landfill Lostorf, Switzerland. J. Contam. Hydrol. 40, 239–259. https://doi.org/10.1016/S0169-7722(99)00052-2

Jones, D.R., 1995. The Leaching of major and trace elements from coal ash, in: Environmental Aspects of Trace Elements in Coal. Springer, Dordrecht, Netherlands, pp. 221–262. https://doi.org/10.1007/978-94-015-8496-8_12

Kim, A.G., Kazonich, G., Dahlberg, M., 2003. Relative solubility of cations in Class F fly ash. Environ. Sci. Technol. 37, 4507–4511. https://doi.org/10.1021/ES0263691

Kogbara, R.B., Al-Tabbaa, A., Stegemann, J.A., 2014. Comparisons of operating envelopes for contaminated soil stabilised/solidified with different cementitious binders. Environ. Sci. Pollut. Res. 21, 3395–3414. https://doi.org/10.1007/s11356-013-2276-7

Kogbara, R.B., Al-Tabbaa, A., Yi, Y., Stegemann, J.A., 2013. Cement–fly ash stabilisation/solidification of contaminated soil: Performance properties and initiation of operating envelopes. Appl. Geochemistry 33, 64–75. https://doi.org/10.1016/J.APGEOCHEM.2013.02.001

Komonweeraket, K., Cetin, B., Aydilek, A., Benson, C.H., Edil, T.B., 2015a. Geochemical analysis of leached elements from fly ash stabilized soils. J. Geotech. Geoenvironmental Eng. 141, 04015012. https://doi.org/10.1061/(ASCE)GT.1943-5606.0001288

Komonweeraket, K., Cetin, B., Aydilek, A.H., Benson, C.H., Edil, T.B., 2015b. Effects of pH on the leaching mechanisms of elements from fly ash mixed soils. Fuel 140, 788–802. https://doi.org/10.1016/J.FUEL.2014.09.068

Komonweeraket, K., Cetin, B., Benson, C.H., Aydilek, A.H., Edil, T.B., 2015c. Leaching characteristics of toxic constituents from coal fly ash mixed soils under the influence of pH. Waste Manag. 38, 174–184. https://doi.org/10.1016/J.WASMAN.2014.11.018

Kosson, D.S., Garrabrants, A.C., DeLapp, R., van der Sloot, H.A., 2014. pH-dependent leaching of constituents of potential concern from concrete materials containing coal combustion fly ash. Chemosphere 103, 140–147. https://doi.org/10.1016/J.CHEMOSPHERE.2013.11.049

Kosson, D.S., van der Sloot, H.A., Sanchez, F., Garrabrants, A.C., 2002. An integrated framework for evaluating leaching in waste management and utilization of secondary materials. Environ. Eng. Sci. 19, 159–204. https://doi.org/10.1089/109287502760079188

Langmuir, D., 1997. Aqueous Environmental Geochemistry. Prentice Hall, Upper Saddle River, New Jersey, USA.

Li, J.-S., Wang, L., Cui, J.-L., Poon, C.S., Beiyuan, J., Tsang, D.C.W., Li, X.-D., 2018. Effects of low-alkalinity binders on stabilization/solidification of geogenic As-containing soils: Spectroscopic investigation and leaching tests. Sci. Total Environ. 631–632, 1486–1494. https://doi.org/10.1016/j.scitotenv.2018.02.247

Loncnar, M., van der Sloot, H.A., Mladenovič, A., Zupančič, M., Kobal, L., Bukovec, P., 2016. Study of the leaching behaviour of ladle slags by means of leaching tests combined with geochemical modelling and mineralogical investigations. J. Hazard. Mater. 317, 147–157. https://doi.org/10.1016/J.JHAZMAT.2016.05.046

Mahedi, M., Cetin, B., Cetin, K.S., 2019. Freeze-thaw performance of phase change material (PCM) incorporated pavement subgrade soil. Constr. Build. Mater. 202, 449–464. https://doi.org/10.1016/J.CONBUILDMAT.2018.12.210

Mahedi, M., Cetin, B., White, D.J., 2018. Performance evaluation of cement and slag stabilized expansive soils. Transp. Res. Rec. J. Transp. Res. Board 036119811875743. https://doi.org/10.1177/0361198118757439

Mudd, G.M., Weaver, T.R., Kodikara, J., 2004. Environmental geochemistry of leachate from leached brown coal ash. J. Environ. Eng. 130, 1514–1526. https://doi.org/10.1061/(ASCE)0733-9372(2004)130:12(1514)

Olmo, I.F., Chacon, E., Irabien, A., 2001. Influence of lead, zinc, iron (III) and chromium (III) oxides on the setting time and strength development of Portland cement. Cem. Concr. Res. 31, 1213–1219. https://doi.org/10.1016/S0008-8846(01)00545-2

Oormila, T.., Preethi, T.V., 2014. Effect of stabilization using flyash and GGBS in soil characteristics. Int. J. Eng. Trends Technol. 11, 284–289. https://doi.org/10.14445/22315381/IJETT-V11P254

Querol, X., Umaña, J.., Alastuey, A., Ayora, C., Lopez-Soler, A., Plana, F., 2001. Extraction of soluble major and trace elements from fly ash in open and closed leaching systems. Fuel 80, 801–813. https://doi.org/10.1016/S0016-2361(00)00155-1

Roy, A., Cartledge, F.K., 1997. Long-term behavior of a Portland cement-electroplating sludge waste form in presence of copper nitrate. J. Hazard. Mater. 52, 265–286. https://doi.org/10.1016/S0304-3894(96)01812-2

Roy, W.R., Griffin, R.A., Dickerson, D.R., Schuller, R.M., 1984. Illinois basin coal fly ashes. 1. Chemical characterization and solubility. Environ. Sci. Technol. 18, 734–739. https://doi.org/10.1021/es00128a003

Sas, W., Głuchowski, A., Radziemska, M., Dzięcioł, J., Szymański, A., 2015. Environmental and geotechnical assessment of the steel slags as a material for road structure. Materials (Basel). 8, 4857–4875. https://doi.org/10.3390/ma8084857

Schulz, K.G., Riebesell, U., Rost, B., Thoms, S., Zeebe, R.E., 2006. Determination of the rate constants for the carbon dioxide to bicarbonate inter-conversion in pH-buffered seawater systems. Mar. Chem. 100, 53–65. https://doi.org/10.1016/J.MARCHEM.2005.11.001

Shi, C., 2004. Steel Slag—its production, processing, characteristics, and cementitious properties. J. Mater. Civ. Eng. 16, 230–236. https://doi.org/10.1061/(ASCE)0899-1561(2004)16:3(230)

Sparks, D.L., 2003. Environmental Soil Chemistry. Academic Press, San Diego, California, USA. https://doi.org/https://doi.org/10.1016/B978-0-12-656446-4.X5000-2

Stronach, S.A., Glasser, F.P., 1997. Modelling the impact of abundant geochemical components on phase stability and solubility of the CaO—SiO2 —H2O system at 25°C: Na+, K+, SO42-, Cl- and CO32-. Adv. Cem. Res. 9, 167–181. https://doi.org/10.1680/adcr.1997.9.36.167

Stumm, W., Morgan, J.J., 1996. Aquatic Chemistry : Chemical Equilibria and Rates in Natural Waters. Wiley & Sons, Hoboken, New Jersey, USA.

Tastan, E.O., Edil, T.B., Benson, C.H., Aydilek, A.H., 2011. Stabilization of organic soils with fly ash. J. Geotech. Geoenvironmental Eng. 137, 819–833. https://doi.org/10.1061/(ASCE)GT.1943-5606.0000502

Thomas, M., 2007. Optimizing the use of fly ash in concrete. Skokie, Ill Portl. Cem. Assoc. 24. https://doi.org/10.15680/IJIRSET.2015.0409047

Tiruta-Barna, L., Rakotoarisoa, Z., Méhu, J., 2006. Assessment of the multi-scale leaching behaviour of compacted coal fly ash. J. Hazard. Mater. 137, 1466–78. https://doi.org/10.1016/j.jhazmat.2006.04.039

U.S. Geological Survey, 2018. Mineral commodity summaries 2018: U.S. Geological Survey. Washington, DC. https://doi.org/https://doi.org/10.3133/ 70194932

van der Sloot, H.., 2002. Characterization of the leaching behaviour of concrete mortars and of cement–stabilized wastes with different waste loading for long term environmental assessment. Waste Manag. 22, 181–186. https://doi.org/10.1016/S0956-053X(01)00067-8

Wang, F., Shen, Z., Al-Tabbaa, A., 2018. An evaluation of stabilised/solidified contaminated model soil using PC-based and MgO-based binders under semi-dynamic leaching conditions. Environ. Sci. Pollut. Res. 25, 16050–16060. https://doi.org/10.1007/s11356-018-1591-4

Wang, T., Wang, J., Burken, J.G., Ban, H., Ladwig, K., 2007. The leaching characteristics of selenium from coal fly ashes. J. Environ. Qual. 36, 1784. https://doi.org/10.2134/jeq2007.0143

Warren, C.J., Dudas, M.J., 1988. Leaching behaviour of selected trace elements in chemically weathered alkaline fly ash. Sci. Total Environ. 76, 229–246. https://doi.org/10.1016/0048-9697(88)90110-6

Warren, C.J., Dudas, M.J., 1985. Formation of secondary minerals in artificially weathered fly ash. J. Environ. Qual. 14, 405. https://doi.org/10.2134/jeq1985.00472425001400030019x

Warren, C.J., Dudas, M.J., 1984. Weathering processes in relation to leachate properties of alkalinefly Ash. J. Environ. Qual. 13, 530. https://doi.org/10.2134/jeq1984.00472425001300040005x

Windt, L. De, Chaurand, P., Rose, J., 2011. Kinetics of steel slag leaching: Batch tests and modeling. Waste Manag. 31, 225–235. https://doi.org/10.1016/J.WASMAN.2010.05.018

Yilmaz, Y., Coban, H.S., Cetin, B., Edil, T.B., 2019. Use of standard and off-spec fly ashes for soil stabilization. J. Mater. Civ. Eng. 31, 04018390. https://doi.org/10.1061/(ASCE)MT.1943-5533.0002599

Zhang, Y., Cetin, B., Likos, W.J., Edil, T.B., 2016. Impacts of pH on leaching potential of elements from MSW incineration fly ash. Fuel 184, 815–825. https://doi.org/10.1016/J.FUEL.2016.07.089

3.8 Tables and Figures

Table 4.1 Chemical compositions, physical properties and metal contents of fly ashes, slag, cement and soil

Chemical Compositrion[*]	Class C FA	Class F FA	Slag	Cement	Soil
pH[a]	12.01	11.64	11.6	12.65	8.57
CaO (%)	25.9	11.8	39.8	64	5.2
MgO (%)	5.2	2.9	10.4	2.2	2.1
K_2O (%)	0.49	1.1	0.41	0.55	2.06
Na_2O (%)	1.65	0.58	0.24	0.14	1.33
$SiO_2 + Al_2O_3 + Fe_2O_3$ (%)	61.5	80.4	46.2	27.4	80.6
SiO_2 (%)	37.6	56.3	35.7	20	67.7
Al_2O_3 (%)	18	18.6	9.9	4.4	9.6
Fe_2O_3 (%)	5.9	5.5	0.6	3	3.3
SO_3 (%)	1.2	0.4	1.1	2.9	0.03
Loss on ignition, LOI (%)	0.24	0.14	N/A	2.45	6.91
Initial moisture, w/w (%)	0.05	0.03	0.07	N/A	1.34
Specific Gravity, G_s	2.7	2.67	2.55	N/A	2.74
Liquid limit, LL (%)	NP	NP	NP	NP	24
Plasticity Index, PI (%)	NP	NP	NP	NP	4
Classification	Class C[b]	Class F[b]	-	Type I/II[c]	ML[d]
Total metal concentration (mg/kg)[**]					
Ca	143142	60300	186228	313810	33100
Mg	24414	10371	64685	9564	11348
Mn	279	295	1,847	280	602
Ba	4379	1440	211	61	222
Cr	70.3	69.3	35.3	35	29.6
S	9103	3176	12600	18200	916

Note: [*]From X-ray fluorescence spectrometry (XRF); FA: Fly ash; [a]EPA 9045D; [b]ASTM C618; [c]ASTM C150/C150M; [d]USGS classification, [**]U.S. EPA Method 3050B; Hyphen: not applicable; NP: nonplastic; N/A: Not available

Table 4.2 Composition of the mixtures with optimum moisture content (OMC) and maximum dry density (MMD)

Component	Soil	Class C Fly Ash				Class F Fly Ash				Slag			
Loess Soil (%)[*]	100	87	84	74	54	87	84	74	54	87	84	74	54
Fly Ash or Slag Content (%)[*]	-	10	10	20	40	10	10	20	40	10	10	20	40
Type I/II Cement Content (%)[*]	-	3	6	6	6	3	6	6	6	3	6	6	6
Optimum Moisture (%)[a]	16.2	18.8	17	14.5	14	17.5	18	17	15.2	18.5	18	17	18.7
Max. Dry Density (kN/m^3)[a]	16.7	16.6	16.6	17	16.7	16.5	16.6	16.8	17	16.3	16.6	16.7	16.8

Note: [*]Dry weight basis; [a]ASTM D698
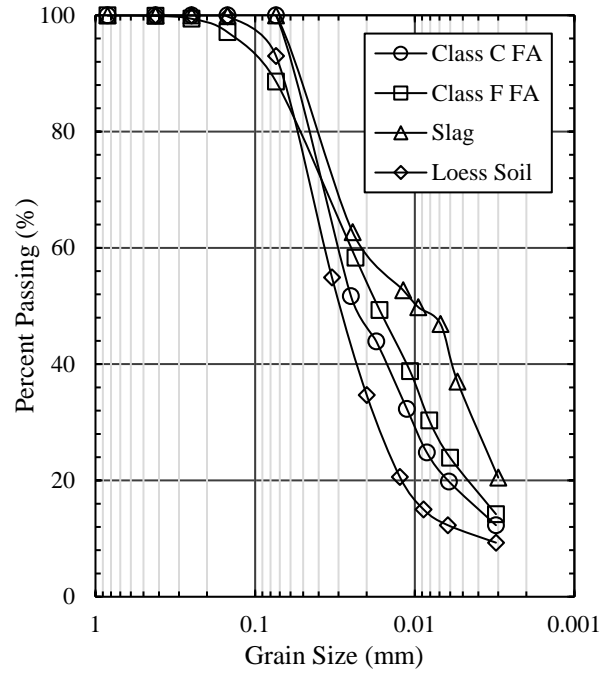
Figure 4.1 Grain size distribution of the materials used in the study
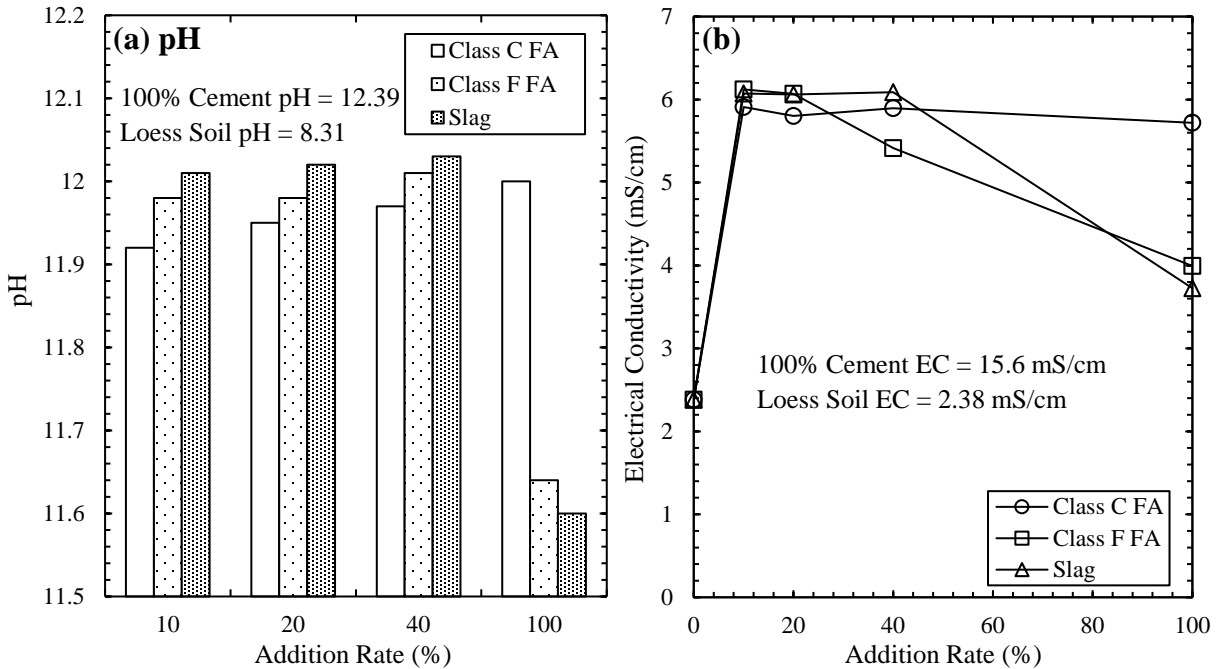
Figure 4.2 Effect of fly ash or slag content on (a) pH, and (b) electric conductivity. Note: In addition to fly ash or slag content, mixtures were prepared with 6% type I/II cement. Zero and hundred percent corresponds to soil and fly ash/slag only
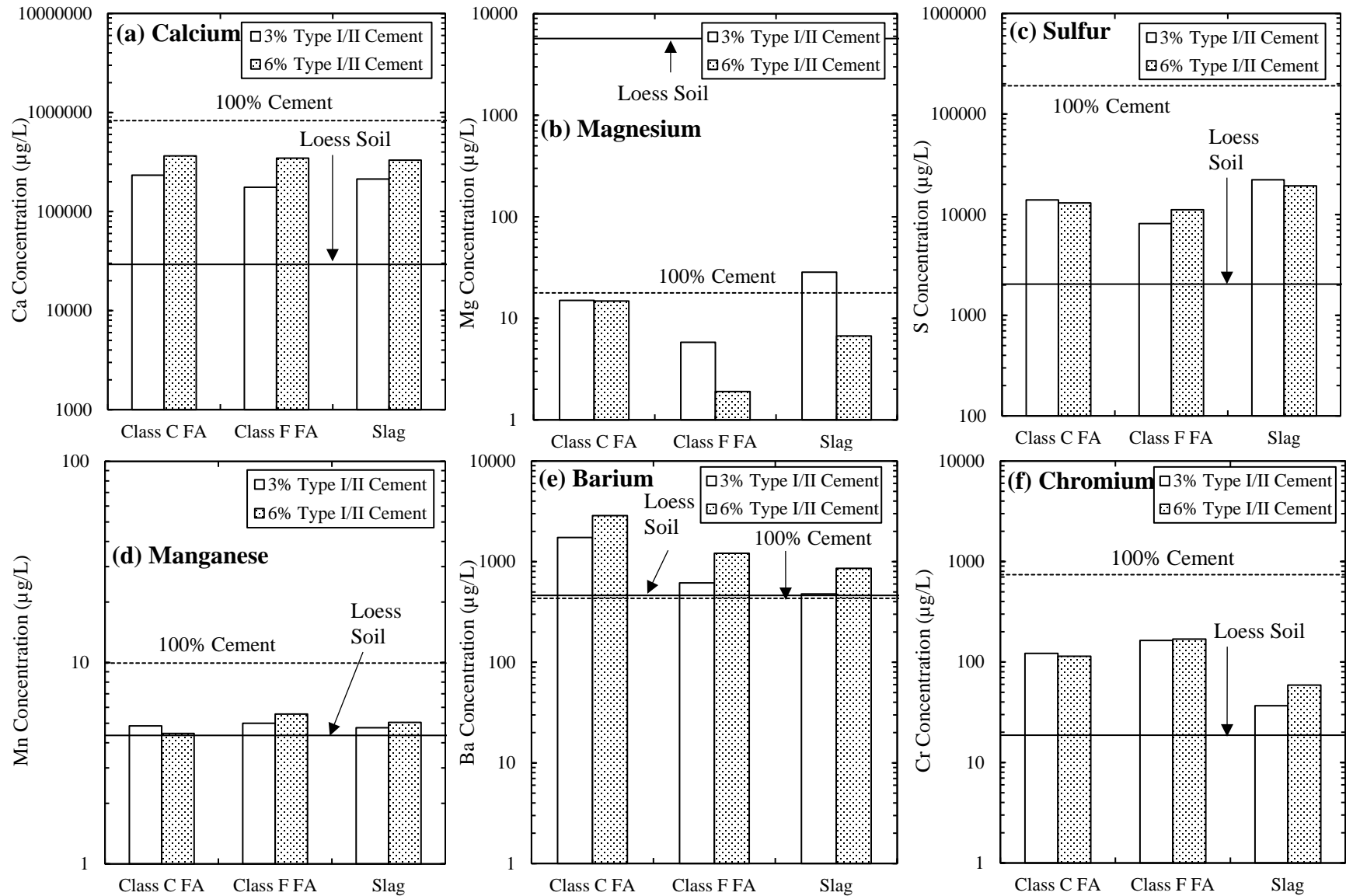
Figure 4.3 Change in (a) Ca, (b) Mg, (c) S, (d) Mn, (e) Ba, and (f) Cr concentrations with type I/II cement content in WLT effluent
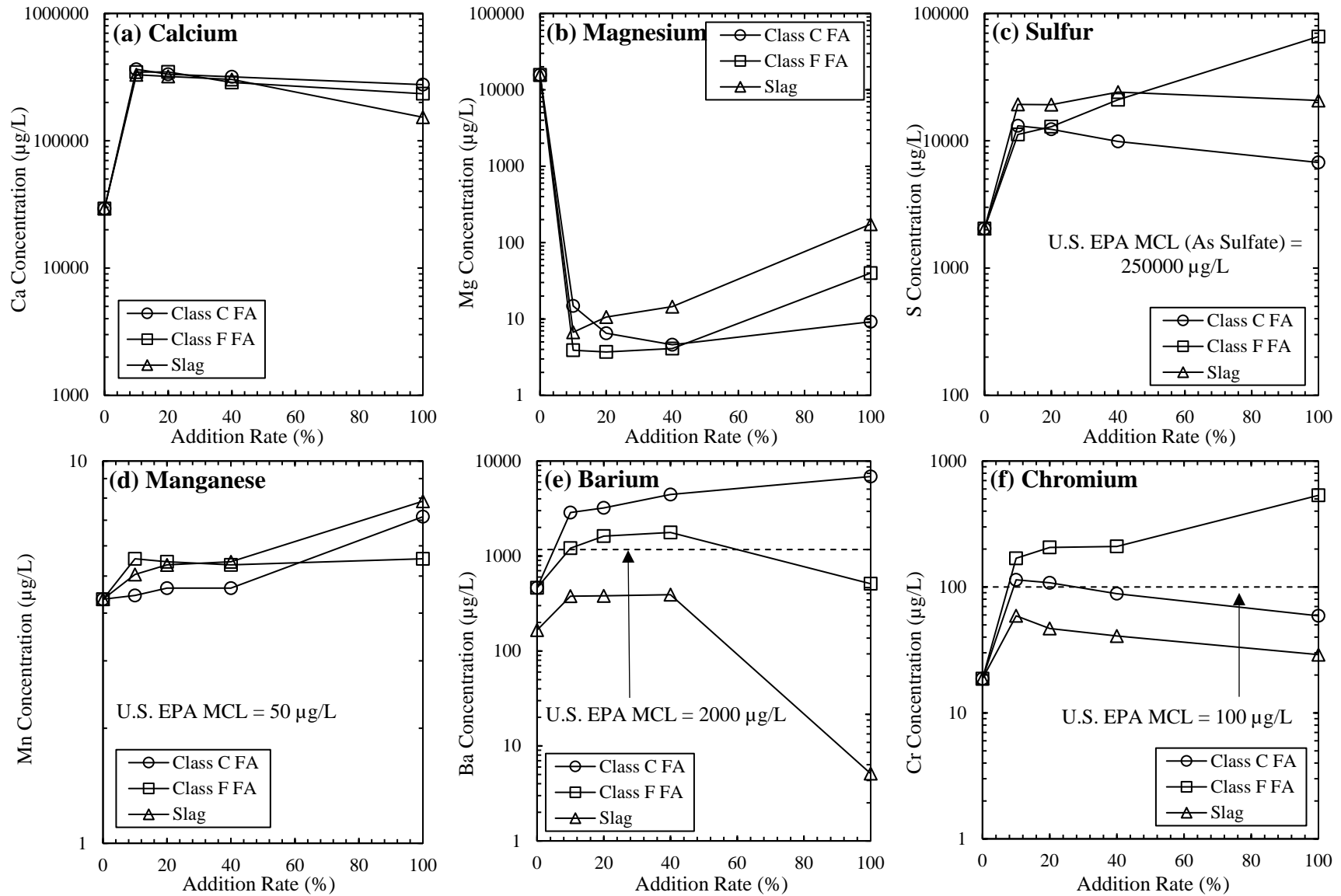
Figure 4.4 Change in (a) Ca, (b) Mg, (c) S, (d) Mn, (e) Ba, and (f) Cr concentrations with fly ash or slag content in WLT effluent
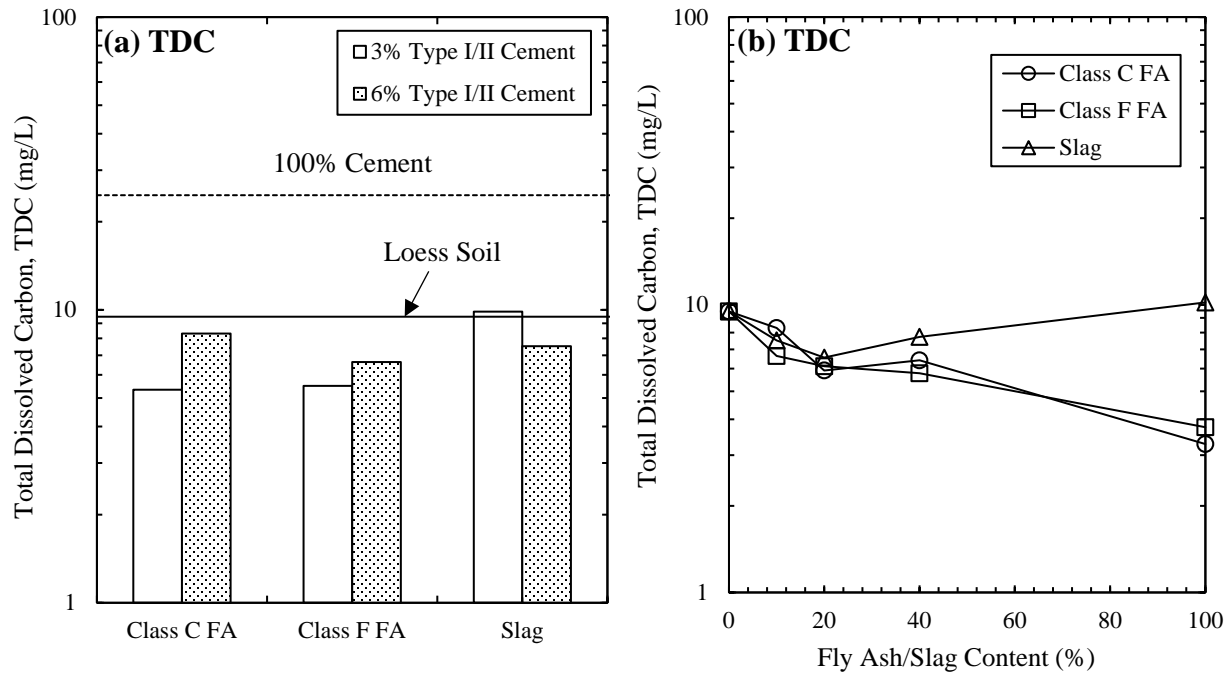
Figure 4.5 Change in Total dissolved carbon (TDC) concentrations with (a) cement content, and (b) fly ash or slag content in WLT effluent. Note: Zero and hundred percent corresponds to soil and fly ash, slag only

134
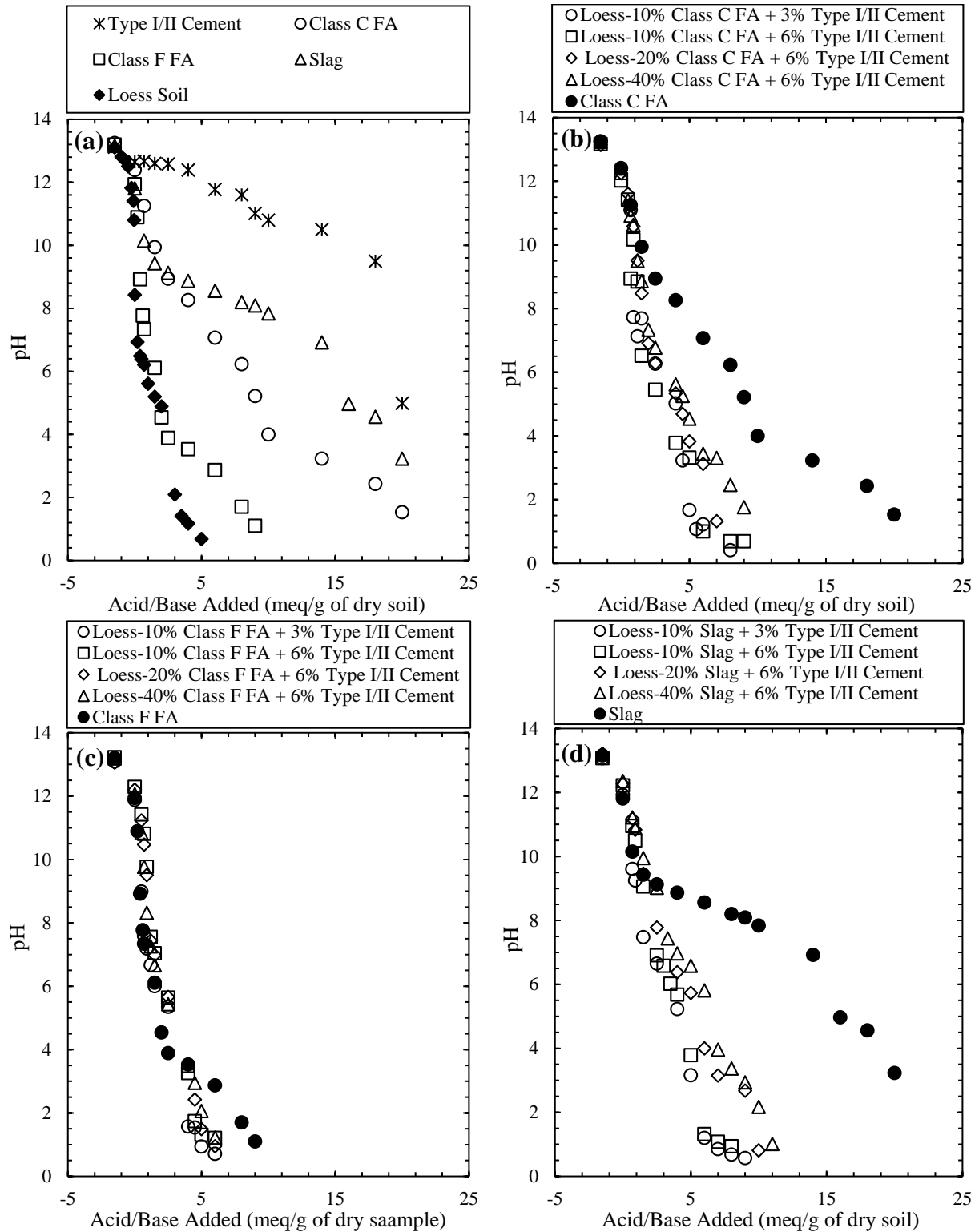
Figure 4.6 Acid neutralizing capacity (ANC) of (a) soil, fly ashes, slag and cement, (b) class C fly ash mixtures, (c) class F fly ash mixtures, and (d) slag mixtures
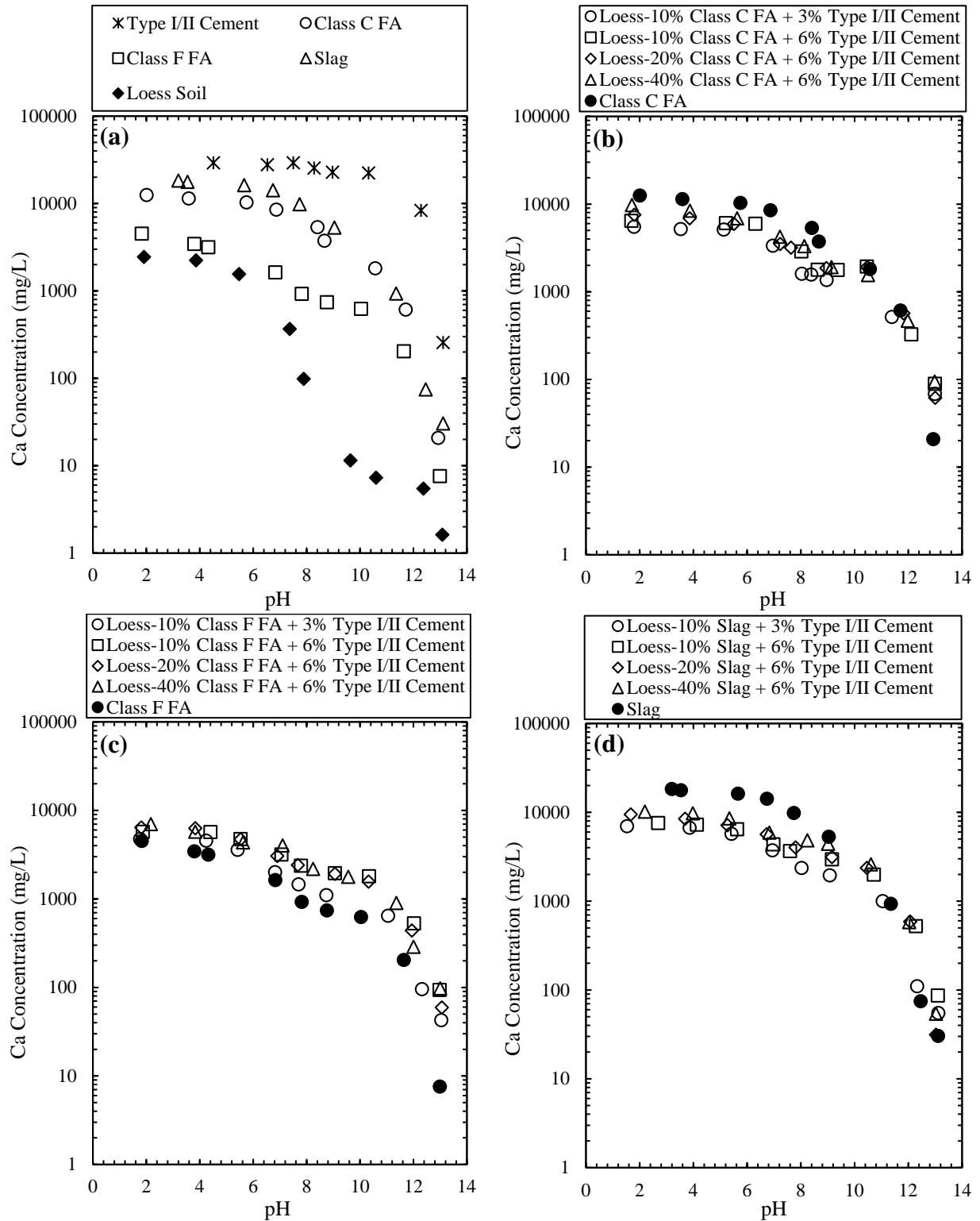
Figure 4.7 pH dependent leaching of Ca in the leachates from (a) soil, cement, fly ashes and slag, (b) Class C FA mixtures, (c) Class F FA mixtures, and (d) slag mixtures. Note: FA- Fly ash

Figure 4.8 pH dependent leaching of Mg in the leachates from (a) soil, cement, fly ashes and slag, (b) Class C FA mixtures, (c) Class F FA mixtures, and (d) slag mixtures. Note: FA- Fly ash

Figure 4.9 pH dependent leaching of S in the leachates from (a) soil, cement, fly ashes and slag, (b) Class C FA mixtures, (c) Class F FA mixtures, and (d) slag mixtures. Note: FA- Fly ash

Figure 4.10   pH dependent leaching of Mn in the leachates from (a) soil, cement, fly ashes and slag, (b) Class C FA mixtures, (c) Class F FA mixtures, and (d) slag mixtures. Note: FA- Fly ash
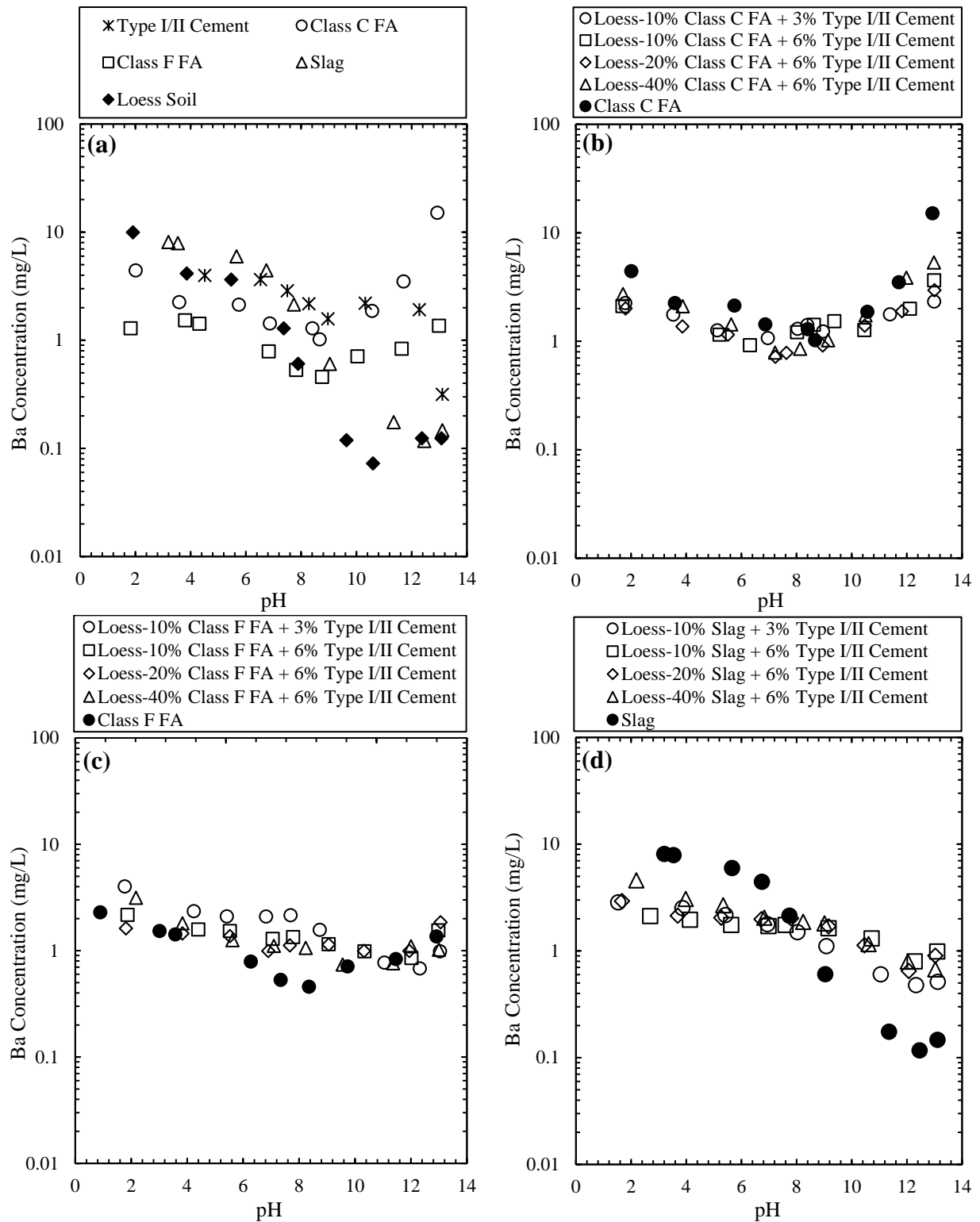
Figure 4.11   pH dependent leaching of Ba in the leachates from (a) soil, cement, fly ashes and slag, (b) Class C FA mixtures, (c) Class F FA mixtures, and (d) slag mixtures. Note: FA- Fly ash

Figure 4.12 pH dependent leaching of Cr in the leachates from (a) soil, cement, fly ashes and slag, (b) Class C FA mixtures, (c) Class F FA mixtures, and (d) slag mixtures. Note: FA- Fly ash

Figure 4.13 pH dependent leaching of TDC in the leachates from (a) soil, cement, fly ashes and slag, (b) Class C FA mixtures, (c) Class F FA mixtures, and (d) slag mixtures. Note: FA- Fly ash

**Figure 4.14**   Ternary diagram for Barium, Manganese and Sulfate for (a) soil, fly ashes, slag and cement (b) soil-class C fly ash mixtures, (c) soil-class F fly ash mixtures, and (d) soil-slag mixtures
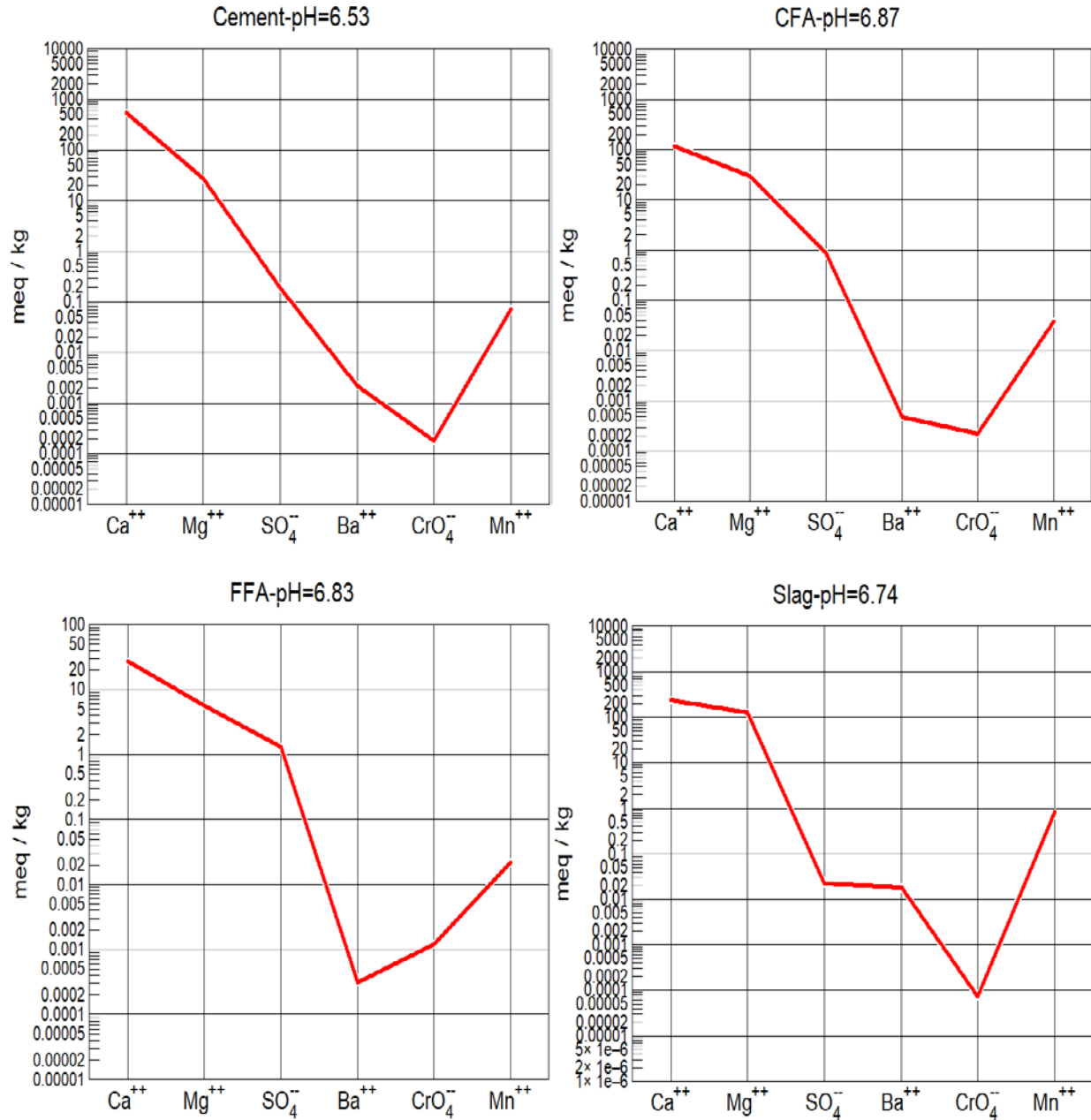
Figure 4.15   Schoeller diagrams for Ba, Ca, Cr, Mg, Mn and SO4-2 for (a) cement, pH=6.53 (b) soil-class C fly ash mixtures, (c) soil-class F fly ash mixtures, and (d) soil-slag mixtures

144
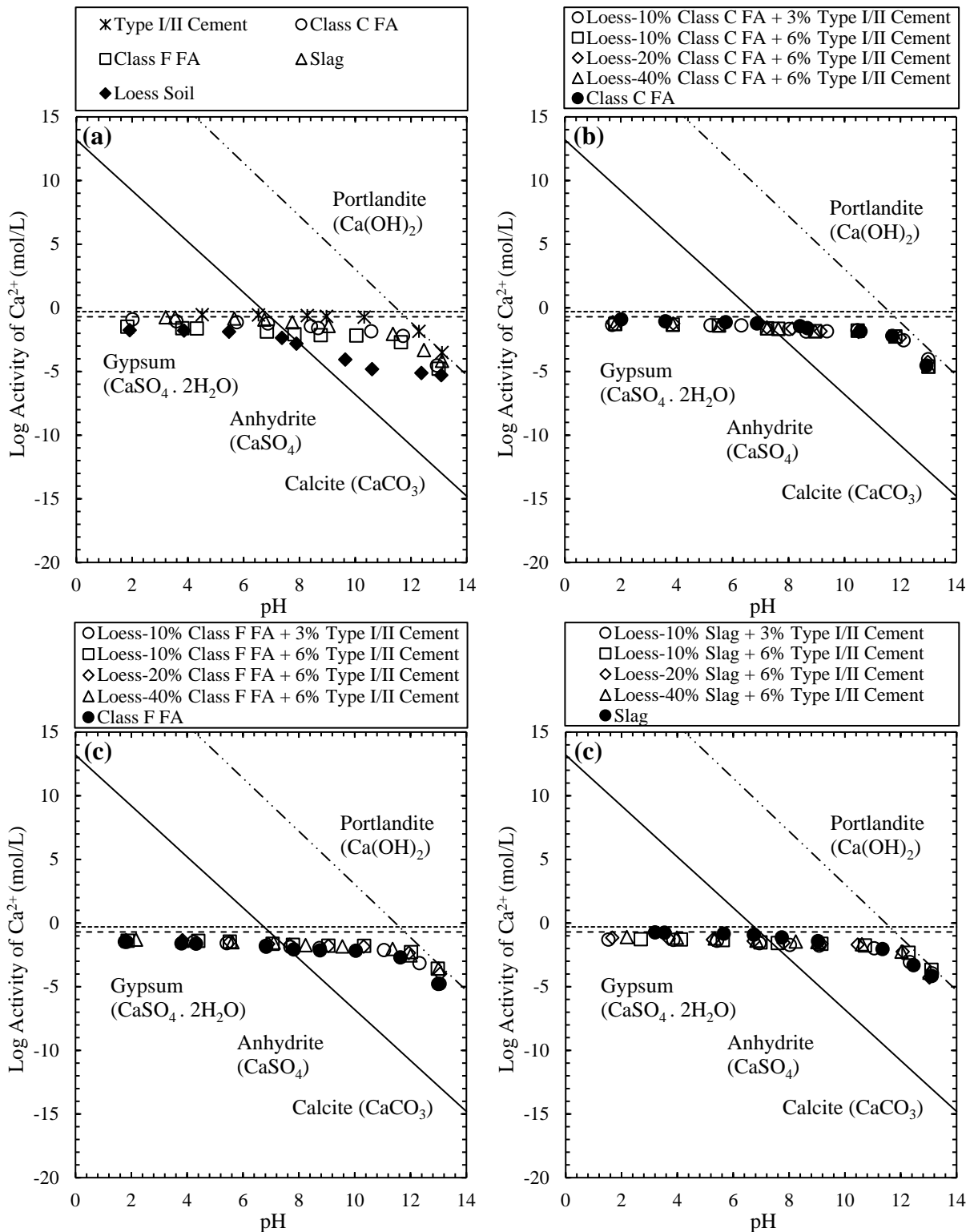
Figure 4.16   Log activity of Ca^{2+} with pH in the effluent from (a) soil, cement, fly ashes and slag, (b) Class C FA mixtures, (c) Class F FA mixtures, and (d) slag mixtures. Note: FA- Fly ash
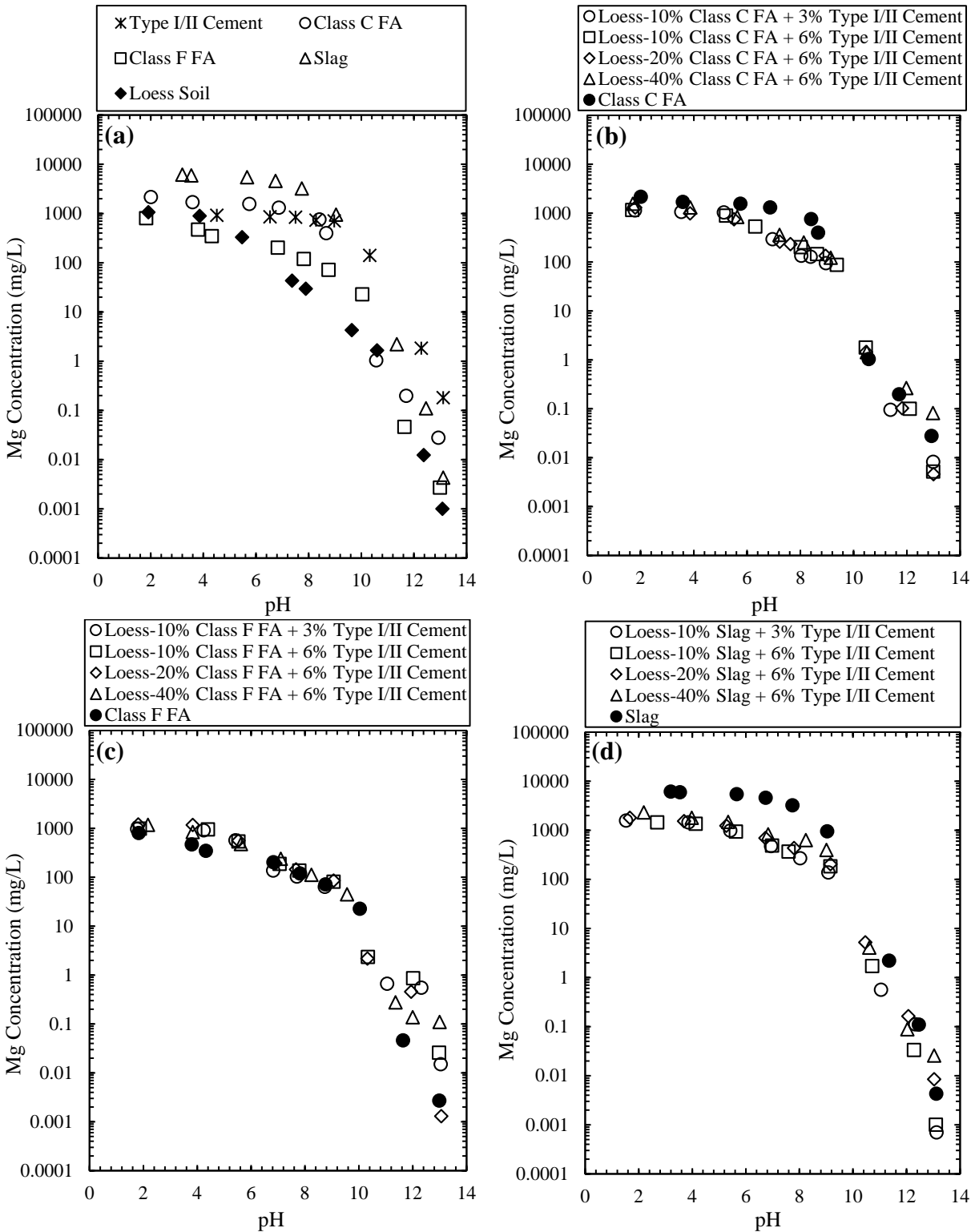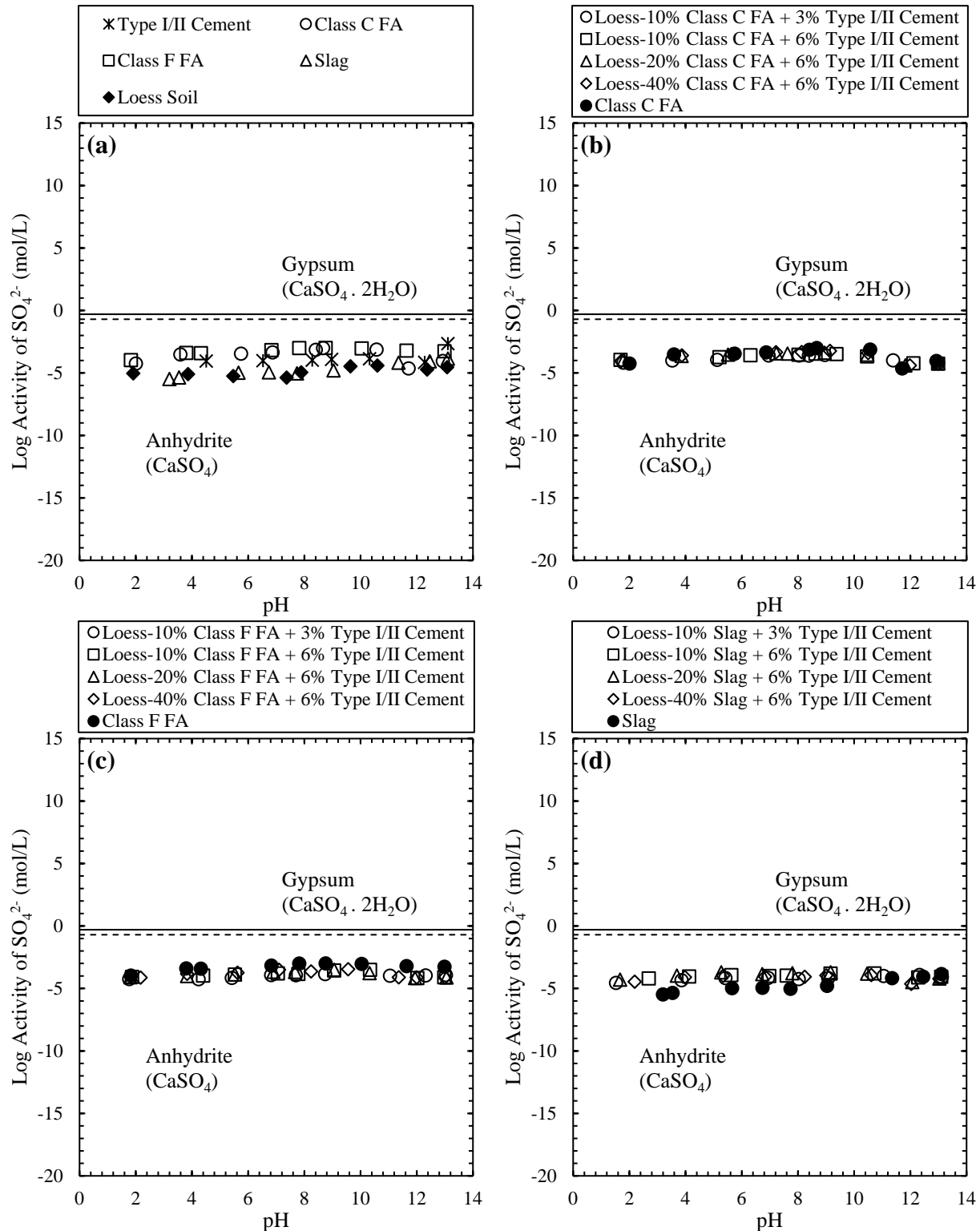
Figure 4.17 Log activity of SO_4^{2-} with pH in the effluent from (a) soil, cement, fly ashes and slag, (b) Class C FA mixtures, (c) Class F FA mixtures, and (d) slag mixtures. Note: FA- Fly ash
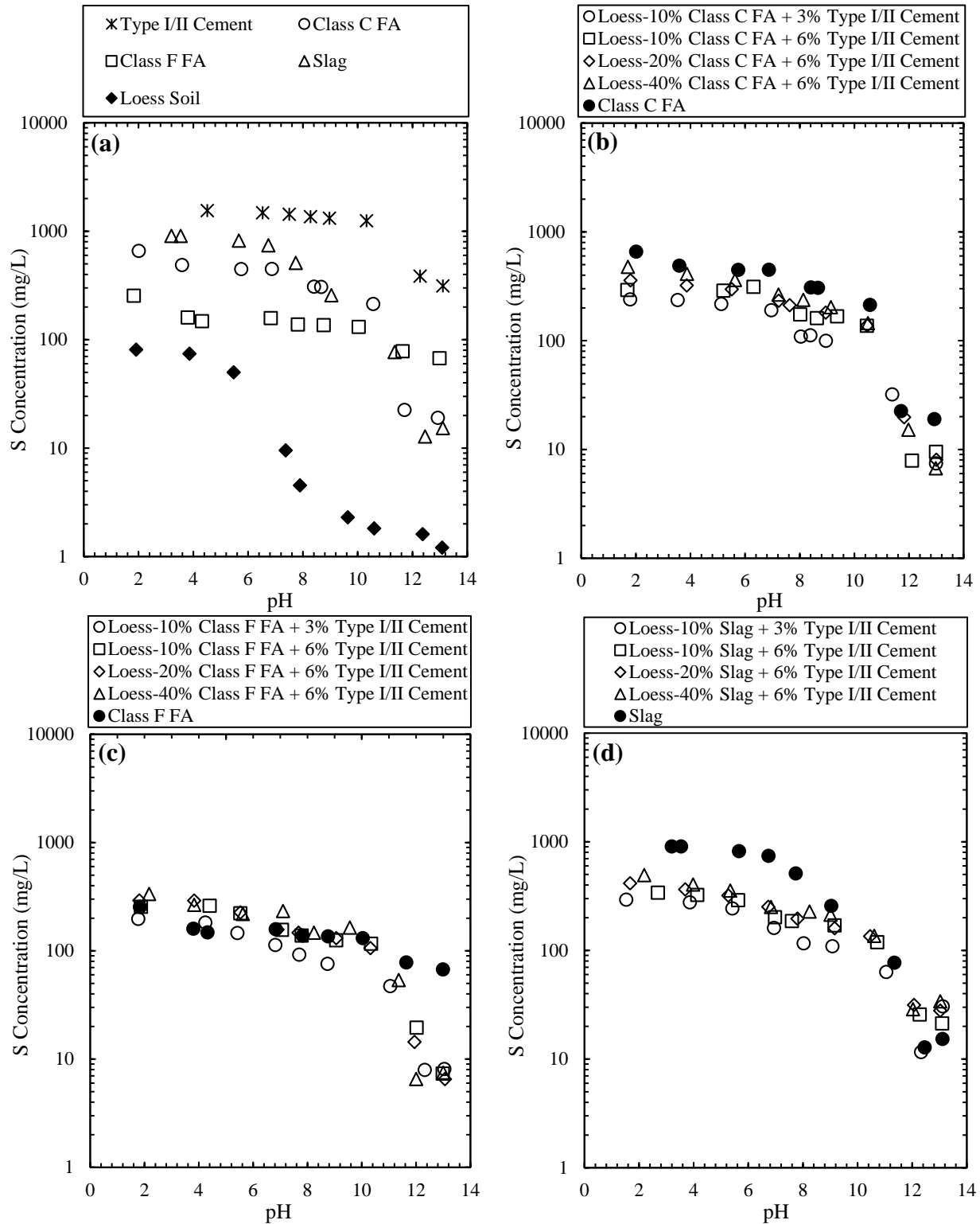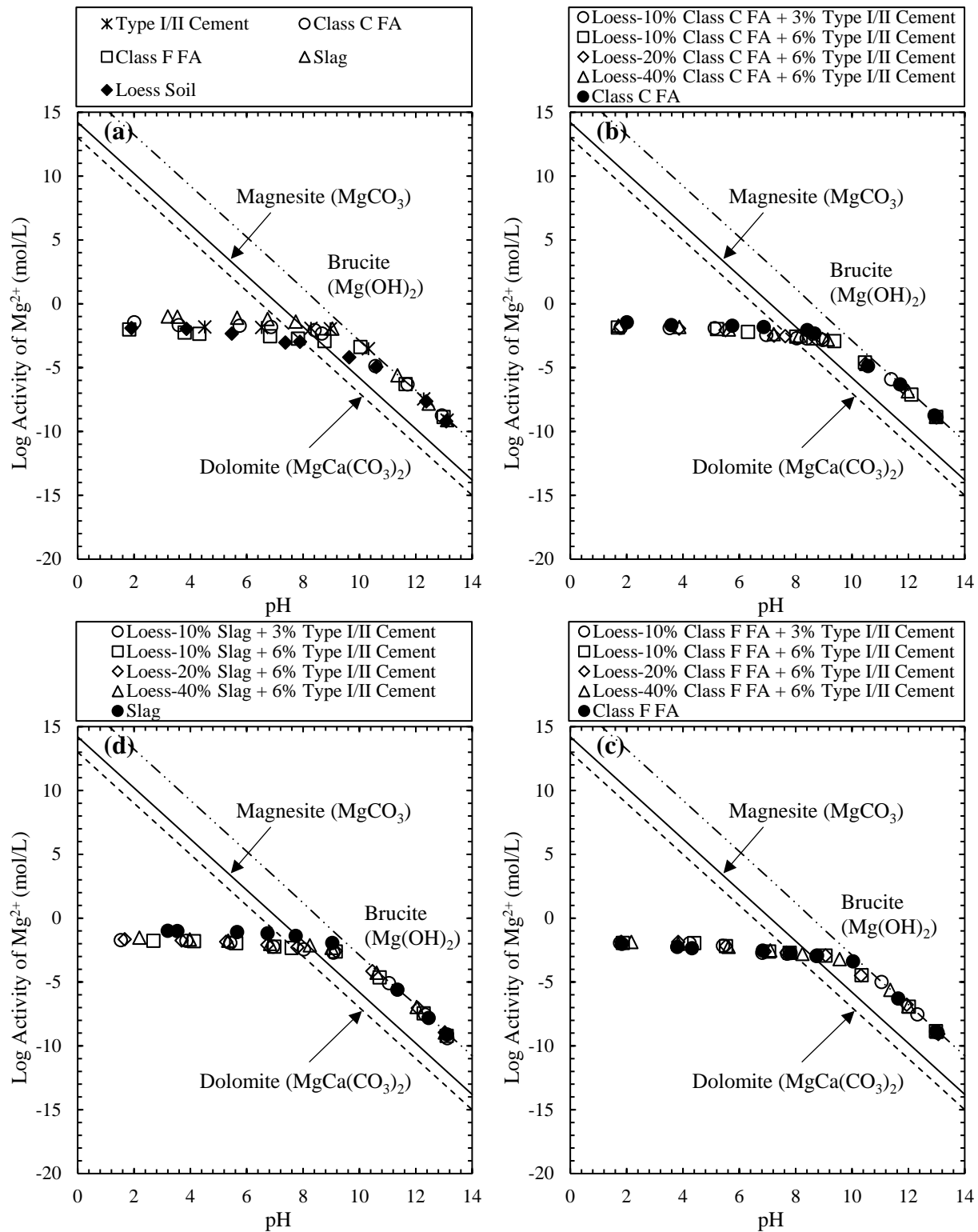
Figure 4.18 Log activity of Mg^{2+} with pH in the effluent from (a) soil, cement, fly ashes and slag, (b) Class C FA mixtures, (c) Class F FA mixtures, and (d) slag mixtures. Note: FA- Fly ash
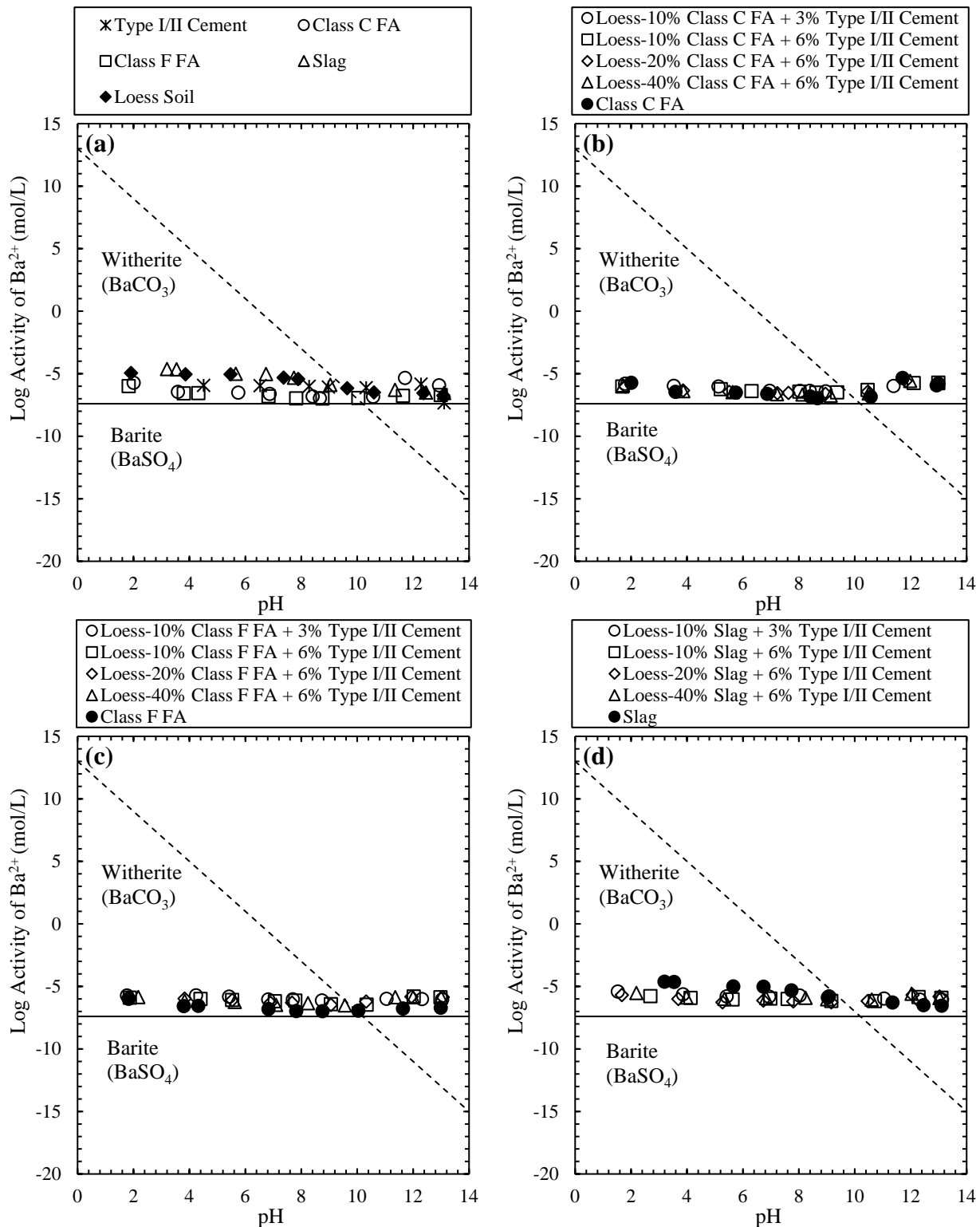
Figure 4.19 Log activity of Ba^{2+} with pH in the effluent from (a) soil, cement, fly ashes and slag, (b) Class C FA mixtures, (c) Class F FA mixtures, and (d) slag mixtures. Note: FA- Fly ash
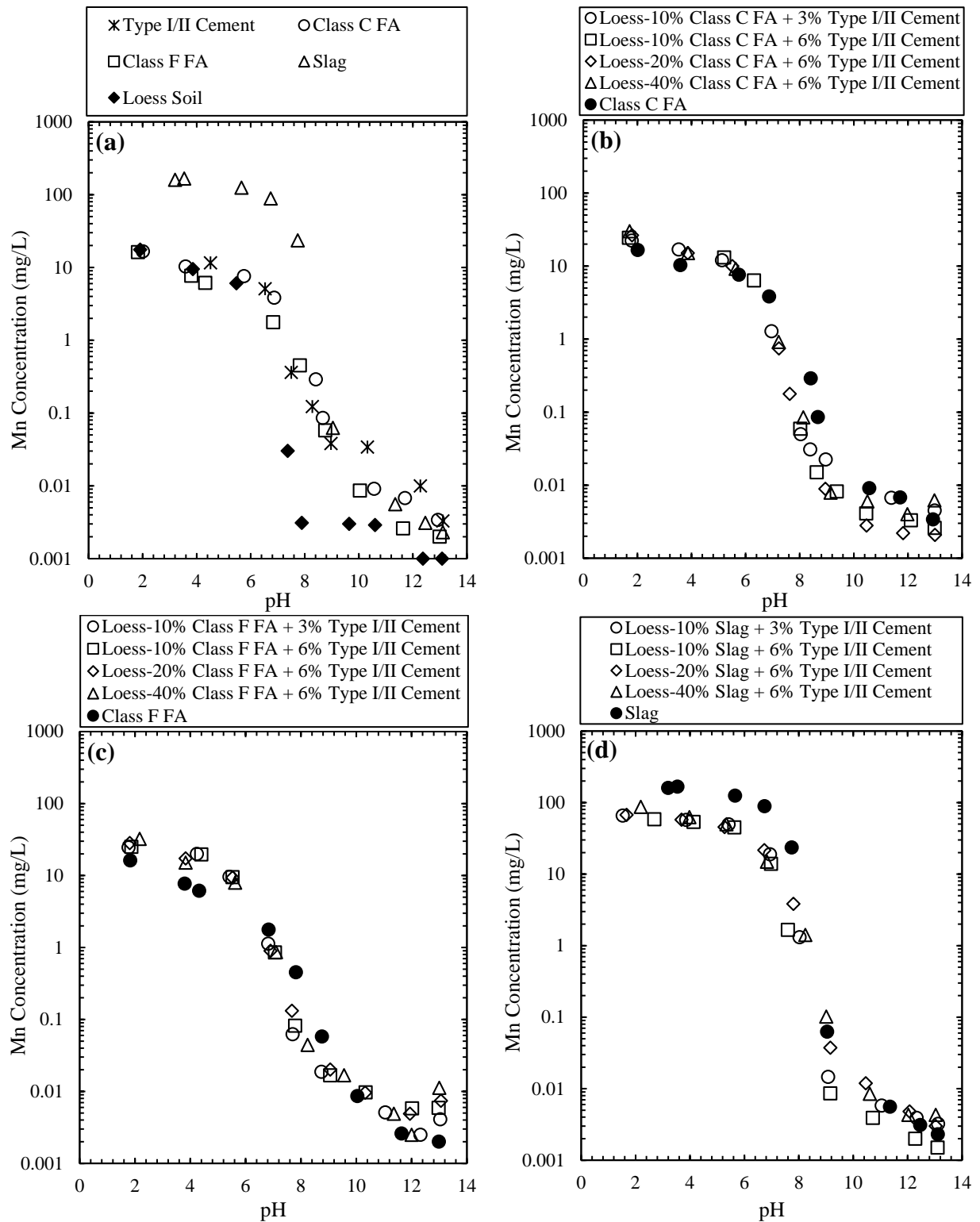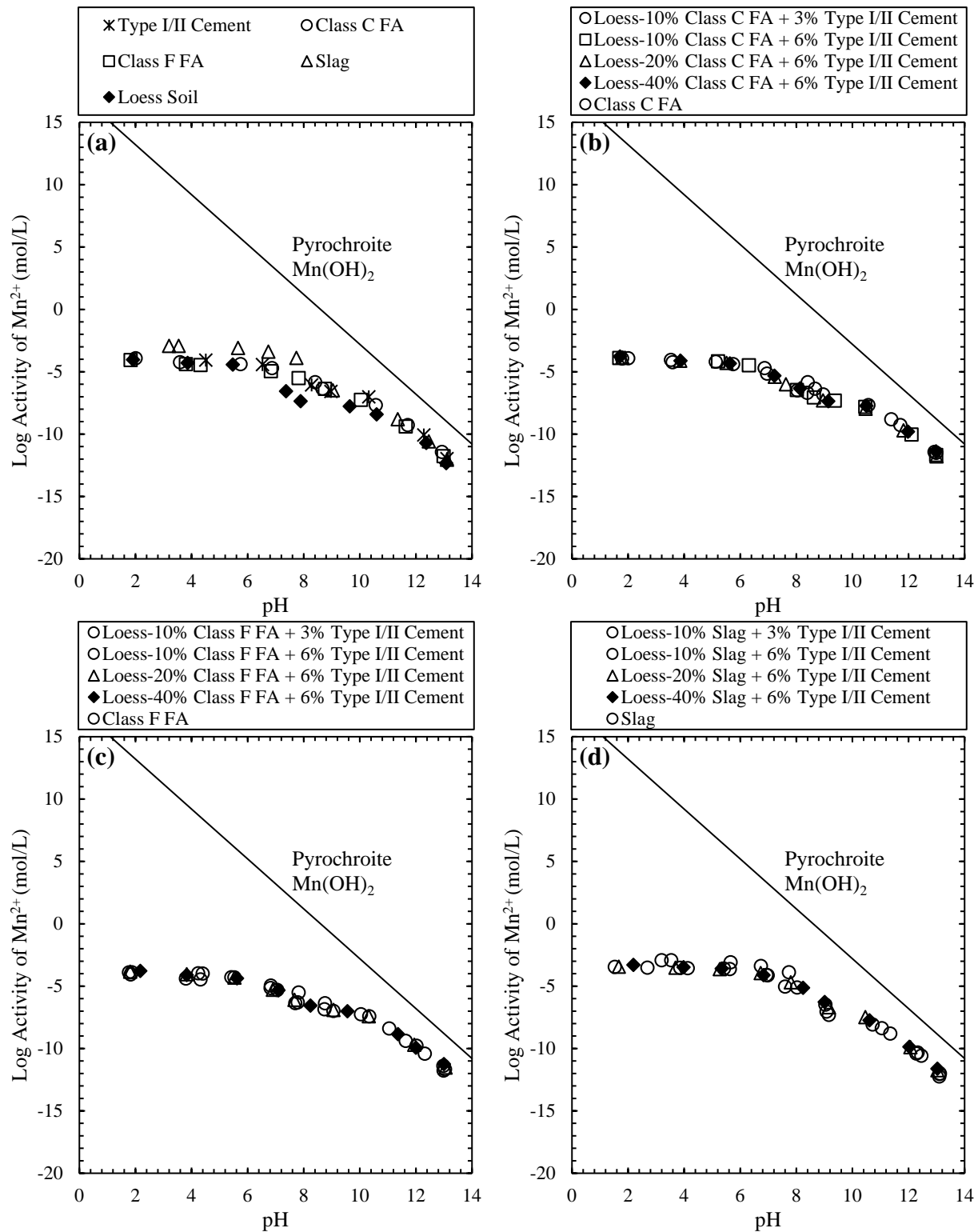
Figure 4.20 Log activity of Mn^{2+} with pH in the effluent from (a) soil, cement, fly ashes and slag, (b) Class C FA mixtures, (c) Class F FA mixtures, and (d) slag mixtures. Note: FA- Fly ash
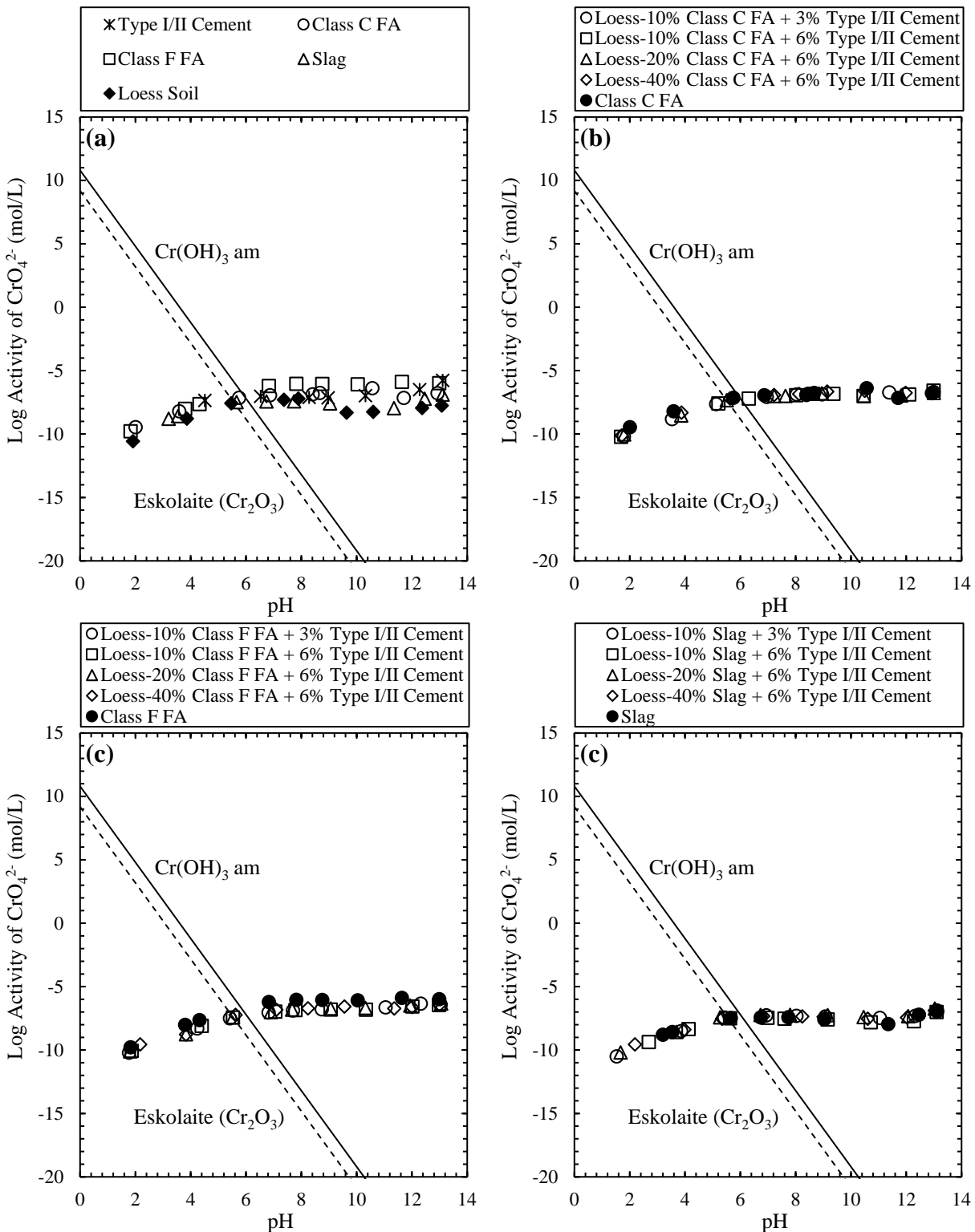
Figure 4.21 Log activity of CrO_4^{2-} with pH in the effluent from (a) soil, cement, fly ashes and slag, (b) Class C FA mixtures, (c) Class F FA mixtures, and (d) slag mixtures. Note: FA- Fly ash
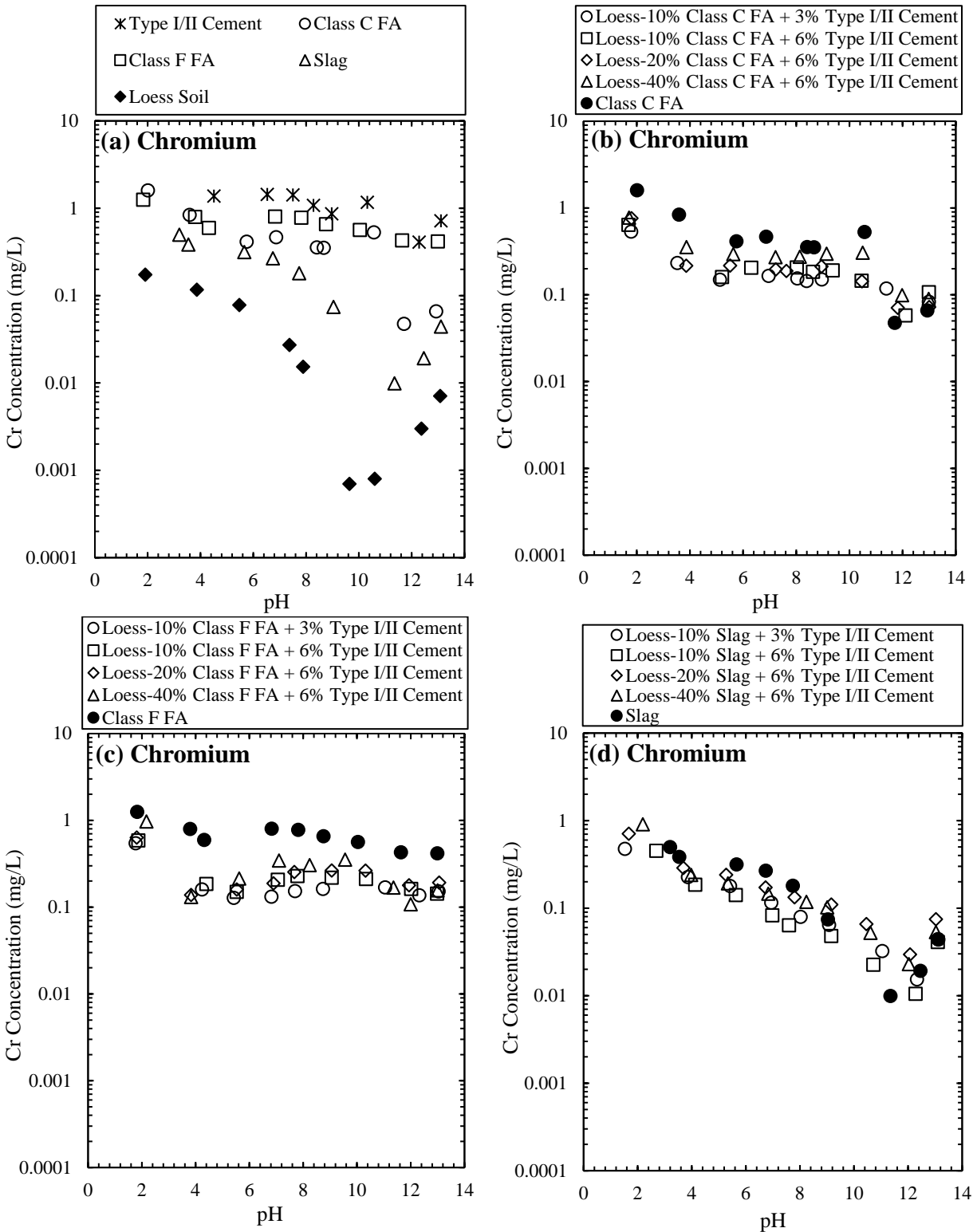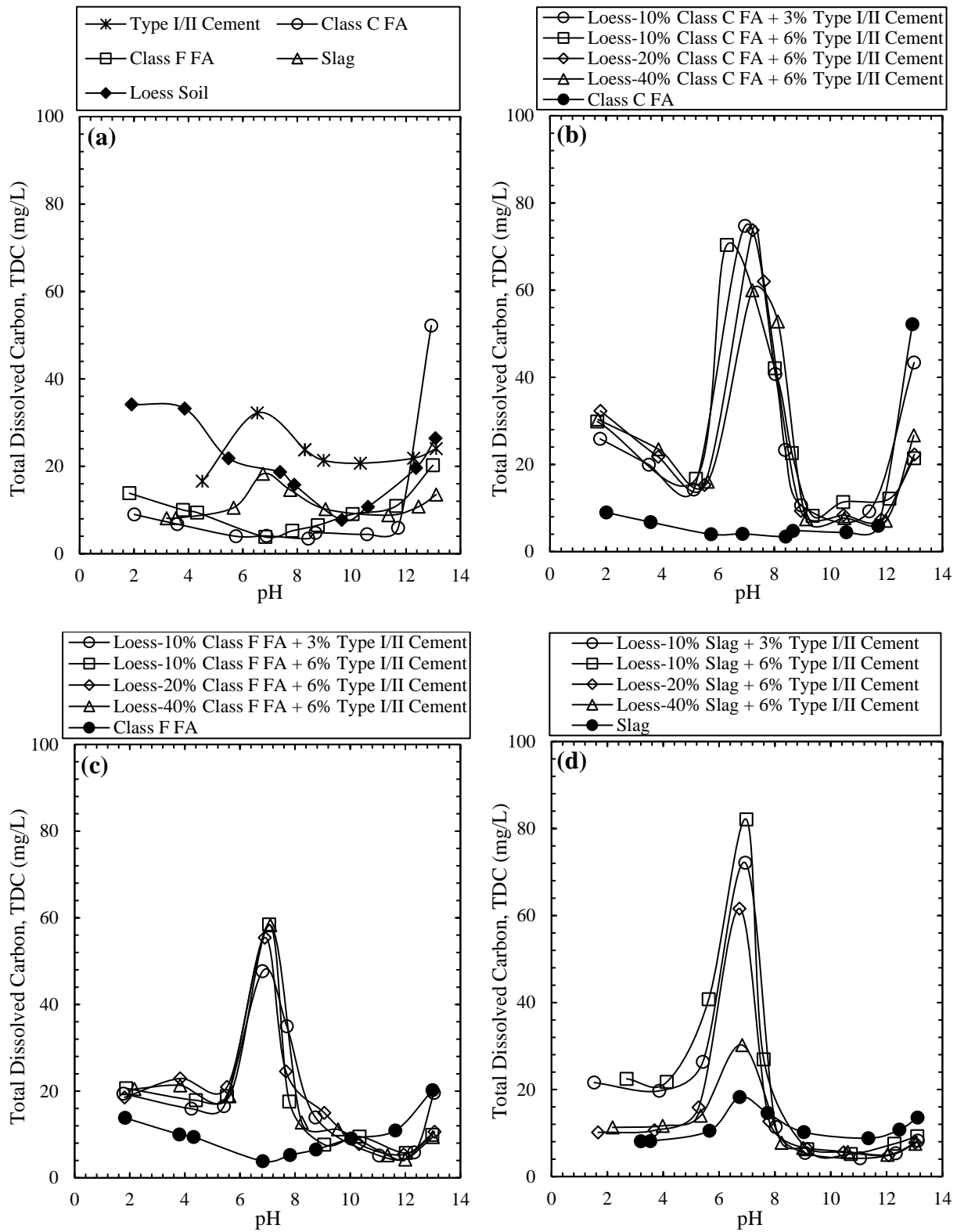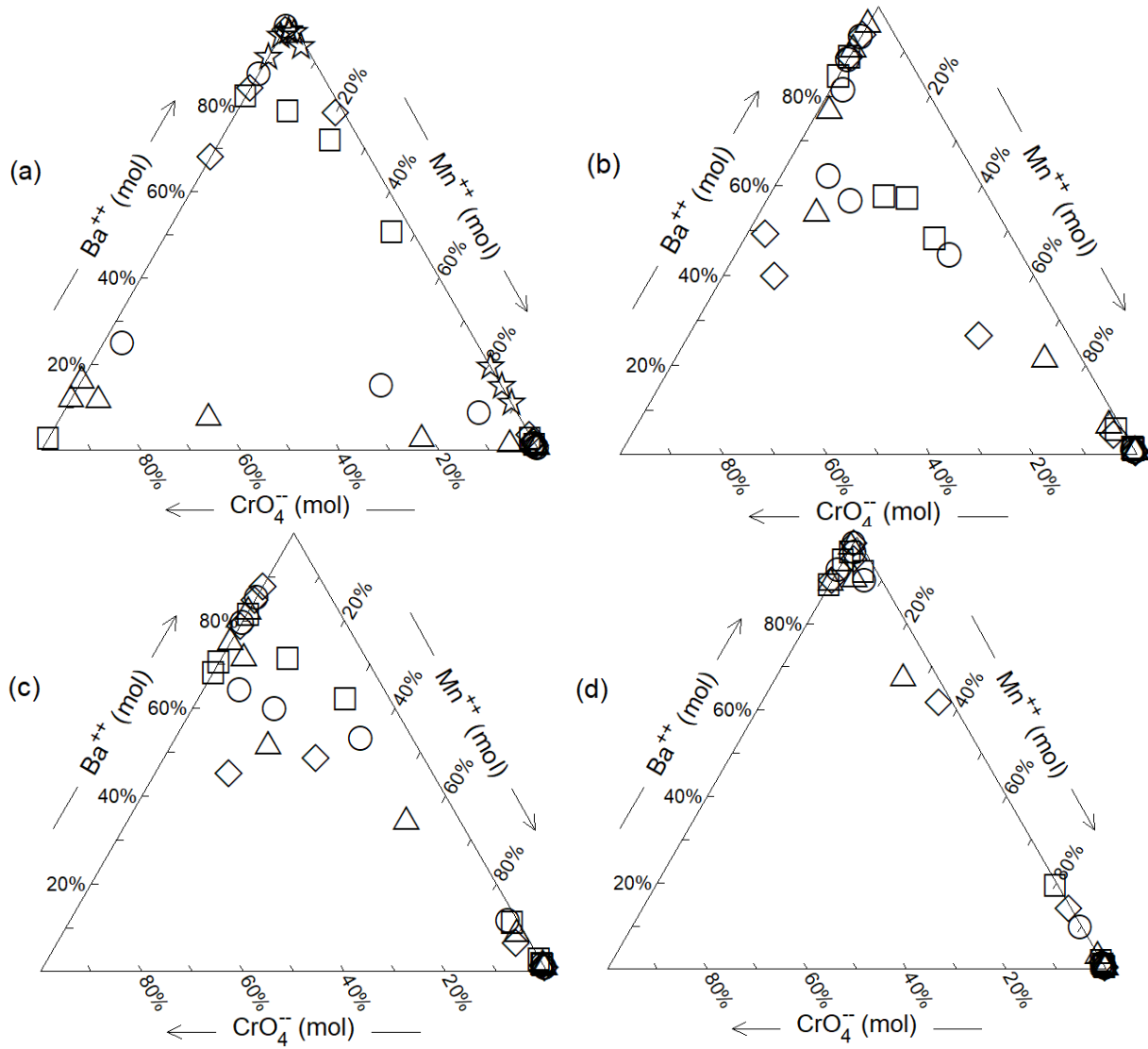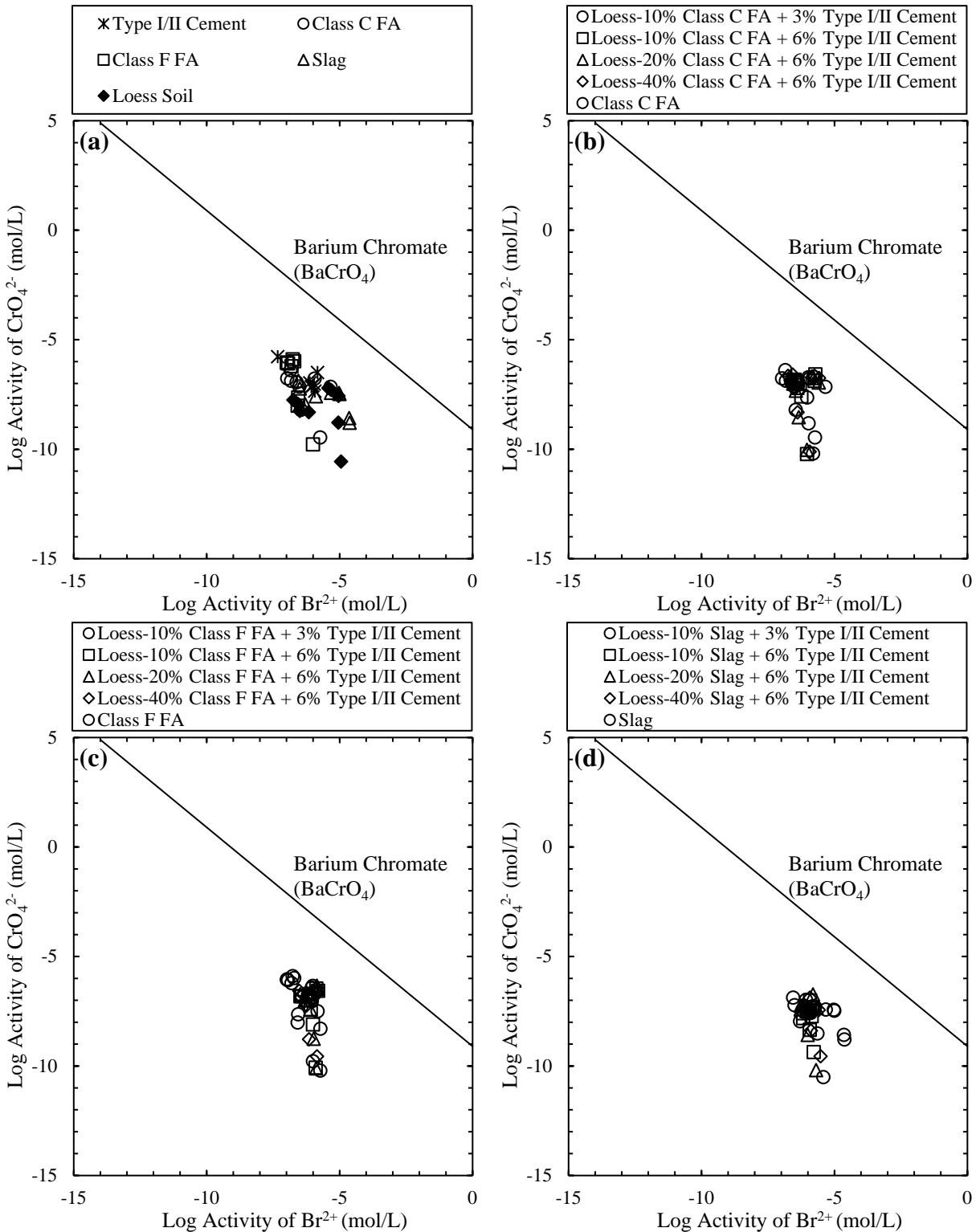
Figure 4.22 Log activity of CrO_4^{2-} versus log activity of Ba^{2+} in leachates of a) soil, fly ashes, slag and cement, (b) Class C FA mixtures, (c) Class F FA mixtures, and (d) slag mixtures. Note: FA- Fly ash

# CHAPTER 5.   LEACHING CHARACTERISTICS OF RECYCLED CONCRETE AGGREGATES: EFFECT OF CARBONATION AND SATURATION

A paper to be submitted to *Journal of Environmental Management*

Masrur Mahedi and Bora Cetin

5.1   Abstract

The effects of carbonation on the pH dependent leaching characteristics of recycled concrete aggregates (RCA) were assessed in the current study. Quantitative comparisons of the leached constituents in the effluent of water leach tests (WLT), toxicity characteristic leaching procedure (TCLP) and synthetic precipitation leaching procedure (SPLP) were performed. Depending on the RCA degree of carbonation, distinct pH dependent leaching patterns of Ca, Mg, Ba, Cr and SO_4 were identified. The selection of an appropriate batch test was largely influenced by both carbonation and the constituent of potential concern. Liquid to solid (L/S) ratios and particle sizes showed diverse influences on the leaching behavior of carbonated and uncarbonated RCAs. At higher L/S ratio, leaching fingerprints of uncarbonated RCAs drifted towards the carbonated ones. Additionally, the effects of matric potentials on the leaching behavior of elements were investigated to access the pore-water chemistry. Geochemical modeling was performed to evaluate the leaching controlling mechanisms of the elements in the pH range of 2 to 13. Results indicated that, higher effluent concentrations were associated in the matric potential range of 2 kPa to 5 kPa. Except for Cr, the leaching of the elements from RCA was controlled by solubility.

Keywords: Leaching, carbonation, matric potential, geochemical modeling, recycled concrete aggregate (RCA)

5.2   Introduction

Aggregates derived from natural sources have been traditionally used for pavement construction. In recent years, the mining of natural aggregates is increasing considerably due to

heightened demand rised by urbanization sprawls, overextraction, depletion of natural sources and subsequent increase in labor and extraction costs (Hoyos et al., 2011). Besides, construction and demolition wastes such as recycled concrete, reclaimed asphalt and recycled brick generated by rehabilitation projects and the consequent declination of landfill spacing have raised the importance to find an alternative way to reuse these materials (Arulrajah et al., 2014). The use of Recycled Concrete Aggregate (RCA) in pavement construction has proven to be a viable and cost effective solution in reducing the depletion of natural aggregates, construction costs and valuable landfill spacing. Demolition of existing structures such as concrete pavements, bridge, curb and gutter are the main sources of recycled crushed concrete aggregates which may also be generated from concrete over-runs associated with new constructions. In the United States approximately 140 millon tons of RCA is generated annually and at least 41 states recycle their concrete pavements (Chen et al., 2012).

RCA tends to be highly alkaline with pH values as high as 12.5, which could negatively impact surface water ecology and groundwater chemistry (Gupta et al., 2018). Even after the process of recycling, cement paste remained attached to the surface of the aggregates which is a potential source of leached constituents (Bestgen et al., 2016; Engelsen et al., 2009). Previous studies showed that RCA materials leach heavy and trace metals of environmental concerns (Butera et al., 2015; Chen et al., 2012; Engelsen et al., 2010; Galvín et al., 2012; Puthussery et al., 2017; Van Praagh and Modin, 2016). Additionally, in most cases the initial mix design of RCA remains unknown which leads to the necessity of gauging their environmental suitability before any practical implications. Certain cement additives such as fly ash, slag, and kiln dust are often used in concrete which are known to leach metals of environmental concern (Cetin et al., 2012a; Daniels and Das, 2006; Zhang et al., 2016). Moreover, several studies have indicated that the pH

of RCA depends on the degree of carbonation reaction (Engelsen et al., 2009; Garavaglia and Caramuscio, 1994; Mulugeta et al., 2011; Sanchez et al., 2002). Carbonation occurs when the cement hydrated phases react with the atmospheric carbon dioxide and precipitate as calcite (Garrabrants et al., 2004a; Mulugeta et al., 2011). Thus, the pH of the RCA varies depending on source, service life of the original concrete structure, storage time and geographical location. Gupta et al. (2018) summarized that the pH of RCA could drop to approximately 8 over time from a pH value of 12.5 due to carbonation. Therefore, focusing the degree of carbonation, the leaching characteristics of RCA need to be investigated for a wide range of pH conditions. Engelsen et al. (2010, 2009) evaluated the pH-dependent release of elements from RCAs of varying degree of carbonation. This study collected partially carbonated RCAs from a single location, and the uncarbonated RCAs were prepared by crushing concrete cubes after 150 days and storing them in air tight containers. However, the pH-dependent leaching of RCA in naturally weathered conditions from diverse geographical locations remained unknown.

Moreover, different standard batch tests such as water leach test (WLT), toxicity characteristic leaching procedure (TCLP), and synthetic precipitation leaching procedure (SPLP) are often used for a quick estimation of the leaching behavior of RCA. To the best of our knowledge, none of the previous studies has provided an assessment on the selection of appropriate test procedures based on RCA carbonation levels. Depending on the degree of carbonation, certain leach test could provide conservative results (higher leaching), while the same test may not be conservative for a different RCA carbonation level. Therefore, inconsistency within previous studies are often apparent (Bestgen et al., 2016). A comprehensive leaching assessment of RCA is required, encompassing widely implemented test procedures with varying degree of RCA carbonation. Besides, the effect of liquid to solid ratios (L/S) and particle sizes in leachate

extraction process from diversely carbonated RCAs need to be evaluated. According to Kosson et al. (2002) L/S ratio could also be considered as a surrogate parameter of time, and hence, probably the RCA degree of carbonation. Crucial physical and chemical properties influencing the leaching behavior of elements are related to RCA particle size distribution. According to Engelsen et al. (2009), more cement paste is available in finer RCA fractions which may control the leaching from RCA. Chen et al. (2012) claimed that carbonation of RCA is greater for finer particle sizes due to higher surface areas. Chen et al. (2012) reported lower pH values for smaller particle sizes of RCA. Therefore, it is important to investigate the influence of RCA particle size on the leaching behavior of elements.

Furthermore, in all batch test procedures influent solutions are added in excess to the materials of interest. Test procedure varies based on extraction fluid type, L/S ratio, shaking period, shaking rate and filtration process. However, these methods may not be representative to the actual field conditions owing to the fact that, RCA may become saturated only during and/or after the precipitation events. In most cases, the RCA used in pavement foundation layers remains unsaturated with negative matric potentials. Yet, there is a continuous infiltration or seepage of water from the unsaturated RCAs towards the groundwater table. The leaching behavior of RCA in unsaturated flow and the effect of matric potential yet remained unexplored. Column leach test has been designed to access the impact on groundwater under percolating condition (LEAF, 2019). However, in column leach test a continuous flow of water is injected into the specimen which makes the samples saturated. Laboratory and field lysimeters could possibly represent the unsaturated conditions of the RCA, but the test methodology does not provide the matric potential measurements which is the most important parameter in unsaturated conditions.

The objectives of this research study were to (1) investigate the pH dependent leaching behaviors of RCA with a varying degree of carbonation, (2) provide quantitative comparisons between different standard batch tests with an assessment on the selection of appropriate methods targeting the RCA carbonation level, (3) access the effect of L:S ratio on the leaching behavior of diversely carbonated RCA, (4) evaluate the influence of RCA particle sizes on the leaching behavior of constituents, and (5) identify the effect of matric potential on the leaching characteristics of RCA. To accomplish these goals, six different RCAs were collected from 3 different states in the U.S. and one RCA was prepared in laboratory condition. A series of WLT, TCLP, SPLP and pH dependent leach tests were performed by implementing different L:S ratios and particle sizes. The physical properties, chemical properties and the degree of carbonation of the RCAs were determined by particle size distribution, Proctor compaction, X-ray diffraction, X-ray fluorescence, acid digestion and thermogravimetric analyses. Pressure cell techinque was employed to extract the RCA pore solutions at known matric potentials. This study analyzed and reported the effluent pH, electrical conductivity (EC), alkalinity and leached Ca, Mg, Ba, Cr and SO_4 concentrations from all the followed test procedures. Furthermore, the leaching mechanisms of the elements from the RCAs were determined via use of geochemical modeling program Visual MINTEQA2.

5.3   Materials

Seven different RCA batches were collected for the test program of this study. Two RCA batches were collected from Texas (TX1 and TX2), three from Iowa (IA1, IA2 and B), one from Minnesota (MN) and one RCA (LAB) was prepared in the laboratory. The RCA-TX1 and RCA-TX2 were stockpiled for several years in concrete recycling facilities located in Dallas and Fort Worth. The RCA-IA1 and RCA-IA2 were collected from Ames and Ankeny in Iowa. RCA-IA1 was taken from a pile stock for 3 months, whereas RCA-IA2 was collected from the production

line. The third RCA from Iowa was prepared by crushing the building demolition waste with a jaw crusher. The RCA from Minnesota was collected from an old pavement demolished for reconstruction. Laboratory based RCA were prepared by crushing waste concrete cylinders from ISU PCC lab and exposing them to the atmosphere for more than a year. The mix design of the laboratory made RCA was unknown as it ought to be in actual conditions.

The RCA used in this study primarily composed of sand to gravel size particles. The laboratory processed RCAs (RCA-B and RCA-LAB) were crushed and grounded to a particle size less than 25.4 mm. The particle size distribution of the RCA materials used in this study are presented in Figure 5.1. Except for RCA-IA1 and RCA-TX2, all the RCA had more than 80% gravel size particles. RCA-IA1 was predominated by sand size particles (51.1%), whereas the gravel content for RCA-TX2 was 68.8%. The compaction characteristics of the materials were determined by implementing standard proctor compaction energy. The optimum moisture content and maximum dry density of the materials varied in the range of 10.9% to 14.4% and 18.3 kN/m^3 to 19.7 kN/m^3, respectively. All the physical properties of the RCA materials are tabulated in Table 5.1. The RCA-MN, TX1, TX2 and LAB were classified as poorly graded gravel (GP) in accordance to USCS classification system. RCA-IA1 and RCA-B were classified as well graded gravel (GW), whereas the USGS classification of RCA-IA1 was poorly graded sand (SP). According to AASHTO classification system, all the RCAs were classified as A-1-a.

The chemical compositions of the RCAs were determined by X-ray fluorescence (XRF) spectrometry analyses. The oxide contents of the RCAs are presented in Table 5.2. All the RCA materials were dominated by silica (SiO$_2$) in the range of 34.7% to 47.7% by weight. The lime (CaO) content varied in the range of 22% to 34.9%. The highest amount of CaO was found in RCA-TX1, while the minimum CaO content was in RCA-B. The RCAs also contained varying

amount of alumina (Al_2O_3) and iron oxide (Fe_2O_3) in the range of 1.7% to 5.8% and 1.2% to 3%, respectively. Additionally, the Ca, Mg, Ba and Cr contents of the RCAs were determined by implementing acid digestion following the U.S. EPA method 3050B and are reported in Table 5.2. A representative 1 g RCA sample was digested with varying amount of concentrated trace metal grade nitric acid (HNO_3) and 30% hydrogen peroxide (H_2O_2). Heating at 95 ± 5 °C temperature and refluxing were involved as per the standard requirements to dissolve all the elements that could become environmentally available. The total elemental concentrations of the RCA were in general agreement with XRF analyses. From acid digestion, the maximum and minimum Ca content were also determined in RCA-TX1 and RCA-B, respectively. The Cr content of the RCAs varied within a narrow range of 21.3 mg/kg to 27.9 mg/kg.

An X-ray diffraction (XRD) spectrometry analyses were conducted to identify the mineralogical compositions of the RCAs used in this study. Table 5.3 lists the RCA mineral phases recognized by XRD analyses. As indicated in Table 5.3, calcite and dolomite were identified in all the RCAs, regardless their source, aging and collection procedures. Except for RCA-TX1 and TX2, portlandite was identified in every RCAs. Therefore, it was anticipated that RCAs from Texas were the most carbonated ones. Besides, ettringite was identified in RCA-MN and IA2. Albite and anorthite (feldspars) were recognized in RCA-IA1, B and LAB which could have contributed by the aggregates in RCAs. As showed in Table 5.2, the pH values of the RCAs were significantly lower compared to the pH of less aged RCA-LAB (pH = 10.5). The lowest pH of RCA-TX1 indicated its higher carbonation level. The carbonation levels of the RCAs were further verified by thermogravimetric analyses (TGA) as shown in Figure 5.2.

5.4   Methods

5.4.1   Laboratory Sample Preparation

The laboratory sample preparation started by dividing the collected RCA materials into small batches based on the quartering method following ASTM C702. The materials were further reduced to 2 kg small sub-batches by implementing alternative quartering method. The sub-batch RCA materials were oven dried at a temperature 60 °C for at least 24 hours. The dry RCAs were then subjected to sieve analyses and divided into particle size fractions of 25.4-9.51 mm, 9.5-4.76 mm, 4.7-2.38 mm, 2.38-1.19 mm, 1.19-0.595 mm, 0.595-0.297 mm, 0.297-0.149 mm and 0.149-0.074 mm. For gravel size particles (25.4-9.51 mm and 9.51-4.76 mm), further crushing was performed by an electric jack hammer. An additional size reduction of the sieved fractions of 25.4-9.51 mm, 9.51-4.76 mm, 4.76-2.38 mm, 2.38-1.19 mm was performed by agate mortar to get the test sample sizes of less than 2 mm. The reduced size test samples (< 2 mm) were stored in air-tight bags for leaching tests. A representative RCA sample was prepared by adding the appropriate amount of materials from each reduced size fractions according to the gradation characteristics determined by sieve analysis. Four different standard leaching tests methods were implemented using the reduced 2 mm RCA samples. All of the leach test samples were prepared on oven dry weight basis. In addition, leaching potential of elements at different saturation conditions (matric potential) was investigated by exploiting the water retention characteristics of the RCA materials.

5.4.2   Batch Water Leach Test

Batch water leach tests (WLT) were performed following the standard test method designated by ASTM D3987. To investigate the influence of diverse field conditions, samples were prepared at four different (5:1, 10:1, 15:1 and 20:1) liquid to solid (L/S) ratios. According to Kosson et al. (2002) L/S ratio could also be considered as a surrogate parameter of time, and release of metals is weakly related to L/S, when L/S ratio is in between 2:1 and 10:1. Additionally,

L/S ratio of 10:1 is widely implemented, since the release of elements at L/S of 10:1 is solubility controlled over the range of pH relevant to the field conditions (Kosson et al., 2002). Therefore, samples were prepared at L/S ratio of 5:1 (between 2:1 and 10:1), 10:1, and at two L/S values higher than 10:1 (15:1 and 20:1). Deionized water was used as an influent solution for the sample preparation. Samples were rotated end-over-end fashion for 18 ± 0.25 hours at a rotation rate of 29 rpm. After rotation, pH and electric conductivity of the supernatant fluid were measured. Next, the solution was pressure filtered through membrane disk filter papers (0.2-µm pore size and 25 mm diameter) into acid washed 50 mL centrifuged tubes. One fraction of extract was acidified with 10% trace metal grade nitric acid (HNO_3) to a pH less than 2 and stored at 4°C temperature for metal analyses. Another not-acidified aliquot of the leachate was immediately subjected to alkalinity and sulfate measurements.

Furthermore, the impacts of RCA particles on the leaching of elements were evaluated by batch water leach tests. Crucial physical and chemical properties influencing the leaching behavior of elements from RCA are related to RCA particle size distribution (Bestgen et al., 2016). According to Engelsen et al. (2009), more cement paste is available in finer RCA fractions which may control the leaching from RCA. Additionally, Chen et al. (2012) claimed that carbonation of RCA is greater for finer particle sizes due to higher surface areas. Chen et al. (2012) reported lower pH values for smaller particle sizes of RCA. Therefore, it is important to investigate the influence of RCA particle size on the leaching behavior of element. The RCA particle size distribution is largely dependent on the crushing procedure, crushing location (in plant or onsite), RCA source (building or pavement demolition) and storage conditions (stockpile or container). In this study the leaching behavior of 8 different (25.4-9.51 mm, 9.5-4.76 mm, 4.7-2.38 mm, 2.38-1.19 mm,

1.19-0.595 mm, 0.595-0.297 mm, 0.297-0.149 mm and 0.149-0.074 mm) RCA size fractions were evaluated through WLT.

5.4.3 TCLP Leach Test

Toxicity characteristic leaching procedure (TCLP) designated by the U.S. EPA method 1311 was followed to access the leaching behavior of RCA at landfill containment conditions. A liquid to solid ratio of 20:1 was implemented following the standard requirement. The influent solution for TCLP was prepared by mixing 64.3 mL 1 N sodium hydroxide (NaOH) and 5.7 mL glacial acetic acid (CH_3COOH) into deionized water and diluting the solution to 1 liter. The prepared influent solution had a pH of 4.93 ± 0.05. Then, the RCA-influent mixture was agitated end-to-end at a rotation rate of 28 rpm for 18 ± 2 hours. After agitation, the pH and conductivity of the effluent solution were measured. Finally, vacuum filtration technique was implemented using 0.7-μm borosilicate glass fiber filters. An aliquot of sample was acidified and stored for metal analysis as described in the WLT section. Another non-acidified portion of filtered sample was used for alkalinity and sulfate measurements.

5.4.4 SPLP Leach Test

To investigate the leaching behavior of RCA in simulated acid rain conditions, SPLP test procedure designated by the U.S. EPA method 1312 was performed. The influent solution for SPLP was prepared by mixing reagent grade sulfuric and nitric acid (60%/40% by weight) into deionized water and diluting the solution to a pH of 5 ± 0.05. A constant liquid to solid ratio of 20:1 was used for leachate extraction. A similar agitation, filtration and storage procedure as described in the TCLP section was implemented for SPLP sample preparation.

5.4.5 pH-dependent Leach Test

The pH dependent leach tests were conducted on RCAs following the U.S. EPA Method 1313 to investigate the influence of pH on the leaching behavior of elements. Samples were

prepared at 9 different target pH values of 2, 4, 5.5, 7, 8, 9, 10.5, 12 and 13 ($\pm$0.5). A constant L/S ratio of 10:1 was implemented for the leachate extraction. The target sample pH values were achieved by adding appropriate amounts of 1 N potassium hydroxide (KOH) or 2 N trace metal grade nitric acid (HNO$_3$) into deionized water. The required amounts of acid or base, and deionized water for a target pH were predetermined by exploring the acid neutralization capacity (ANC) of the RCAs. To investigate the ANC of the RCAs, varying amounts of acid or base in regular intervals, and water was added to the RCA samples at a L/S ratio of 10:1. The mixtures were then agitated end-over-end at a rotation rate of 28 rpm for 48$\pm$2 hours. After agitation, the pH of the supernatant was measured to quantify the acid/base buffering capacity of the RCAs. For the final pH-dependent leach test samples, similar rotation frequency and agitation period were implemented. Following shaking, the pH and electrical conductivity of the samples were determined. Finally, samples were filtered and stored for further analyses following the same method described in the WLT section.

5.4.6 Leaching at Unsaturated Conditions

To evaluate the leaching behaviors of metals at different saturated conditions, a pressure cell technique was adopted. Test size ($<$ 2 mm) RCAs were compacted into 76.2 mm diameter and 76.2 mm height cores at optimum moisture content by implementing standard Proctor compaction energy. A polyethylene membrane was provided to avoid undue contact between RCA particles and the core metal wall. To reduce contamination of the RCA samples while compacting, the compaction hammer was covered with cloth and polyethylene layers. Upon compaction, the samples were placed in separate saturation chambers with deionized water and vacuum saturation was applied for 48 hours. The saturated cores were then placed in pressure cells.

A schematic of a pressure cell with RCA core is shown in Figure 5.3. The pressure cells were made of acrylic with a leachate collection funnel and a graduated cylinder. In each cell, a

saturated 0.45 µm pore size and 90 mm diameter nylon membrane filter paper was placed on the perforated bottom plate, upon which saturated RCA core was placed. The cells were made airtight by using vacuum grease and placing O-rings at the top and bottom. Next, eight different matric potentials were induced in RCA cores by applying air pressures of 0.37, 1.96, 2.94, 4.91, 9.81, 19.61, 32.36 and 49.03 kPa. Smaller matric potentials were selected, since the RCA materials had inferior water retention capacities due to minor fine contents (Table 5.1). Precise measurements of matric potentials were ensured by using a hand-held digital manometer. Each pressure was sustained for 24 hours except for 32.36 and 49.03 kPa, where the duration of sustained pressure was 48 hours. Due to applied pressure, a hydraulic gradient was induced in the RCA cores, since the bottom of the core was exposed to atmospheric condition through the filter paper and the perforated bottom plate. Therefore, to reach an equilibrium with the induced suctions (matric potentials), RCA cores drained pore solution which was collected into a 100 mL graduated cylinder. The weight and volume measurements of the drainage were performed for the investigation of water retention characteristics of the RCAs. Additionally, the drainage was pressure filtered through 0.2-µm pore size membrane filter papers and stored in centrifuge tubes by acidifying with 10% nitric acid at a pH lower than 2. Before acidifying the samples, pH and electric conductivity of the drainage were also quantified. To avoid the cross contamination between the leachates, a new filter paper, and acid washed leachate collection funnels and graduated cylinders were used for each pressure cycles. Washing the bottom plate was not possible since the bottom plate was firmly attached on a wooden table. However, the bottom plate was sprayed with 2% trace metal grade nitric acid (HNO_3) solution and subsequently washed with deionized water.

5.4.7 Chemical Analyses

Inductively coupled plasma optical emission spectroscopy (ICP-OES) (Shimadzu, Japan) was used to determine the effluent concentrations of major elements (Ca, Mg, Al, Ba and Fe), common metals (Cu, Mn and Zn) and oxyanion Cr. Commercially produced known concentrations of multi-elemental standards were used to calibrate the ICP. Multiple calibration curves were prepared for pH-dependent leach test samples due to a wide range of metal concentrations in the eluates. The calibration curves were verified by running check standards and blanks at every 9 samples and at the end of an analysis session. In this study only the leached concentrations of Ca, Mg, Ba and Cr are reported, discussing the other elements elsewhere. The minimum detection limits for Ca, Mg, Ba and Cr were 0.002 mg/L, 0.001 mg/L, 0.0004 mg/L and 0.005 mg/L, respectively.

The effluent concentrations of sulfate (SO_4) in non-acidified samples were quantified by the SEAL AQ2 analyzer, implementing the standard method designated by the U.S. EPA method No: EPA 123-A. The instrument was calibrated by anhydrous sodium sulfate (Na_2SO_4) standard solutions. A new calibration curve was generated for every analysis session. The calibration curve was verified by running check standard of 20 mg/L and blank solution at every 15 analyses. The method detection limits for the sulfate was 1 mg SO_4/L.

The alkalinity of the non-acidified effluent was determined through titration by 0.035 N standard sulfuric acid (H_2SO_4) solution. Phenolphthalein and bromcresol green-methyl red indicators were used to determine phenolphthalein and methyl orange alkalinity, respectively. The solution turned into pink when phenolphthalein indicator was added. Acid was added dropwise into the solution until it became colorless. Next, bromcresol green-methyl red indicators was used and titration was performed until the solution turned into pink. The RCA samples showed very

little phenolphthalein alkalinity compared to the methyl orange alkalinity. Therefore, only the methyl orange alkalinity is reported in this study and indicated as the alkalinity of the RCA eluates.

5.4.8 Geochemical Modeling

Two key equilibrium mechanisms, solubility and sorption are recognized to control the leaching of constituents from the waste materials. Solubility controls the leaching when the effluent is saturated with respect to the constituent species and is known to be reliant on the dissolution/precipitation of oxide and hydroxide minerals (Komonweeraket et al., 2015a). Constituents with sorption affinity to the active sites such as solid surfaces, organic matter, oxides and oxyhydroxides are controlled by the sorption process (McBride, 1994). In this study, geochemical modeling was performed to investigate whether the leaching of elements was controlled by solubility. Geochemical model program Visual MINTEQA2, developed by the U.S. EPA was implemented. The pH and effluent concentrations from pH-dependent leach tests were considered as the input data. An equilibrium with the atmospheric carbon dioxide at 25 °C was assumed, since the filtration was performed in a laboratory setting. Aqueous phase equilibrium concentrations of the constituents, constituents' activities and saturation indices of the leachate with respect to MINTEQA2 predicted minerals were calculated. The pH-log activity diagrams for each of the elements were generated along with the solubility line of the MINTEQA2 predicted mineral phases. The activities of a constituent fell in close proximity to the solubility line of the constituent minerals, if the leaching was controlled by solubility (Garavaglia and Caramuscio, 1994).

5.5 Results and Discussions

5.5.1 Influence of L/S Ratio on the Leaching Behavior

The influence of liquid to solid ratio (L/S) on the leaching behavior of elements is illustrated in Figure 5.4. As indicated in Figure 5.4(a), except for RCA-LAB, the effluent

concentrations of Ca decreased with an increase of L/S ratio. For laboratory made RCA, Ca concentrations remained unchanged. The leached concentrations of Ca from RCA-B did not change significantly up to the L/S ratio of 10 but decreased gradually at higher L/S values (15 and 20). Among all the RCAs used in this study RCA-LAB and B were the least carbonated ones. For moderate to highly carbonated RCAs, Ca concentrations decreased progressively with the increase of L/S ratio. Garrabrants et al. (2004) also reported that leached concentrations of Ca from carbonated cement mortar decreased with an increase in L/S ratio. An increase in L/S ratio increased the liquid content of WLT, which diluted the leachate and subsequently decreased effluent Ca concentrations. Similar behavior was observed for effluent pH and electrical conductivity (EC). The pH and EC values decreased at an increased L/S ratio (Table 5.3). From TGA analyses, the RCAs in terms of descending carbonation levels were LAB, B, MN, IA2, IA1, TX2 and TX1. The leached concentrations of Ca, effluent pH and EC also followed the same order. In contrast, the leached concentrations of Mg fluctuated with L/S ratio (Figure 5.4b). However, it could be concluded that Mg concentrations were inclined to an increasing trend with the increase in L/S ratio. With the increase in L/S ratio, effluent pH decreased which could increase the leached concentrations of Mg. Figure 5.4(c) represents the variation of effluent alkalinity with the increase in L/S ratio. Following the leaching of Ca, effluent alkalinity decreased with an increase in L/S ratio. Moreover, the alkalinity of the RCAs followed the same order of carbonation determined from TGA analyses. The eluates of RCA-LAB were the most alkaline ones, whereas the RCA-TX1 showed the least alkalinity. This was expected, since the carbonates of Ca and Mg are known to be insoluble at alkaline pH (pH > 10) conditions (Komonweeraket et al., 2015b).

Leached concentration of Ba and Cr decreased noticeably with the increase in L/S ratio. This finding is coherent with previous studies conducted on RCA, concrete demolition waste and

bottom ash (Bestgen et al., 2016; Di Gianfilippo et al., 2016; Van Praagh and Modin, 2016). Phoungthong et al. (2016) indicated that, both the dilution and solubility of the heavy metals are affected by L/S ratio, which eventually change the effluent metal concentrations. It is well known that Ba and Cr follow amphoteric leaching pattern with elevated concentrations at both acidic and alkaline conditions, and the minimum at neutral/near neutral pH values. With the increase in L/S ratio, effluent pH decreased (Table 5.4) which led to an overall reduction in effluent Ba and Cr concentrations. In case of SO_4, diverse leaching behaviors with respect to L/S ratio was observed. For aged RCAs (TX1 and TX2), SO_4 concentration decreased with an increase in L/S ratio. In contrast, less carbonated RCAs leached higher concentrations SO_4 at higher L/S ratios. It was anticipated that dilution affected the leaching of SO_4 from aged RCAs, whereas sorption/desorption controlled SO_4 leaching from the less carbonated RCAs. The decrease in pH with an increase in L/S ratio led to the desorption of SO_4 from calcite surface and increased the effluent concentrations.

5.5.2 Effect of Carbonation on the Leaching Potentials

To understand the effect of carbonation on the leaching of elements and for a quantitative comparison of leachate quality, Schoeller diagrams at four different L/S ratios were utilized and are presented in Figure 5.5. The milliequivalent concentrations were calculated assuming the Ca^{2+}, Mg^{2+}, Ba^{2+}, Cr^{6+} and SO_4^{2-} oxidation states. Cr is a redox sensitive element and could be in Cr (III) or Cr (IV) oxidation states. However, Cr (IV) was assumed in this study because of the higher natural pH (pH > 11) of the RCAs. Previous studies reported oxidized Cr (IV) at higher pH conditions (Bestgen et al., 2016; Quina et al., 2009; Zhang et al., 2016). For simplicity, alkalinity of the leachates was represented by CO_3^{2-}, since alkalinity was reported as equivalent $CaCO_3$ in this study.

As indicated in Figure 5.5, the RCAs could be sorted into 3 groups based on their carbonation levels such as highly carbonated (TX1 and TX2), moderately carbonated (MN, IA1 and IA2) and least carbonated (B and LAB). Least carbonated RCAs showed similar leaching fingerprints with almost parallel lines in all L/S ratios. Significant variations on the leaching of Mg were observed, where the lines joining Cr^{6+} and Mg^{2+} became oblique. This is due to higher leaching potential of Mg from RCA-B compared to other RCAs. As indicated in Table 5.2, higher MgO content and elemental concentration of Mg were determined in RCA-B by XRF and total elemental analysis, respectively. Lines joining Ca^{2+} and CO_3^{2-} were almost horizontal in all L/S ratios. This signifies that for the least carbonated RCAs, alkalinity mostly resulted from the dissolution of major calcium minerals such as portlandite, gypsum and calcite. However, the concentrations of SO_4^{2-} were well below the concentrations of Ca^{2+}. Therefore, dissolution of gypsum may not be the primary contributor for the leaching of Ca^{2+} from the least carbonated RCAs. The slopes (positive or negative) of the lines joining Ba^{2+} and Cr^{6+} were close to zero, which indicated possible interdependent leaching of these two elements. For moderately carbonated RCAs, almost identical leachate chemistry was identified by the lines overlapping on each other. RCA-MN leached higher Cr^{6+} compared to other two RCAs in this group. Moderately carbonated RCAs showed distinct behavior from the least carbonated ones in terms of alkalinity and the leaching of Ca^{2+}. The lines joining Ca^{2+} and CO_3^{2-} concentrations had positive slopes, indicating that the contribution of other minerals to alkalinity became significant with an increase in RCA carbonation level.

The highly carbonated RCAs (TX1 and TX2) showed unique leaching behavior with relatively lower concentrations of Ca^{2+} and alkalinity. Higher amounts of SO_4^{2-} and Cr^{6+} leached from highly carbonated RCAs compared to the moderate and least carbonated ones. Previous

studies showed enhanced leaching of SO_4^{2-} and Cr from carbonated materials (Kosson et al., 2014; Mulugeta et al., 2011). The leached concentrations of Mg^{2+} from the most carbonated RCA-TX1 were the highest in all L/S ratios. The slopes of the lines joining Ca^{2+} and CO_3^{2-} were negative, whereas the molar ratios of Ca^{2+}/SO_4^{2-} were close to 1, especially for TX1. These signify that the leaching of Ca^{2+} from highly carbonated RCAs were dominated by the dissolution of gypsum and/or anhydrite. Additionally, the leached concentrations of Ba^{2+} were lower. Therefore, it was anticipated that leaching of Ba^{2+} from highly carbonated RCAs was controlled by poorly soluble witherite rather than barite. Additionally, at higher pH with the presence of SO_4^{2-}, Ba^{2+} precipitates as barite(Kosson et al., 2014). Moreover, for highly carbonated RCAs, Ca^{2+}/CO_3^{2-} molar ratios decreased with the increase in L/S ratios. In contrast, Ca^{2+}/CO_3^{2-} molar ratios consistently increased with L/S ratios for less carbonated RCAs. With the increase in L/S ratio, leaching fingerprints of less carbonated RCAs drifted toward the highly carbonated ones. Thus, as seen from Figure 5.5(d), the differences in eluate cation and anion concentrations decreased significantly at L/S of 20, irrespective to the degree of carbonations of the RCAs.

5.5.3   Influence of Particle Size on the Leaching Behavior

It was found that the RCA particle sizes had significant influences on the effluent pH, electrical conductivity (EC), alkalinity and elemental concentrations. As indicated in Table 5.5, the pH and EC decreased with the increase in RCA particle size. For least carbonated RCA-B and LAB, maximum pH was found at 0.074 mm of particle sizes, whereas for carbonated RCAs the highest pH values were found in between 1.19 mm to 0.149 mm. In a few cases an increase in pH was observed for the 2.38 mm particle size, which could have happened due to size reductions of RCA particles to the test size (2 mm) as described in the method sections. The leached concentrations of Ca and eluate alkalinity followed the same pattern (Figure 5.6) as the pH. With the increase in RCA particle size, leached Ca concentrations and alkalinity decreased. With few

exceptions, the maximum Ca concentrations and alkalinity were found for 1.19 mm to 0.149 mm particle sizes. Leached Mg concentrations fluctuated with RCA particle sizes (Figure 5.6b). The highest concentrations of Mg were leached from larger particle sizes of RCA-TX1.

Additionally, Figure 5.6d-e shows that the effluent concentrations of Ba and Cr also decreased at higher particle sizes. Larger particle sizes yielded lower pH which decreased Ba and Cr concentrations. Additionally, carbonated RCAs (TX1 and TX2) leached lower concentrations of Ba but higher Cr concentrations. As presented in Figure 5.6f, except for RCA-B, SO_4 concentrations also decreased with the particle sizes of the RCAs. It was speculated that the leaching of SO_4 from RCAs was mostly from the hydrated cement paste. Engelsen et al. (2009) indicated that more cement paste was available in finer fractions of RCA particles.

5.5.4 Factors Effecting Eluate Properties and Leaching

The U.S. EPA does not provide any specific guideline for effluent Ca concentration. However, Ca is one of the most abundant elements present in cementitious products such as cement, mortar, concrete and different types of fly ash, bottom ash and blast furnace slags. The presence of Ca critically influences the effluent chemistry, and subsequently the leaching of the poisonous elements. Therefore, an attempt was made to access the influence of Ca on the effluent pH, EC, alkalinity and leaching of Ba and Cr. The results from all the WLT performed at different L/S ratios and particle sizes were considered for the evaluation purpose.

As shown in Figure 5.7(a), the pH of the effluent consistently increased with an increase in Ca concentrations. Dissociation of remaining $Ca(OH)_2$ in RCAs increased the effluent pH and Ca concentration significantly (Bin-Shafique et al., 2006). From XRD analyses portlandite was detected in all the RCAs, except for highly carbonated TX1 and TX2 (Table 5.3). Thus, RCA-TX1 and TX2 resulted lower pH values with minor dependence on effluent Ca concentrations. Similarly, the EC and alkalinity of the solutions were largely controlled by leached Ca

concentrations (Figure 5.7b-c). Both the EC and alkalinity considerably increased with the increase in effluent Ca concentrations. As seen in Figure 5.7(c), the Alkalinity values of RCA-TX1 were aligned with Ca to alkalinity ratio of 1:1, whereas alkalinity of the other RCAs were closely associated to 1:2 line. This indicated that the alkalinity of TX1 could be controlled by calcium carbonate, while calcium bicarbonate may have controlled the alkalinity of other RCAs.

5 5.7(d) shows the influence of alkalinity on the leaching behavior of Ba. Leached concentrations of Ba increased with the increase in alkalinity. This signifies that carbonate minerals controlled the leaching of Ba from RCA materials. Previous studies reported that at strongly alkaline conditions (pH > 10) Ba-carbonate mineral, witherite controls the leaching of Ba (Komonweeraket et al., 2015a; Mudd et al., 2004). Moreover, the leached concentrations of Cr were influenced positively by the solution Ca concentrations (Figure 5.7e). For highly carbonated RCAs, the leaching of Cr was more sensitive with respect to Ca. Leisinger et al. (2010) indicated that chromate concentrations increased with an increased in Ca concentrations. It is well known that for alkaline waste materials, CrO_4^{2-} is the relevant oxidation of Cr (Quina et al., 2009; Zhang et al., 2016). CrO_4^{2-} can substitute for SO_4^{2-} and may incorporate to ettringite as CrO_4^{2-}-ettringite solid solution (S/S) (Leisinger et al., 2010). It was anticipated that dissolution of CrO_4^{2-}-ettringite S/S was the most probable reason of enhanced Cr leaching with Ca. This assumption was further stressed by Figure 5.7(f), indicating that Cr concentrations also increased with an increase in solution SO_4 concentrations. Quina et al. (2009) indicated that SO_4 reduced the sorption of Cr (VI) in ettringite. Therefore, a partial replacement (loosely bonded) of SO_4^{2-} by CrO_4^{2-} was possible and dissolution of such phases increased the solution Ca, Cr and SO_4 concentrations.

5.5.5 Method Comparisons

To access the leaching potentials of RCA in different test conditions, ternary phase diagrams of leached metal concentrations, alkalinity and SO_4 in WLT, TCLP and SPLP were

plotted. Effluent concentration of a metal (or SO_4/alkalinity) in a test method was normalized as the percent fraction of the total leached concentrations of that metal (or SO_4/alkalinity) in all three leach tests. For quantitative comparison, effluent pH, EC, alkalinity, SO_4 and leached metal concentrations in WLT, TCLP and SPLP are provided in Table 5.6. As shown in Figure 5.8(a), leached concentrations of Ca were always higher in TCLP effluents. Ca concentrations in TCLP were 1 to 10 times higher compared to WLT, and 2 to 15 times higher than the SPLP concentrations. This observation is in agreement with a previous study conducted on RCA materials (Bestgen et al., 2016). Additionally, the leaching of Ca in different test methods was greatly influenced by the degree of carbonation of RCA particles. Less carbonated RCAs leached higher Ca in WLT, whereas highly carbonated RCAs showed higher Ca in TCLP effluents. Solution Ca concentrations were comparable in TCLP and WLT for less carbonated ones (B and LAB). For other highly carbonated RCAs, WLT and SPLP effluent Ca concentrations were equivalent.

Mg was poorly leached in WLT, regardless of the carbonation levels of the RCAs (Figure 5.8b). Least carbonated RCAs (B and LAB) leached the highest amount of Mg in SPLP solution. For elevated carbonation levels, TCLP effluents provided the highest leaching of Mg. In the case of alkalinity, TCLP effluents were found to be highly alkaline followed by WLT and SPLP effluents (Figure 5.8c). TCLP alkalinity decreased as the carbonation level of the RCAs decreased, whereas the observed trend was completely opposite for WLT and SPLP effluent. WLT and SPLP effluent alkalinity decreased with an increase in RCA carbonation. Among these three test methods, TCLP effluent was the most acidic one which degraded the calcite in RCA vigorously. Thus, the release of carbonate and bicarbonate anions in the solution increase the acid buffering capacity of the TCLP effluents. With the decrease in carbonation, portlandite became readily

available in neutralizing protons in TCLP influent. Neutralization of the protons produced water which did not contribute to effluent alkalinity. The alkalinity of SPLP effluents decreased with RCA carbonation levels, since the SPLP influent is not a buffer solution as TCLP influent. WLT effluent alkalinity decreased with RCA carbonation due to the insoluble nature of calcite in water. Additionally, the WLT-TCLP-SPLP phase diagram of Ca and alkalinity suggested the same carbonation order of the RCAs determined by TGA analyses.

Figure 5.8(d) indicates that, except for RCA-TX1 the highest amount of Ba leached into WLT effluent. The Ba concentrations in WLT effluent were approximately twice compared to SPLP effluent concentrations and 1 to 5 times higher compared to TCLP. It was theorized that relatively higher pH (Table 5.6) of WLT effluents had increased the leached Ba concentrations significantly. In few cases (MN, IA1 and IA2) SPLP effluent pH values were slightly larger compared to WLT pH values, yet Ba concentrations were higher in WLT. This could have happened due to higher ionic strength of WLT effluents (Cetin et al., 2012a). The EC provided an indication of effluent ionic strength, and higher EC were determined in WLT (Gräfe et al., 2009). Additionally, for RCA-TX1, the maximum Ba concentration was found in TCLP effluent followed by WLT and SPLP concentrations. TCLP and SPLP effluent Ba concentrations were found to be comparable for moderately carbonated RCAs (IA1, IA2 and MN). RCA-LAB leached the highest amount of Ba in WLT effluent because of its largest pH in all leaching methods (Table 5.6).

In case of Cr and SO_4, as seen in Figure 5.8(e-f), the higher concentrations were found in WLT effluent for highly carbonated RCAs (TX1 and TX2), whereas, leached concentrations were the highest in TCLP effluents for moderately to least carbonated ones. Except for highly carbonated RCAs (TX1 and TX2), the WLT and SPLP effluent concentrations of Cr and SO_4 were equivalent. Additionally, Cr and SO_4 concentrations were inclined to increase with increased

carbonation in WLT effluent. However, this behavior was reverse in TCLP effluents. The leachability of Cr and SO4 in SPLP effluents varied within a narrow range (0.2 line) due to the presence of SO4 in influent solution as sulfuric acid.

5.5.6 pH dependent Leaching Behavior

To access the pH buffering ability, acid/base neutralization capacities of the RCAs were determined. Figure 5.9(a) shows the ANC of the RCAs used in this study. The negative values of acid equivalents indicated the addition of base. As seen in Figure 5.9(a), depending on the degree of carbonation of the RCAs, significant differences in the shape of ANC curves were observed. Highly carbonated RCA-TX1 showed lower acid neutralization capabilities in the pH range of 12 to 6. In contrast, less carbonated RCAs showed higher resistance to pH changes in this zone, requiring more acid for the same pH adjustment. The difference was attributed to the carbonation of the RCA and subsequent disappearance of hydrated cement phases (Engelsen et al., 2009). Except for RCA-TX1, all other RCAs showed slight buffering capacity up to the pH of 11.5. This was ascribed due to the presence of portlandite, AFt, AFm and calcium-silicate-hydrates in RCAs (Isenburg and Moore, 1992). In the pH range of 5 to 6, a plateau was identified, signifying that RCAs were least sensitivity to the acid additions. The presence of calcium carbonate due to RCA carbonation, gypsum and gibbsite were the reasons of higher buffering capacity in this pH zone. Previous studies indicated that these minerals have the buffering capacities in the pH range of 5 to 6 (Chen et al., 2009; Komonweeraket et al., 2015b). RCAs with higher degree of carbonation showed larger acid neutralizing capacities in this pH region. The order of RCA carbonations from ANC analyses were determined based on the acid requirements to drop the solution pH below 4.5. The ANC analyses indicated that the ascending order of RCA carbonation was: LAB, B, MN, IA2, IA1, TX2 and TX1. This observation was analogous with the TGA analyses, effluent alkalinity and Ca leaching in method comparisons section.

Figure 5.9(b-c) shows the leaching behavior of Ca and Mg from RCAs as a function of solution pH. Both the Ca and Mg showed strong cationic leaching behaviors where concentrations decreased progressively with an increase in effluent pH. At lower pH, higher concentrations of cationic elements were observed due to the dissolution of metal bearing minerals and reduced sorption. Higher pH promoted the precipitation and sorption of dissolved ions, leading to a consequent decrease in effluent concentrations (Komonweeraket et al., 2015b). Comparing the Ca and Mg leaching patterns, significant differences were observed depending on RCA carbonation levels. The variations were more prominent at neutral to alkaline pH conditions. The leaching of Ca and Mg were the minimum for the most carbonated RCA-TX1. The least carbonated RCA-LAB leached the highest concentrations of Ca throughout the pH range. For Mg, the highest concentrations were found for RCA-B, which was the second least carbonated RCA used in this study. As indicated in Table 5.2, RCA-B had the highest Mg content determined by both XRF and total elemental analyses. Additionally, the differences in the leaching of Mg reduced noticeably at natural pH conditions.

As indicated in Figure 5.9(d), the leaching of Cr from the RCAs showed significant pH dependence. The maximum Cr concentrations were associated with highly acidic pH environments (pH < 4). Except for RCA-MN and IA2, the leached concentrations of Cr decreased at slight acidic to neutral pH conditions. In the pH range of 7 to 10.5, a concentration plateau was identified which was followed by subsequent decreased and increase in Cr leachability at pH values of 12 and 13, respectively. As mention earlier, Cr is likely to leach as chromate in alkaline and oxidizing conditions. The oxyanionic leaching pattern of Cr observed in this study evidently supported this claim. Previous studies also reported similar leaching behavior of Cr from alkaline waste materials such as fly ashes, air pollution control (APC) residues and RCAs (Engelsen et al., 2010; Izquierdo

and Querol, 2012; Quina et al., 2009). In case of RCA-MN and IA2, the leaching plateau was not observed, and thus the Cr concentration decreased gradually up to the pH value of 12. From XRD analyses the presence of ettringite was identified in these two RCAs. Several studies pointed out that CrO_4^{2-} can be incorporated in ettringite by substituting SO_4^{2-} (Izquierdo and Querol, 2012; Zhang and Reardon, 2003). Therefore, it was theorized that the presence of ettringite and consequent immobilization of CrO_4^{2-} decreased the effluent Cr concentrations from these RCAs. According to Engelsen et al. (2009), calcium sulphoaluminate hydrates (ettringite) started to destabilized at pH lower than 9.5. As shown in Figure 5.9(d), Cr concentrations of RCA-MN and IA2 deviated from oxyanionic leaching patters at pH higher than 8.8, indicating the possible formation and precipitation of CrO_4^{2-}-ettringite solid solution. Additionally, RCA carbonation had relatively less influence on the leaching of Cr. However, effluent Cr concentrations were inclined to be higher for higher degree of RCA carbonation. Furthermore, except for RCA-MN and IA2, leached Cr concentrations from all the other RCAs exceeded the U.S. EPA specified maximum contaminant level (MCL) of 0.1 mg/L for almost the whole pH range.

The concentrations of Ba were higher in acidic pH conditions which dropped at neutral pH values (Figure 5.9e). For RCA-LAB, B, IA1 and TX2, the leaching of Ba was almost pH independent in the pH range of 7 and 10 but increased slightly when the solution pH was 12. Diversely, RCA-TX1 showed cationic leaching pattern of Ba with the lowest effluent concentrations in neutral to alkaline pH range. Similar leaching patterns of Ba were observed from fly ashes (Zhang et al., 2016) and fly ash treated soils (Komonweeraket et al., 2015b) and steel slag (Fällman, 2000) in association with the dissolution/precipitation of barite ($BaSO_4$), witherite ($BaCO_3$) and and/or $(Ba,Sr)SO_4$. The leaching patters of Ba and Cr from RCA-MN and IA2 were

identical, indicating possible formation and precipitation of $Ba(S, Cr)O_4$ solid solution in alkaline conditions (Astrup et al., 2006).

The pH dependent leaching of SO_4^{2-} was the highest in acidic conditions (pH < 7) with a monotonic decrease in concentrations at elevated pH conditions. Distinct leaching behaviors of SO_4^{2-} were identified depending on the degree of carbonation of the RCA. The least carbonated RCA-LAB leached the highest concentrations of SO_4^{2-} in the pH range of 2 to 11, while highly carbonated RCA-TX1 leached the lowest concentrations in this pH zone. In material pH range, the observed trend was opposite. Highly carbonated RCA leached higher SO_4^{2-} compared to less carbonated RCAs in the pH range of 11 to 13. Additionally, a V-shape of SO_4^{2-} leaching curves was observed for all the RCAs in this pH region which was also reported by previous studies (Engelsen et al., 2009; Zhang et al., 2016). The V-shape of SO_4^{2-} leaching curve also indicated the possible substitution of SO_4^{2-} by oxyanions (Butera et al., 2015). The leaching curve of Ba, Cr and SO_4^{2-} showed the similar V-shapes in alkaline pH conditions.

5.5.7 Geochemical Modeling

Geochemical modeling was performed on all the RCAs to evaluate whether the leaching of elements from the RCAs was controlled by solubility or sorption mechanism. Previous studies indicated that geochemical equilibria models are successful in predicting the aqueous concentrations of elements based on thermodynamics data, if the leaching was controlled by solubility (Allison et al., 1991; Bestgen et al., 2016; Komonweeraket et al., 2015a). Therefore, Visual MINTEQA2 was implemented in calculating aqueous phase equilibrium concentrations and saturation indices of the leachate with respect to the solubility controlling solids or minerals. Aqueous complexation reactions at a fixed pH was allowed as recommended by Apul et al. (2005). The pH and effluent concentrations from pH-dependent leach tests were considered as the input data. The dominant oxidation states of the elements were assumed to be Ca^{2+}, Mg^{2+}, Ba^{2+} and

CrO_4^{2-}. Among all the elements reported in this study, Cr is the redox sensitive element and could occur in Cr^{3+} and Cr^{6+} oxidation states. However, as discussed in the preceding sections, alkaline material pH, WLT effluent concentrations and pH dependent leaching pattern of Cr from RCAs suggested Cr^{6+} oxidation state.

Despite of the differences in RCA source of origin and degree of carbonation, homogeneity in leaching behavior and leaching controlling mechanisms was observed. As indicated in Figure 5.10(a), Gypsum and anhydrite were identified as the solubility controlling minerals for Ca^{2+} in the pH range of 2 to 9. Under alkaline conditions, carbonate minerals became important and calcite could potentially control the aqueous concentrations of Ca. However, oversaturation with respect to calcite was observed which could happen due to the presence of gypsum (Langmuir, 1997). According to Langmuir (1997), gypsum is much more soluble than calcite and consequently precipitate calcite by providing Ca as a common ion in the leachate. Additionally, at pH higher than 10 portlandite may play a significant role on the leaching of Ca.

As seen from Figure 5.10(b), magnesite and dolomite have comparable solubility and may control the leaching of Mg in alkaline pH conditions (Komonweeraket et al., 2015a). Previous studies identified dolomite as the solubility controlling mineral for Mg leaching from alkaline waste materials such as fly ash (Garavaglia and Caramuscio, 1994), fly ash stabilized soils (Komonweeraket et al., 2015a) and steel slag (Apul et al., 2005). However, at acidic pH conditions, Mg leaching from the RCAs was not controlled by solubility.

Depending on eluate pH, carbonate and sulfate minerals had the most significant role on the leaching of Ba from the RCAs (Figure 5.10c). Sulfate mineral of barium (barite) appeared to control the leaching of Ba in acidic to moderate alkaline pH values (pH 2 to 10). At highly alkaline conditions, witherite is less soluble compared to barite, and therefore controlled the leaching of Ba

(Mudd et al., 2004). Oversaturated was observed in the leachate with respect to barite and witherite. Zhang et al. (2016) also reported oversaturation with respect to Ba minerals in fly ash leachate. From geochemical modeling, Komonweeraket et al. (2015a) claimed that the oversaturation was due to the possible formation and dissolution/precipitation of $(Ba, Sr)SO_4$ and $Ba(S, Cr)O_4$ solid solutions. However, the claim on $(Ba, Sr)SO_4$ solid solutions formation could not be tested in this study since the effluent concentrations of Sr was not quantified.

Figure 5.10(d) indicates that the leaching of Cr^{6+} in RCA leachates was not controlled by solubility. A number of studies also concluded that the leaching of Cr^{6+} from alkaline waste materials could not be described by solubility mechanism (Bestgen et al., 2016; Engelsen et al., 2010; Zhang et al., 2016). Astrup et al. (2006) claimed that $CaCrO_4$ and Cr(VI)-ettringite solid solution may control the leaching of Cr^{6+} from alkaline waste materials (pH > 10). Figure 5.10(e) provides the variation of log activity of Cr^{6+} corresponding to the log activities of Ca^{2+} along with the solubility line of $CaCrO_4$. The log activities of Cr^{6+} were in close proximity to $CaCrO_4$ solubility line, indicating that the leaching of Cr^{6+} in RCA leachate could be controlled by $CaCrO_4$. Figure 5.7 also suggested that Cr^{6+} solubility was controlled by $CaCrO_4$, where positive correlations between the effluent Cr-Ca and Cr-SO_4 concentrations were observed. Additionally, an attempt was made to investigate the probable formation of $Ba(S, Cr)O_4$ solid solutions, as suggested by the oversaturated log activity diagram of Ba. Figure 5.10(f) shows the log activities of Cr^{6+} as a function of the activities of Ba^{2+}. The solubility line of $CaCrO_4$ was approximately 6 to 12 order of magnitude higher than the log activities of Cr^{6+}-Ca^{2+}, whereas solubility line of $BaCrO_4$ was approximately 3 to 8 order of magnitude higher. This indicated that the leaching of Cr^{6+} in RCA effluent was dominated by $BaCrO_4$ rather than $CaCrO_4$ alone. Moreover, when the WLT effluent concentrations of Cr were plotted against the concentrations of Ba, a positive

correlation was found (not included). The trend was stronger for highly carbonated RCAs compared to the less carbonated ones. Zhang et al. (2016) also found that the solubility of Cr^{6+} was controlled by $BaCrO_4$ in highly alkaline fly ash leachate.

5.5.8 Saturation Conditions and Leaching of Elements

The water retention characteristics of the RCAs are presented in Figure 5.11. All of the RCAs showed low water retention capacities. Depending on RCA type, the volumetric moisture content of the RCAs at saturated conditions varied within the range of 30% to 37% (Figure 5.11a). RCA-MN had the lowest saturated moisture content, while RCA-IA1 had the highest. RCA-IA1 had the maximum amount of sand size particles and was classified as poorly graded sand (Table 5.1). Smaller particle sizes are known to have larger water retention capacities due to higher surface areas for water adsorption (Gupta and Larson, 1979). RCA-MN was the second most coarse grained RCA after RCA-LAB, and hence was expected to have relatively low saturated moisture content. Additionally, it was observed that volumetric moisture content of the RCAs did not change up to the matric potential of 2 kPa, indication the air entry pressure. At higher suction values, moisture contents of the RCAs varied within a narrow range. RCA-MN and TX2 showed relatively greater water holding capacities at higher matric potentials. Furthermore, the degree of saturation of the RCAs as a function of matric potential is presented in Figure 5.11(b). The RCAs became unsaturated with the increase in matric potential by discharging pore solutions. RCA-MN and TX2 had higher degree of saturation compared to the others at similar matric potentials.

The effluent pH values at different matric potentials are provided in Table 5.7. As seen from Table 5.7, the solution pH was the highest in the matric potential (suction) range of 2 to 5 kPa. This may have happened due to first-flush leaching of alkaline substances at near saturation conditions (Cetin et al., 2012c). As indicated in Figure 5.12, first-flush leaching patterns of Ca and Ba were also observed with higher leached concentrations in this suction range. Except for RCA-

TX1, after the initial first-flush release, Ca concentrations decreased to minimum at 10 kPa matric potential. For RCA-MN, IA1 and IA2, Ca concentrations increased at matric potential higher than 10 kPa. Conversely, leached concentrations of Ca remained at lower levels for RCA-TX2, B and LAB. RCA-TX1 showed a unique leaching pattern depending on matric suction. The concentrations of Ca increased with an increase in matric potential, though the increase rates were lower at higher matric potential values. Regardless of RCA degree of carbonation, similar leaching patterns of Ba were observed for all of the RCAs. RCA-B and LAB leached higher amounts of Ba, while Ba concentrations were lower in RCA-TX1 and TX2 pore solutions. As seen in Figure 5.13, three distinct leaching behaviors of Mg were observed depending on matric potential. The initial high Mg concentrations decreased to minimum values when matric potentials were approximately 3 kPa. For RCA-MN, IA1 and B a subsequent increase in Mg concentrations was observed. From XRF and total elemental analyses, maximum Mg contents were identified in these three RCAs. With the increase in matric potential, pH of the pore solutions decreased which led to an increase in solution Mg concentrations. For RCA-IA2 and TX2 an increase in Mg concentrations was detected at around 5 kPa matric potentials, which eventually decreased at 10 kPa matric potential values. A subsequent slight increase in Mg concentrations were observed for IA2 and TX2 at higher potentials. For RCA-TX1 and LAB, Mg concentrations remained almost unchanged in between 3 and 20 kPa matric potentials. Elevated Mg concentrations were observed for TX1 and LAB pore solutions at a matric potential of 32 kPa. Pore-water concentrations of Cr were found to be influenced by RCA degree of carbonation (Figure 5.13d-f). For RCA-MN, B and LAB, Cr concentrations were the highest at near saturation conditions, which subsequently decreased at 2 kPa matric potentials and remained stable for rest of the matric potential range. For other RCAs, Cr concentrations increased up to 2 kPa of matric potentials and became relatively stable with

respect to matric potential. Highly carbonated RCA-TX1 and TX2 tended to leach higher Cr at unsaturated conditions.

5.6   Conclusions

A study was conducted to investigate the leaching behavior of elements (Ca, Mg, Ba and Cr), sulfate (SO_4) and eluate alkalinity from RCAs collected from a variety of geographical locations. Laboratory batch water leach tests (WLT), toxicity characteristic leaching procedure (TCLP), synthetic precipitation leaching procedure (SPLP) and pH-dependent leach tests were performed. Comparisons between the effluent leaching characteristics were provided depending on RCA degree of carbonation, leach test method, saturation condition, particle size and liquid to solid ratio. Additionally, geochemical equilibrium model Visual MINTEQ was implemented to access the leaching controlling mechanisms of the elements. Some of the salient features of this study are summarized as follow:

When the RCAs were fractionized into different particle sizes, it was found that the effluent pH, electric conductivity (EC), alkalinity and leached concentrations of Ca, Ba, Cr and SO_4 generally decreased with an increase in RCA particle sizes. The Mg concentrations fluctuated, with a propensity to increase at larger particle sizes.

For carbonated RCAs, the maximum pH, EC, alkalinity and Ca concentrations were associated with the particle of 1.19 mm to 0.149 mm in size. Particles finer than 0.149 resulted the highest pH, EC, alkalinity and Ca concentrations for less carbonated RCAs.

With an increase in liquid to solid ratio (L/S), effluent pH, EC, alkalinity and leached concentrations of Ca, Ba and Cr decreased. Mg concentrations were inclined to increase with an increase in L/S ratio. Less carbonated RCAs leached higher amount of SO_4 at larger L/S ratios, while the observed behavior was opposite for highly carbonated ones.

Leaching of constituents was considerably influenced by the degree of RCA carbonation. RCAs with greater degree of carbonation leached higher concentrations of Cr and SO_4 compared to the less carbonated ones. The effluent pH, EC, alkalinity and leached concentrations of Ca and Ba were higher for less carbonated RCAs.

Schoeller diagrams indicated that the effluent alkalinity of less carbonated RCAs could be associated with the dissolution of calcium minerals, whereas other alkaline minerals became important with an increase in RCA carbonation level. Leaching of Ca from highly carbonated RCAs was possibly dominated by gypsum and/or anhydrite.

Probable interdependent leaching of Cr and Ba from less carbonated RCAs was predicted by the Schoeller diagram. For highly carbonated RCAs, it was anticipated that the leaching of Ba was controlled by witherite rather than barite.

Leaching fingerprints of the RCAs indicated that with the increase in L/S ratio, the leaching behavior of less carbonated RCA drifted towards the highly carbonated ones with less variation in effluent concentrations of the constituents.

Effluent pH, EC, alkalinity and Cr concentrations significantly increased with an increase in leached Ca concentrations. Ba concentrations increased when the effluent alkalinity was higher. The leaching of Cr from highly carbonated RCAs was more sensitive with respect to Ca.

For less carbonated RCAs, Ca concentrations were comparable in WLT and TCLP effluents, whereas similar concentrations of Ca were observed in WLT and SPLP effluents of highly carbonated RCAs. In general, TCLP effluent concentrations of Ca were higher compared to WLT and SPLP effluent Ca concentrations.

Least carbonated RCAs leached the highest concentrations of Mg in SPLP effluent, while for moderately to highly carbonated RCAs, TCLP effluent concentrations of Mg were the highest.

The TCLP effluent of the RCAs was found to be the most alkaline which was followed by WLT and SPLP alkalinity. TCLP alkalinity increase with an increase in RCA carbonation level. For WLT and SPLP, effluent alkalinity decreased at elevated RCA degree of carbonation.

Generally, the WLT effluent Ba concentrations were the highest, whereas the lowest concentrations of Ba were found in TCLP effluent. In case of Cr and SO_4, WLT effluent concentrations were the highest for higher degree of carbonation. Diversely, fresher RCAs leached higher Cr and SO_4 concentrations in TCLP effluents.

Depending on the degree of carbonation, RCAs showed distinct acid neutralization capacities. Highly carbonated RCAs showed higher buffering capacities in the pH range of 5 to 6 compared to the less carbonated ones.

The pH-dependent leaching of Ca, Mg and SO_4 followed a cationic leaching pattern. In the pH range of 7 to 13, Ca and Mg concentrations were lower for highly carbonated RCAs compared to the fresher ones. In material pH conditions, carbonated RCAs resulted higher SO_4 concentrations, while SO_4 leaching were lower for aged RCAs at every other pH values.

Cr showed an oxyanionic leaching pattern with lesser influence of RCA degree of carbonation. The presence of ettringite significantly altered the leaching pattern of Cr. The most carbonated RCA showed a cationic leaching pattern of Ba, whereas for the other RCAs, Ba concentrations were found to be pH independent.

Geochemical modeling indicated that the leaching of Ca, Mg and Ba from the RCAs were controlled by solubility. The solubility mechanism was ineffective in describing the leaching of Cr. Geochemical modeling suggested that leaching of Cr from the RCAs could be controlled by $BaCrO_4$ and $CaCrO_4$ solid solutions.

Effluent pH, Ca and Ba concentrations were the highest in the matric potential range of 2 to 5 kPa. Depending on carbonation level, leached Ca concentration varied with the RCA degree of saturation/matric potential. Leaching of Mg with matric potential was influenced by Mg content of the RCA. Cr leaching at different saturation conditions was greatly influenced by carbonation.

Briefly, results indicated that the leaching characteristics of RCA are needed to be evaluated focusing the RCA degree of carbonation. For the leaching assessment of RCA, the selection of the most appropriate method was found to be dependent on RCA degree of carbonation. The pH dependent leaching of the elements were also controlled by RCA carbonation level.

5.7   References

Allison, J.D., Brown, D.S., Novo-Gradac, K.J., 1991. MINTEQA2/PRODEFA2, A geochemical assessment model for environmental systems: Version 3.0 User's Manual. Environmental Research Laboratory, Office of Research and Development, US Environmental Protection Agency, Athens, Georgia.

Apul, D.S., Gardner, K.H., Eighmy, T.T., Fällman, A.M., Comans, R.N.J., 2005. Simultaneous application of dissolution/precipitation and surface complexation/surface precipitation modeling to contaminant leaching. Environ. Sci. Technol. 39, 5736–5741. https://doi.org/10.1021/ES0486521

Arulrajah, A., Piratheepan, J., Disfani, M.M., 2014. Reclaimed asphalt pavement and recycled concrete aggregate blends in pavement Ssubbases: Laboratory and field evaluation. J. Mater. Civ. Eng. 26, 349–357. https://doi.org/10.1061/(ASCE)MT.1943-5533.0000850

Astrup, T., Dijkstra, J.J., Comans, R.N.J., Sloot, H.A. van der, Christensen, T.H., 2006. Geochemical modeling of leaching from MSWI air-pollution-control residues. Environ. Sci. Technol. 40, 3551–3557. https://doi.org/10.1021/ES052250R

Bestgen, J.O., Cetin, B., Tanyu, B.F., 2016. Effects of extraction methods and factors on leaching of metals from recycled concrete aggregates. Environ. Sci. Pollut. Res. 23, 12983–13002. https://doi.org/10.1007/s11356-016-6456-0

Bin-Shafique, S., Benson, C.H., Edil, T.B., Hwang, K., 2006. Leachate concentrations from water leach and column leach tests on fly ash-stabilized soils. Environ. Eng. Sci. 23, 53–67. https://doi.org/10.1089/ees.2006.23.53

Butera, S., Hyks, J., Christensen, T.H., Astrup, T.F., 2015. Construction and demolition waste: Comparison of standard up-flow column and down-flow lysimeter leaching tests. Waste Manag. 43, 386–397. https://doi.org/10.1016/J.WASMAN.2015.04.032

Cetin, B., Aydilek, A.H., Guney, Y., 2012a. Leaching of trace metals from high carbon fly ash stabilized highway base layers. Resour. Conserv. Recycl. 58, 8–17. https://doi.org/10.1016/J.RESCONREC.2011.10.004

Cetin, B., Aydilek, A.H., Li, L., 2012b. Experimental and numerical analysis of metal leaching from fly ash-amended highway bases. Waste Manag. 32, 965–978. https://doi.org/10.1016/J.WASMAN.2011.12.012

Cetin, B., Aydilek, A.H., Li, L., 2012c. Experimental and numerical analysis of metal leaching from fly ash-amended highway bases. Waste Manag. 32, 965–978. https://doi.org/10.1016/j.wasman.2011.12.012

Chen, J., Bradshaw, S., Benson, C.H., Tinjum, J.M., Edil, T.B., 2012. pH-dependent leaching of trace elements from recycled concrete aggregate, in: GeoCongress 2012. American Society of Civil Engineers, Reston, VA, pp. 3729–3738. https://doi.org/10.1061/9780784412121.382

Chen, Q., Zhang, L., Ke, Y., Hills, C., Kang, Y., 2009. Influence of carbonation on the acid neutralization capacity of cements and cement-solidified/stabilized electroplating sludge. Chemosphere 74, 758–764. https://doi.org/10.1016/J.CHEMOSPHERE.2008.10.044

Daniels, J.L., Das, G.P., 2006. Leaching behavior of lime–fly ash mixtures. Environ. Eng. Sci. 23, 42–52. https://doi.org/10.1089/ees.2006.23.42

Di Gianfilippo, M., Costa, G., Verginelli, I., Gavasci, R., Lombardi, F., 2016. Analysis and interpretation of the leaching behaviour of waste thermal treatment bottom ash by batch and column tests. Waste Manag. 56, 216–228. https://doi.org/10.1016/J.WASMAN.2016.07.034

Engelsen, C.J., van der Sloot, H.A., Wibetoe, G., Justnes, H., Lund, W., Stoltenberg-Hansson, E., 2010. Leaching characterisation and geochemical modelling of minor and trace elements released from recycled concrete aggregates. Cem. Concr. Res. 40, 1639–1649. https://doi.org/10.1016/J.CEMCONRES.2010.08.001

Engelsen, C.J., van der Sloot, H.A., Wibetoe, G., Petkovic, G., Stoltenberg-Hansson, E., Lund, W., 2009. Release of major elements from recycled concrete aggregates and geochemical modelling. Cem. Concr. Res. 39, 446–459. https://doi.org/10.1016/J.CEMCONRES.2009.02.001

Fällman, A.-M., 2000. Leaching of chromium and barium from steel slag in laboratory and field tests — a solubility controlled process? Waste Manag. 20, 149–154. https://doi.org/10.1016/S0956-053X(99)00313-X

Galvín, A.P., Ayuso, J., Jiménez, J.R., Agrela, F., 2012. Comparison of batch leaching tests and influence of pH on the release of metals from construction and demolition wastes. Waste Manag. 32, 88–95. https://doi.org/10.1016/J.WASMAN.2011.09.010

Garavaglia, R., Caramuscio, P., 1994. Coal fly-ash leaching behaviour and solubility controlling solids. Stud. Environ. Sci. 60, 87–102. https://doi.org/10.1016/S0166-1116(08)71450-X

Garrabrants, A.C., Sanchez, F., Kosson, D.S., 2004a. Changes in constituent equilibrium leaching and pore water characteristics of a Portland cement mortar as a result of carbonation. Waste Manag. 24, 19–36. https://doi.org/10.1016/S0956-053X(03)00135-1

Garrabrants, A.C., Sanchez, F., Kosson, D.S., 2004b. Changes in constituent equilibrium leaching and pore water characteristics of a Portland cement mortar as a result of carbonation. Waste Manag. 24, 19–36. https://doi.org/10.1016/S0956-053X(03)00135-1

Gräfe, M., Power, G., Klauber, C., 2009. Review of bauxite residue alkalinity and associated chemistry, CSIRO Document DMR-3610. Project ATF-06-3: Management of Bauxite Residues.

Gupta, N., Kluge, M., Chadik, P.A., Townsend, T.G., 2018. Recycled concrete aggregate as road base: Leaching constituents and neutralization by soil Interactions and dilution. Waste Manag. 72, 354–361. https://doi.org/10.1016/J.WASMAN.2017.11.018

Gupta, S.C., Larson, W.E., 1979. Estimating soil water retention characteristics from particle size distribution, organic matter percent, and bulk density. Water Resour. Res. 15, 1633–1635. https://doi.org/10.1029/WR015i006p01633

Hoyos, L.R., Puppala, A.J., Ordonez, C.A., 2011. Characterization of cement-fiber-treated reclaimed asphalt pavement aggregates: Preliminary investigation. J. Mater. Civ. Eng. 23, 977–989. https://doi.org/10.1061/(ASCE)MT.1943-5533.0000267

Isenburg, J., Moore, M., 1992. Generalized acid neutralization capacity test, in: Stabilization and Solidification of Hazardous, Radioactive, and Mixed Wastes: 2nd Volume. ASTM International, 100 Barr Harbor Drive, PO Box C700, West Conshohocken, PA 19428-2959, pp. 361-361–17. https://doi.org/10.1520/STP19564S

Izquierdo, M., Querol, X., 2012. Leaching behaviour of elements from coal combustion fly ash: An overview. Int. J. Coal Geol. 94, 54–66. https://doi.org/10.1016/J.COAL.2011.10.006

Komonweeraket, K., Cetin, B., Aydilek, A., Benson, C.H., Edil, T.B., 2015a. Geochemical analysis of leached elements from fly ash stabilized soils. J. Geotech. Geoenvironmental Eng. 141, 04015012. https://doi.org/10.1061/(ASCE)GT.1943-5606.0001288

Komonweeraket, K., Cetin, B., Benson, C.H., Aydilek, A.H., Edil, T.B., 2015b. Leaching characteristics of toxic constituents from coal fly ash mixed soils under the influence of pH. Waste Manag. 38, 174–184. https://doi.org/10.1016/J.WASMAN.2014.11.018

Kosson, D.S., Sloot, H.A., Garrabrants, A.C., Seignette, P.F.A.B., 2014. Leaching test relationships, laboratory-to-field comparisons and recommendations for leaching evaluationusing the leaching environmental assessment framework (LEAF).

Kosson, D.S., van der Sloot, H.A., Sanchez, F., Garrabrants, A.C., 2002. An integrated framework for evaluating leaching in waste management and utilization of secondary materials. Environ. Eng. Sci. 19, 159–204. https://doi.org/10.1089/109287502760079188

Langmuir, D., 1997. Aqueous Environmental Geochemistry. Prentice Hall, Upper Saddle River, New Jersey, USA.

LEAF, 2019. Method 1314 – Percolation Column | LEAF | Vanderbilt University [WWW Document]. URL https://www.vanderbilt.edu/leaching/leaching-tests/test-method-1314/ (accessed 3.17.19).

Leisinger, S.M., Lothenbach, B., Saout, G. Le, Kägi, R., Wehrli, B., Johnson, C.A., 2010. Solid Solutions between CrO4- and SO4-Ettringite Ca6(Al(OH)6)2[(CrO4)x(SO4)1-x]3*26 H2O. Environ. Sci. Technol. 44, 8983–8988. https://doi.org/10.1021/es100554v

McBride, M.B., 1994. Environmental Chemistry of Soils., Environmental chemistry of soils. Oxford University Press, NY, USA.

Mudd, G.M., Weaver, T.R., Kodikara, J., 2004. Environmental geochemistry of leachate from leached brown coal ash. J. Environ. Eng. 130, 1514–1526. https://doi.org/10.1061/(ASCE)0733-9372(2004)130:12(1514)

Mulugeta, M., Engelsen, C.J., Wibetoe, G., Lund, W., 2011. Charge-based fractionation of oxyanion-forming metals and metalloids leached from recycled concrete aggregates of different degrees of carbonation: A comparison of laboratory and field leaching tests. Waste Manag. 31, 253–258. https://doi.org/10.1016/J.WASMAN.2010.05.003

Phoungthong, K., Xia, Y., Zhang, H., Shao, L., He, P., 2016. Leaching toxicity characteristics of municipal solid waste incineration bottom ash. Front. Environ. Sci. Eng. 10, 399–411. https://doi.org/10.1007/s11783-015-0819-5

Puthussery, J. V., Kumar, R., Garg, A., 2017. Evaluation of recycled concrete aggregates for their suitability in construction activities: An experimental study. Waste Manag. 60, 270–276. https://doi.org/10.1016/J.WASMAN.2016.06.008

Quina, M.J., Bordado, J.C.M., Quinta-Ferreira, R.M., 2009. The influence of pH on the leaching behaviour of inorganic components from municipal solid waste APC residues. Waste Manag. 29, 2483–2493. https://doi.org/10.1016/j.wasman.2009.05.012

Sanchez, F., Gervais, C., Garrabrants, A.C., Barna, R., Kosson, D.S., 2002. Leaching of inorganic contaminants from cement-based waste materials as a result of carbonation during intermittent wetting. Waste Manag. 22, 249–260. https://doi.org/10.1016/S0956-053X(01)00076-9

Van Praagh, M., Modin, H., 2016. Leaching of chloride, sulphate, heavy metals, dissolved organic carbon and phenolic organic pesticides from contaminated concrete. Waste Manag. 56, 352–358. https://doi.org/10.1016/J.WASMAN.2016.07.009

Zhang, M., Reardon, E.J., 2003. Removal of B, Cr, Mo, and Se from wastewater by incorporation into hydrocalumite and ettringite. Environ. Sci. Technol. 37, 2947–2952. https://doi.org/10.1021/ES020969I

Zhang, Y., Cetin, B., Likos, W.J., Edil, T.B., 2016. Impacts of pH on leaching potential of elements from MSW incineration fly ash. Fuel 184, 815–825. https://doi.org/10.1016/J.FUEL.2016.07.089

5.8   Tables and Figures

Table 5.1 Physical properties of recycled concrete aggregates used in this study

Properties	RCA-MN	RCA-IA1	RCA-IA2	RCA-TX1	RCA-TX2	RCA-B	RCA-LAB
Gravel Content (%)	94.1	48.8	82	93.4	68.8	86.4	94.8
Sand Content (%)	4.9	51.1	17.8	5.8	31.1	12.9	4.8
C_u	2.1	7.9	7.6	2.1	32	4.6	2.7
C_c	1.4	0.6	1.8	1.1	3.6	2.4	1.2
θ (%)	2.1	2.2	3.2	1.1	1.7	2.5	1.4
ω_{opt} (%)	12.6	14.8	14.3	10.9	14.4	13.8	13.6
γ_{dmax} (kN/m^3)	18.3	19	18.4	19	19.7	18.2	18.8
USCS Classification	GP	SP	GW	GP	GP	GW	GP
AASHTO Classification	A-1-a	A-1-a	A-1-a	A-1-a	A-1-a	A-1-a	A-1-a

Note: Gravel content: > 4.75 mm, Sand content: 4.75 – 0.075 mm, Fines Content: < 0.075 mm, C_u: Coefficient of uniformity, C_c: Coefficient of curvature, θ : Air-dry moisture content by weight, ω_{opt} : Optimum moisture content, γ_{dmax} : Maximum dry density

Table 5.2 Chemical composition of recycled concrete aggregates used in this study

Oxide Content (%)	RCA-MN	RCA-IA1	RCA-IA2	RCA-TX1	RCA-TX2	RCA-B	RCA-LAB
SiO_2	46	37	41.6	30.8	38.1	47.7	34.7
Al_2O_3	5.6	4.4	4.6	1.7	2.3	5.8	4.3
Fe_2O_3	2.2	1.8	1.9	2.3	2.1	3	1.2
CaO	23.9	28.5	28.2	34.9	30.9	22.0	33.4
MgO	3.2	3.3	2.2	1.5	2	4	1.7
SO_3	0.61	0.66	0.7	0.41	0.46	0.58	0.93
K_2O	0.97	0.8	0.79	0.25	0.42	1.11	0.82
Na_2O	0.99	0.94	0.88	0.08	0.08	1.22	0.91
BaO	0.03	0.03	0.04	0.01	0.01	0.04	0.02
SrO	0.04	0.04	0.04	0.08	0.07	0.04	0.04
Mn_2O_3	0.08	0.08	0.09	0.08	0.08	0.15	0.04
LOI	18.7	22.3	21.8	27.7	23.3	17.1	14.2
pH	12.05	11.84	12.02	11.12	12.03	12.43	12.5
Total Metal Content (mg/kg)							
Ca	84,286	93,333	100,343	140,381	103,086	73,943	126,857
Mg	9,933	11,581	8,337	6,401	8,411	13,143	6,406
Ba	80	71.8	62.2	45.9	52.9	54.1	46.7
Cr	27	21.3	25	26.8	27.9	25	23.7
S	7,667	8,160	7,829	9,051	7,509	7,246	11,211

Table 5.3 Mineralogical compounds of the recycled concrete aggregates (RCA) identified by X-ray diffraction (XRD)

RCA Type	Minerals	Ideal Formula
RCA-MN RCA-IA2	Quartz, calcite, dolomite, portlandite, ettringite	SiO_2, $CaCO_3$, $CaMg(CO_3)_2$, $Ca(OH)_2$, $Ca_6Al_2(SO_4)_3(OH)_{12} \cdot 26H_2O$
RCA-IA1 RCA-B RCA-LAB	Quartz, calcite, dolomite, portlandite, albite, anorthite	SiO_2, $CaCO_3$, $CaMg(CO_3)_2$, $Ca(OH)_2$, $NaAlSi_3O_8$, $CaAl_2Si_2O_8$
RCA-TX1 RCA-TX2	Quartz, calcite, dolomite	SiO_2, $CaCO_3$, $CaMg(CO_3)_2$

Table 5.4 Effect of L/S ratio on pH and electric conductivity of WLT effluent

RCA ID	Liquid to Solid Ratio (L/S)							
	5	10	15	20	5	10	15	20
	pH				Electric Conductivity (mS/cm)			
RCA-MN	12.12	12.05	11.98	11.91	9.46	7.64	6.67	6.02
RCA-IA1	12.09	11.84	11.84	11.82	6.56	5.33	4.95	4.74
RCA-IA2	12.15	12.02	11.88	11.84	6.49	5.82	5.01	4.83
RCA-TX1	11.14	11.12	11.13	11.12	2.94	2.79	2.72	2.71
RCA-TX2	12.12	12.03	12	11.87	4.45	4.29	4.08	3.94
RCA-B	12.52	12.43	12.38	12.37	9.28	8.67	7.35	7.5
RCA-LAB	12.56	12.5	12.47	12.45	10.73	10.3	9.63	8.65

Table 5.5 Effect of particle size on pH and electric conductivity of WLT effluent

Sieve Number	Sieve Opening (mm)	RCA-MN	RCA-IA1	RCA-IA2	RCA-TX1	RCA-TX2	RCA-B	RCA-LAB
				pH				
3/8"	9.51	11.75	11.61	11.43	9.54	10.29	12.18	12.3
#4	4.76	12.01	11.64	12.12	9.22	11.41	12.19	12.27
#8	2.38	11.92	11.9	12.03	9.15	11.49	12.31	12.41
#16	1.19	11.91	11.93	11.98	8.93	11.8	12.29	12.46
#30	0.595	12.03	11.93	11.87	11.33	11.96	12.43	12.53
#50	0.297	11.97	11.92	11.82	11.31	11.92	12.49	12.54
#100	0.149	11.78	11.91	11.94	11.3	11.98	12.49	12.56
#200	0.074	11.77	11.88	11.9	11.33	11.95	12.54	12.61
				Electric Conductivity (mS/cm)				
3/8"	9.51	3.593	3.15	2.821	2.489	2.422	3.725	6.74
#4	4.76	5.028	3.164	5.059	2.573	2.865	3.871	6.96
#8	2.38	4.101	3.807	4.265	2.633	3.017	5.916	8.8
#16	1.19	3.903	4.097	4.067	2.665	2.922	5.968	9.75
#30	0.595	4.905	3.825	4.011	2.912	4.398	7.093	10.04
#50	0.297	4.224	3.823	3.949	2.865	4.286	7.676	10.15
#100	0.149	3.557	3.885	4.229	3.011	4.475	9.439	10.59
#200	0.074	3.531	3.437	4.012	3.158	4.33	9.159	10.72

Table 5.6 RCA effluent pH, electric conductivity, alkalinity and leached concentrations of elements in different leach tests

Tests	RCA ID	pH	Conductivity (mS/cm)	Ca (mg/L)	Mg (mg/L)	Ba (mg/L)	Cr (mg/L)	SO$_4$ (mg/L)	Alkalinity (mg/L CaCO$_3$)
	RCA-MN	12.05	7.64	303	0.014	0.485	0.071	20.24	1060
	RCA-IA1	11.84	5.33	167	0.015	0.555	0.049	30.24	500
Batch Water	RCA-IA2	12.02	5.82	206	0.011	0.626	0.037	19.64	780
Leach Test	RCA-TX1	11.12	2.79	55	0.057	0.037	0.175	133.98	60
(L/S = 10)	RCA-TX2	12.03	4.29	113	0.017	0.224	0.204	92.24	240
	RCA-B	12.43	8.67	436	0.025	0.306	0.048	14.67	1280
	RCA-LAB	12.5	10.3	504	0.012	0.889	0.054	19.92	1480
	RCA-MN	11.57	7.65	525	0.642	0.243	0.106	86.22	2660
Toxicity	RCA-IA1	11.03	7.38	477	5.57	0.241	0.08	166.35	2840
characteristic	RCA-IA2	11.62	7.74	515	0.684	0.356	0.076	75.41	2760
leaching	RCA-TX1	7.12	7.84	504	9.79	0.181	0.141	100.39	3000
procedure	RCA-TX2	10.18	7.26	494	9.68	0.202	0.122	87.05	2520
(TCLP)	RCA-B	11.81	7.99	522	0.34	0.211	0.065	74.89	2680
	RCA-LAB	11.92	8.24	553	0.368	0.169	0.139	90.09	2400
	RCA-MN	12.24	4.07	249	0.078	0.228	0.066	31.17	640
Synthetic	RCA-IA1	11.94	1.82	133	0.072	0.209	0.048	33.16	300
Precipitation	RCA-IA2	12.09	2.82	168	0.061	0.35	0.036	15.91	360
Leaching	RCA-TX1	10.94	0.34	35	0.183	0.019	0.087	62.87	20
Procedure	RCA-TX2	11.7	1.04	76	0.518	0.081	0.149	57.14	120
(SPLP)	RCA-B	12.25	4.69	282	0.694	0.181	0.037	16.02	660
	RCA-LAB	12.33	4.84	299	0.654	0.349	0.065	19.08	740

Table 5.7 pH and electric conductivity of the RCA effluent at different matric potentials

Matric Potential (kPa)	RCA-MN	RCA-IA1	RCA-IA2	RCA-TX1	RCA-TX2	RCA-B	RCA-LAB
				pH			
0.37	NA	NA	12.07	NA	8.95	10.47	12.05
1.96	9.36	11.9	12.09	8.21	11.76	12.39	12.61
2.94	12.03	12	11.2	8.69	11.89	12.49	12.72
4.9	12.02	12.01	10.28	9.02	10.81	12.25	12.49
9.81	10.38	11.06	10.79	8.66	10.88	11.92	12.57
19.61	9.32	9.19	10.69	8.11	10.19	9.91	11.43
32.36	NA	8.98	NA	7.96	9.1	9.56	10.06

Note: NA: Not available due to low drainage volume
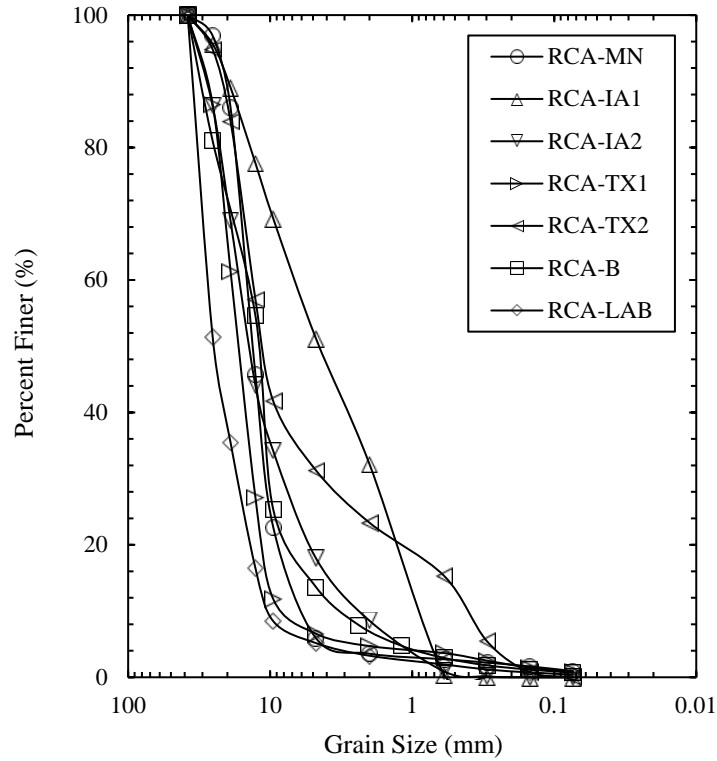
Figure 5.1 Particle size distribution curves of recycled concrete aggregates (RCA)
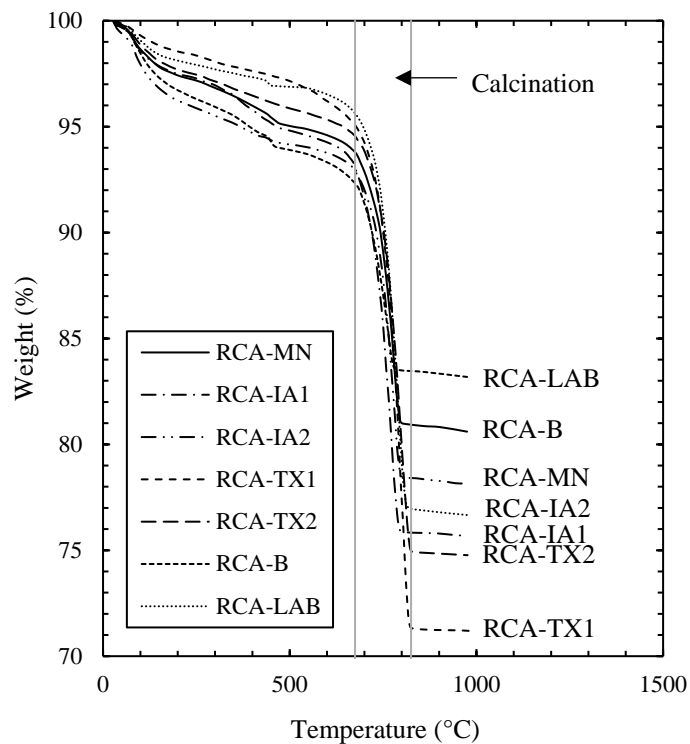
Figure 5.2 TGA analyses of the recycled concrete aggregates (RCA) used in this study
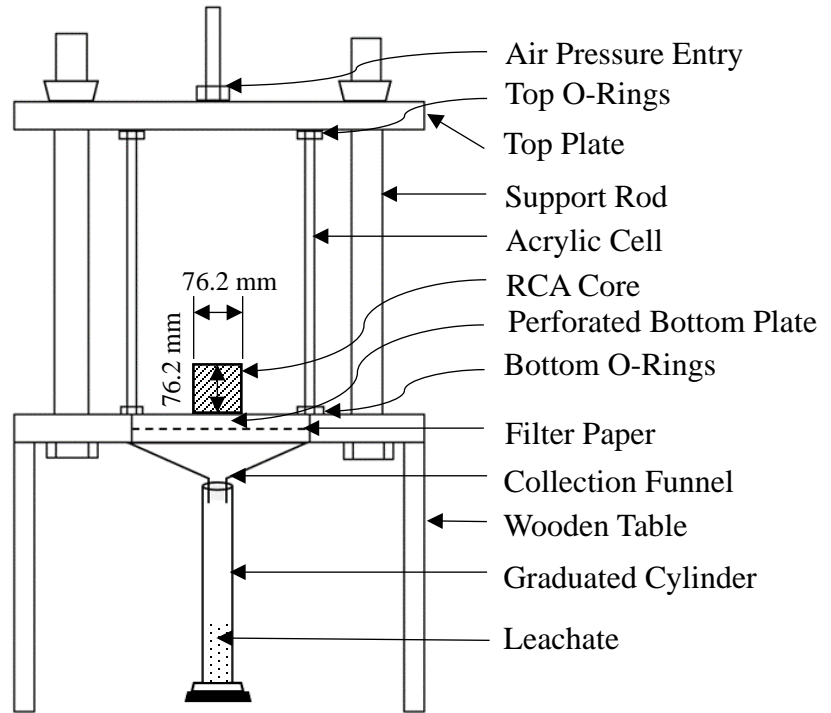
Figure 5.3 Pressure cell arrangement with RCA core to investigate the water retention characteristic and leaching behavior at different matric potentials
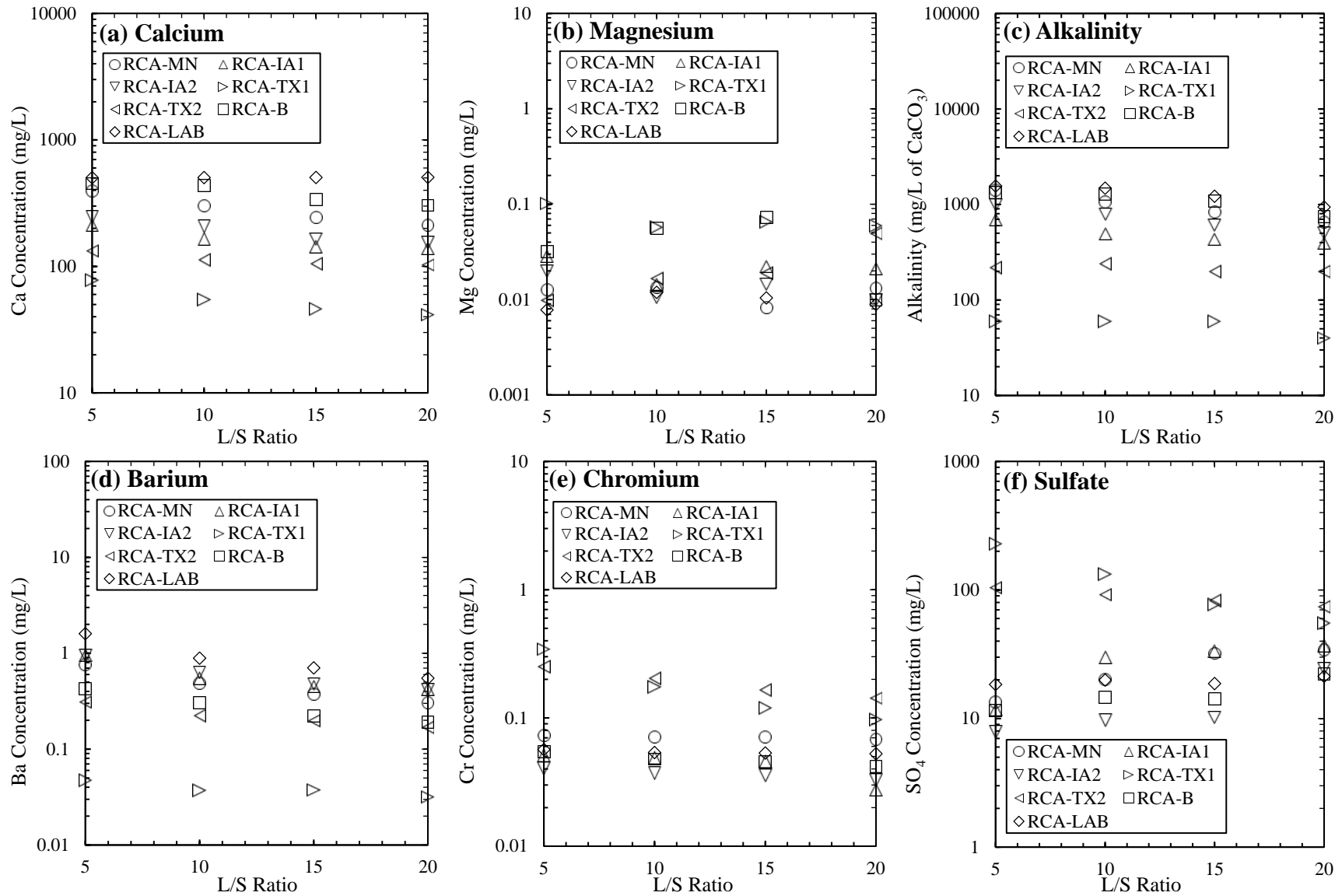
Figure 5.4 Effect of liquid to solid (L/S) ratio on the leaching of (a) Ca, (b) Mg, (c) alkalinity, (d) Ba, (e) Cr, and (d) SO₄
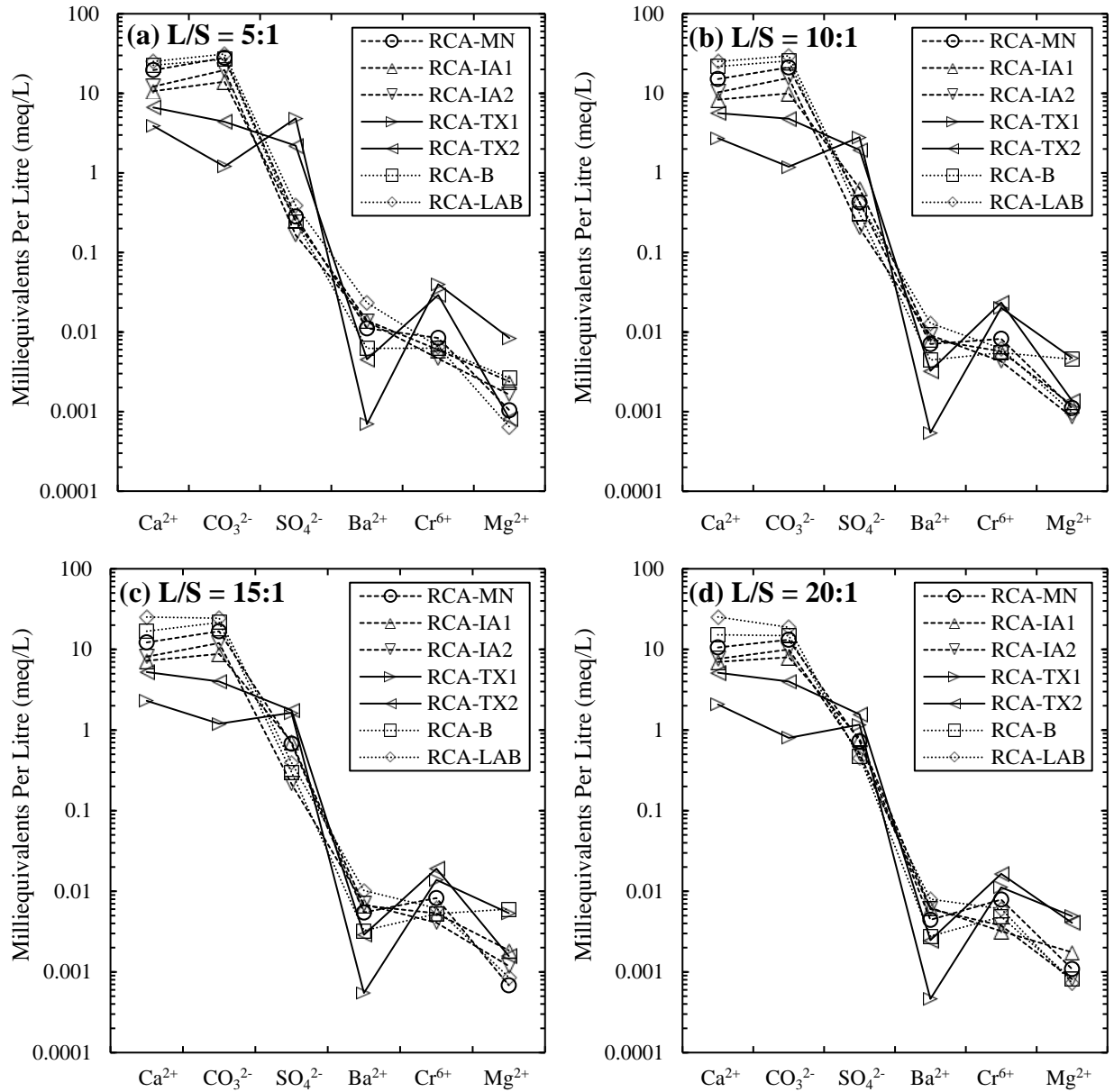
Figure 5.5 Schoeller diagram of the effluent concentrations at liquid to solid ratios (L/S) of (a) 5:1, (b) 10:1, (c) 15:1, and (d) 20:1
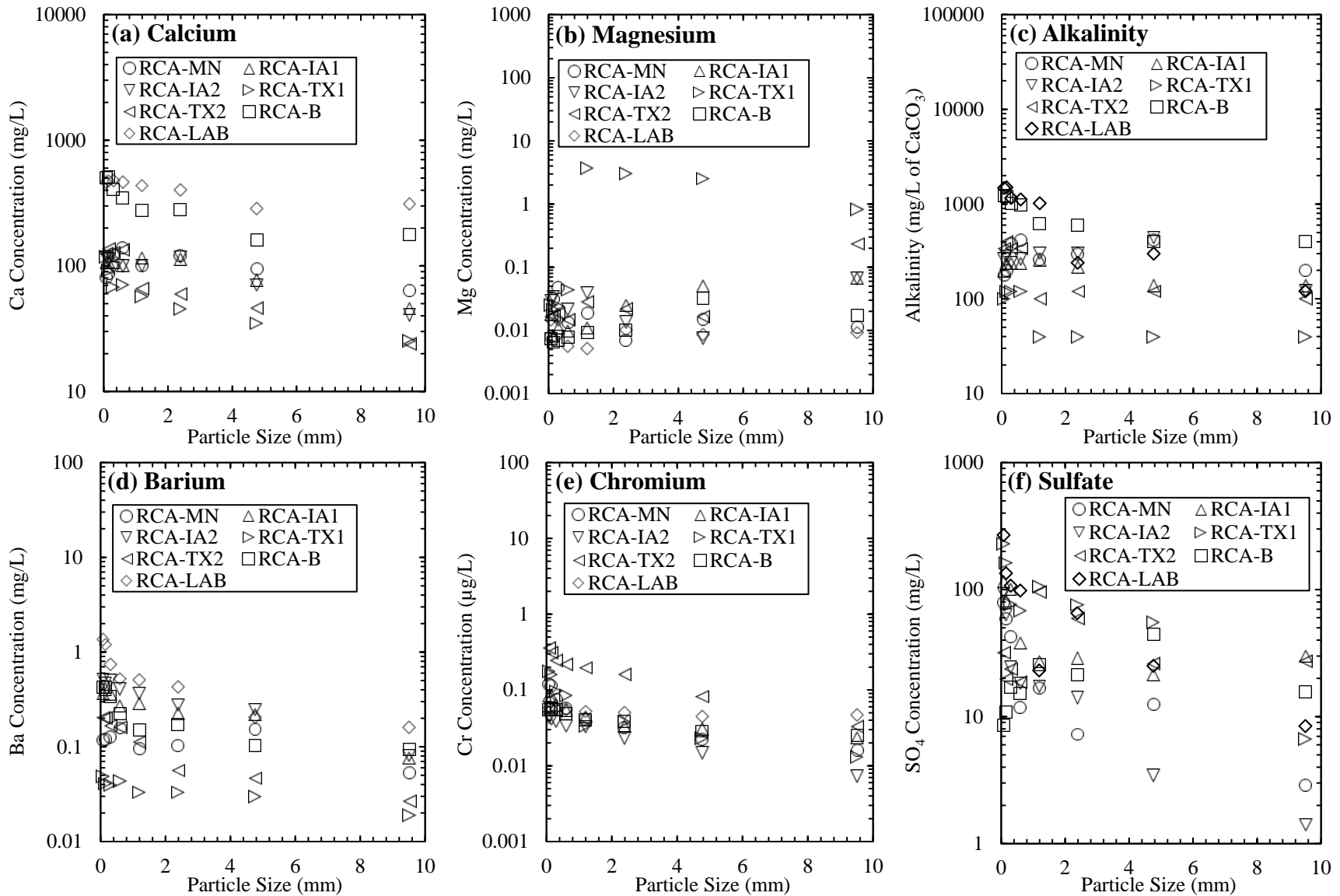
Figure 5.6 Effect of particle size on the leaching of (a) Ca, (b) Mg, (c) alkalinity, (d) Ba, (e) Cr, and (f) SO4
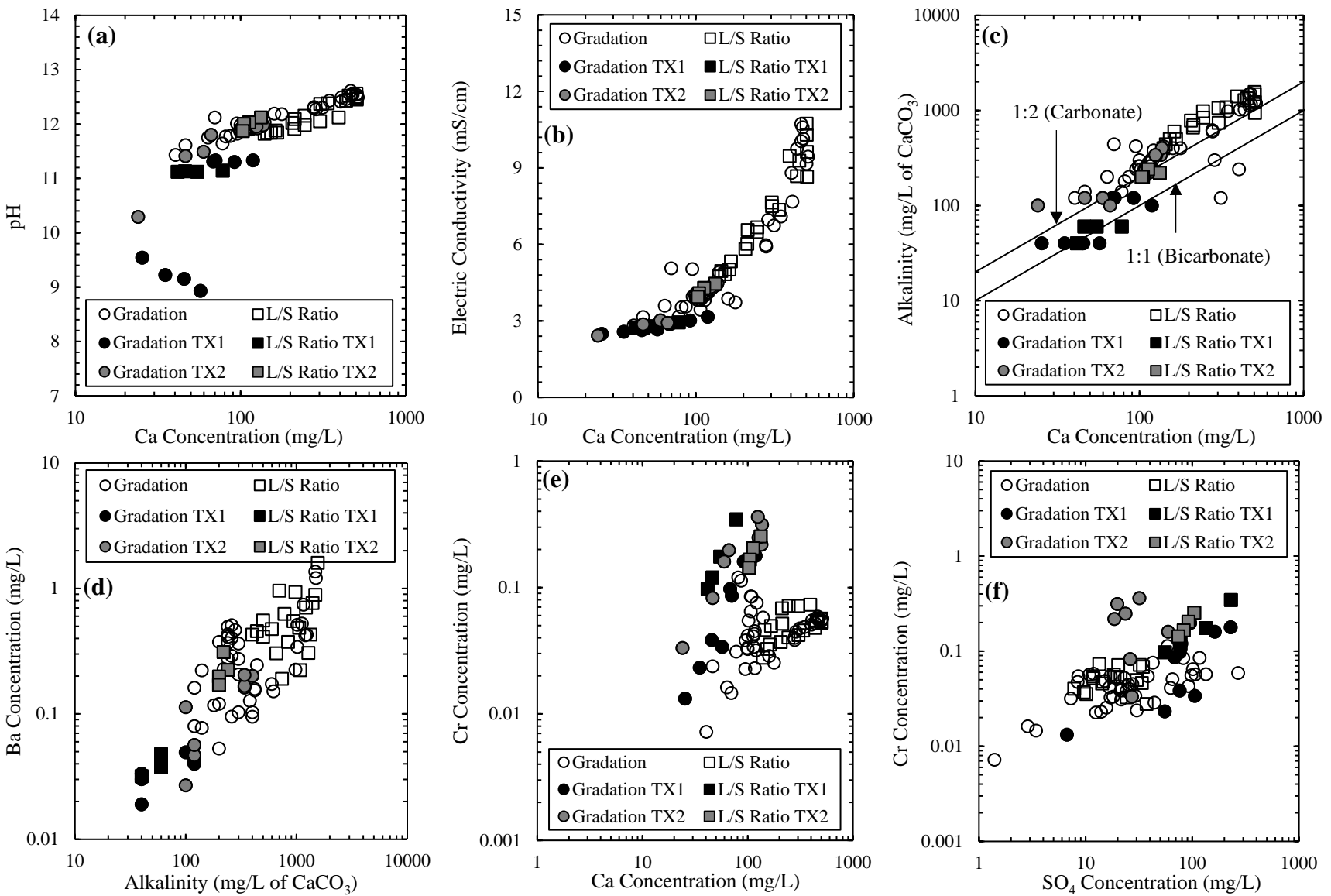
Figure 5.7 Effect of leached Ca on (a) pH, (b) EC, (c) Alkalinity, (d) leached Ba, (e) leached Cr, and (f) effect of SO₄ on Cr in WLT
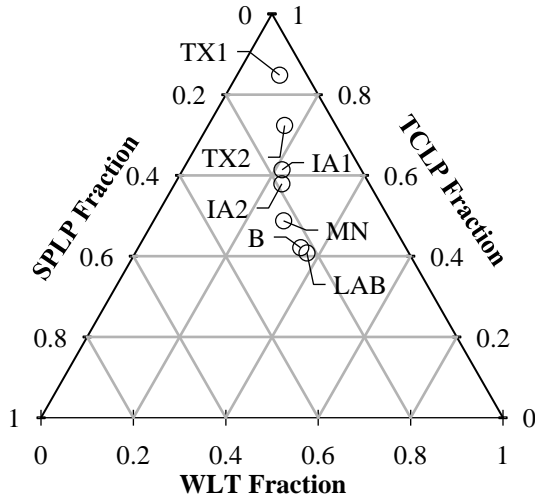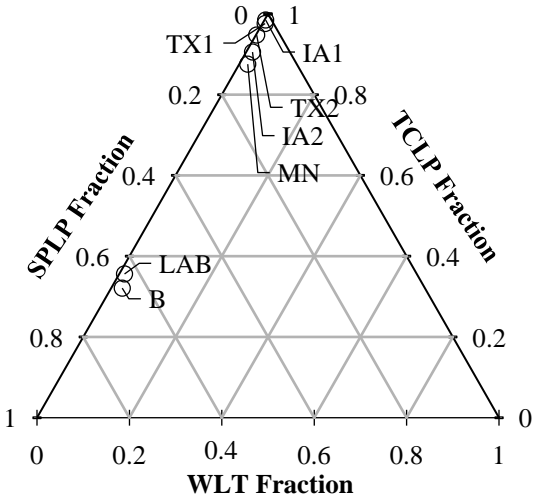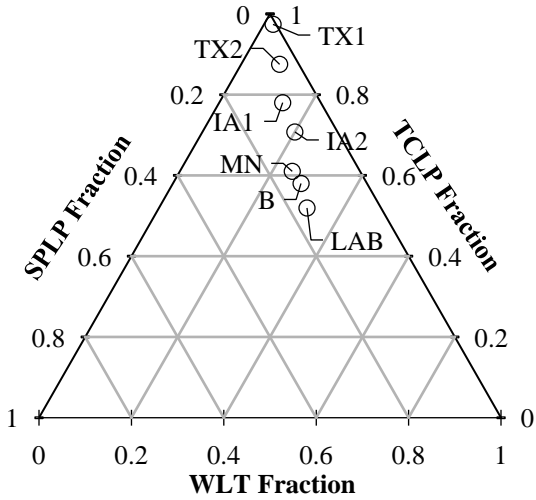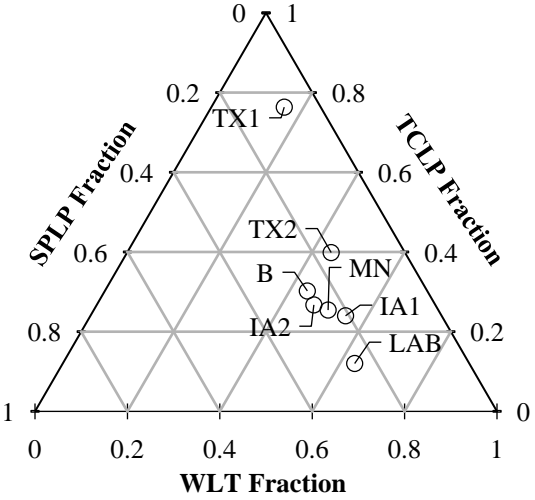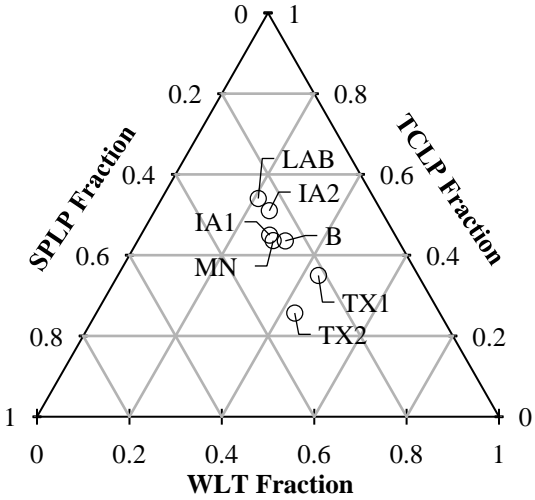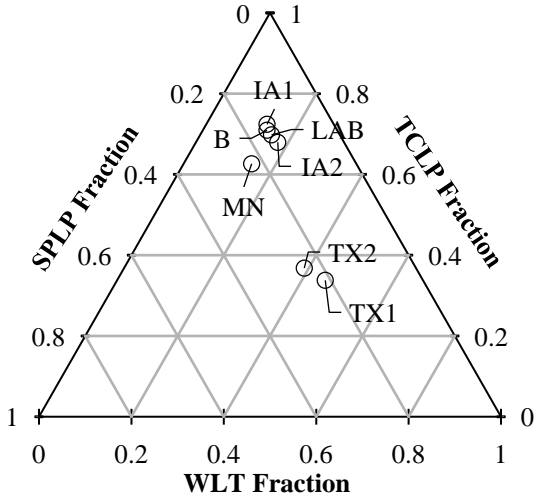
Figure 5.8 Method comparisons of leached concentrations of (a) Ca, (b) Mg, (c) alkalinity, (d) Ba, (e) Cr, and (f) SO₄
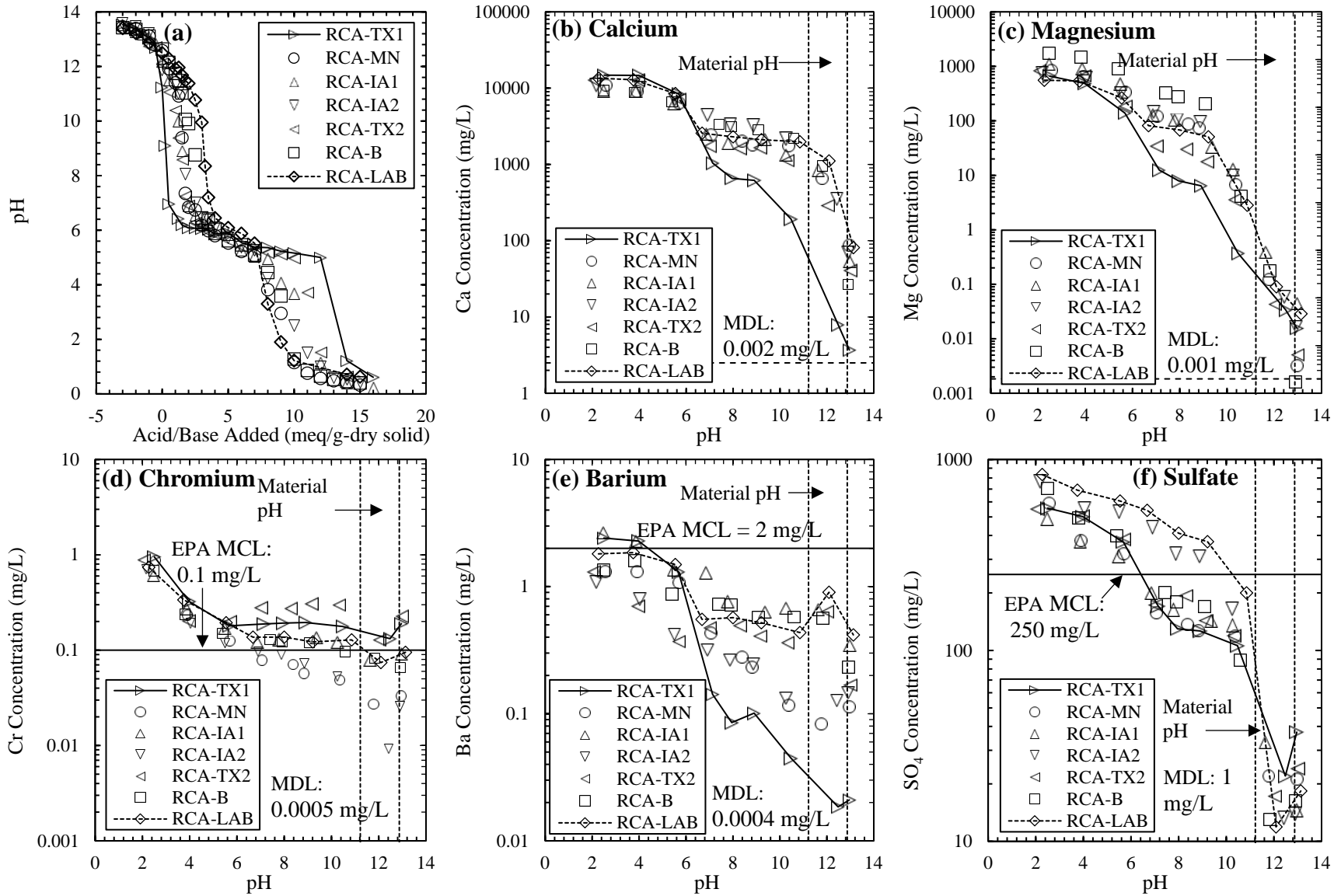
Figure 5.9 (a) Acid neutralization capacity, pH dependent leaching of (b) Ca, (c) Mg, (d) Ba, (e) Cr, and (f) SO₄
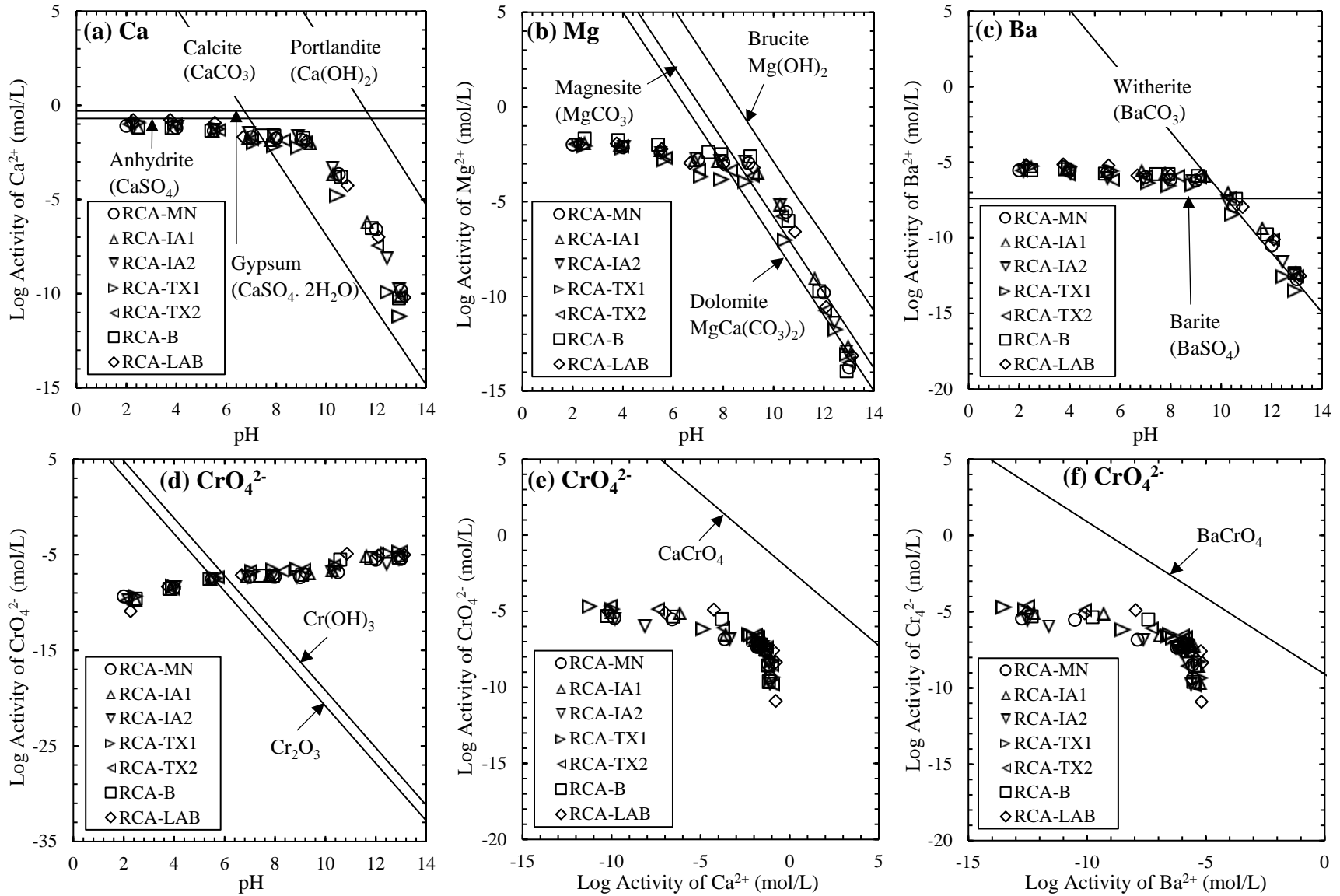
Figure 5.10 Log activity of (a) Ca, (b) Mg, (c) Ba, (d) Cr, (e) Cr vs Ca, and (f) Cr vs Ba
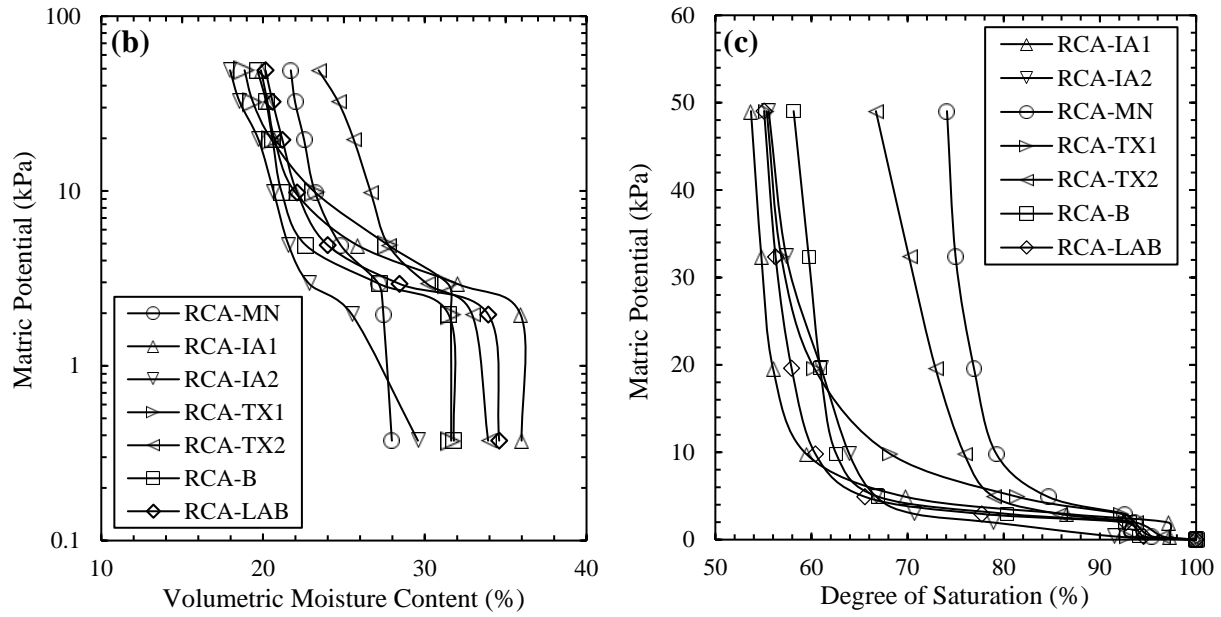
Figure 5.11   (a) Water retention characteristics, and (c) degree of saturation vs matric potential
relationship
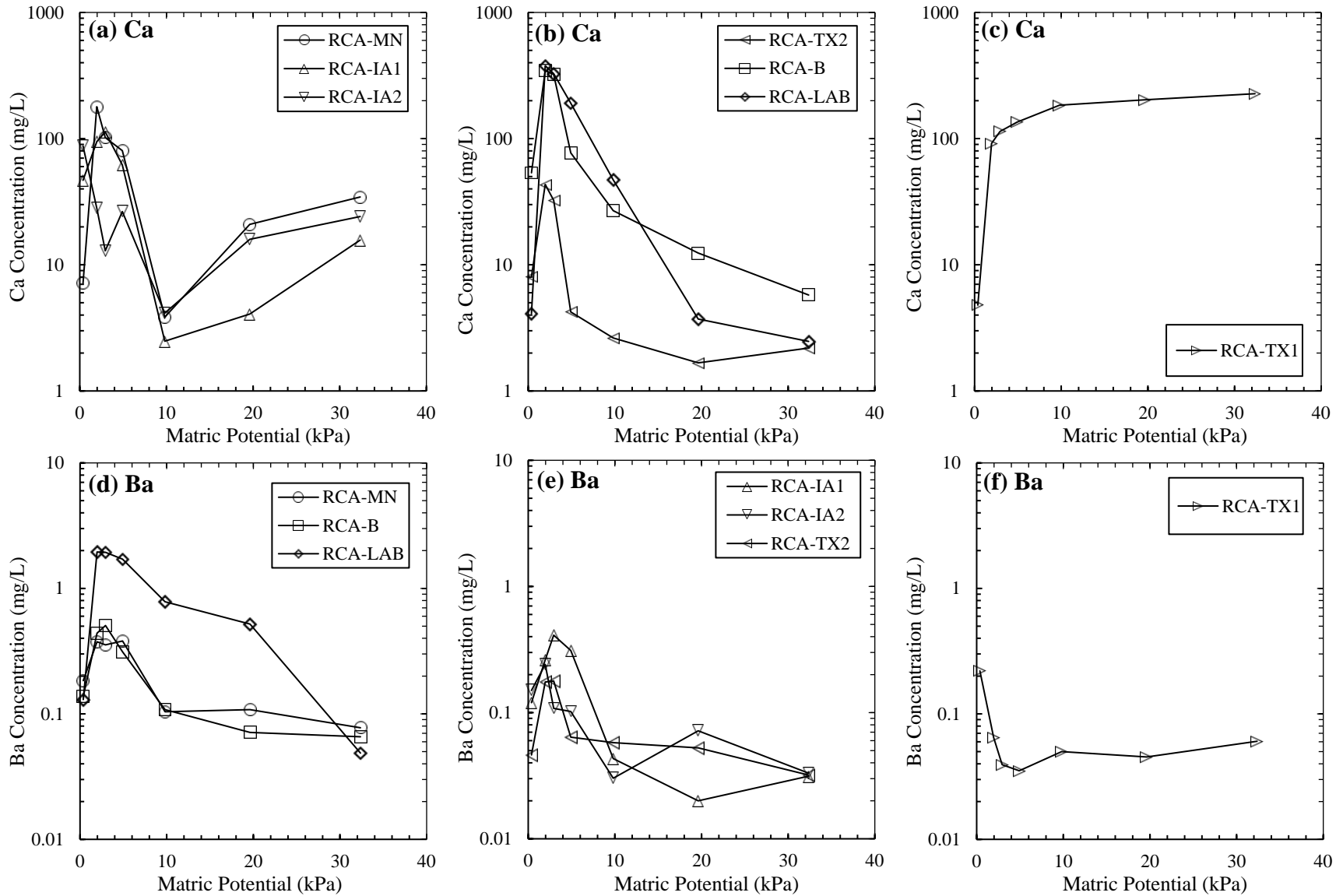
Figure 5.12 Effect of metric potential on the leaching behavior of Ca and Ba from the RCA used in this study
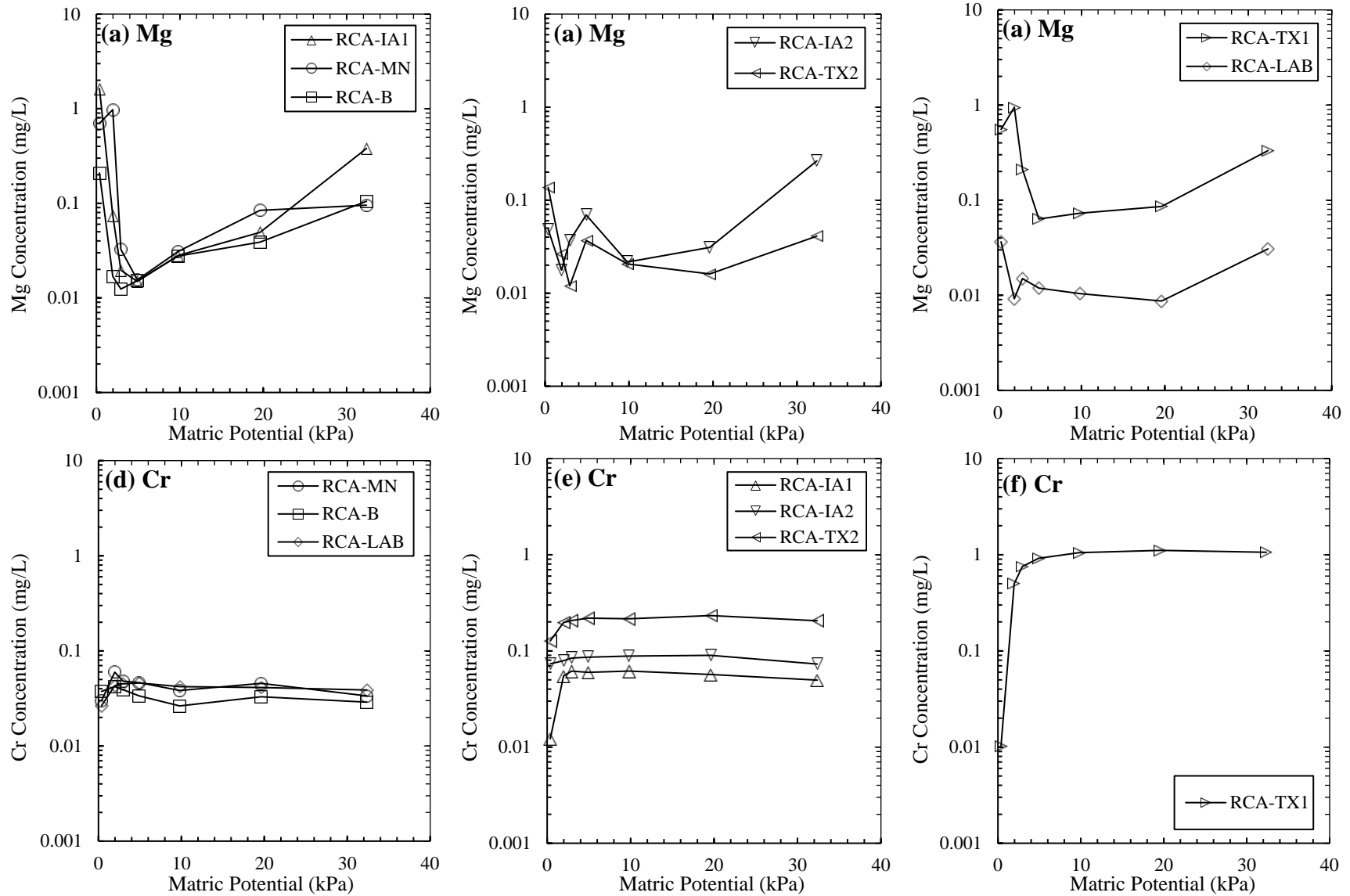
Figure 5.13 Effect of metric potential on the leaching behavior of Mg and Cr a from the RCA used in this study

CHAPTER 6. CONCLUSIONS AND RECOMMENDATIONS

The main objective of this study is to investigate the leaching behavior of elements from recycled materials that are commonly used in pavement constructions. As part of the research endeavor, leaching characteristics of cement activated fly ash and slag treated pavement subgrade soils, and soil, fly ashes, cement and slag alone were investigated. In addition, laboratory evaluation of the leaching behavior of elements from recycled concrete aggregate (RCA) were performed. Leaching controlling mechanisms of the elements from fly ash/slag-cement treated soils and RCAs were assessed by using geochemical modeling program Visual MINTEQA2. Preceding chapters provided specific conclusions and key findings from each research work. The more generalized conclusions and recommendations are provided in this chapter as follows:

6.1 Leaching Characteristics of Cement Activated Fly Ash and Slag Treated Soils

- Effluent pH and electrical conductivity (EC) initially increased with the addition of fly and slag content. However, the influence of fly ash and slag at higher addition rates were less pronounced. The addition of cement was found to be the most dominating factor controlling the pH and EC of the effluent.

- Addition of cement had diverse influences on the leaching characteristics of soil-fly ash and soil-slag system. The effluent concentrations of Ca, Ba, Al, SO_4 increased, Mg, Cu and dissolved inorganic carbon (DIC) concentrations decreased, Fe, Zn and dissolved organic carbon (DOC) fluctuated, Cr and Mn concentrations remained almost unaffected with the addition of cement.

- Cr, Cu and SO_4 concentrations were the highest in TCLP, intermediate in WLT and the lowest in SPLP effluents. The highest concentrations of Fe were observed in

WLT and were the lowest in TCLP leachates. Therefore, it was concluded that, multiple batch leach test methods were required for a comprehensive leaching assessment of cement activated fly ash and slag treated soils.

- Acid/base neutralizing capacity test showed an indication of the hydration products and minerals of soil, fly ashes, slag, cement and their mixtures, along with a basis for qualitative comparisons. Besides, ANCs revealed that the fly ashes and slag used in this study can produce pozzolanic reactions.

- Ca, Mg, Fe, Mn and SO_4 followed cationic leaching patterns, where concentrations decreased with the increase in solution pH. Al, Cu and Zn followed amphoteric patterns with minimum concentrations at neutral/near neutral pH values and higher concentrations at acidic and alkaline conditions.

- Cr showed oxyanionic leaching behavior with a concentration plateau in the pH range of 5.5-10, which was followed by subsequent decrease and increase in concentrations at pH of 11.5 and 13, respectively. Cement activation caused highly alkaline pH of soil-fly ash and soil-slag mixtures which resulted Cr^{6+} oxidation state of Cr.

- The leaching of Ba followed both cationic and amphoteric patterns depending on material and mixture types. Soil, fly ashes and their mixtures showed amphoteric leaching patterns, whereas cement, slag and slag mixtures showed cationic leaching of Ba. Effluent Ca concentrations were found to be a controlling factor for the leaching of Ba.

- The DIC concentrations were maximum at neutral and/or near neutral pH conditions. In contrast, the maximum concentrations of DOC were associated with highly acidic and alkaline pH values.

- Geochemical modeling indicated that, except for Cr, the releases of elements from cement activated fly ash and slag stabilized soils were controlled by solubility. The leaching mechanism of Cr could be sorption controlled.

- As an overall conclusion, elemental concentrations of soil, fly ash, slag and cement, influence of pH, sulfate, dissolved organic and inorganic carbon concentrations should be taken into consideration when cement is used as an activator for fly ash and slag amended soils. Moreover, it is important to identify the oxidation states of redox sensitive elements such as Cr, rather than measuring total leached concentrations.

6.2   Leaching Characteristics of Recycled Concrete Aggregates

- The eluate concentrations of Ca, Ba, Cr and SO_4 and pH, electric conductivity (EC) and alkalinity decreased with an increase in RCA particle sizes. For carbonated RCAs, particles ranging from 1.19 mm to 0.149 mm in sizes resulted higher pH, EC, alkalinity and Ca concentrations whereas particles finer than 0.149 mm resulted higher pH, EC and Ca concentrations when the RCAs were uncarbonated.

- Effluent pH, EC, alkalinity and leached concentrations of Ca, Ba and Cr decreased with an increase in L/S ratios. As the L/S ratio increased, the leaching characteristics of uncarbonated RCAs drifted towards the carbonated ones. This

indicated that L/S ratio could be implemented as a surrogate parameter of time, and, hence may represent RCA degree of carbonation.

- The effluent pH, EC, alkalinity and leached concentrations of Ca and Ba were higher for less carbonated RCAs. In contrast, carbonated RCAs leached higher concentrations of Cr and SO_4.

- The selection of an appropriate leach test for a quick assessment of RCA`s contaminant leaching potential considerably depends on carbonation and constituent of potential concern. Multiple batch leach tests are required for a comprehensive leaching assessment of the RCA.

- Highly carbonated RCAs showed higher pH neutralization capacities at the pH range of 5 to 6 compared to the less carbonated ones. Acid buffering capacity could be used as a possible indicator RCA degree of carbonation.

- Ca, Mg and SO_4 followed cationic leaching patterns, Cr followed oxyanionic leaching. The effect of carbonation was greatly pronounced on the pH dependent release of the elements. Depending on carbonation, the pH dependent leaching of Ba could be cationic or pH independent.

- Geochemical modeling indicated that the leaching of Ca, Mg and Ba from the RCAs were controlled by solubility. Solubility mechanism was ineffective in describing the leaching of Cr. Geochemical modeling suggested that leaching of Cr from the RCAs could be controlled by $BaCrO_4$ and $CaCrO_4$ solid solutions.

- The highest solution pH and leached concentrations of Ca and Ba were found in the matric potential range of 2 kPa to 5 kPa. The leaching of Ca varied with matric potential, whereas Cr showed a stable leaching at different matric potentials.

6.3 Recommendations

Several recommendations for future studies on the leaching characterization of cement activated fly ash and slag treated soils and different construction and demolition (C&D) wastes are provided as follow:

- This research study is based on the laboratory investigations of the leaching characteristics of cement activated fly ash and slag treated soils and RCAs. Field investigations along with the laboratory assessments are recommended for a comprehensive understanding of the leaching behavior of these materials.

- Column leach test and a quantitative comparison of the leaching behavior of RCA at different saturation condition is recommended. The in-situ and laboratory lysimeter tests instrumented with matric potential sensors are recommended to investigate the leaching characteristics at different saturation conditions and matric potentials.

- The impact on curing time on the leaching behavior of elements could be investigated. An investigation on the effects of curing on the leaching characteristics of RCA at different matric suctions is recommended.

- A groundwater transport modeling is recommended to investigate the constituents' concentrations in soil vadose zone, and groundwater as a function of time and space. For this purpose, different numerical modeling programs could be employed using the results reported in this study.

REFERENCES

ACAA, 2018. Coal combustion products production & use statistics. Farmington Hills, MI.

Bestgen, J.O., Cetin, B., Tanyu, B.F., 2016a. Effects of extraction methods and factors on leaching of metals from recycled concrete aggregates. Environ. Sci. Pollut. Res. 23, 12983–13002. https://doi.org/10.1007/s11356-016-6456-0

Bestgen, J.O., Hatipoglu, M., Cetin, B., Aydilek, A.H., 2016b. Mechanical and environmental suitability of recycled concrete aggregate as a highway base material. J. Mater. Civ. Eng. 28, 04016067. https://doi.org/10.1061/(ASCE)MT.1943-5533.0001564

Bin-Shafique, S., Benson, C.H., Edil, T.B., Hwang, K., 2006. Leachate concentrations from water leach and column leach tests on fly ash-stabilized soils. Environ. Eng. Sci. 23, 53–67. https://doi.org/10.1089/ees.2006.23.53

Cappuyns, V., Alian, V., Vassilieva, E., Swennen, R., 2014. pH dependent leaching behavior of Zn, Cd, Pb, Cu and As from mining wastes and slags: Kinetics and mineralogical control. Waste and Biomass Valorization 5, 355–368. https://doi.org/10.1007/s12649-013-9274-3

Cetin, B., Aydilek, A.H., 2013. pH and fly ash type effect on trace metal leaching from embankment soils. Resour. Conserv. Recycl. 80, 107–117. https://doi.org/10.1016/J.RESCONREC.2013.09.006

Cetin, B., Aydilek, A.H., Guney, Y., 2010. Stabilization of recycled base materials with high carbon fly ash. Resour. Conserv. Recycl. 54, 878–892. https://doi.org/10.1016/J.RESCONREC.2010.01.007

Cetin, B., Aydilek, A.H., Li, L., 2013. Leaching behavior of aluminum, arsenic, and chromium from highway structural fills amended with high-carbon fly ash. Transp. Res. Rec. J. Transp. Res. Board 2349, 72–80. https://doi.org/10.3141/2349-09

Chen, J., Bradshaw, S., Benson, C.H., Tinjum, J.M., Edil, T.B., 2012. pH-dependent leaching of trace elements from recycled concrete aggregate, in: GeoCongress 2012. American Society of Civil Engineers, Reston, VA, pp. 3729–3738. https://doi.org/10.1061/9780784412121.382

Chen, Q., Zhang, L., Ke, Y., Hills, C., Kang, Y., 2009. Influence of carbonation on the acid neutralization capacity of cements and cement-solidified/stabilized electroplating sludge. Chemosphere 74, 758–764. https://doi.org/10.1016/J.CHEMOSPHERE.2008.10.044

Dayioglu, A.Y., Aydilek, A.H., Cimen, O., Cimen, M., 2018. Trace metal leaching from steel slag used in structural fills. J. Geotech. Geoenvironmental Eng. 144, 04018089. https://doi.org/10.1061/(ASCE)GT.1943-5606.0001980

Engelsen, C.J., van der Sloot, H.A., Wibetoe, G., Justnes, H., Lund, W., Stoltenberg-Hansson, E., 2010. Leaching characterisation and geochemical modelling of minor and trace elements released from recycled concrete aggregates. Cem. Concr. Res. 40, 1639–1649. https://doi.org/10.1016/J.CEMCONRES.2010.08.001

Engelsen, C.J., van der Sloot, H.A., Wibetoe, G., Petkovic, G., Stoltenberg-Hansson, E., Lund, W., 2009. Release of major elements from recycled concrete aggregates and geochemical modelling. Cem. Concr. Res. 39, 446–459. https://doi.org/10.1016/J.CEMCONRES.2009.02.001

Engelsen, C.J., Wibetoe, G., van der Sloot, H.A., Lund, W., Petkovic, G., 2012. Field site leaching from recycled concrete aggregates applied as sub-base material in road construction. Sci. Total Environ. 427–428, 86–97. https://doi.org/10.1016/J.SCITOTENV.2012.04.021

Engström, F., Adolfsson, D., Samuelsson, C., Sandström, Å., Björkman, B., 2013. A study of the solubility of pure slag minerals. Miner. Eng. 41, 46–52. https://doi.org/10.1016/j.mineng.2012.10.004

Faysal, M., Mahedi, M., Aramoon, A., Thian, B., Hossain, M.S., Khan, M.S., 2016. Strength Characterization of Untreated and Cement-Treated Recycled Flex-Base Materials, in: Geotechnical and Structural Engineering Congress 2016 - Proceedings of the Joint Geotechnical and Structural Engineering Congress 2016.

Gomes, J.F.P., Pinto, C.G., 2006. Leaching of heavy metals from steelmaking slags. Rev. Metal. 42, 409–416. https://doi.org/10.3989/revmetalm.2006.v42.i6.39

Jones, D.R., 1995. The Leaching of major and trace elements from coal ash, in: Environmental Aspects of Trace Elements in Coal. Springer, Dordrecht, Netherlands, pp. 221–262. https://doi.org/10.1007/978-94-015-8496-8_12

Kogbara, R.B., Al-Tabbaa, A., 2011. Mechanical and leaching behaviour of slag-cement and lime-activated slag stabilised/solidified contaminated soil. Sci. Total Environ. 409, 2325–2335. https://doi.org/10.1016/J.SCITOTENV.2011.02.037

Kogbara, R.B., Al-Tabbaa, A., Yi, Y., Stegemann, J.A., 2013. Cement–fly ash stabilisation/solidification of contaminated soil: Performance properties and initiation of operating envelopes. Appl. Geochemistry 33, 64–75. https://doi.org/10.1016/J.APGEOCHEM.2013.02.001

Komonweeraket, K., Cetin, B., Aydilek, A., Benson, C.H., Edil, T.B., 2015a. Geochemical analysis of leached elements from fly ash stabilized soils. J. Geotech. Geoenvironmental Eng. 141, 04015012. https://doi.org/10.1061/(ASCE)GT.1943-5606.0001288

Komonweeraket, K., Cetin, B., Aydilek, A.H., Benson, C.H., Edil, T.B., 2015b. Effects of pH on the leaching mechanisms of elements from fly ash mixed soils. Fuel 140, 788–802. https://doi.org/10.1016/J.FUEL.2014.09.068

Komonweeraket, K., Cetin, B., Benson, C.H., Aydilek, A.H., Edil, T.B., 2015c. Leaching characteristics of toxic constituents from coal fly ash mixed soils under the influence of pH. Waste Manag. 38, 174–184. https://doi.org/10.1016/J.WASMAN.2014.11.018

Mahedi, M., Cetin, B., White, D.J., 2018. Performance evaluation of cement and slag stabilized expansive soils. Transp. Res. Rec. J. Transp. Res. Board 036119811875743. https://doi.org/10.1177/0361198118757439

Shi, C., 2004. Steel Slag—its production, processing, characteristics, and cementitious properties. J. Mater. Civ. Eng. 16, 230–236. https://doi.org/10.1061/(ASCE)0899-1561(2004)16:3(230)

Thomas, M., 2007. Optimizing the use of fly ash in concrete. Skokie, Ill. Portl. Cem. Assoc. 24. https://doi.org/10.15680/IJIRSET.2015.0409047

U.S. Geological Survey, 2018. Mineral commodity summaries 2018: U.S. Geological Survey. Washington, DC. https://doi.org/https://doi.org/10.3133/ 70194932

Wen, H., Baugh, J., Edil, T., Wang, J., 2011. Cementitious high-carbon fly ash used to stabilize recycled pavement materials as base course. Transp. Res. Rec. J. Transp. Res. Board 2204, 110–113. https://doi.org/10.3141/2204-14

Windt, L. De, Chaurand, P., Rose, J., 2011. Kinetics of steel slag leaching: Batch tests and modeling. Waste Manag. 31, 225–235. https://doi.org/10.1016/J.WASMAN.2010.05.018

Zhang, Y., Cetin, B., Likos, W.J., Edil, T.B., 2016. Impacts of pH on leaching potential of elements from MSW incineration fly ash. Fuel 184, 815–825. https://doi.org/10.1016/J.FUEL.2016.07.089

APPENDIX A.   CEMENT ACTIVATED FLY ASH, SLAG TREATED SOILS
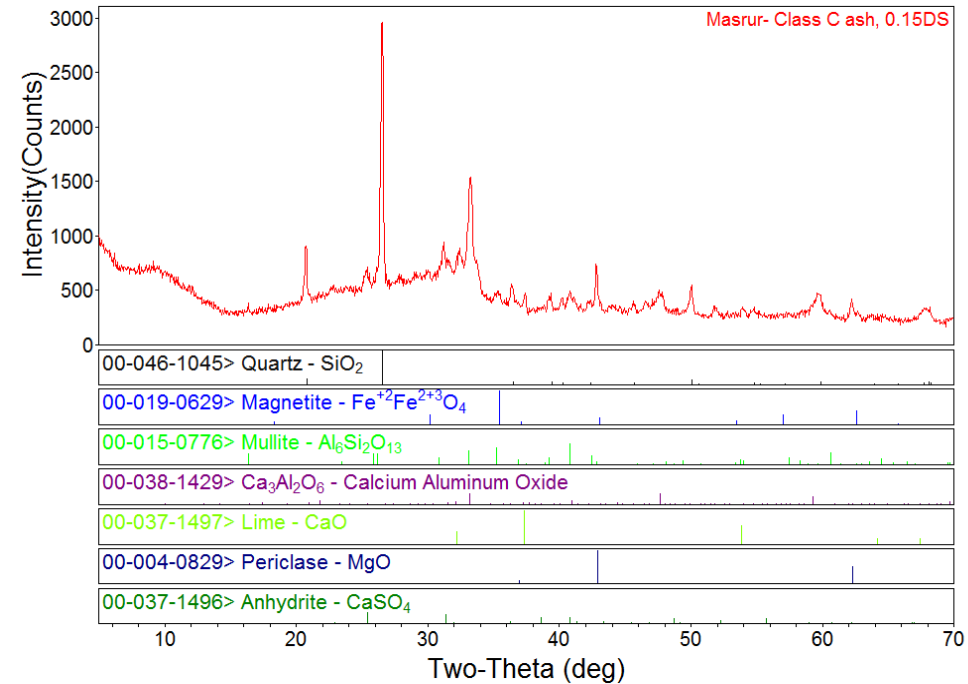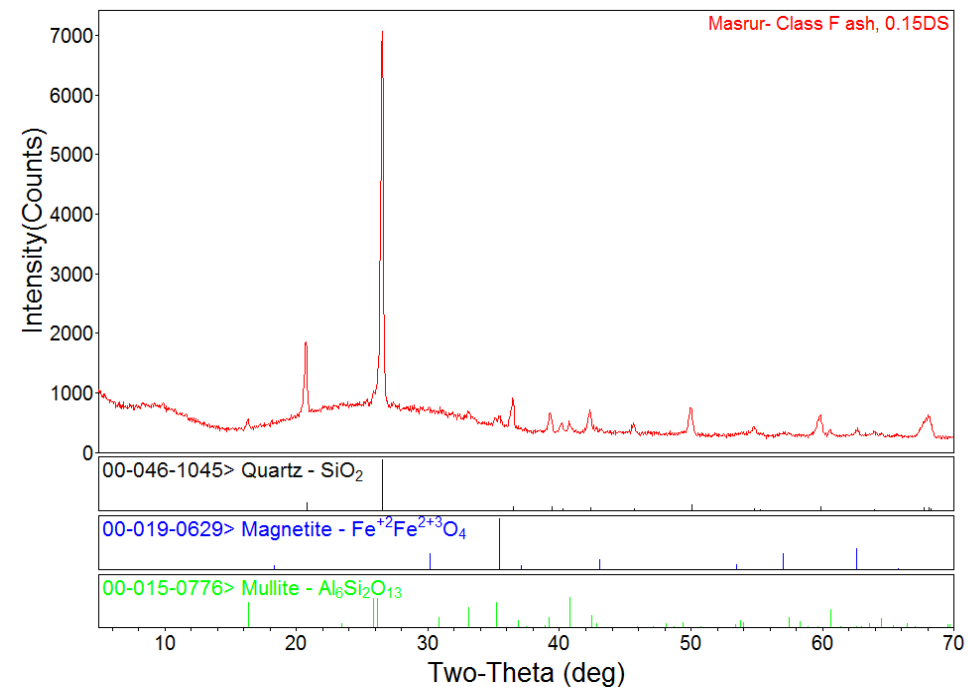
Figure A.1 XRD analyses of Class C and F fly ash
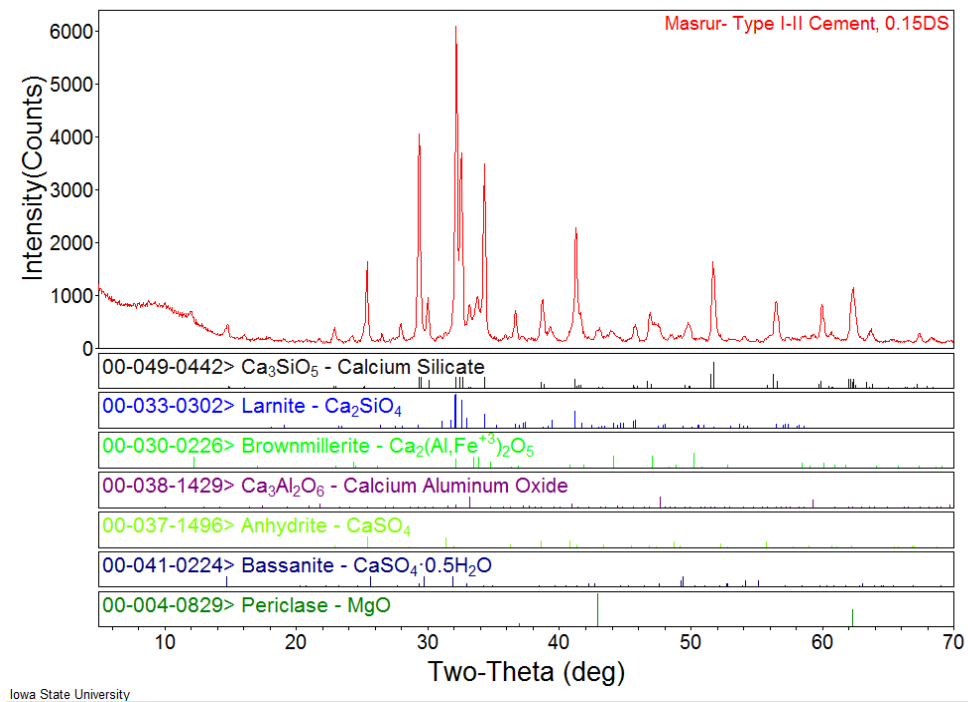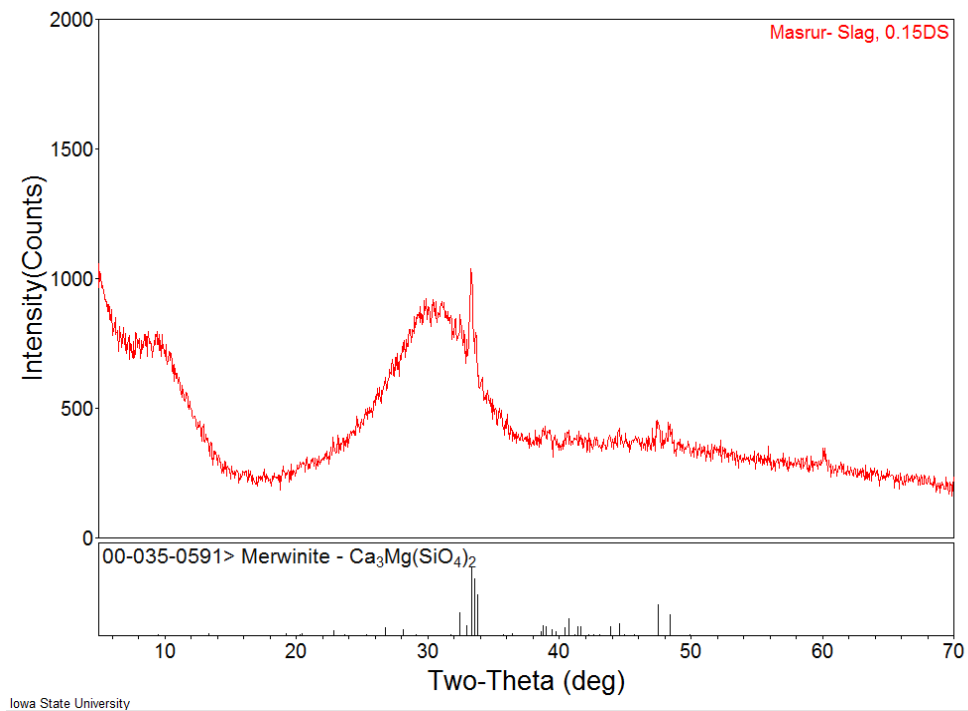
Figure A.2   XRD analyses of slag and cement
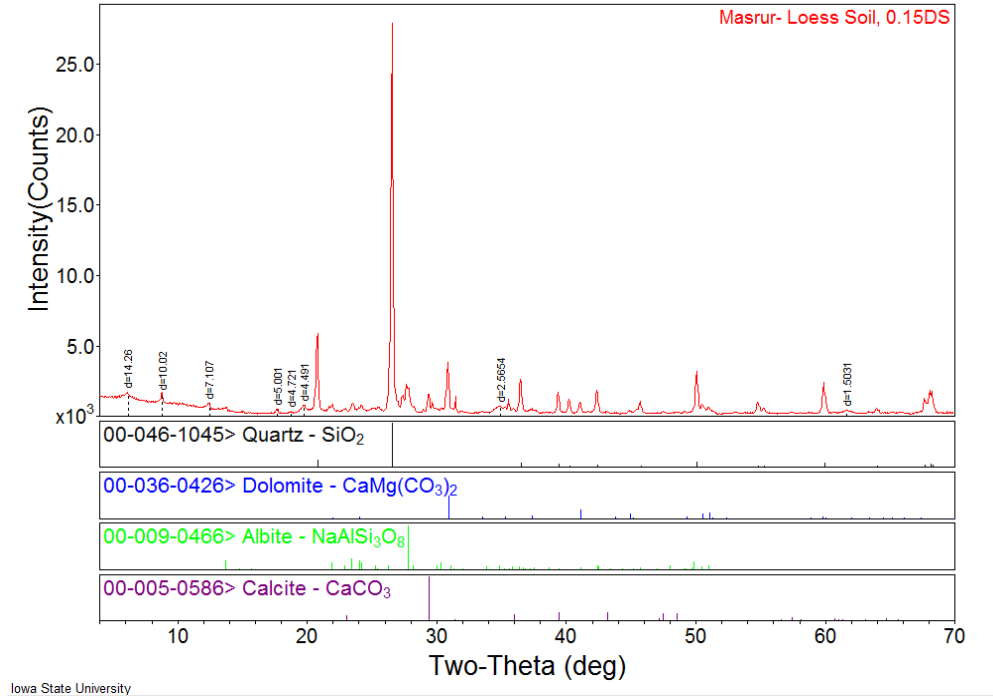
Figure A.3   XRD analyses of Iowa loess soil
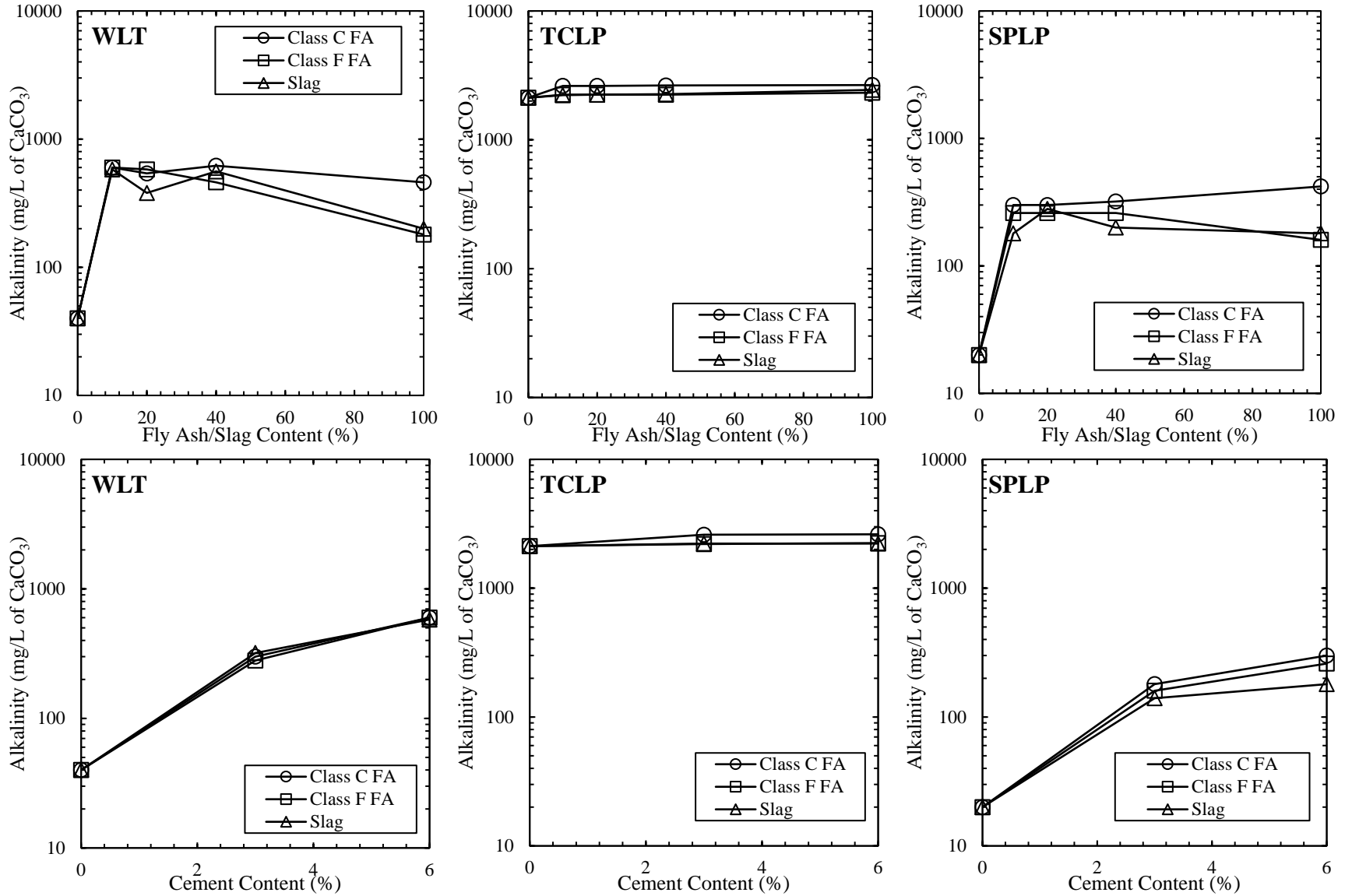
Figure A.4   Change in Alkalinity with FA, slag, cement content in WLT, TCLP and SPLP test
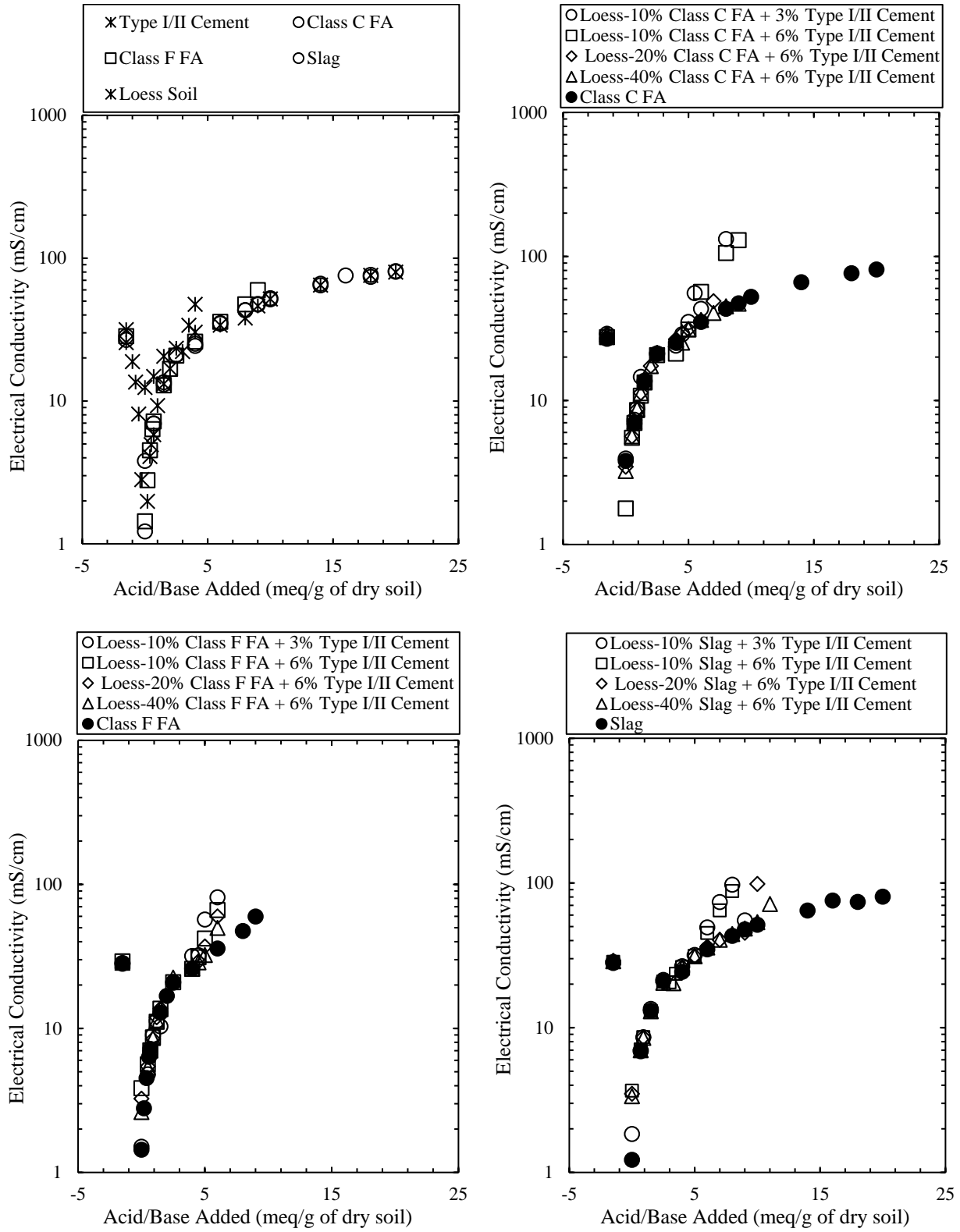
Figure A.5   Change in electrical conductivity with acid/base addition

APPENDIX B.   RECYCLED CONCRETE AGGREGATES (RCA)

B.1   X-Ray Diffraction Analyses (XRD)
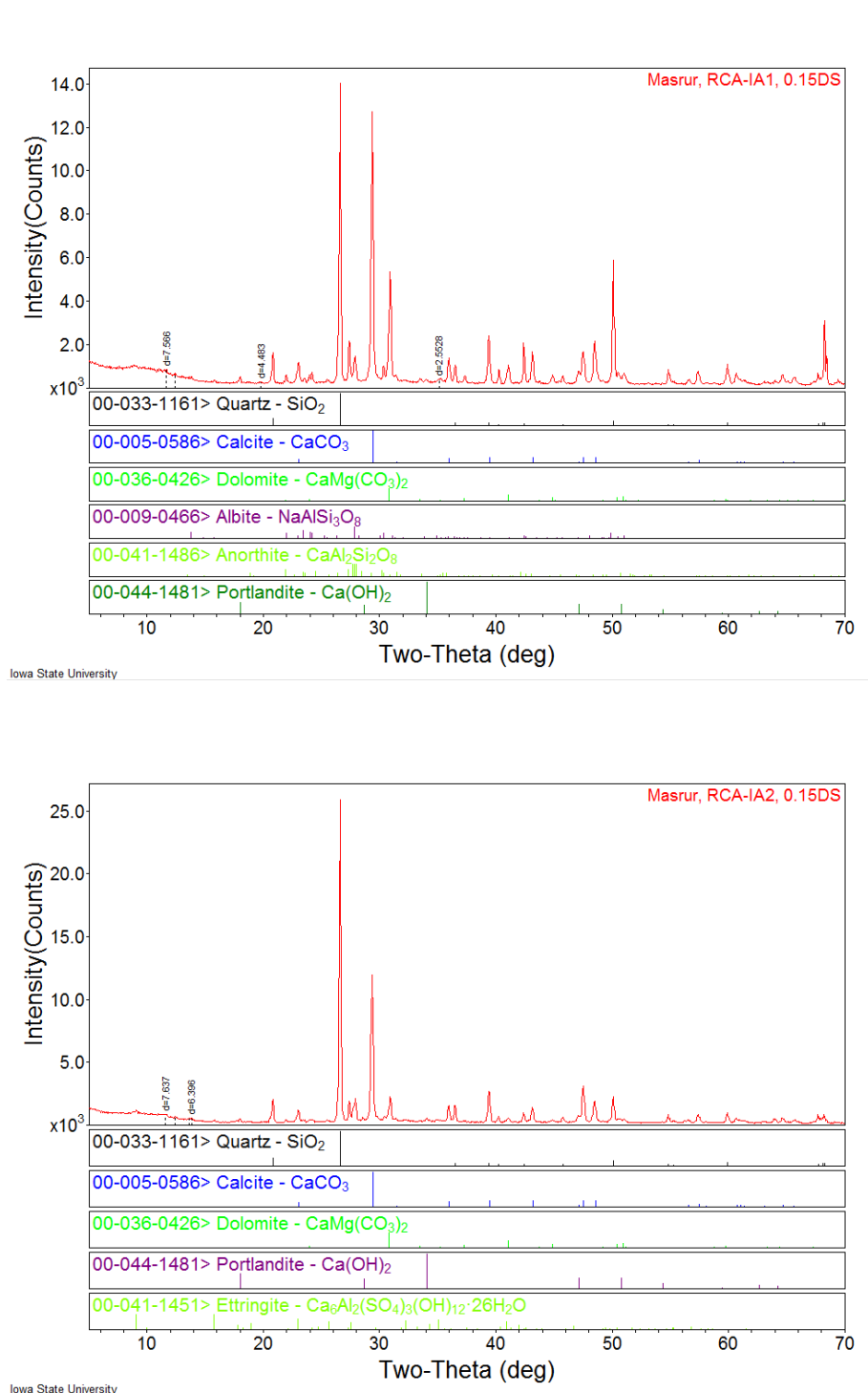
Figure B.1   XRD analyses of RCA-IA1 and RCA-IA2
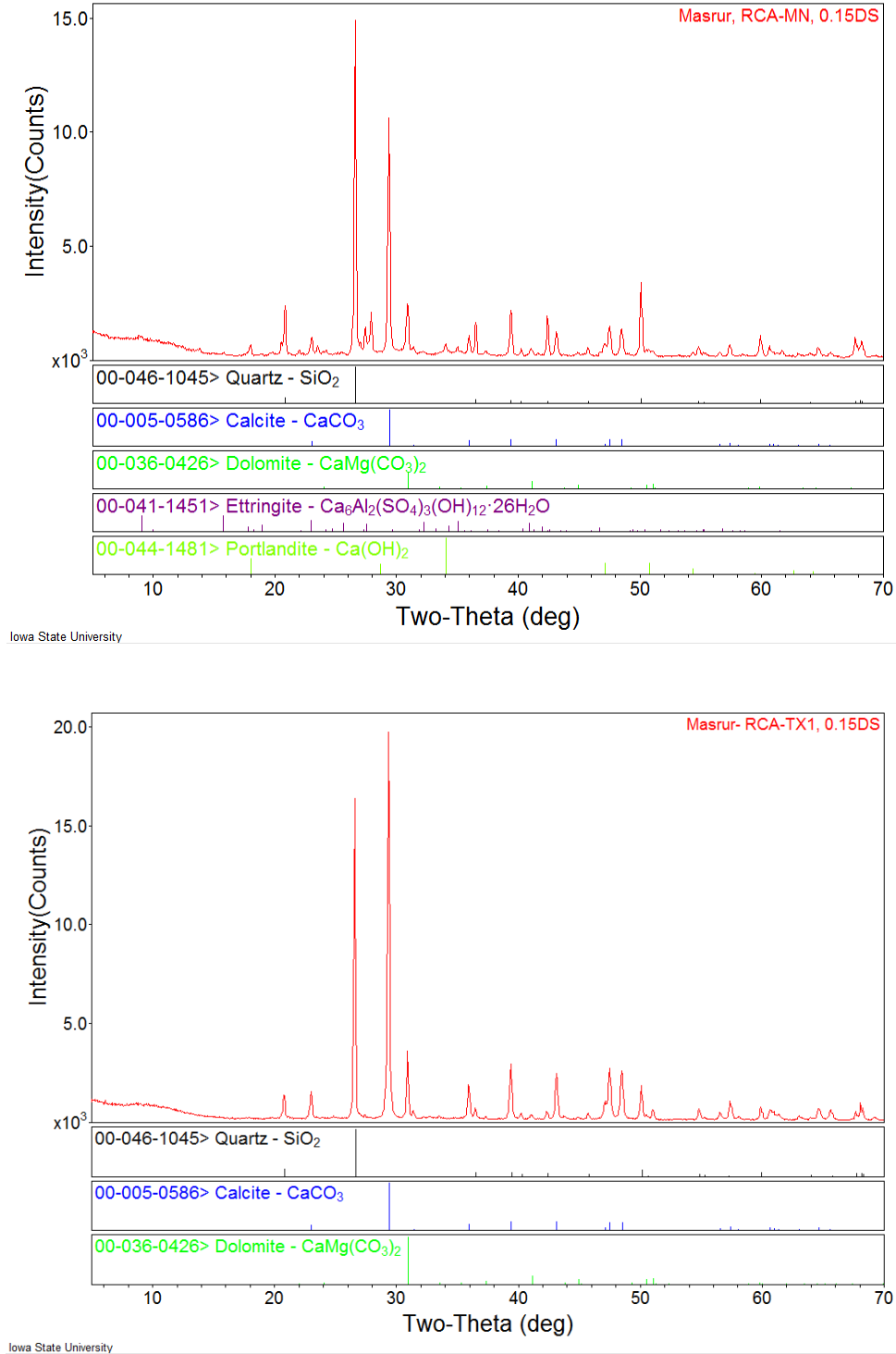
Figure B.2   XRD analyses of RCA-MN and RCA-TX1
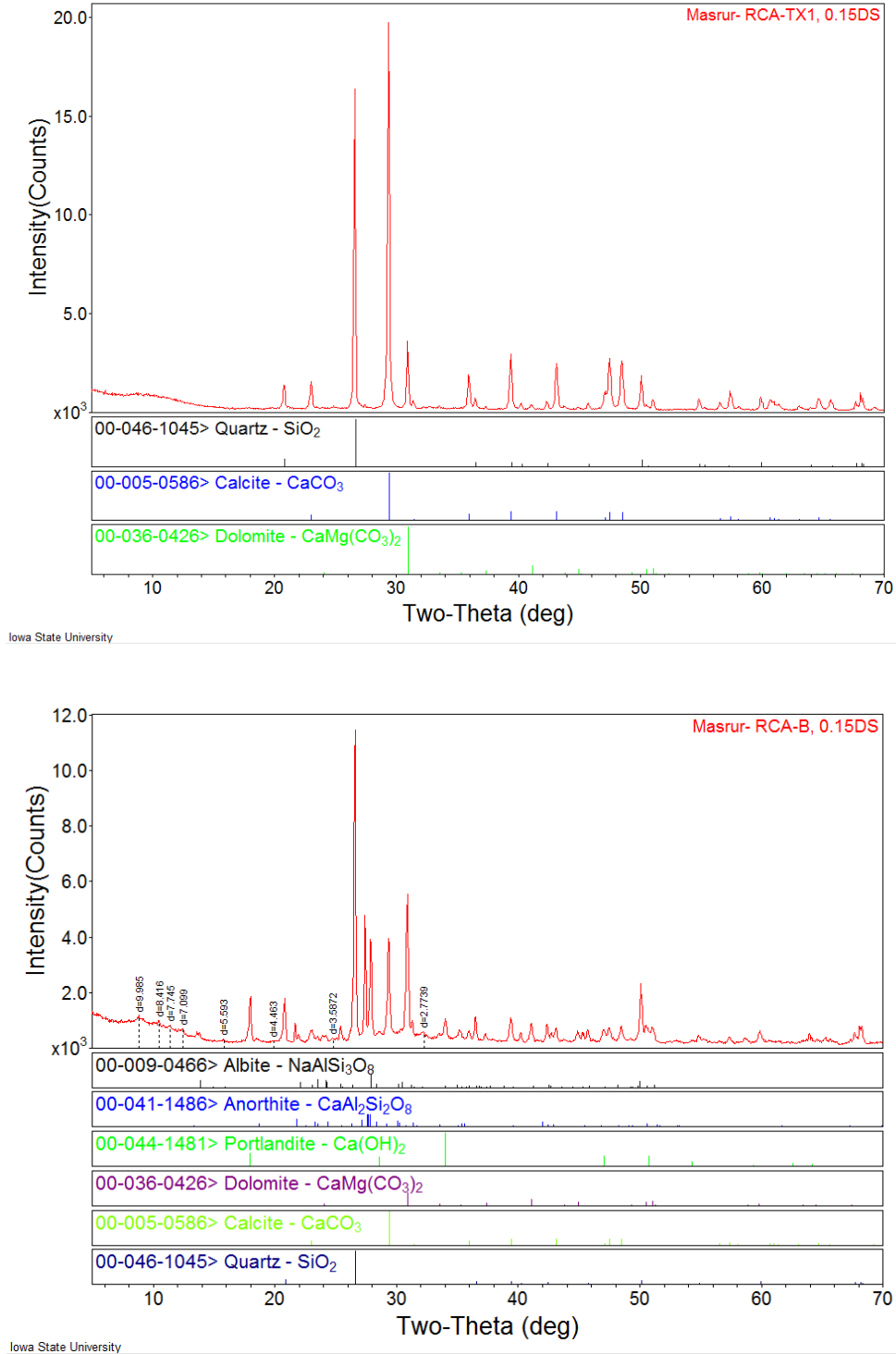
Figure B.3 XRD analyses of RCA-TX2 and RCA-B
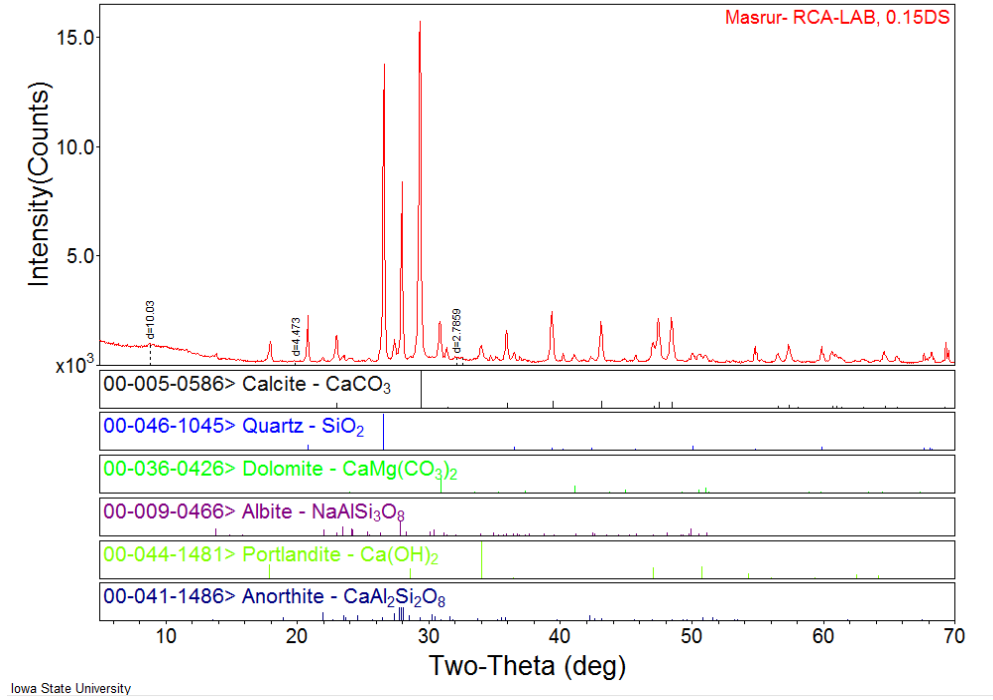
Figure B.4 XRD analyses of RCA-B

B.2 Leaching of Trace Elements from RCA

Table B.1 Physical and chemical properties of the recycled concrete aggregates (RCA) used in this study

Physical Properties	RCA-MN	RCA-IA1	RCA-IA2	RCA-TX1	RCA-TX2	RCA-B	RCA-LAB
Gravel Content (%)	94.1	48.8	82	93.4	68.8	86.4	94.8
Sand Content (%)	4.9	51.1	17.8	5.8	31.2	12.9	4.8
Fines Content (%)	1	0.03	0.13	0.8	0.02	0.7	0.4
C_u	2.1	7.9	7.6	2.1	32	4.6	2.7
C_c	1.4	0.6	1.8	1.1	3.6	2.4	1.2
θ (%)	2.1	2.2	3.2	1.1	1.7	2.5	1.4
ω_{opt} (%)	12.6	14.8	14.3	10.9	14.4	13.8	13.6
γ_{dmax} (kN/m^3)	18.3	19	18.4	19	19.7	18.2	18.8
USCS Classification	GP	SP	GW	GP	GP	GW	GP
AASHTO Classification	A-1-a	A-1-a	A-1-a	A-1-a	A-1-a	A-1-a	A-1-a
Chemical Properties (%)							
SiO_2	46	37	41.6	30.8	38.1	47.7	34.7
Al_2O_3	5.6	4.4	4.6	1.7	2.3	5.8	4.3
Fe_2O_3	2.2	1.8	1.9	2.3	2.1	3	1.2
CaO	23.9	28.5	28.2	34.9	30.9	22.0	33.4
MgO	4.2	3.3	2.2	1.5	2	4	1.7
SO_3	0.61	0.66	0.7	0.41	0.46	0.58	0.93
K_2O	0.97	0.8	0.79	0.25	0.42	1.11	0.82
Na_2O	0.99	0.94	0.88	0.08	0.08	1.22	0.91
BaO	0.03	0.03	0.04	0.01	0.01	0.04	0.02
SrO	0.04	0.04	0.04	0.08	0.07	0.04	0.04
Mn_2O_3	0.08	0.08	0.09	0.08	0.08	0.15	0.04
LOI	17.1	22.3	18.7	27.7	23.3	14.2	21.8
Total Metal Content (mg/kg)							
Al	5,668	4,629	5,766	5,148	5,634	5,309	5,154
Cu	26.4	23.1	24.3	23.2	22.2	23	23
Fe	10,922	9,482	9,749	12,457	11,303	19,086	6,554
Mn	387	388	449	420	397	650	180
Zn	75.6	53.4	54.3	37.2	81.3	35.6	22.4
S	7,667	8,160	7,829	9,051	7,509	7,246	11,211

Table B.2 pH, electric conductivity, metal concentrations, and total dissolved carbon, dissolved inorganic carbon and dissolved organic carbon concentrations in WLT, TCLP and SPLP effluent

Test Type	RCA Type	pH	EC (mS/cm)	Al (mg/L)	Cu (mg/L)	Fe (mg/L)	Mn (mg/L)	Zn (mg/L)	S (mg/L)	TDC (mg/L)	DIC (mg/L)	DOC (mg/L)
WLT (L/S = 10)	MN	12.05	7.64	1.92	0.267	0.0704	0.0113	0.042	16.9	14.09	6.762	7.326
	IA1	11.84	5.33	1.81	0.255	0.0427	0.0104	0.041	12.2	9.601	2.667	6.934
	IA2	12.02	5.82	1.66	0.229	0.0488	0.0092	0.0192	13.7	7.119	2.984	4.135
	TX1	11.12	2.79	0.694	0.201	0.0289	0.0074	0.0237	27.8	12.54	4.14	8.4
	TX2	12.03	4.29	3.06	0.222	0.0522	0.0081	0.0774	12.3	14.44	5.517	8.927
	B	12.43	8.67	0.667	0.241	0.055	0.0119	0.0463	22.3	13.37	6.461	6.905
	LAB	12.5	10.3	0.577	0.251	0.0461	0.0104	0.0559	23.1	9.367	5.246	4.121
TCLP	MN	11.57	7.65	0.778	0.112	0.0296	0.015	0.054	41.2	1147	2.935	1144
	IA1	11.03	7.38	0.464	0.108	0.0366	0.0109	0.0317	43.2	1147	4.295	1143
	IA2	11.62	7.74	0.989	0.11	0.0297	0.0114	0.0588	40.4	1147	2.761	1144
	TX1	7.12	7.84	0.485	0.113	0.0402	0.0115	0.0309	37.4	1147	123.3	1024
	TX2	10.18	7.26	0.647	0.121	0.0607	0.016	0.0722	33.4	1147	2.741	1144
	B	11.81	7.99	0.786	0.1	0.0176	0.0128	0.0302	32.6	1147	3.472	1144
	LAB	11.92	8.24	0.48	0.111	0.0208	0.011	0.0371	48.6	1147	2.611	1144
SPLP	MN	12.24	4.07	1.96	0.0807	0.0477	0.0097	0.0362	18	6.93	3.54	3.39
	IA1	11.94	1.82	2.41	0.0632	0.0412	0.0081	0.0377	13.7	12.38	2.575	9.804
	IA2	12.09	2.82	2.36	0.0617	0.0558	0.0086	0.0342	12.9	5.075	2.38	2.695
	TX1	10.94	0.34	0.429	0.0371	0.0279	0.007	0.0186	23.6	4.476	2.239	2.237
	TX2	11.69	1.04	2.78	0.055	0.125	0.0082	0.0463	18.7	4.56	2.191	2.37
	B	12.25	4.69	0.846	0.0785	0.0639	0.0099	0.0462	17.2	5.484	3.018	2.465
	LAB	12.33	4.84	0.754	0.0738	0.0584	0.0096	0.0422	18.4	4.228	2.772	1.456

Table B.3 Acid neutralization capacity of the recycle concrete aggregates (RCA)

RCA Type	Acid/base Added*	Target pH								
	Final pH	**2**	**4**	**5.5**	**7**	**8**	**9**	**10.5**	**12**	**13**
RCA-MN	meq/g-dry	9.55	7.86	5	1.92	1.67	1.55	1.32	0.5	-0.79
	Final pH	2.56	3.91	5.70	7.06	8.37	8.83	10.36	11.78	12.96
RCA-IA1	meq/g-dry	11.35	9.21	5.62	2	1.73	1.5	1	0.38	-0.84
	Final pH	2.47	3.86	5.47	6.85	7.78	9.35	10.26	11.63	12.96
RCA-IA2	meq/g-dry	10.5	8.25	5.62	2.5	1.75	1.68	1.55	-0.11	-0.86
	Final pH	2.17	4.03	5.50	6.90	7.88	8.86	10.25	12.42	12.90
RCA-TX1	meq/g-dry	13.59	12.53	6.3	0.5	0.38	0.26	0.09	-0.27	-0.94
	Final pH	2.50	3.98	5.68	7.13	7.95	8.9	10.47	12.48	12.96
RCA-TX2	meq/g-dry	11.79	10.78	5.54	1.94	1.61	1.37	0.92	0.053	-0.94
	Final pH	2.06	3.94	5.69	7.01	8.28	9.14	10.32	12.02	12.98
RCA-B	meq/g-dry	9.69	8.55	6	2.88	2.67	2.4	1.64	0.69	-0.75
	Final pH	2.48	3.81	5.40	7.41	7.92	9.08	10.59	11.82	12.91
RCA-LAB	meq/g-dry	12.63	11.62	7.15	3.46	3.31	3.15	2.66	0.89	-1.37
	Final pH	2.27	3.75	5.54	6.68	8	9.21	10.85	12.09	13.13

227
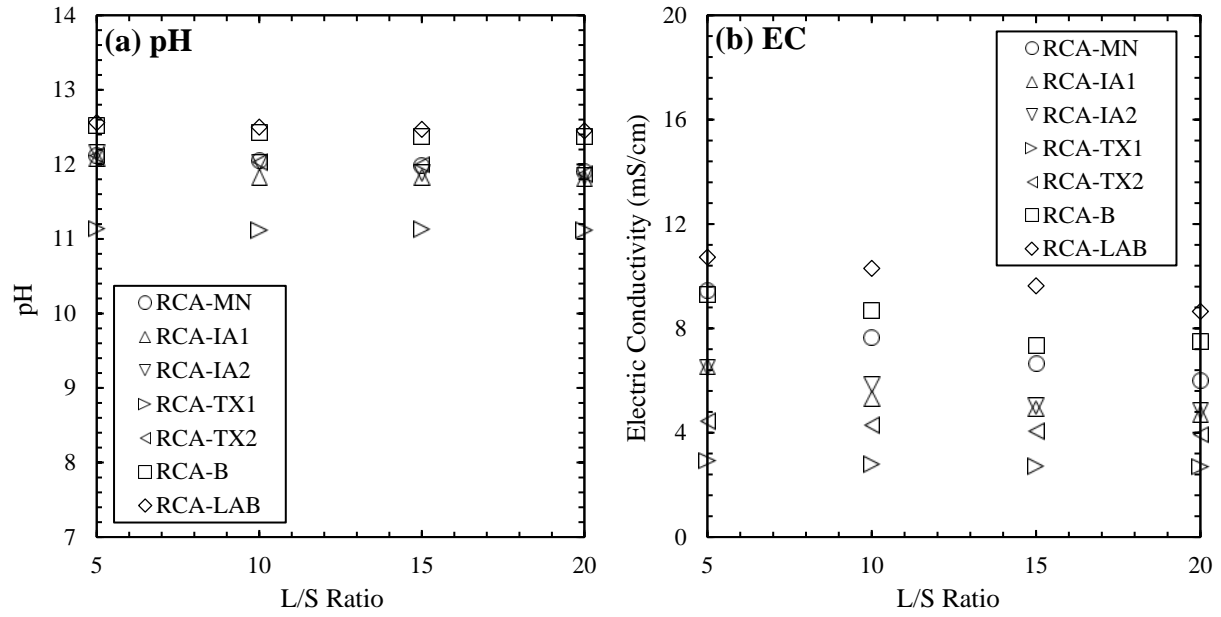
Figure B.5 Change in pH and EC with L/S ratio
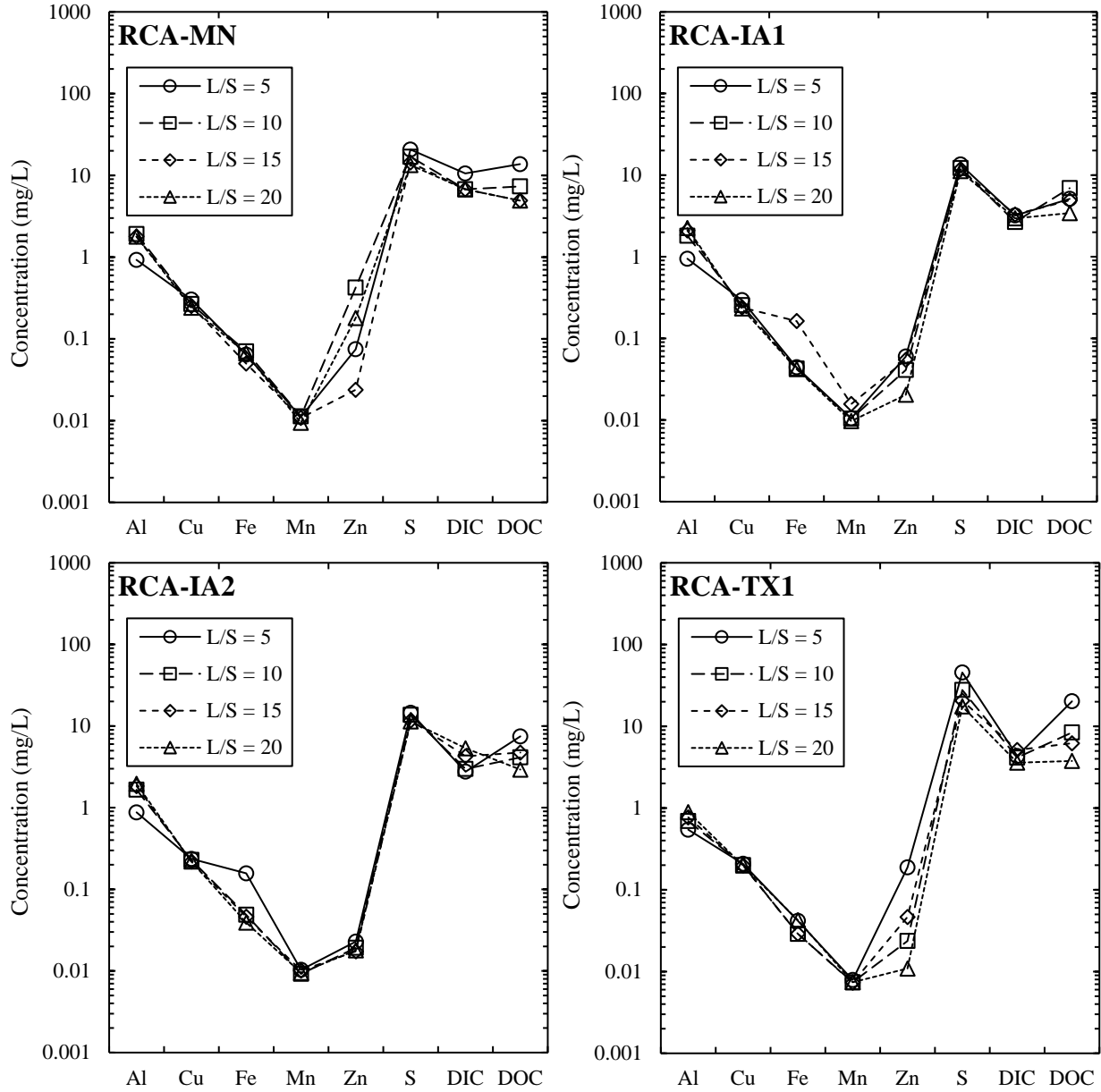
Figure B.6 Schoeller diagram of the leached concentrations at different L/S ratios
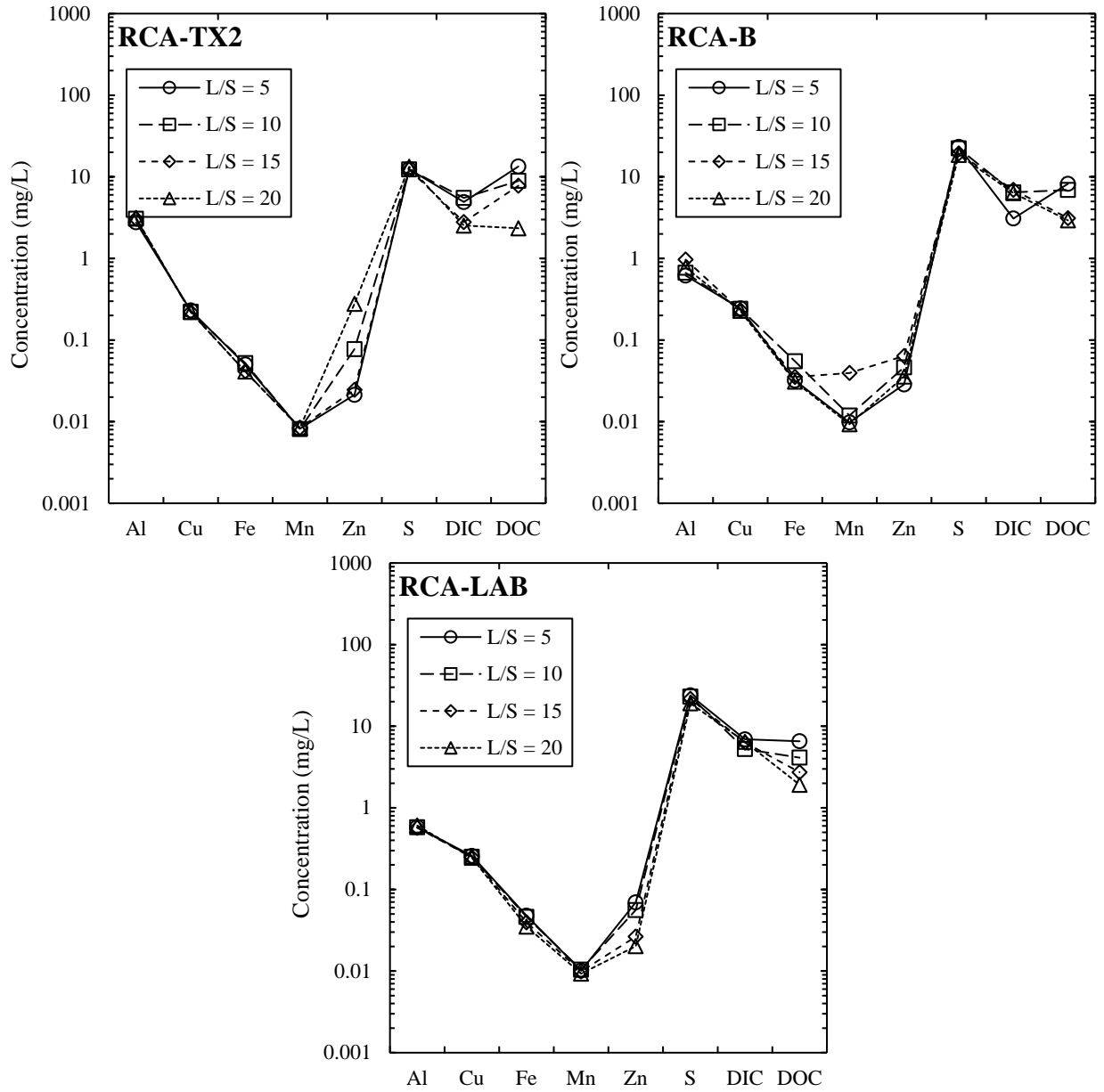
Figure B.6 (Continued). Schoeller diagram of the leached concentrations at different L/S ratios
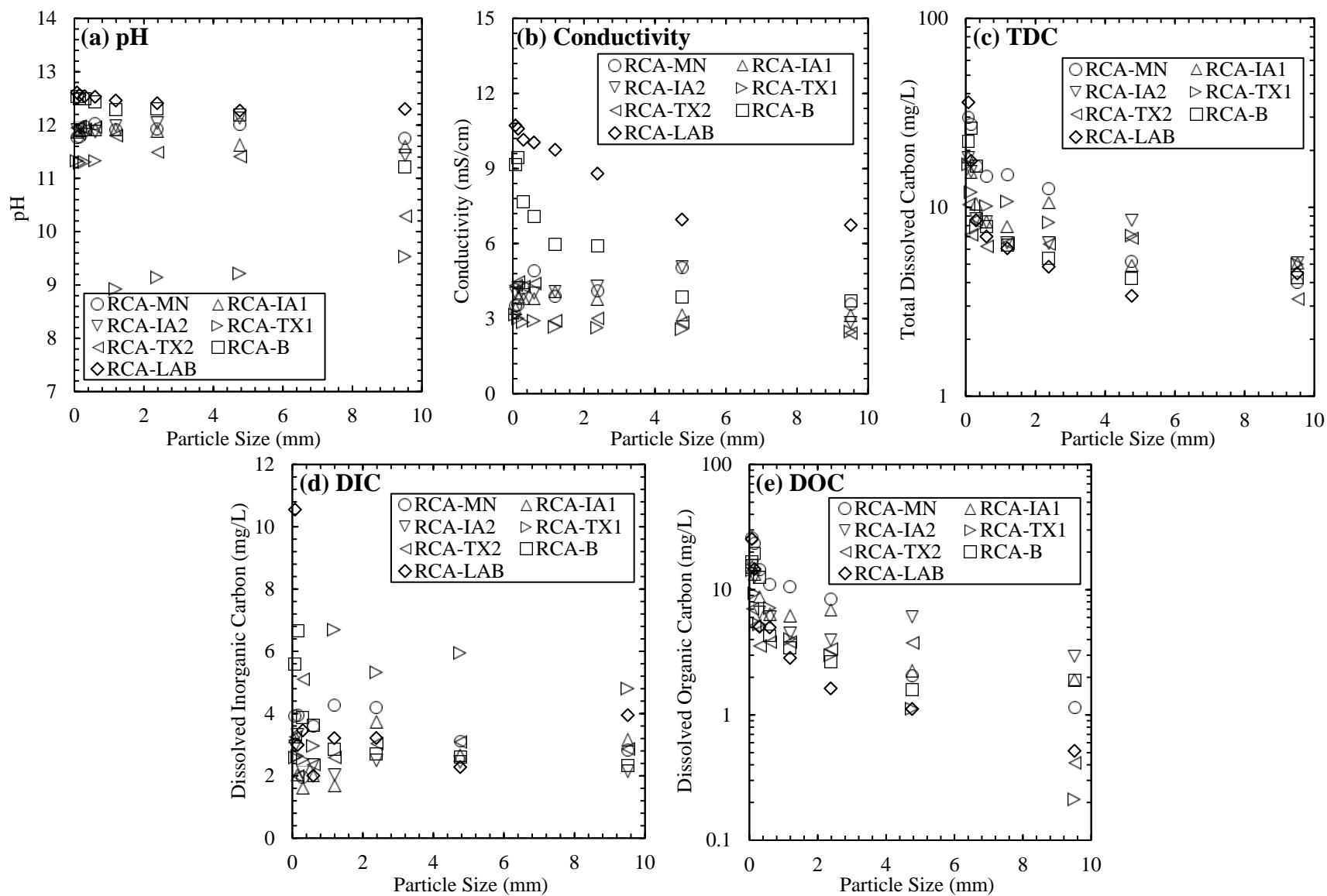
Figure B.7 Effect of particle size on the leaching characteristics of the RCA
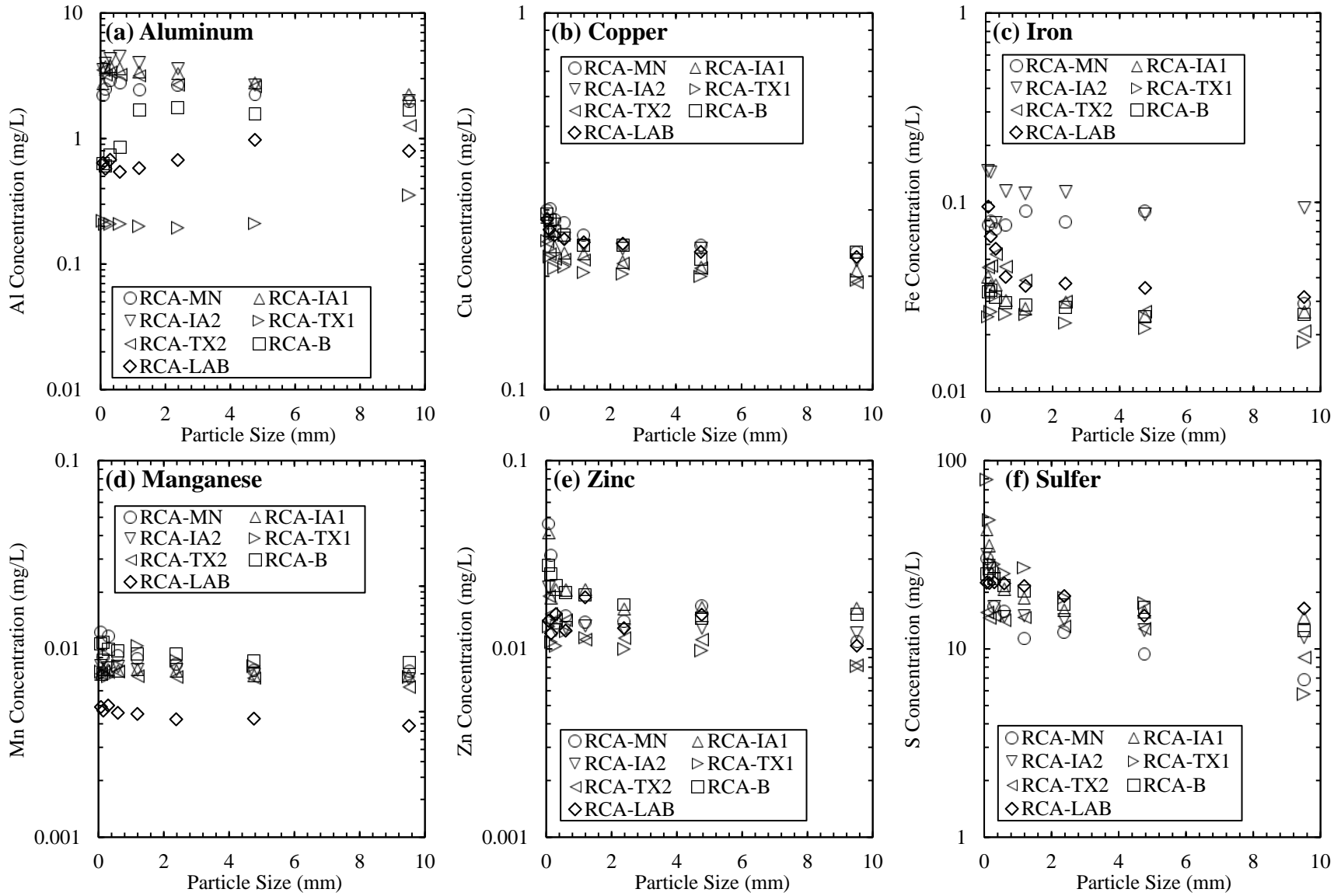
Figure B.8 Leached concentrations of the elements at different particle sizes of RCA
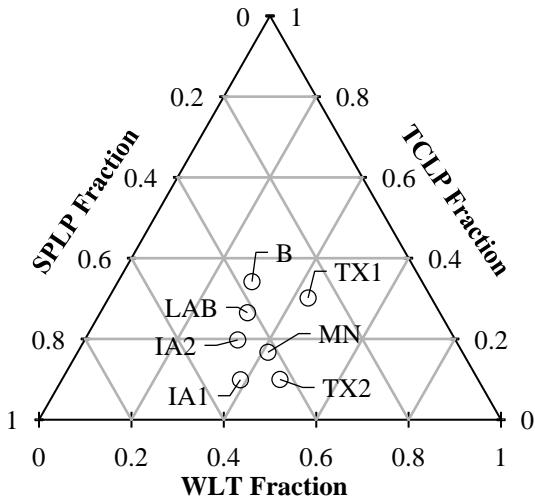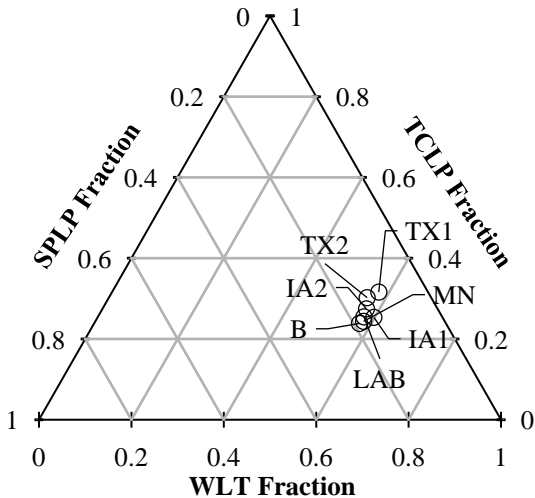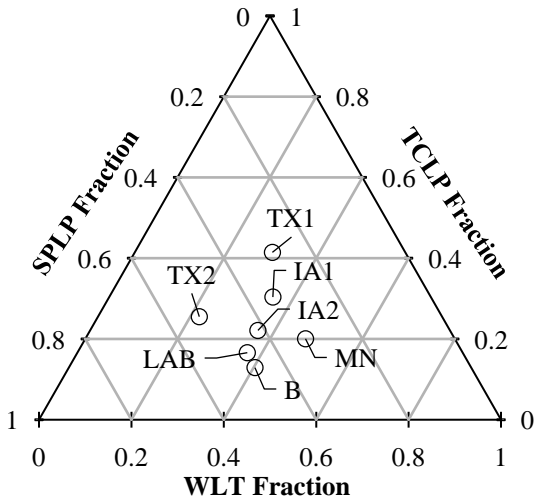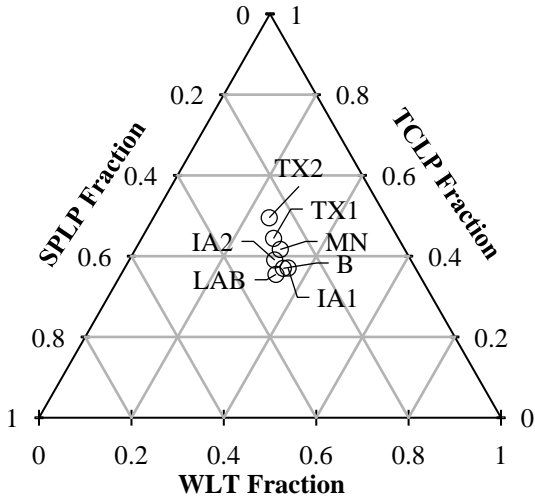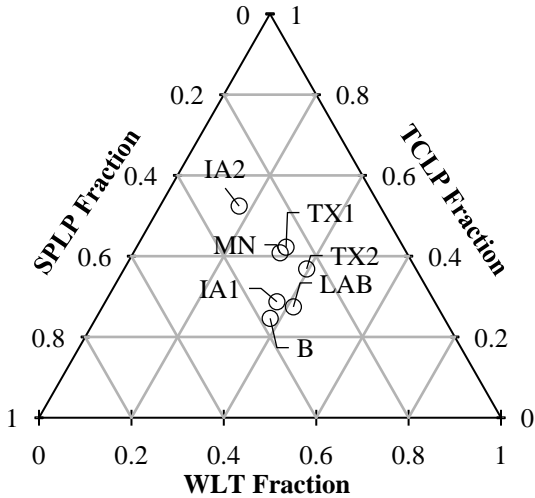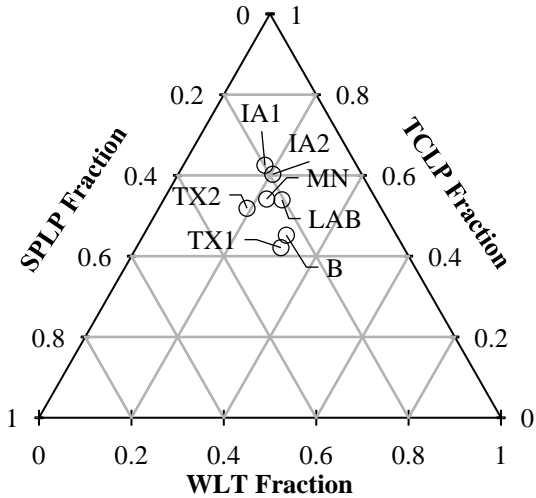
Figure B.9 Ternary diagrams of the leached concentrations of elements in different test methods

(a) TDC

(b) DOC

(c) DIC

234
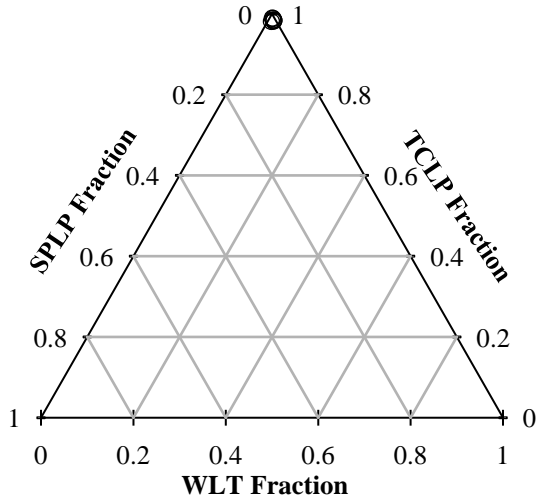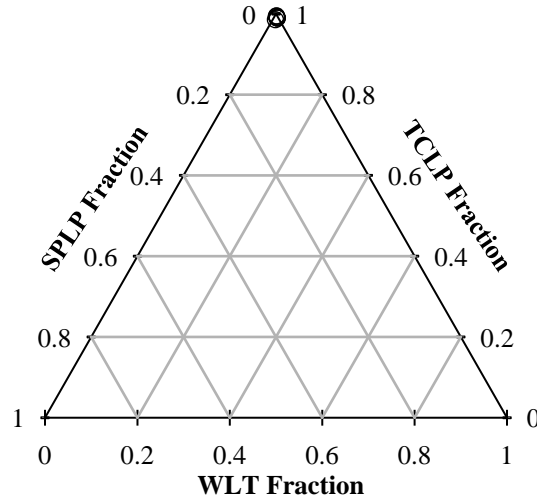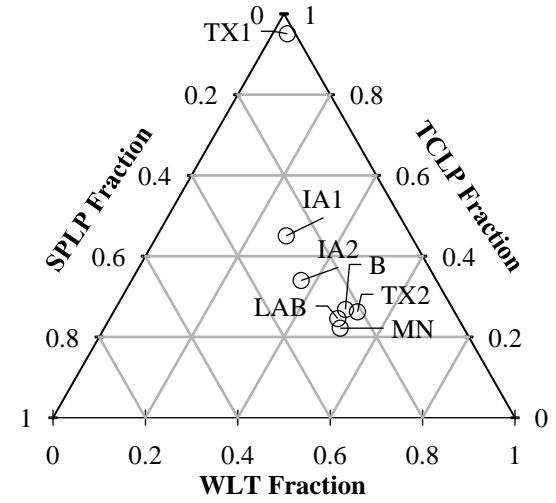
Figure B.10　Effluent concentrations of TDC, DOC and DIC in different test methods
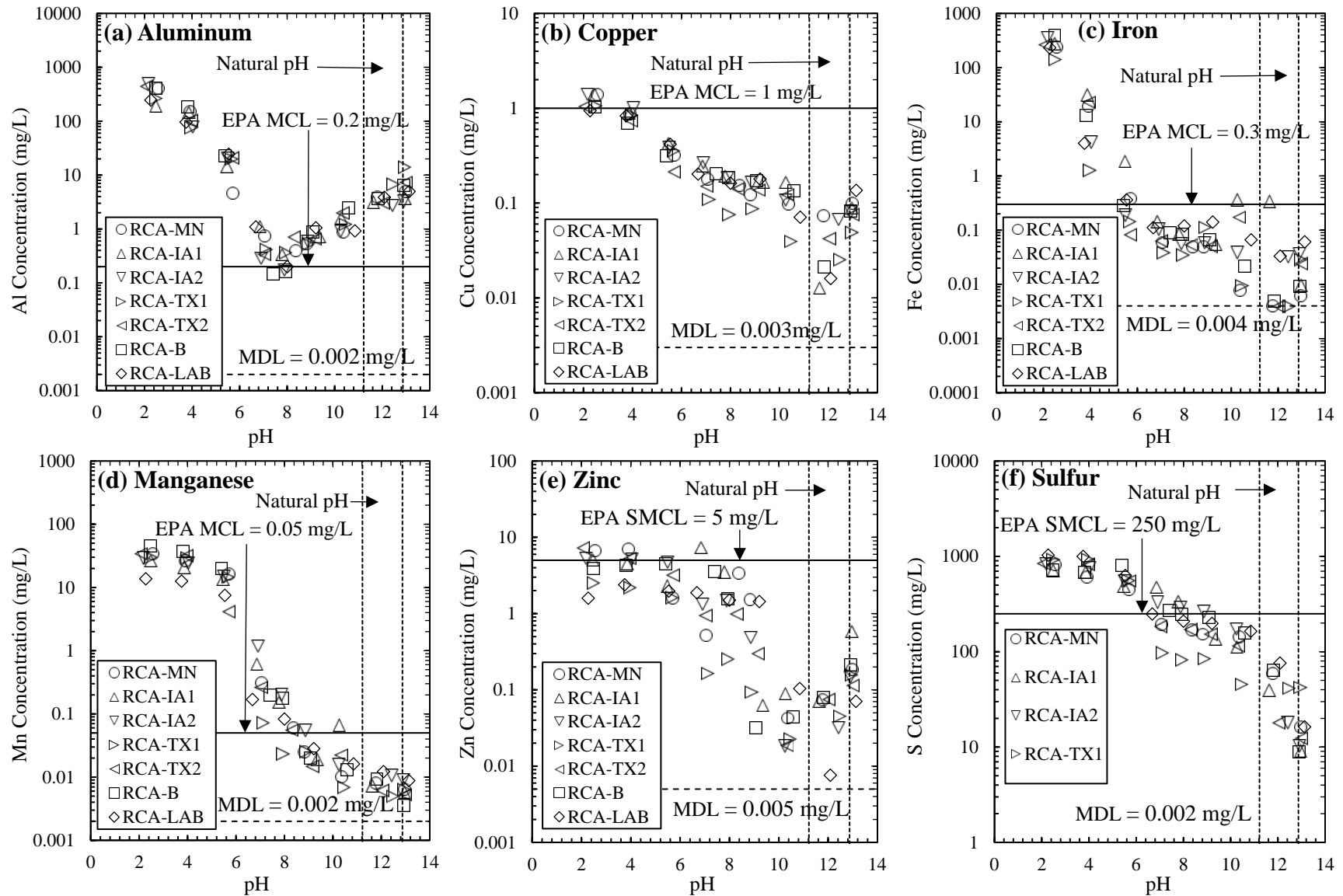
Figure B.11 pH dependent leaching behavior of elements
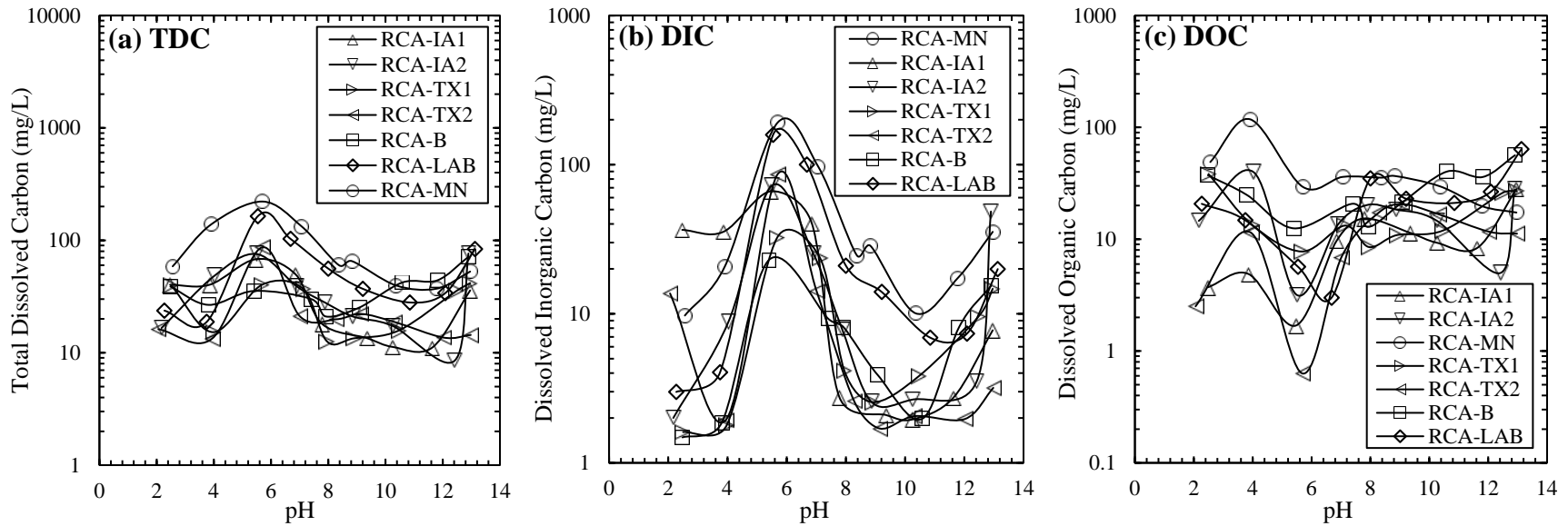
Figure B.12   pH dependent leaching of TDC, DIC and DOC
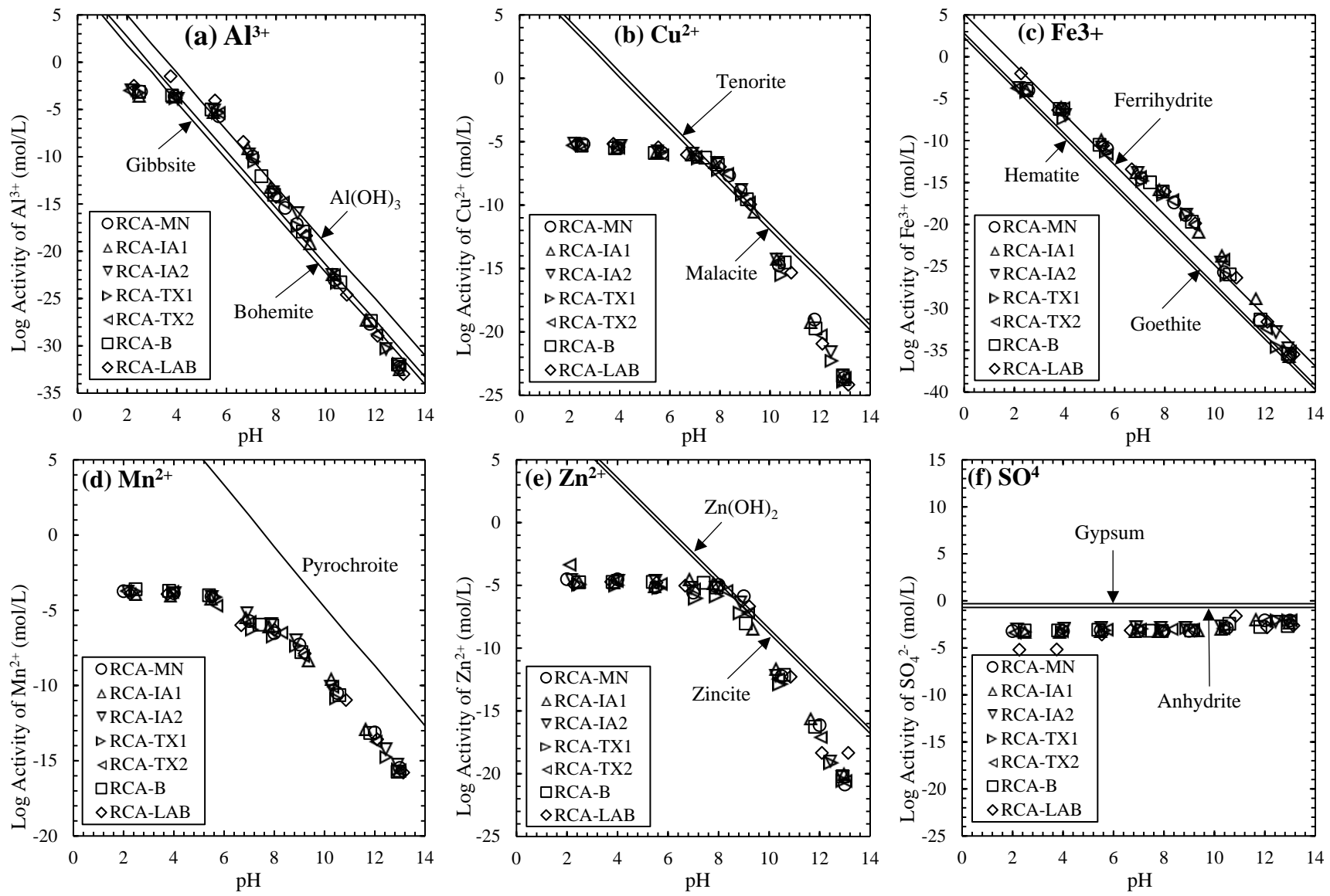
Figure B.13 pH-log activity diagrams of the elements
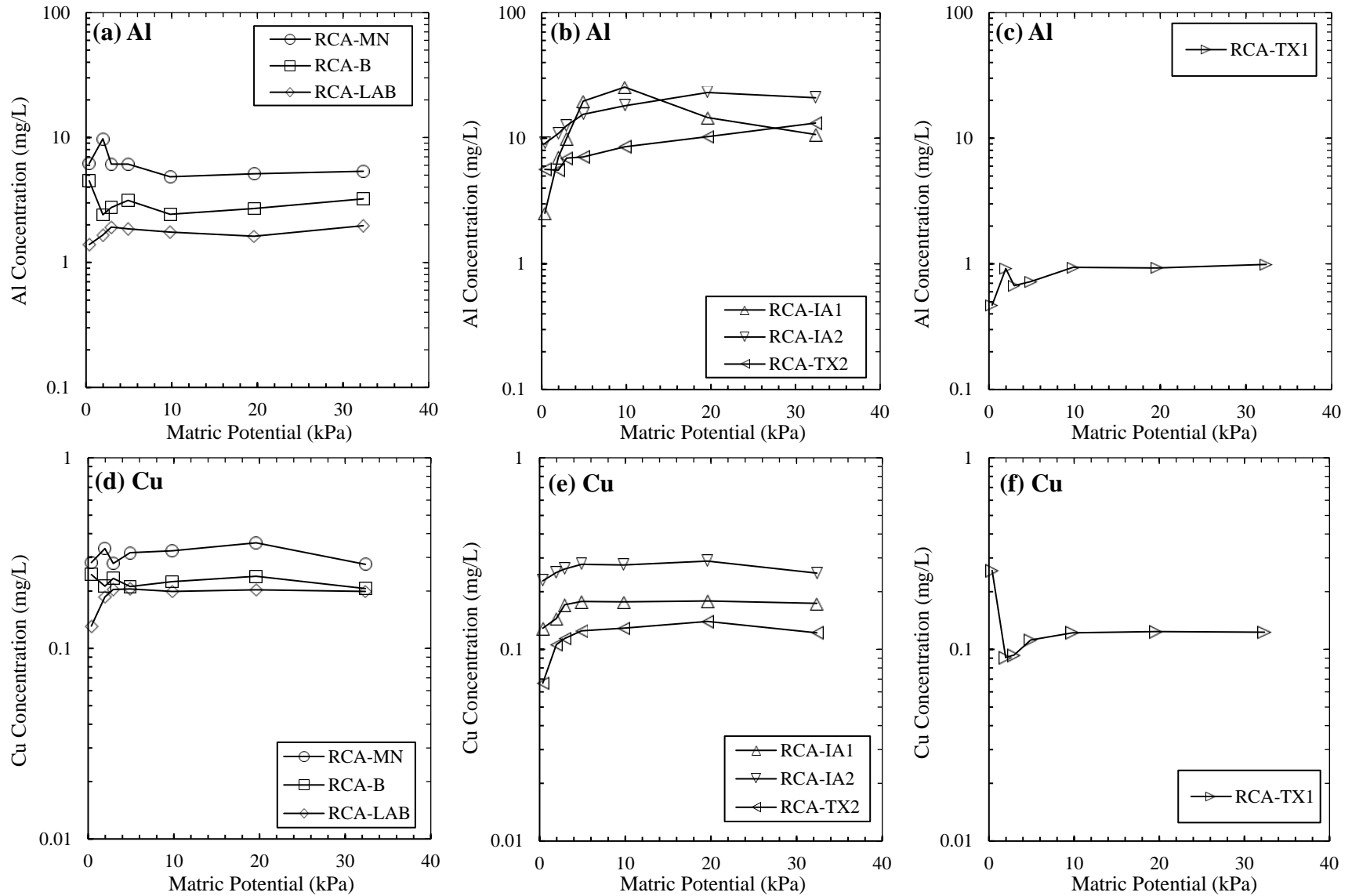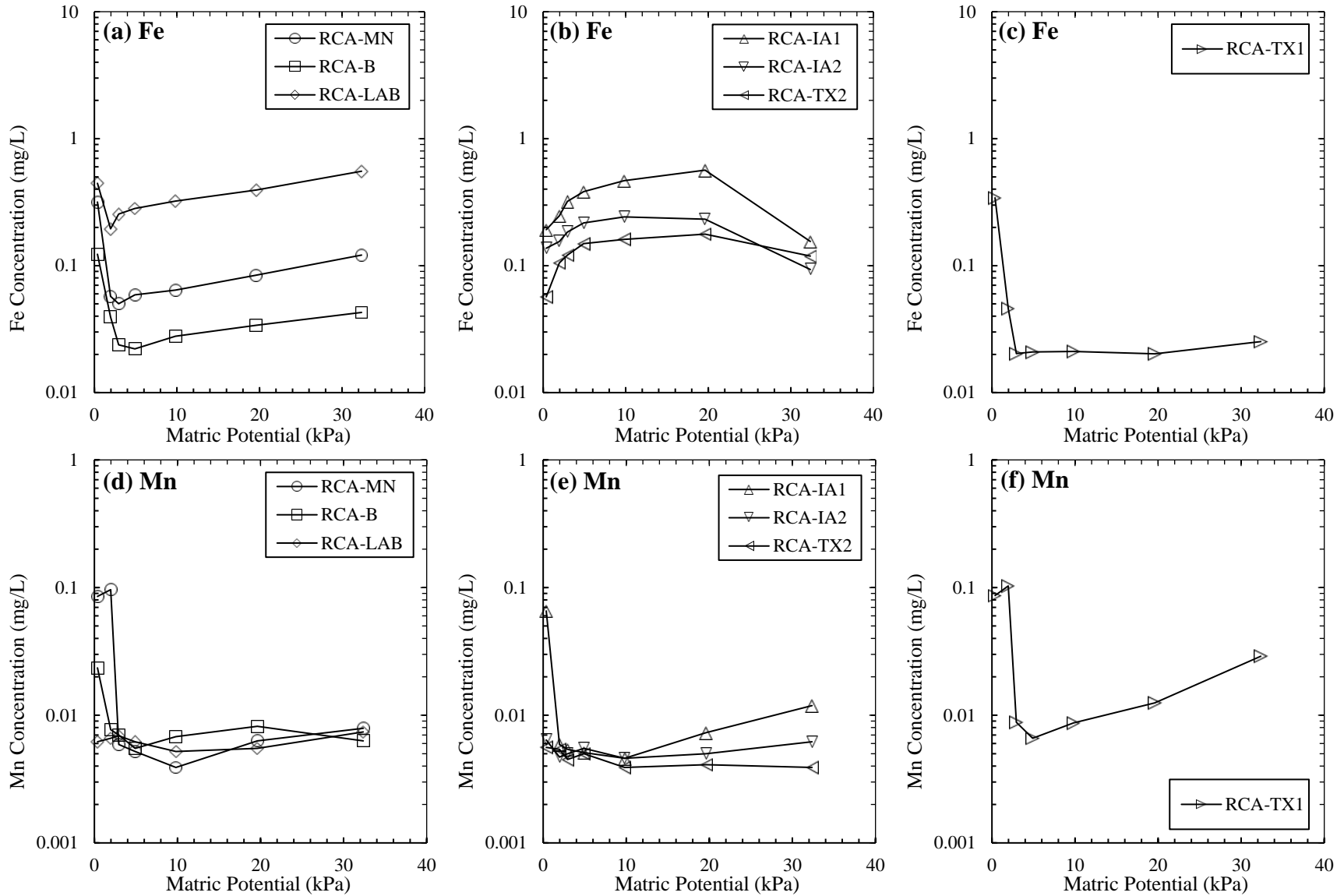
Figure B.14 Effect of matric potential on the leaching of Al and Cr

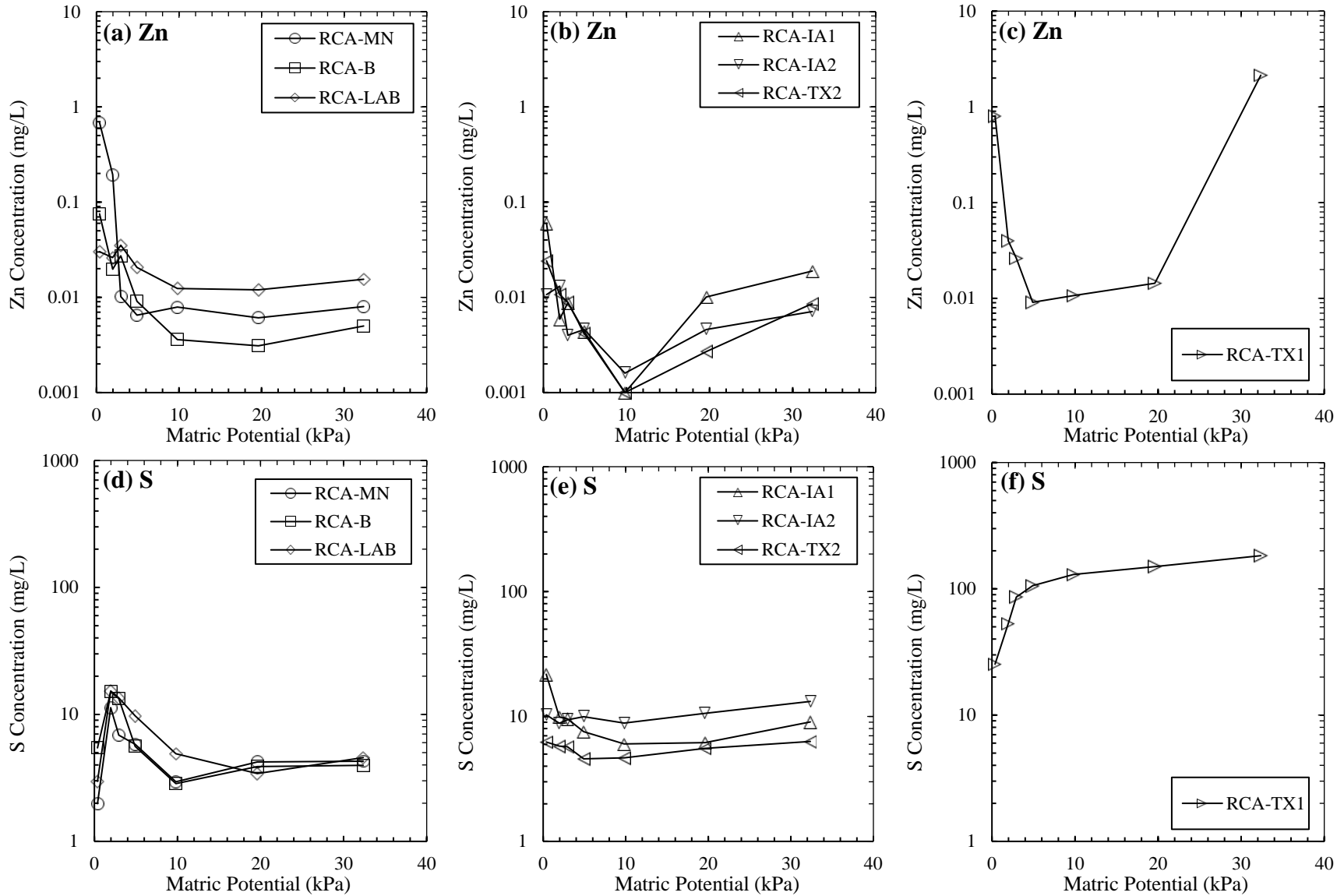**Figure B.15**   Effect of matric potential on the leaching of Fe and Mn

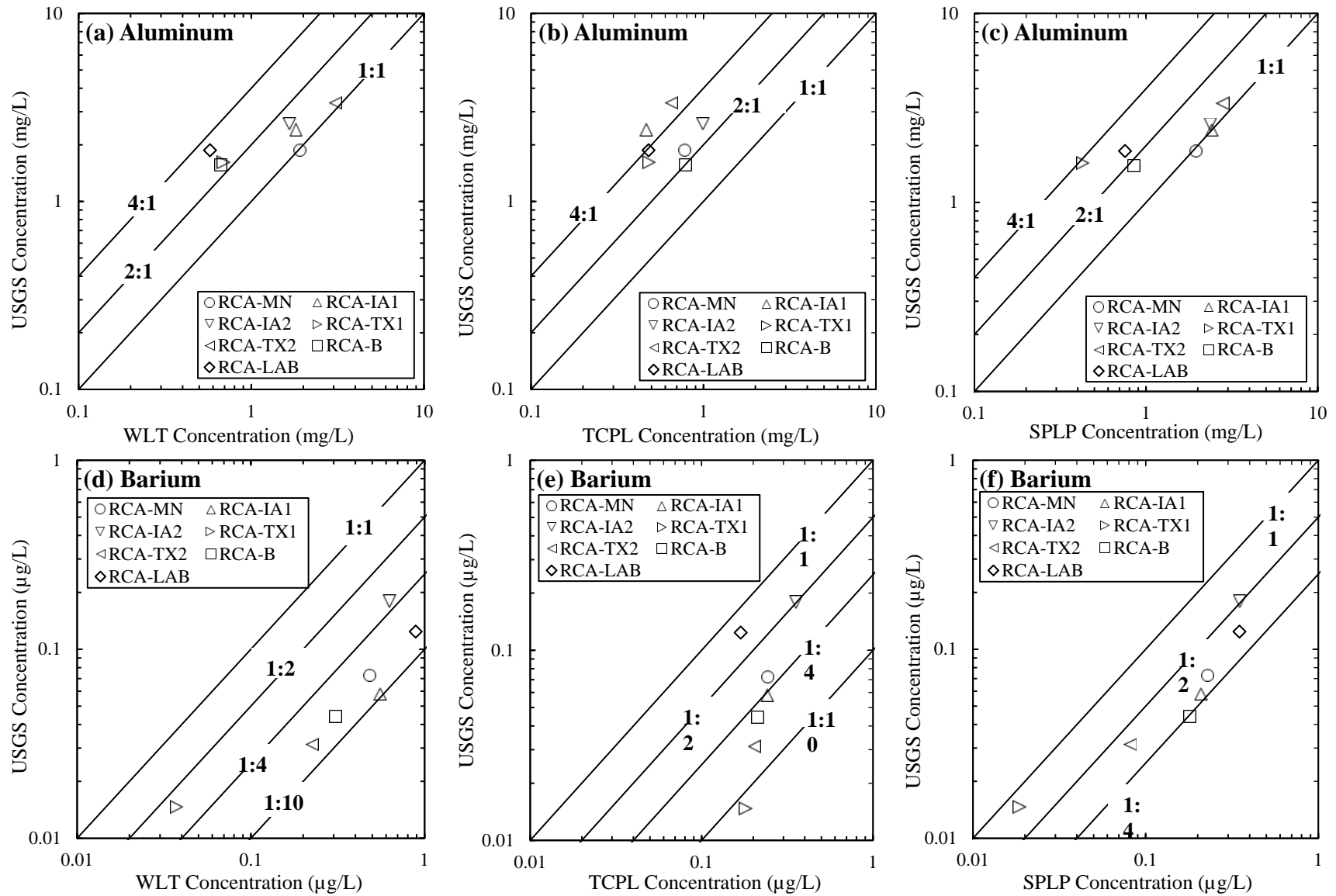**Figure B.16** Effect of matric potential on the leaching of Zn and S

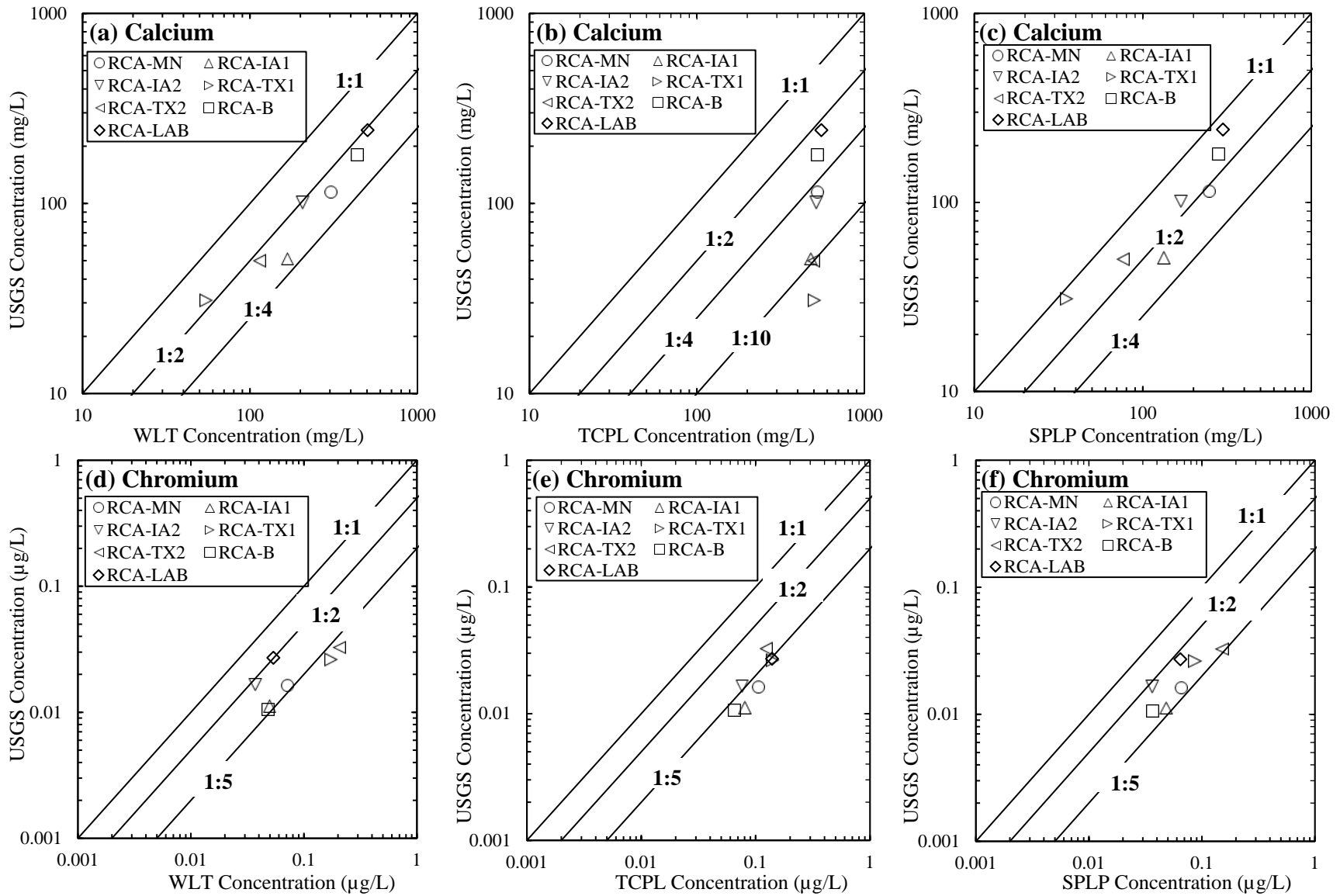**Figure B.17**   Leaching of Al and Ba from the RCAs in USGS leach tests

Figure B.18   Leaching of Ca and Cr from the RCAs in USGS leach tests